FLUORESCENT SELF-ASSEMBLED MONOLAYERS

AS NEW SENSING MATERIALS

Fluorescent Self-Assembled Monolayers as New Sensing Materials

Lourdes Basabe Desmonts

Thesis University of Twente, Enschede, The Netherlands

ISBN 90-365-2303-6

This research has been financially supported by the Council for Chemical Sciences of the Netherlands Organization for Scientific Research (CW-NWO), in the Young Chemist programme (grant number 70098305). The research was carried out at the Supramolecular Chemistry and Technology group (SMCT), MESA$^+$ Institute for Nanotechnology, University of Twente.

Publisher: Wöhrmann Print Service, Zutphen, The Netherlands

© Lourdes Basabe Desmonts, Enschede, 2005

Cover Design Lourdes Basabe Desmonts

No part of this work may be reproduced by print, photocopy or any other means without the permission in writing of the author.

Cover picture: Fluorescence microscopy image of a fluorescent sensor array confined in a microfluidic chip (Chapter 6).

FLUORESCENT SELF ASSEMBLED MONOLAYERS

AS NEW SENSING MATERIALS

PROEFSCHRIFT

ter verkrijging van
de graad van doctor aan de Universiteit Twente,
op gezag van de rector magnificus,
prof. dr. W.H.M. Zijm,
volgens besluit van het College voor Promoties
in het openbaar te verdedigen
op vrijdag 13 januari 2006 om 13.15 uur

door

Lourdes Basabe Desmonts

geboren op 11 maart 1978
te Cartagena, Spanje

Dit proefschrift is goedgekeurd door:

Promotor:	Prof. dr. ir. D. N. Reinhoudt
Assistent-promotor:	Dr. M. Crego Calama

Learning is a treasure that will follow its owner everywhere.

Chinese Proverb

A mis padres y Vicente

Contents

Chapter 5

Cross-reactive metal ion sensor array based on SAMs in a microtiter plate format

Chapter 6

Fluorescent Sensor Array in a Microfluidic Chip

Chapter 7

Combinatorial Fabrication of Fluorescent Patterns with Metal Ions on Glass by Soft and Probe Lithography

Chapter 1

Introduction

Chemical sensing is a critical aspect of life. Our ability to sense the environment is essential for vision, reproduction, olfaction, and auditory or tactile stimulation. In analogy with “natural sensing”, chemical sensing is essential for the evolution of science. Sensing is the tool to discover and quantify analytes in any chemical or biological environment. It has been an active area involving scientists from many disciplines. Despite many efforts, there is still a large number of interesting analytes that cannot be easily detected. Thus, new probes for rapid and low-cost testing methods must be designed for application in medical diagnostics, industrial manufacturing, and national security. Among the different types of chemical sensors, optical sensors and biosensors are expected to grow the fastest. Fluorescence appears one of the most powerful transduction mechanisms[1] due to its high sensitivity and the number of different analytical parameters that can change in the presence of the target analytes.[2] Additionally, and in contrast with electrochemical methods, light can travel without a physical wave-guide, facilitating the technical requirements.[2] In the last two decades a large number of new fluorescent sensing probes have been synthesized. Until now the general trend in the production of sensing materials has been the immobilization of those sensing probes in polymeric matrices. A new emerging tendency in chemical sensing is the production of functional materials with intrinsic sensing properties. This has simplified the sensor device implementation and allowed the production of nanosensors.[3] In Chapter 2 of this thesis, the latest advances in the design of functional materials for chemical sensing are reviewed.

This thesis describes the study and development of a new sensing strategy for the fabrication of a novel fluorescent sensing material. In contrast to classical design based on the synthesis of specific receptors for the target analyte, this sensing approach disconnects the receptor and the fluorophore and organizes them in a self-assembled monolayer on glass to create a large number of sensing pockets on a surface.[4] These surfaces are not designed to complex selectively a unique analyte but rather they are intended to produce fingerprint type responses to a range of analytes by less specific interactions (differential sensing).[5] The approach described in this thesis offers advantages such as direct immobilization of the sensing probes at glass surfaces. It avoids probe leaching and facilitates device implementation like modular immobilization of the building blocks comprising the sensing probe, i.e. ligands and fluorophores, allowing parallel combinatorial methods to generate libraries of sensing surfaces and/or the generation of sensing arrays.[6,7] The speed and ease of synthesis, the high-throughput character of the fabrication, and the screening of the surfaces properties further strengthens this approach.[5]

Initially, and to prove the concept, the synthesis and the characterization of two small libraries of fluorescent sensing monolayers were performed. Subsequently, the sensitivity and selectivity of these surfaces towards the presence of cations and anions in acetonitrile were studied (Chapter 3). However, due to the fact that the most interesting analytes are present in aqueous environment, sensing in water is more important, especially for medical and environmental applications. Thus, the extension of the approach to metal ion sensing in water was the next step. The synthesis of new fluorescent monolayers stable in water was performed, and their sensing abilities towards cations and anions in aqueous environment were investigated (Chapter 4).

The intrinsic characteristics of this sensing system, i.e. flat and transparent surfaces, make it a good candidate for the fabrication of cross-reactive fluorescent sensor arrays.[6,8] This emerging sensing approach[9] has been inspired by the mammalian natural way of sensing, where the olfactory system, with a set of non-specific receptors, generates a response pattern that is perceived by the brain as a particular odor. In Chapter 5 the applicability of the new approach for the generation of such cross-reactive sensor arrays is studied. A sensing array containing 21 different monolayers was prepared in a

25 x 75 mm^2 microtiter-plate. The exposure of the monolayer array to several metal ions and the analysis of the resulting "fingerprint" responses for the recognition of individual analytes were explored.

It is well accepted that miniaturization and automation are essential issues for the development of high-throughput processes. In this context, microfluidics appears a powerful tool for miniaturization of analytical assays.[10-14] On the other hand, glass microchannels are very suitable platforms for the formation of fluorescent sensing monolayers.[15] Thus, the generation of sensing channels arrays by the combination of glass microchannels and sensing monolayers was investigated in Chapter 6. In this chapter, the simultaneous covalent immobilization of different fluorescent self-assembled monolayers in five different microchannels (2 μm deep) confined to a single glass chip was performed. The fluorescent emission of the functionalized channels and its sensitivity to the flow of metal ions were also explored.

In Chapter 7, the application of these fluorescent sensing monolayers towards the development of nanodevices is studied.[16] The generation of luminescent patterns with metal ions on the micro and nano scale by microcontact printing (μCP) and dip-pen nanolithography (DPN) has been studied.

References and Notes

1 Encyclopedia of Sensors, 10-volumen set, Ed. Craig A. Grimes, Elizabeth C. Dickey, and Michael V. Pishko, The Pennsylvania State University, University Park, USA***, 2005***.

2 Lakowicz, J. R., Topics in Fluorescence Spectroscopy. Vol.1, Techniques. Lakowicz, Joseph R. Publication: Kluwer Academic Publishers, New York ***2002***.

3 Medintz, I. L.; Uyeda, H. T.; Goldman, E. R.; Mattoussi, H. Quantum Dot Bioconjugates for Imaging, Labelling and Sensing. *Nature Materials* ***2005***, 4(6), 435-446.

4 Crego-Calama, M.; Reinhoudt, D. N. New Materials for Metal Ion Sensing by Self-Assembled Monolayers on Glass. *Adv. Mater.* ***2001***, 13(15), 1171-1174.

5 Lavigne, J. J.; Anslyn, E. V. Sensing a Paradigm Shift in the Field of Molecular Recognition: From Selective to Differential Receptors. *Angew. Chem., Int. Ed.* ***2001***, 40(17), 3119-3130.

6 Rakow, N. A.; Suslick, K. S. A Colorimetric Sensor Array for Odour Visualization. *Nature* ***2000***, 406(6797), 710-713.

7 Albert, K. J.; Gill, S. D.; Pearce, T. C.; Walt, D. R. Automatic Decoding of Sensor Types Within Randomly Ordered, High-Density Optical Sensor Arrays. *Anal. Bioanal. Chem.* ***2002***, 373(8), 792-802.

8 Suslick, K. S.; Rakow, N. A.; Sen, A. Colorimetric Sensor Arrays for Molecular Recognition. *Tetrahedron* ***2004***, 60(49), 11133-11138.

9 Lundstrom, I. Artificial Noses - Picture the Smell. *Nature* ***2000***, 406(6797), 682-683.
10 Andersson, H.; Van den Berg, A. Microfluidic Devices for Cellomics: a Review. *Sens. Actuators, B* ***2003***, 92(3), 315-325.
11 Buranda, T.; Huang, J. M.; Perez-Luna, V. H.; Schreyer, B.; Sklar, L. A.; Lopez, G. P. Biomolecular Recognition on Well-Characterized Beads Packed in Microfluidic Channels. *Anal. Chem.* ***2002***, 74(5), 1149-1156.
12 Sato, K.; Hibara, A.; Tokeshi, M.; Hisamoto, H.; Kitamori, T. Microchip-Based Chemical and Biochemical Analysis Systems. *Adv. Drug Delivery Rev.* ***2003***, 55(3), 379-391.
13 Vilkner, T.; Janasek, D.; Manz, A. Micro Total Analysis Systems. Recent Developments. *Anal. Chem.* ***2004***, 76(12), 3373-3385.
14 Rudzinski, C. M.; Young, A. M.; Nocera, D. G. A Supramolecular Microfluidic Optical Chemosensor. *J. Am. Chem. Soc.* ***2002***, 124(8), 1723-1727.
15 Mela, P.; Onclin, S.; Goedbloed, M. H.; Levi, S.; García-Parajó, M. F.; Van Hulst, N. F.; Ravoo, B. J.; Reinhoudt, D. N.; Van den Berg, A. Monolayer-Functionalized Microfluidics Devices for Optical Sensing of Acidity. *Lab Chip* ***2005***, 5(2), 163-170.
16 Saxl, O. Nanotechnology a Key Technology for the Future of Europe. Institute of Nanotechnology, UK, for the European Commission Expert Group on Key Technologies for Europe, ***2005***.

Chapter 2

Design of Fluorescent Materials for Chemical Sensing

There is an enormous demand for chemical sensors for many areas and disciplines. High sensitivity and ease of operation are two main issues for sensor development. Fluorescence techniques can easily fulfill these requirements and therefore fluorescent-based sensors appear as one of the most promising candidates for chemical sensing. However, the development of sensors is not trivial; material science, molecular recognition and device implementation are some of the aspects that play a role in the design of sensors. The use of polymers, sol-gels, mesoporous materials, surfactant aggregates, quantum dots, and glass or gold surfaces, combined with different chemical approaches for the development of fluorescent sensing probes is reviewed and illustrated with representative examples.

2.1. Introduction

Chemical sensing refers to the continuous monitoring of the presence of chemical species.[1] It is hardly necessary any longer to stress the importance of the development of new chemical sensors. Many disciplines need sensing systems, including chemistry, biology, clinical biology and environmental science. For example, analytical methods to study the chemistry of the living cell and to understand the mechanisms that make cells work are highly desirable. Therefore, sensors for biomolecules such as neurotransmitters, glutamate and acetylcholine, glycine, aspartate and dopamine, NO and ATP would be very helpful.[2] Along the same line it is interesting to develop sensors for metal ions like sodium, potassium, and calcium which are involved in biological processes such as transmission of nerve pulses, muscle contraction and regulation of cell activity. Interesting as well is the detection of aluminum which is toxic and whose possible implication in Alzheimer's disease is being discussed. In the field of environmental science, it is well known that mercury, lead and cadmium are toxic for living organisms, and thus early detection in the environment is desirable. Additionally, sensors for explosives and hazardous chemicals are being extensively investigated for the detection of landmines[3] and warfare chemicals. With the war on terrorism, the need for accurate, reliable, real-time biological and chemical sensing is in the spotlight.[4,5] Finally, chemical sensing allows for the study and control of chemical processes from the laboratory to the industrial scale, and plays an important role in the food industry for the control of food quality and safety.[6]

The list of interesting analytes to be detected is lengthly[2] and there is a need for rapid and low-cost testing methods for a wide range of clinical bioprocesses and in areas of chemical and environmental applications.[7] On the other hand it has been pointed out before that there is a large gap between the importance of certain types of organic molecules and the availability of sensors for these target compounds. This is probably due to lack of communication between the communities that need chemosensors and those that might fabricate them.[8] Thus it is important to expand the range of analytes that can be detected and quantified as well as improve the communication between both mentioned communities. In the case of biomolecules, nature provides us with a large

number of specific interactions that can be used for biosensors. However, there are also a large number of molecules that are not easily detectable, and therefore new probes must be designed.[8]

Many features make fluorescence one of the most powerful transduction mechanisms to report the chemical recognition event.[9] A number of fluorescence microscopy and spectroscopy techniques based on the life-time, anisotropy or intensity of the emission of fluorescent probes have been developed over the years.[10] These are enormously sensitive techniques that allow even the detection of single molecules. Fluorescence does not consume analytes and no reference is required. Light can travel without a physical wave-guide in contrast to electrochemical methods, facilitating the technical requirements.[11] Additionally, using fluorescence it is possible to perform remote monitoring. For example, it is possible to monitor simultaneously concentrations of the target analytes in all regions of a living cell.[12] A big advantage of fluorescence spectroscopy is that different assays can be designed based on different aspects of the fluorescence output (lifetime, intensity, anisotropy and energy transfer).[11,13] Additionally, laser fiber optics and detection technologies are well established. Therefore, fluorescence techniques are also envisioned as the most important future detection method for miniaturized ultra-high-throughput screening.[13]

Chemical sensing using fluorescence to signal a molecular recognition event was first demonstrated during the early 80's when Roger Y. Tsien reported the synthesis of the first fluorescent calcium indicators.[14,15] They were comprised of a calcium ion chelate receptor covalently linked to simple aromatic rings or other dyes as chromophores. Since then an enormous amount of work has been done for the rational design of fluorescent indicators.[16,17] However, only a few sensors are currently available because the implementation of sensing probes in functional devices without loss of sensitivity is still very challenging. Previously, the common habit of organic chemists to refer to new molecular indicators as "sensors" has been criticized since only by the integration of such fluorescent indicators into a device will a sensor be obtained.[18] To avoid such confusion, Czarnik introduced the concept of "Chemosensor" in 1993.[19] A chemosensor was defined as: "A compound of abiotic origin that complexes to an anlyte reversibly with a concominant fluorescent signal transducition" and it constitutes only the active

transduction unit of a sensor. New approaches based on materials in which molecular indicators are already integrated are increasingly captivating the attention of scientists, because their implementation as a truly sensory system is more straightforward.

The strategies and ideas that chemists have invented to develop new fluorescent chemosensing materials for the integration of the sensory system in sensor devices are reviewed here. Fluorescent sensors are divided in two groups, fluorescent biosensors[20] and fluorescent chemosensors.[21] Even though biosensors represent a very important area in the sensing industry[22,23] they fall outside of the scope of this review. This report will be limited to the development of chemosensors based on new artificial materials that are able to signal reversibly the presence of other chemical species. Additionally, new trends in the development of fluorescent sensors such as the fabrication of nanosensors,[24] the use of combinatorial methods and the fabrication of high density sensor arrays[3] will be discussed.

2.2 Classical design of fluorescent indicators

The classical design of a fluorescent indicator includes two moieties, a receptor responsible for the molecular recognition of the analyte and a fluorophore responsible for signaling the recognition event. There are three main strategies to approach the design of fluorescent molecular indicators for chemical sensing in solution. The first results in *intrinsic fluorescent probes*,[25,26] which are fluorescent molecules where the mechanism for signal transduction involves interaction of the analyte with a ligand that is part of the π-system of the fluorophore. The second are *extrinsic fluorescent probes*, in which the receptor moiety and the fluorophore are covalently linked but are electronically independent.[25,27-29] These approaches involve different receptor molecules that might be synthesized and afterwards attached to a fluorophore to make the sensitive probe. Due to the covalent linking through a spacer the moieties are in close proximity, and thus interaction of the analyte with the receptor induces a change in the fluorophore surroundings and alters its fluorescence. The third strategy is called *chemical ensemble*. This approach is based on a competitive assay in which a receptor–fluorophore ensemble

is selectively dissociated by the addition of an appropriate competitive analyte that is able to interact efficiently with the receptor, and resulting in a detectable response of the fluorophore.[30-33]

2.3 Fluorescent materials for chemical sensing

Traditinally, after the production of a fluorescent indicator the next step toward the fabrication of a sensor is the production of the sensing material by the incorporation of the indicator into a solid support. Until today the most common approach for the immobilization step has been the physical entrapment of the sensitive probe in a polymer matrix.[34] After the entrapment the polymer is deposited on a device such as an optical fiber or the surface of a waveguide to create the working sensor. However, physical entrapment of the dyes in a polymer matrix produces inhomogeneity in the materials and causes stability problems due to the leaching of the fluorescent probe, thus reducing the life time and reproducibility of the sensor. Thus, despite the easy preparation of these materials, they are rarely incorporated into commercial instrumentation. To solve the instability of these materials, the alternative has been the covalent attachment of the probes into the polymeric matrices.[35] Parallel to the production of polymeric materials, new trends in materials science for chemical sensing are emerging. Other materials have been developed where the components of a sensing system (receptor and fluorophore) are directionally confined in space, i.e. they are covalently immobilized at a surface or form surfactant aggregates. A number of materials such as silica particles, glass and gold surfaces,[36] quantum dots,[37] Langmuir-Blodgett films,[38] vesicles, liposomes, and others[39] are used presently to create sensitive fluorescent materials.

2.3.1 Fluorescent polymers

Polymers are still the most common support for chemical sensors. They are convenient due to the fact that they are easily processable as small particles and thin films that can be deposited onto optical fibers[40] and waveguides[41,42] for sensor fabrication

(Figure 2.1). During the last two decades chemical indicators have been immobilized in polymeric matrices mainly by simple impregnation,[3] doping[43] or covalent attachment.[44] Other strategies such as electrostatic layer-by-layer assembly have also been used.[45] Polymers used in sensor devices either participate in the sensing mechanism or they are used to immobilize the component responsible for analyte sensing.[46] The use of polymers for physical, chemical and biochemical sensing applications have been recently reviewed by Adhikari.[46]

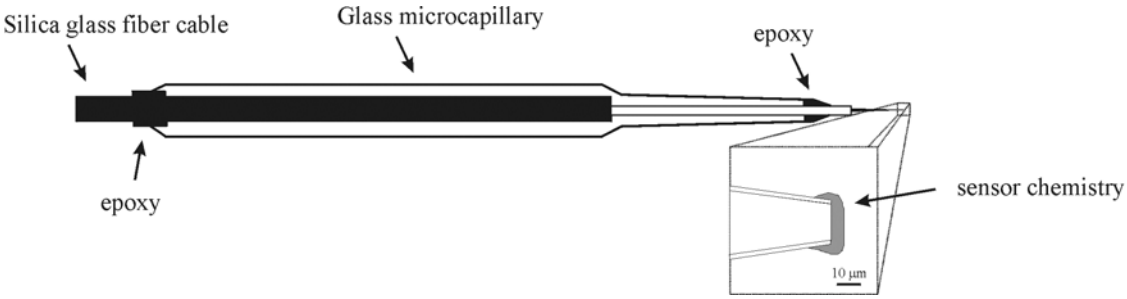

Figure 2.1. *Cross section through a fiber optic with a polymeric sensing layer deposited on the tip.*

Physical entrapment of the dyes in the polymer matrix is the simplest method for immobilization of dyes and indicators into polymer materials. In general these methods produce unstable materials because leaching of the probes limits their use for long time monitoring. Nevertheless, this method is widely used for the preparation of sensitive thin films or microspheres.[47,48] Polymeric thin films with embedded organic dyes are often immobilized on the tip of optical fibers to perform the sensing measurements.[49] The specific incorporation of fluorescent probes in polymers has been recently reviewed by Bosch.[50] Entrapment of organic dyes and transition metal complexes has also been used to design probes for sensing O_2.[47,51] Yang et al. recently reported the immobilization of pyrene-labeled metalloporphyrins in a plastized poly(vinyl chloride) (PVC) membrane for the sensing of imidazole derivatives such as histidine.[52] Approaches based on dye-doped thin films have been used in the analysis of organic vapors,[53-55] the detection of metal ions,[56-58] and the determination of pH.[59,60]

Processing of polymers can also yield polymeric particles with sizes ranging from nanometers to micrometers. These particles are easily transformed into sensing systems by staining them with dye molecule solutions.[61] [62,63]Because sensing particles can act as an individual probe, they can easily be used for the fabrication of sensor arrays.[48] Their small size and their polymeric nature make them suitable candidates for the generation of nanosensors for intracellular analysis.[64] The production of sensor arrays and nanosensors by incorporation of dye molecules into polymeric particles will be discussed later.

As an alternative for dye-impregnated polymers, fluorescent polymers have been synthesized. Covalent attachment of the fluorescent molecules into polymeric materials can be achieved after polymerization if the polymer contains reactive functional groups,[65] or by co-polymerization with a fluorescent polymerizable monomer.[44] Initially, covalent functionalization of polymers with fluorescent molecules was performed by covalent attachment of fluorophores to natural polymers such as cellulose. For example, in 1992 Wolfbeis et al. already reported the immobilization of pH sensitive dyes in cellulose matrices,[66] and recently Ueno's group described the covalent immobilization of dansyl functionalized cyclodextrins in a cellulose membrane for the detection of neutral molecules.[67,68] Depending on properties such as permeability, polarity, mechanical strength, biocompatibility and solubility of the polymers they are suitable for the use in several media and for different analytes. Synthetic polymers with specific functionalities are used currently for the production of specific sensors. A large variety of probes containing covalently linked dyes have been developed. Walt et al. published in 1991[69] the photopolymerization of appropriate dye indicators on the surface of an imaging fiber tip for pH, CO_2 and O_2 sensing.[70] They also reported the covalent attachment of fluorophores to the surface of silica, poly(methylstyrene), and poly(ethylene glycol) (PEG) microspheres[48,71] to generate a collection of small sensors that afterwards could be used for the fabrication of sensor arrays on the tips of optical fibers for organic vapors[3] and DNA detection.[72] An optical fiber coated with a fluorescent membrane containing anthracene has been reported for the sensing of tetracycline antibiotics by Yu et al.[73] Anslyn's group has used poly(ethylene glycol)- polystyrene (PEG-PS) resin beads derivatized with a variety of indicator molecules to generate an array of microsize pH sensors.[74] Wolfbeis has shown the co-immobilization of transition metal complexes and

pH indicators in a hydrogel matrix to design a pH sensor with long luminescence decay times.[75] Polymers labeled with naphthalimide have been shown to be sensitive to transition metal ions and pH.[76] Recently a fluorescent pH sensitive hydrogel thin film has been prepared by copolymerization of a modified dye and poly(ethylene glycol) diacrylate.[77] Using a similar strategy a new commercial optical sensor for glucose under physiological conditions has been developed by the group of Singaram.[44] They used boronic acid derivatives together with a fluorophore derivative to form a thin film hydrogel, because boronic acids are known to bind glucose reversibly under physiological conditions. They specifically combined a cationic boronic-acid (a functional quencher) and an anionic dye (Figure 2.2). The electrostatic interactions between both produce a quenching of the fluorescence of the dye which is modulated upon interaction between the boronic acid and the glucose.

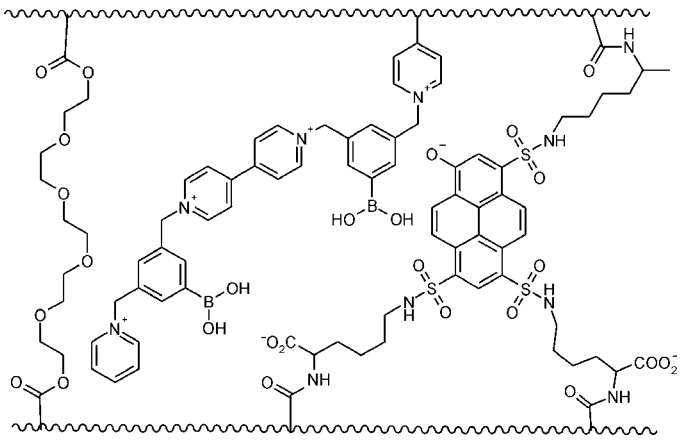

Figure 2.2. *Glucose-sensing polymer comprised of in boronic acids and pyrene derivatives, which are in close proximity due to electrostatic interactions.*

Another approach involving boronic acids for the recognition of sugars was reported by Rivero et al.,[78] who immobilized dansylphenylboronic acid in polymeric microspheres for the recognition of fructose.

A special case of polymeric fluorescent systems is luminescent dendrimers. These are macromolecules with a well-defined chemical structure in which chemical units can be easily included for the recognition of ions or neutral molecules (Figure 2.3).

Luminescent dendrimers have been recently reviewed by Balzani.[79] Dendritic structures containing luminescent metal complexes, fluorescent organic chromophores, porphyrins and fullerenes have been reported.[79] Signal amplification processes in these dendrimers have been well characterized[80] and could be advantageous for sensor design. In the field of chemical sensing, it has been demonstrated that luminescent dendrimers could be used for sensing chiral amino alcohols[81-83] and metal ions.[80,84-86]

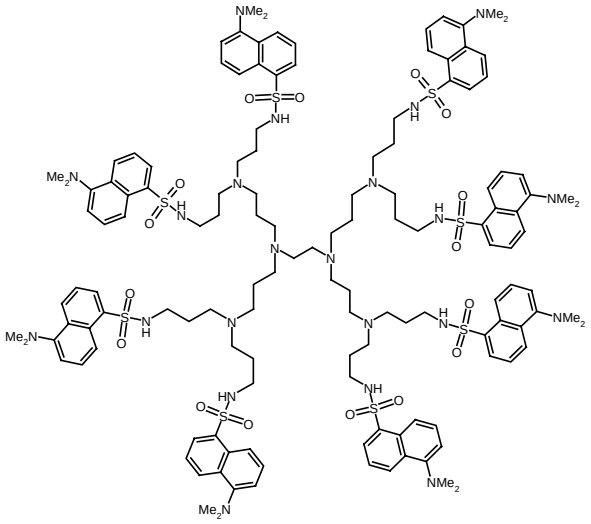

Figure 2.3. *Structure of a dansyl dendrimer sensitive to the presence of Co^{2+} ions.*[84]

2.3.1.1 Molecular imprinted polymers

A special case of fluorescent polymers are molecular imprinted polymers (MIPs).[87] Molecular imprinting was used already in 1949 by Dickey,[88] and is one of the strategies that offers a synthetically efficient route to artificial receptors. It is a very interesting approach for the fabrication of new fluorescent sensitive probes because it does not require the exact prior knowledge of the three dimensional structure of the target molecule and the complete synthesis of a receptor. Ideally this method could be used for the detection of a wide range of compounds. The imprinting process involves the co-polymerization of functional monomers and a cross-linker in the presence of target

analytes which act as a molecular template (imprint molecule). The functional monomer initially forms a complex with the imprint molecule, and following polymerization, their functional groups are held in position by the highly cross-linked polymeric structure. After removal of the imprinted molecule a cavity is formed that is complementary in size and shape to the analyte. The cavity is also lined with complementary functionality, which is provided by the functional monomer. In this way the polymer now has a "molecular memory" and exhibits specific binding characteristics for the template and structurally related compounds (Figure 2.4).

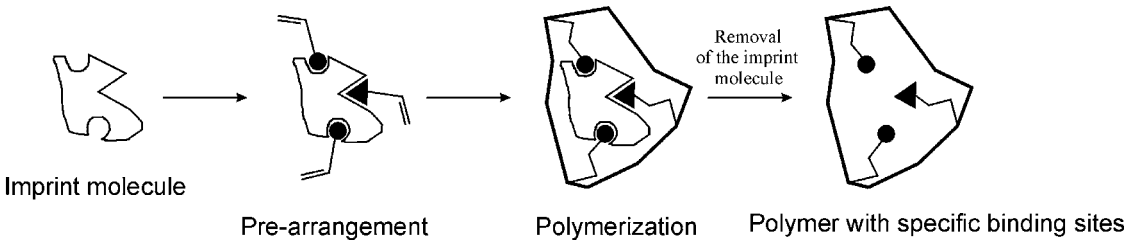

Figure 2.4. *Schematic representation of the polymer imprinting process showing one binding site within the polymer matrix. Cross-linking functionalities may be covalently or no covalently linked to the template.*

The recognition properties of MIPs have been combined with a variety of transducers to generate different sensors, such as capacitance sensors and sensors based on mass-sensitive acoustic or conductimetric transduction, ellipsometry, surface plasmon resonance, etc.[89] Competitive binding based sensors have also been described for these types of polymers.[89] In 1997 the first examples where fluorescent reporter groups were incorporated into the MIP appeared.[89-91] Upon binding to the imprinted binding sites the analyte interacts with the fluorescent molecules and their fluorescence is quenched. Powel et al. reported the synthesis of a polymer imprinted with cyclic adenosine monophosphate (cAMP) using the fluorescent monomer, trans-4-[*p*-(N,N-dimethylamino)styryl]-N-vinylbenzylpyridinium chloride together with a conventional functional monomer.[90] In this way, the fluorophore is part of the recognition site and is quenched upon complexation of the cAMP in water.

In the last five years several reports have appeared where intrinsically fluorescent imprinted polymers have been used for the sensing of L-tryptophan[92], cyclic GMP[93], histamine,[94] cyclic AMP,[90] D-fructose,[95] creatinine[96] and other analytes.[93,97-101] In most of these systems, recognition of the analytes results in the quenching of the fluorescence emission. However, in sensor design enhancement of the signal is more desirable to avoid false positives. Recently, a new fluorescent imprinted polymer that responds to the binding event with a high enhancement in fluorescence intensity has been reported by Takeuchi et al.[102] The co-polymerization of ethylene glycol dimethylacrylate, cross-linker, and the functional monomer 2-acrylamidoquinoline (***1***) (Figure 2.5) in the presence of cyclobarbital (***2***) yields a fluorescent hydrogen-bonded polymer able to bind selectively to the imprinted analyte. Cyclobarbital showed higher affinity for the imprinted polymer than two structurally related compounds (***3*** and ***4***) having the same two-point hydrogen-bonding pattern to the functional monomer (***1***).

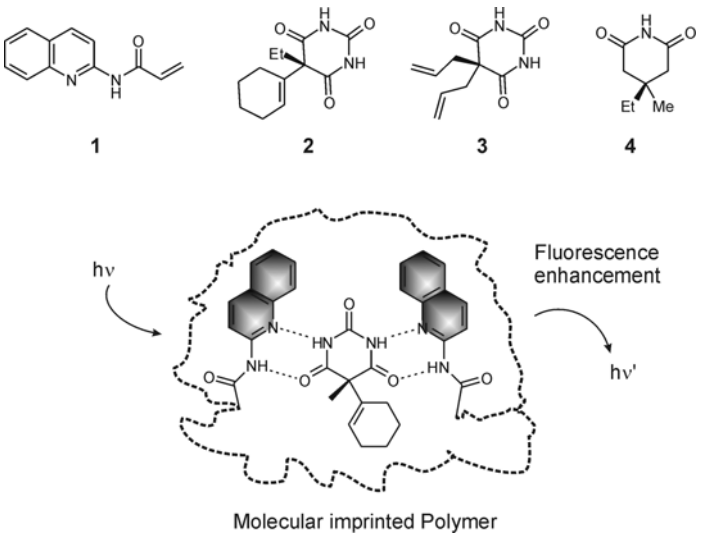

Figure 2.5. *Chemical structures of the functional monomer 2-acrylamidoquinoline* ***(1)****, cyclobarbital* ***(2)****, the structurally related compounds allobarbital* ***(3)*** *and 3-ethyl-3-methylglutarimide* ***(4)****, and a schematic representation of one binding site of the cyclobarbital imprinted polymer.*

One of the advantages of these systems is the easy synthesis. However, this is offset by the relatively poor affinity and selectivity. It is believed that only part of the created binding sites have high affinity and selectivity for the template molecule.[35] Despite their poor selectivity, MIPs are suitable candidates for use in sensor arrays where the collection of responses of these unspecific sensors to the presence of an analyte can create a characteristic pattern for analyte recognition.[103]

2.3.1.2 Conjugated polymers

A different type of fluorescent polymers are the so-called conjugated polymers (CP). Conjugated polymers are polyunsaturated compounds with alternating single and double bonds along the polymer chain in which all backbone atoms are *sp*- or sp^2-hybridized. This *electronic* conjugation between each repeat unit creates a semiconductive "molecular wire". The resulting interaction between orbitals creates a semiconductor band structure having a valence band (filled with electrons) and a conduction band (devoid of electrons). The semiconductive nature of these organic polymers gives them very useful optical and optoelectronic properties. Figure 2.6 shows the structure of some representative conjugated polymers.

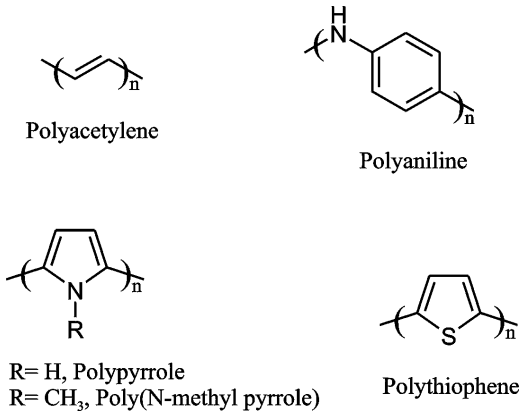

Figure 2.6. *Chemical structures of some representative conjugated polymers.*

The group of Swager demonstrated in 1995 that "wiring molecular recognition sites in series" leads to ultra-high sensitivity.[104,105] This sensitivity arises from the collective optical and conducting properties of the CP. These polymers are extremely sensitive to minor external structural perturbations or to electron density changes within the polymer, due to their ability to self-amplify their fluorescence quenching response upon perturbation of the electronic network by binding of analytes. Depending on the system, a CP can exhibit a strong luminescence. The luminescence efficiency is related to the delocalization and polarization of the electronic structure. These polymers are good candidates as materials for fluorescent sensing. Figure 2.7 shows schematically how conjugated polymers amplify the molecular recognition signal via migration of electrons along the polymer chain. It shows a basic band diagram illustrating the mechanism known as photoinduced electron transfer fluorescence quenching. Irradiation of the polymer with a photon causes promotion of an electron to the conduction band (which is now of a much higher energy), which then migrates along the polymer backbone. Analyte binding produces a trapping site whereby the excitation is effectively deactivated by electron transfer quenching. The low energy LUMO orbital can accept the electron from the excited state of the polymer in an exergonic process. This destroys the polymer based excited state, and the polymer can no longer fluoresce. The final step of reverse electron transfer from the quencher's LUMO to the polymer valence band is a non-radiative process.

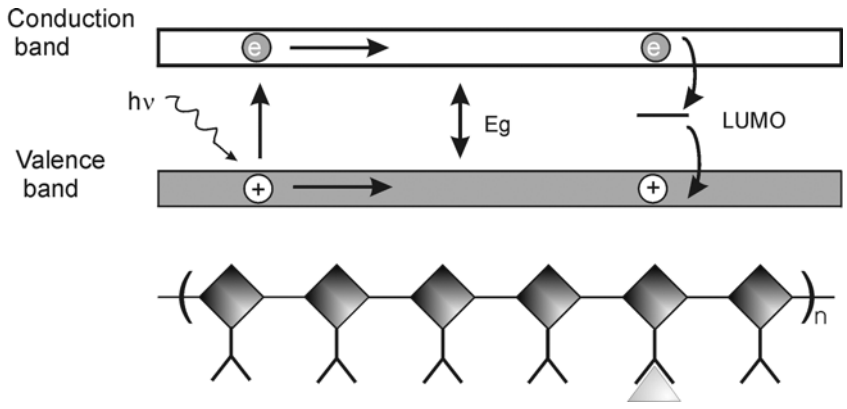

Figure 2.7. *Band diagram illustrating the mechanism for exciton transport and electron transfer fluorescence quenching of a conjugated polymer upon interaction with the analyte.*

Figure 2.8 compares schematically the CP and the classical chemosensor approach. Whereas complete fluorescence quenching would be observed in the case of the conjugated polymer upon interaction with an analyte, in the case of non-conjugated sites exposed to the same analyte concentration only a small percentage of quenching would be observed. Each analyte is confined to its particular molecule and can only sample one binding site. Therefore, the emission is observed from those molecules which did not bind an analyte. In the CP approach one single interaction can quench a large number of fluorophores and the signal obtained in the presence of the analyte is amplified.

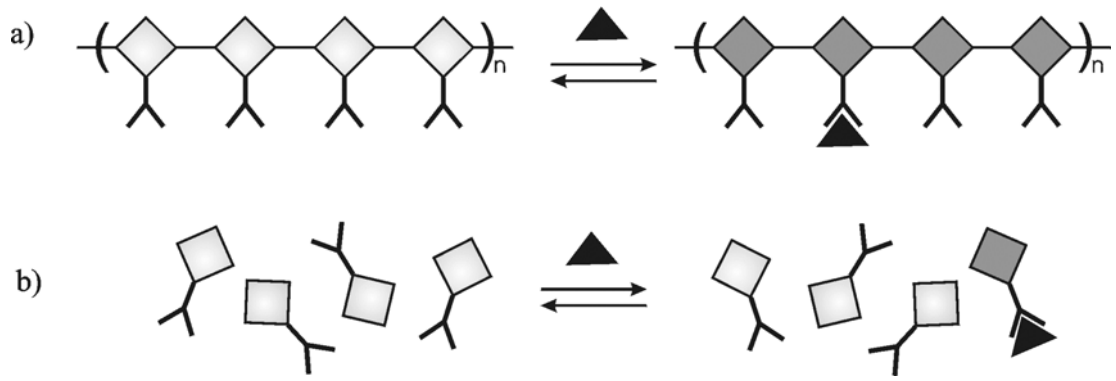

Figure 2.8. *a) Conjugated polymer interacting with a low concentration of quencher giving complete quenching of the polymer chain. b) Individual receptor-chromophore molecules exposed to a low concentration of quencher. This situation results only in a partial quenching.*

Fluorescent conjugated polymers such as 2,2'-bipyridyl-phenylene-vinylene-based polymers,[106] terpyridine-based poly(*p*-phenylene-ethynylene)-*alt*-(thienylene-ethylene) polymers,[107] poly(*p*-phenylene-ethynylene)[108] and others[109] have been reported as sensitive probes for the detection of metal ions. There are only a few examples of anion sensing with conjugated polymers. The groups of Wang,[110,111] Fujiki,[112] and Swager[113] have reported the synthesis of fluorescent conjugated polymers able to detect fluoride anions, and the group of Schanze studied the sensing of other anionic quenchers.[114] Sensing of neutral compounds have also been investigated.[55,115,116]

The most successful use of these semiconductor material as fluorescent probes has been the design of sensors for the detection of vapors of nitroaromatic explosives such as trinitrotoluene (TNT) and dinitrotoluene (DNT).[5,116] These semiconductive materials have been incorporated into sensors used for ultra-trace explosive detection in the search for hidden landmines. Devices with femtogram detection limits of TNT have been fabricated.[117,118] In addition to fluorescent sensors, conductimetric, potentiometric and colorimetric sensors based on CPs have been studied.[119]

2.3.2 Sol-gel materials

Sol-gel materials encompass a wide number of inorganic and organic/inorganic composite materials which share a common preparation strategy. The sol-gel process is a method for the synthesis of ceramic and glass materials at low temperature. In a typical sol-gel process, a colloidal suspension, or a "sol" is formed via hydrolysis of alkoxy metal groups in the precursors and subsequent polycondensation. The result is a network with a glass-like structure which after the synthesis can be processed to a variety of shapes such as thin films, gels and ceramics.[120] Based on the sol-gel process many different materials can be prepared and envisioned. Fluorescent dyes can be easily incorporated yielding doped glasses with powerful sensing applications.[121] They have good optical properties,[122] lack of spectral interference (transparency and high refractive index), high mechanical and chemical stability, minimal quenching of fluorescence reagents and ease of fabrication. They can be fabricated at low temperatures and this allows the incorporation of organic molecules and polymers, leading to materials with added functionality which cannot be obtained otherwise.[123] Additionally, these materials are obtained from solution, which allows the convenient production of films and bulk materials of any possible shape. A major advantage of the sol-gel method is that it produces porous materials whose pore-size distribution can be controlled by the chemical composition of the starting material and by the processing conditions.[124] Another feature of sol-gels is their excellent adhesion to glass and other silica substrates due to the covalent linkage that is formed with the silanol groups of the glass surface.[125,126]

Organic molecules can be entrapped in a sol-gel matrix while still being accessible from solution. The main problem with these materials is that the diffusion of the analyte to reach the recognition site is very slow. Leaching of the probes is also a big problem when continuous monitoring is needed. The first successful attempt to incorporate organic dyes and stabilize them within a sol-gel was reported in 1984 by Avnir et al.[127]

There are three methods to immobilize fluorophores or indicators in sol-gels.[120] Impregnation, which involves the chemical or physical adsorption on the glass surface, chemical doping incorporation of the dye during the formation of the sol-gel glasses, and covalent immobilization. Sensors made by physical entrapment cannot be used any longer after several weeks because a fraction of the dye molecule is usually leaching into solution.[128,129] More stable sensors are prepared by covalent attachment of the dye to the polymer.[130] Pyrene for oxygen sensitivity,[131] fluorescein isocyanate for fluorometric pH measurements,[130] and ruthenium complexes for oxygen[132,133] or for pH sensing,[134] have been covalently attached to sol-gel glass films. However, doping is actually the most common method for entrapment of the fluorophore in the glass. Some authors have suggested that covalent attachment might compromise the sensor performance by slower response times and smaller signal changes.[135]

Hydrophobic sol-gels based on precursors modified with organic groups, also referred to as ormosils glasses, show low penetration of water that makes them appropriate for sensing of gases. Wolfbeis et al. reported the immobilization of ruthenium complexes on ormosils films and their use for O_2 sensing.[125]

Using a different approach Rosenzweig et al. reported the immobilization of liposomes that encapsulate fluorescent dyes in a sol-gel film.[136] Liposomes are miniaturized containers for fluorescent sensing reagents that form an alternative to covalent conjugation of the fluorescent molecules to phospholipid membranes or dextran chains. The encapsulated fluorophores keep their solution properties, high emission, quantum yield and sensing capability. Carboxyfluorescein was used as a pH sensing reagent because it is easily encapsulated in the liposomes. Encapsulation of the fluorescent probe is an effective way to prevent dye leaking because it increases the size of the dye system and reduces the desorption of the dye from the matrix.[137] In addition to

the incorporation in a sol-gel material, individual loaded liposomes have been used as nanosensors for intracellular pH and molecular oxygen sensing.[138-140]

In 2002 Bright et al. combined sol-gel processing methods with pin printed technologies to fabricate a micrometer-scale xerogel sensor on a planar substrate.[141] Sensor elements on the order of 100 μm in diameter and 1-2 μm thickness at a rate of one sensor element per second and per pin can be made. Arrays of sensor elements for O_2 and pH sensing based on xerogels doped with tris(4,7'-diphenyl-1,10'-phenanthroline)ruthenium(II) and fluorescein, respectively, were fabricated.[142] High reproducibility was obtained for the detection of O_2 and pH changes in aqueous samples. Afterwards the same concept was applied to create pin-printed biosensor arrays based on protein-doped xerogels.[143]

Another study of a pH sensor made by co-polymerized poly(vinyl alcohol) with tetramethoxysilane doped with fluorescein was reported by Werner et al.[144] Special attention was paid to the long-term stability and flexibility of the material.

Nocera et al. showed the integration of optical chemosensors and nanoscience by combination of a supramolecular chemosensor, thin film sol-gel, and microfluidics technologies.[145] They fabricated a microfluidic device based on a fluorescent cyclodextrin modified with a Tb^{3+} macrocycle, which enhances its fluorescence emission upon interaction with biphenyl in aqueous solution. Thin films of the acryloyl polymer of the Tb^{3+}-cyclodextrin complex were immobilized by sol-gel techniques on quartz surfaces patterned by photolithography methods. The thin film showed the same sensing properties as the Tb^{3+}-cyclodextrin complex in solution. Monitoring of the concentration from 5 μM of biphenyl in aqueous solution was successfully performed.[146,147]

By varying the sol-gel processing conditions, molecularly imprinted sol-gel materials (MIP) with controlled porosity and surface area have been prepared. They have been used for separation, catalysis, receptor synthesis, selective adsorption and preconcentration of the template molecules.[148] While molecular imprinted sol-gels have been prepared for several applications,[149] there are only a few reports about fluorescent sensing with molecular imprinted sol-gels. In 2001 Lam et el. reported a fluorescent MIP material fabricated by conventional sol-gel processes which showed enhancement of fluorescence upon interaction with the analyte.[150] The material made by the

polymerization of 3-[N,N-bis(9-anthrylmethyl)amino]propyltriethoxysilane, which acts as a photoinduced electron transfer (PET) monomer, was used for the detection of a non-fluorescent herbicide, 2,4-dichlorophenoxyacetic acid in water (Figure 2.9). This new type of organic-inorganic hybrid MIP showed a significant affinity and selectivity for the analyte in aqueous media. However, the authors concluded that the sensitivity in neutral aqueous solution was not high compared with other MIP materials which are not based on PET.

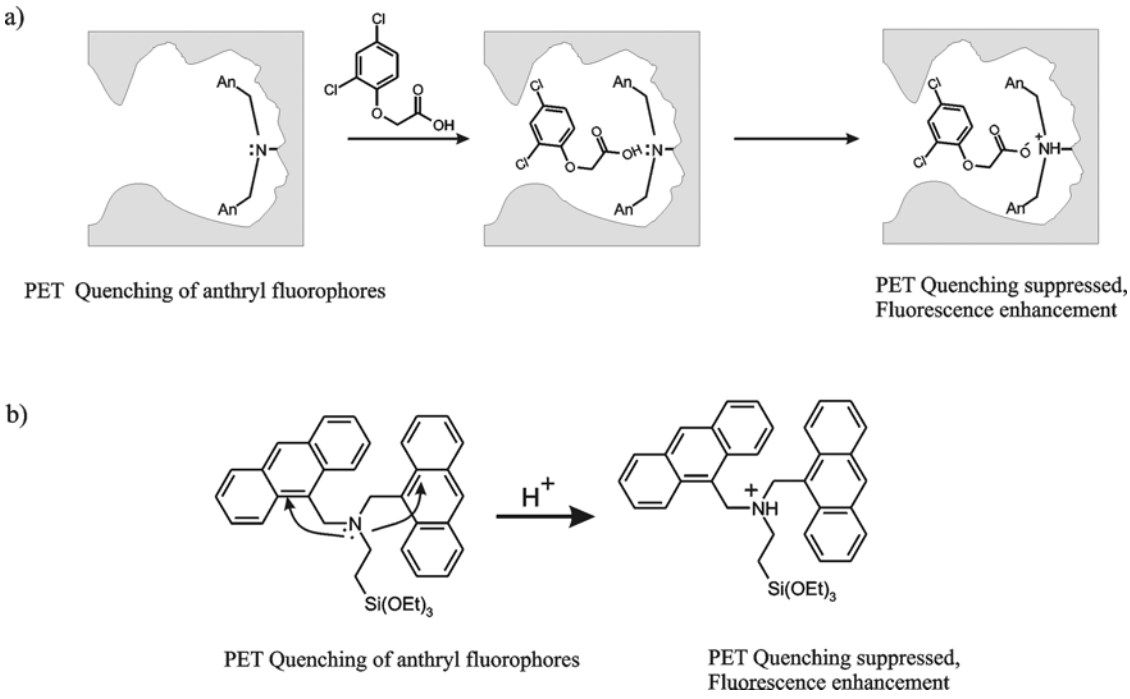

Figure 2.9. *a) Schematic representation of the interaction of 2,4-dichlorophenoxyacetic acid with the binding sites in the sol-gel derived MIP. PET processes lead to fluorescent responses. b) Schematic representation of the PET process in the sensing of the anthrylmethyl monomer.*

A fluorescent molecular imprinted sol-gel for the fluorescent detection of 1,1-bis(4-chlorophenyl)-2,2,2-trichloro-ethane (DDT) in aqueous solutions was reported by Edmiston et al,[151] They used so-called sacrificial spacer molecular imprinting. The template used to generate the binding site for the analyte on the polymer is covalently linked to the polymer. Subsequently, the template is cleaved off and the recognition

pocket is formed. Additionally, a polarity sensitive fluorophore, 7-nitrobenz-2-oxa-1,3-diazol-4-yl (NBD), was incorporated close to the recognition site to signal the binding of the DDT within a imprinted binding pocket. The fluorescence intensity of the NBD dye increases in non polar solvents, so displacement of water or other polar solvent close to the NBD by the analyte results in a fluorescence enhancement.

2.3.3 Mesoporous materials

In 1992 researchers of Mobil Company discovered a new class of silica-based materials, which they called MCM (Mobil Composition of Matter).[152] MCM materials are ordered mesoporous materials which display a honeycomb-like structure of uniform mesopores (3 nm diameter) running through a matrix of amorphous silica. They are the result of using surfactant/block copolymer as a template in sol-gel chemistry. Since the discovery of these materials various routes of functionalizing their inner surface have been reported to yield hybrid materials with improved adsorption, extraction, ion exchange, or catalytic abilities.[153] Due to their high porosity (pore volume 1.0 $mL \cdot g^{-1}$), concomitant large surface area (approximately 1000 $m^2 \cdot g^{-1}$) as well as their facile synthesis and robustness, MCMs are in principle ideally suited as a support material for sensitive probes. Selective functionalization of the exterior and interior surface of structurally uniform mesoporous materials with different organic moieties allows precise regulation of the penetration of selective molecules with certain sizes and chemical properties into the nanoscale pores. The large surface area permits doping them with high concentrations of sensitive probes, and the highly uniform porosity facilitates diffusion making them excellent hosts for sensing molecules or ions.[154] Inner surface monofunctionalization or successive inclusion of different organic moieties can be achieved by co-condensation or post-synthetic covalent grafting of organic compounds[155] yielding higher-order hybrid materials that can be seen as a first step toward “biomimetic”, “enzyme mimicking” or sensitive nanomaterials.[156] From the point of view of engineering optical hybrid materials, microscopic mesoporous siliceous hosts possess the advantage of optical transparency in the visible to UV range, high dye dispersion,

mechanical robustness, and high processability.[157] The main differences with sol-gel glasses are the ordered sequence of surfactant and block copolymer/silica and holes (pores)/silica on the nanometer scale. Sol-gel synthesis of mesoporous silica with functional templates is very attractive for the fabrication of optoelectronic nanocomposite materials.[156]

Applications of these fluorescent mesoporous materials for optical sensing require stability against extraction or leaching of the dye molecules, which can be obtained by the covalent attatchment of dye molecules to these materials. This goal was achieved in 1998 by co-condensation of fluorescently-modified triethoxysilyl anchor groups with tetraethoxysilane (TEOS).[158] Since this success numerous examples have been reported of covalent attachment of functional fluorescent dyes in mesoporous materials either by co-condensation with a fluorescent derivative or attaching the fluorescent dyes to nanosieve surfaces.[159] The first examples of fluorescent mesoporous materials used for optical sensing were reported in 2001.[159] Mesoporous thin films covalently modified with fluorescein dyes showed a very fast response to pH variations. The response time of the thin films is on the order of 7 s for a 95 % change in the emission intensity. The high porosity of the mesoporous thin film facilitates the fast diffusion of the solution towards the dye molecules. Brinker and coworkers fabricated a fluorescent pH sensor using a more elaborate approach involving patterning of surfaces with mesoporous materials.[160] Mesostructures were formed by selective de-wetting of self-assembled monolayer (SAM) modified substrates, followed by covalent modification of the mesoporous material with a fluorescent probe to form a microfluidic system for pH sensing.

The use of hybrid materials, such as the fluorescently modified MCM solids for anion-sensing systems, was demonstrated in 2002 by Martínez-Máñez et al. They showed that the combination of the binding properties of molecular receptors with the structure of the mesoporous materials results in an enhancement of the anion selectivity and sensing response in water.[161] This micro-sized fluorescent probe was made by grafting aminoanthracene groups onto mesoporous silica materials. The amino groups bind ATP anions while the inorganic matrix provides the recognition pocket. Detection limits of 10^{-6} M were obtained. The response of the grafted silica mesoporous material was better than silica membranes with the same functionalization and much better than the response

of the aminoanthracene moiety free in solution. The solids exhibit cooperative effects that resulted in an improvement in ATP response with respect to the free probe in solution. This surface effect may arise from the cooperativity of the confined components of the system and the solid support itself.[162]

Lin et al. synthesized a poly(lactic acid) (PLA) coated, MCM type mesoporous silica nanosphere that served as a fluorescent probe for selective detection of amino-containing neurotransmitters under physiological conditions (Figure 2.10).[163,164] They utilized the PLA layer as a gatekeeper to regulate the penetration of molecules in and out of the nanopores, while monitoring the molecular recognition between the amino-neurotransmitters (dopamine, tyrosine, and glutamic acid) and a surface-anchored *o*-phthalic hemithioacetal (OPTA) group. The OPTA is a non-fluorescent moiety which reacts with these neurotransmitters that contain primary amines, forming a fluorescent isoindole derivative.

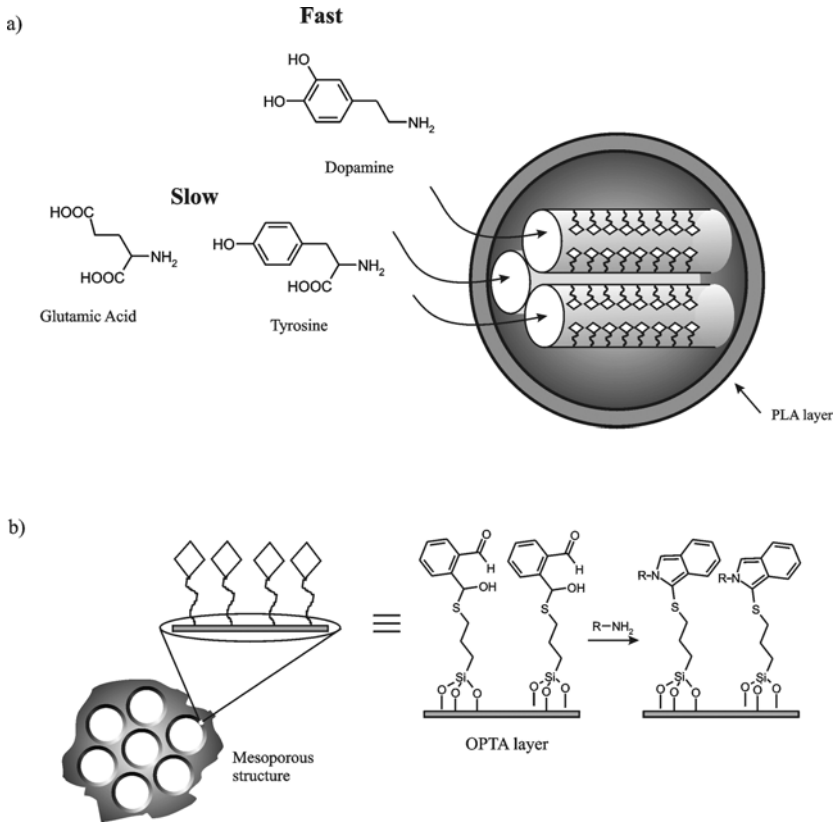

Figure 2.10. *a) Schematic representation of the PLA-coated MCM based fluorescence sensor system for detection of amine-containing neurotransmitters. b) Graphical and molecular representation of the functionalized internal walls of the nanopores.*

Optical sensing of different gas mixtures has been carried out with mesoporous molecular sieves that have covalently anchored rhodamine dyes.[165] The concentration of SO_2 in a gas can be deduced from the quenching of the fluorescence of the dye. Rurack et al. reported recently the synthesis of hybrid optical chemosensor materials for the detection of long-chain carboxylates.[166] The mesoporous material was synthesized by the polymerization of 1-methyl-7-[N'-(triethoxysilyl)propylureido]-3H-phenoxazin-3-one, which is the signaling moiety.

Recently, specific ionophores like calixarenes bearing two dansyl groups have been grafted on large porous silica materials via two long alkyl chains containing triethoxysilane groups to sense Hg^{2+} in water.[167] The material responded reversibly to the presence of Hg^{2+} within a few seconds and displayed a detection limit close to 10^{-7} M. Functionalized mesoporous solids can also act as binding pockets for anion-recognition in water using displacement colorimetric assays.[168] With this method citrate and borate in water with a detection limit of 10^{-5} M was selectively detected.

2.3.4 Surfactant aggregates

In 1987 Wolfbeis et al. published the first fluorescent chemical sensor built in a lipid bilayer.[169] In this example the two parts of a fluorescent probe, fluorophore and receptor, are not covalently linked to each other.[170] Langmuir-Blodgett films containing a lipophilic derivative of a potentiometric fluorophore (Rhodamine-C_{18}-ester) and the K^+ selective ion-carrier valinomycin were prepared and used successfully for selective K^+ sensing.

Nevertheless, the first material where the fluorophore and the receptor are independently covalently attached to a solid substrate was published by Crego-Calama et al.[36] They fabricated new fluorescent self-assembled monolayers on glass for ion sensing (see section 2.3.5) avoiding in this way the leaching of the sensing components.

In 2002 Leblanc and Andreopoulos demonstrated that the disconnection of receptor and fluorophore moiety of a fluorescent sensor could also be applied for lipid bilayers-based fluorescent sensors for Cu^{2+}.[38] This system was based on lipophilic peptides as selective receptors for the metal ions and lipophilic dansyl derivatives. They compared the systems that have receptor and fluorophore covalently bound to the same lipid (***1***, Figure 2.11), to the system with each moiety tailored to individual lipids (***2*** and ***3***, Figure 2.11). In the first case an intermolecular interaction is responsible for the quenching of the fluorescence intensity of the dansyl fluorophore. In the second case, due to the proximity of both receptor and fluorophore after the self-assembly of the lipidic layer, the quenching is due to a through-space interaction. Additionally, the fluorescence quenching properties of the Langmuir monolayers were transferred to the one-layer Langmuir Blodgett (LB) films. The LB films showed sensitivity to Cu^{2+} even in the presence of other metal ions, with a detection limit of 10^{-5}-10^{-6} M.

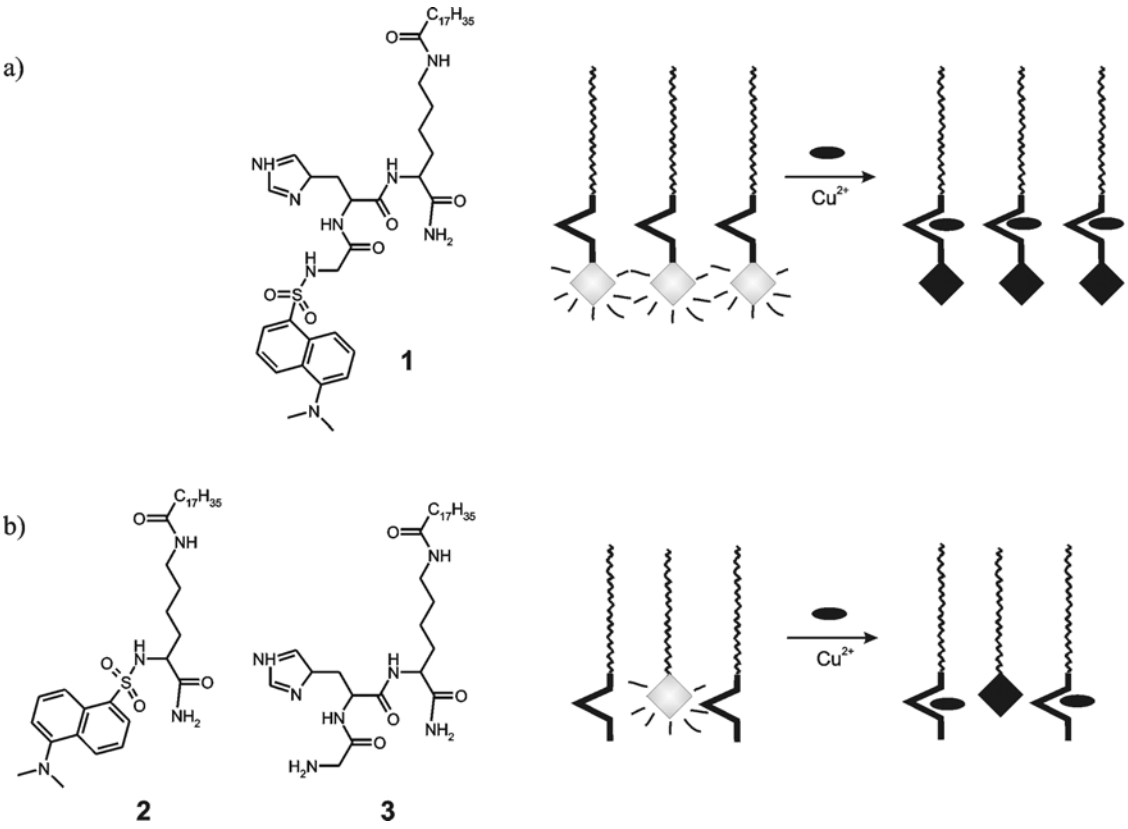

Figure 2.11. *Scheme depicting of the proposed mechanism of the fluorescence quenching of the LB monolayers due to the interaction of the peptide derivate lipids with Cu^{2+} ions. a) Scheme of the intramolecular sensing of Cu^{2+} with the monolayer of lipid **1**. b) Scheme of the intermolecular sensing of Cu^{2+} with the mixed monolayer of lipids **2** and **3**.*

Pallavicini et al. have shown recently that a hydrophobic fluorophore, self-assembled inside a micelle which contains receptor molecules, can act as fluorescent sensing probe for metal ions in water.[171,172] In this approach the receptor is covalently linked to a lipophilic tail which makes it insoluble in water. When the lipophilic receptor derivative is mixed with water containing a suitable amount of surfactant, micelles are formed. A pyrene fluorophore is encapsulated in each micelle by simple addition of the hydrophobic fluorophore to the micellar water solution (Figure 2.12). Binding of a metal cation to the receptor results in quenching of the fluorescence intensity by intramicellar electron-transfer (or energy transfer) processes. These micelles offer a certain degree of freedom since both receptor and fluorophores can be easily varied to create a system with the desired properties.

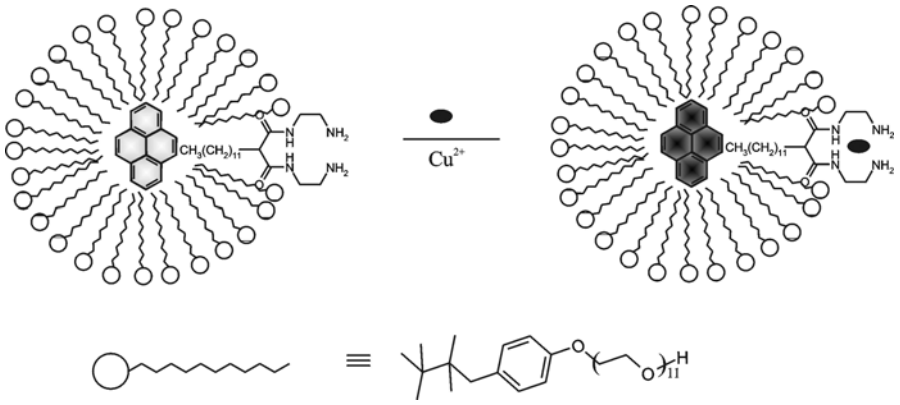

Figure 2.12. *Schematic representation of a sensitive micelle formed by mixing of a neutral surfactant (〰〰○), a selective receptor for divalent cations (dioxo-2,3,2 lipophilized with a linear C12 chain) and pyrene.*

Jalinek et al. reported the selective detection of catecholamines by synthetic receptors embedded in chromatic phospholipid/polydiacetylene (PDA) vesicles.[173] Due to

the conjugated (ene-yne) PDA backbone these vesicles show chromatic properties and fluorescence emission which can change upon surface perturbations.

2.3.5 Glass and gold surfaces

Surface confined chemical sensing offers many advantages over physical entrapped methods of fluorophores in polymers or sol-gels. Surface confinement avoids leaking problems and offers long-term stability. Self-assembled monolayers (SAMs) adsorbed on gold surfaces or covalently bound to silicon oxide surfaces (glass, silicon or quartz) are suitable interfaces for sensing.[174] They produce fast responses since all the receptors are exposed to the surface-liquid interface. Self-assembled monolayers are synthetically flexible so that they can be tailored to be chemically independent, they are cheap, durable and easy to immobilize on the transducer surface.[175] SAMs can be easily and inexpensively manipulated to yield families of materials that provide independent chemical responses in the presence of target analytes.[174] In spite of the fact that different functionalization of SAMs seems to be a convenient method for fabrication of fluorescent chemosensors the realization of such sensors is very rare. SAMs on gold or other metallic surfaces have been extensively applied to chemo- and biosensing by electrochemical methods. The first examples of fluorescent sensing by SAMs used gold as the substrate. But SAMs-based fluorescent sensors development has encountered difficulties due to an efficient fluorescent quenching by the metal surfaces.[176,177] Only a few reports have been published on the detection of fluorescence from self-assembled monolayers on gold. Myles et al. reported in 1998 the preparation of layers of a fluorescent isophthalic acid adsorbate on gold.[178] The binding of barbituric acid derivatives from acetonitrile was detected by a shift of the emission maximum of 15 nm. More recently, Sun et al. have shown a monoboronic acid based self-assembled bilayer (SAB) fluorescent sensor for glucose and other saccharides with nanomolar sensitivity.[179] They fabricated a stable fluorescent self-assembled bilayer on a gold surface using the amino acid cystein and a fluorescent monoboronic acid. After the formation of the cysteine monolayer on the gold

substrate, 3-aminophenylboronic acid (PBA) was assembled on the monolayer via electrostatic interaction with the cysteine (Figure 2.13). They showed that bilayer formation avoided the quenching of the fluorescence of PBA, which was enhanced upon interaction with glucose.[177]

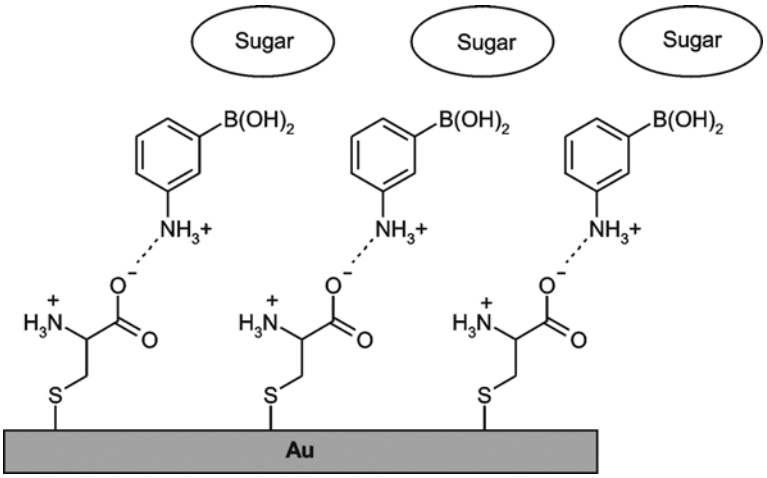

Figure 2.13. *Schematic representation of a self-assembled bilayer sensitive to the presence of sugars.*

Recent developments in the chemistry of SAMs on glass have opened a new possibility for fluorescent chemosensor design. The parts of a fluorescent sensor can be covalently attached to glass, silica and quartz in one or more synthetic steps relying on the ability of trialkoxysilanes or chlorosilanes to react with the hydroxylated surfaces of the substrates and to form self-assembled monolayers (SAMs).[180] Glass does not display the problems of gold (related to fluorescence quenching), it is transparent to light and has been frequently used for fluorescent bioassays for biological studies (protein, DNA microchips, etc…)[181,182] and to prove energy transfer by assembly of donor and acceptor chromophores as mixed monolayers.[183,184]

The first effective sensing systems using covalently bonded dyes to glass were used for pH sensing.[185,186] Almost 20 years ago Wolfbeis[187] et al. reported the covalent immobilization of fluorescent acridinium and quinolinium indicators on a glass surface to create the first optical sensor for halides and pseudohalides. The sensors are able to

indicate the concentration of halides in solution by virtue of the decrease in fluorescence intensity due to the quenching process. Another example of specific sensing probes covalently bound to glass surfaces was reported by Xavier et al.[188] They developed a molecular oxygen sensor in non aqueous media by covalently attaching luminescent Ru(II) complexes via sulfonamide bonds to amino-derivatized porous glass (Figure 2.14). In this very interesting work, the authors outline the influence of the immobilization procedure used for optical sensing in terms of sensitivity and stability. In contrast to physical techniques such as dissolution, adsorption and entrapment in a porous network, covalent immobilization of the luminescent indicator has been probed to increase the long-term stability of the sensitive system. Porous glass materials provide robust non-swelling rigid supports that can be easily modified with a number of chemical reactions. The resulting material displays strong emission above 600 nm, which is effectively quenched by oxygen in both organic solvents and aqueous media, with a detection limit of 6.2 μM.

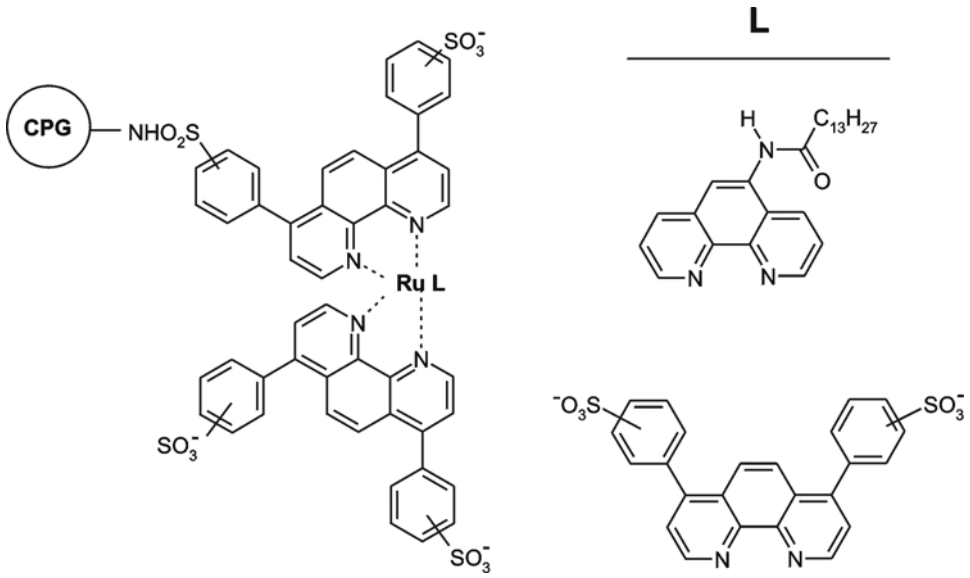

Figure 2.14. *Chemical structures of the controlled pore glass (CPG)-immobilized Ru(II) complexes.*

The first examples of fluorescent sensing on glass using self-assembled monolayers were reported by Reinhoudt et al.[189] They monitored the concentration of an aqueous β-cyclodextrin solution in the millimolar range using a dansyl modified amino-terminated SAM on glass.[189] SAMs of dansyl adsorbates were prepared by attaching a 3-amino-propyltriethoxysilane (APTES) monolayer to a glass plate and converting this layer into the desired dansyl SAM by reaction with dansyl chloride. The selective binding of β-cyclodextrin to the dansyl moieties produces an enhancement of the fluorescence intensity of the monolayer accompanied by a shift of the fluorescence maximum from 510 nm to 480 nm. Soon after another paper from our group reported the covalent attachment of a selective fluorescent calyx[4]arene-based receptor to a SAM for the detection of Na^+ in methanol down to 3.6 μM.[190] This was the first example of the detection of metal ions by fluorescence using a monolayer of a selective receptor. The novelty of this work was that it offers an alternative to physical immobilization of fluoroionophores in membranes. This study proved that the fluoroionophore on the surface functions independently and that the confinement in the monolayer does not affect the complexation behavior. Similar work has been published recently by Wasielewski et al.[191] They attached two identical fluorophores to the upper ring of a calix[4]arene, while the lower ring was functionalized to be attached either directly to a glass surface or to an amino terminated monolayer. Nevertheless, they have not reported the use of this fluorescent monolayer for sensing purposes.

The success of the approaches reported above relies on the synthesis and optimization of highly specific ionophores, which is a difficult and laborious task. Crego-Calama et al. developed a novel approach based on self-assembled monolayers on glass showing for the first time that disconnection between fluorophore and receptor can be applied to preparation of stable sensitive fluorescent materials for metal ion sensing.[36] They used SAMs on glass substrates as a 2D scaffold to impart sufficient molecular orientation to separately deposit various binding functionalities (rather than the entire receptor molecule) and the fluorophore on the surface to achieve analyte selectivity.

Recently, the immobilization of a fluorescent pH sensitive SAM on the glass surface of a microchannel has yielded the first monolayer-functionalized microfluidic devices for optical sensing of pH (Figure 2.15).[192]

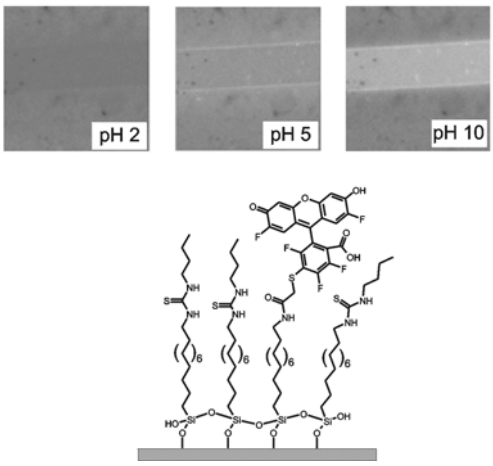

Figure 2.15. *Representation of the composition of a fluorescent pH sensitive monolayer on glass (bottom); confocal microscopy images of a channel with the functionalized glass slide at three different pH values(top). Fluorescence emission intensity increases with the pH.*

π-π Supramolecular interactions have been recently exploited to make sensitive glass surfaces. Raymo et al. have reported the functionalization of glass surfaces (quartz, glass slides and silica particles) with 2,7-diazapyrene derivatives for the detection of catecholamine neurotransmitters as dopamine (Figure 2.16).[193] The association of the 2,7-diazapyrenium acceptors with dopamine donors at the solid liquid interface produces a fluorescent quenching. The layers responded to sub-millimolar concentrations of dopamine and they showed selectivity for dopamine in the presence of ascorbic acid, which is the main interference in conventional dopamine detection protocols. In contrast to polymer-based sensors, the response time of SAMs is normally faster since all the recognition sites are directly exposed to the liquid interface. However, their sensitivity and dynamic range are restricted by the limited number of receptors inherent to a planar surface. Probably in the future new strategies such as functionalization of the monolayers with dendrimers to increase the number of recognition sites[183] will be used.

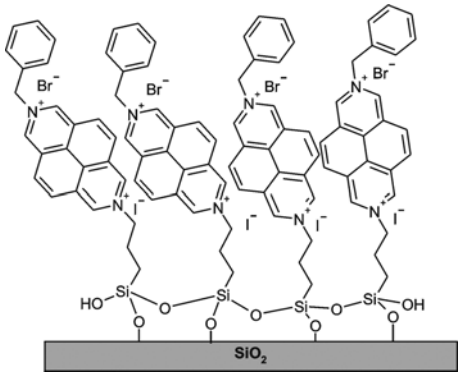

Figure 2.16. *Schematic structure of the dopamine sensitive 2,7-diazapyrenium monolayers on silicon substrates.*

2.3.6 Nanoparticles

There is a trend to miniaturize sensing materials for the production of nanosize sensors, generally in the form of nanoparticles.[194-196] Miniaturization of sensors to nano-dimensions decreases their typical response time down to the millisecond time scale, and exhibits also spatial resolution at the nanometer scale. Due to their small dimensions, typically smaller than 100 nm, nanosensing probes will find applications in intracellular analysis and in the fabrication of high density sensor arrays.[24,72] The photostability of these miniaturized sensors is still a problem despite development of highly sensitive fluorescence detectors and the use of low light levels for excitation.[195]

Fluorescent sensing nanoparticles have been developed based on the attachment of a silanized receptor and silanized fluorophore on the surface of commercial silica colloids,[65] the polymerization of a fluorescent derivative of a silanized receptor,[197,198] and the binding of selective receptors to dye doped polymeric particles[43] or to quantum dots.[199]

2.3.6.1. Silica and polymer-based nanoparticles

Since 1996 when Sasaki et al. demonstrated the employment of a single fluorescent nanoparticle as an optochemical sensor,[200] many groups have devoted their efforts to the design and development of new nanosensors. Sasaki et al. reported a pH-sensitive dye (fluorescein) entrapped in a polyacrylamine nanoparticle that was used to measure the pH distribution in the water glass interface.[200] Modification of silica particles with fluorescent probes for pH sensing was first reported by Soumillon et al.[201] They generated pH sensitive particles by the covalent attachment of an anthracene fluorophore to the surface silica. Recently, Montalti et al. synthesized silica nanoparticles bearing covalently linked luminescent chemosensors and used them for the sensing of Co^{2+}, Cu^{2+}, Ni^{2+} and Pb^{2+} in the nanomolar range.[197,198] The nanoparticles with dimensions between 20 and 50 nm are generated by polymerization of a fluorescein-labeled (3-aminopropyl)triethoxysilane (Figure 2.17). The result is a silica colloid with a high density of fluorescent probes. In this case both the receptor and the fluorophores are coupled in a monomeric chemosensor-like unit as in classical chemosensors. Different photophysical processes can occur in these particles due to the non-homogeneous distribution of the fluorophores. Depending on the distance between the fluorophores, energy transfer and quenching between fluorophores in close proximity are possible.

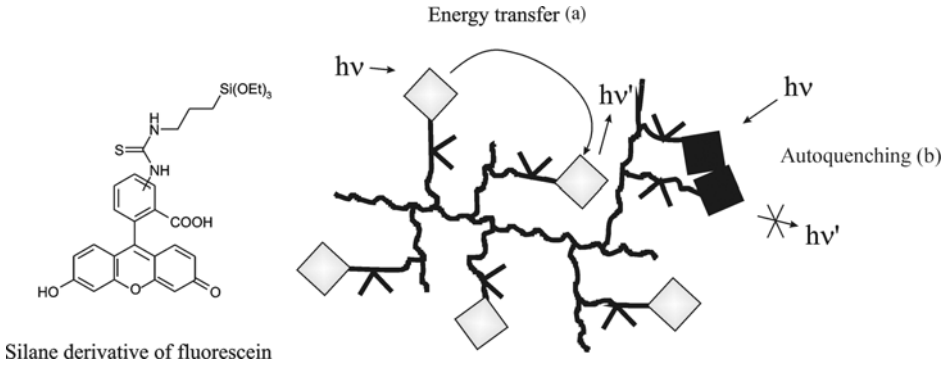

Figure 2.17. *Chemical structure of a silane derivative of fluorescein used to form the polymeric sensitive nanoparticle and a representation of the possible photophysical processes that can occur in the nanoparticles. Both energy transfer between distal fluorophores (a) or autoquenching between adjacent dyes are possible (b).*

Tonellato et al. modified silica nanoparticles via the reaction of commercially available silica nanoparticles with an average size of 18 nm, with a trimethoxysilane derivatized dansylamide as reporter and a picolinamide as Cu^{2+} binding subunit.[65] In this case receptor and fluorophore are not bound together but the spatial proximity is ensured by self-assembly of the sensing elements. The coated silica nanoparticles detected Cu^{2+} selectively down to micromolar concentrations in 9:1 DMSO/water solution. This approach is more versatile than the process of Montalti, since simple combinations of different silanes easily yield nanoparticles with different sensing properties[202] without the need for additional synthesis of fluorescent probes (Figure 2.18).

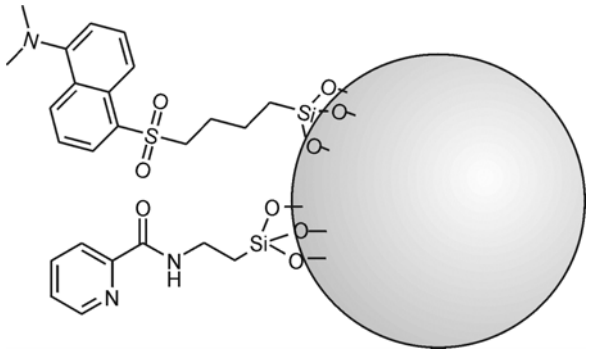

Figure 2.18. *Representation of the self-organized fluorescence chemosensor for Cu^{2+} ions obtained by surface functionalization of silica nanoparticles.*

Similarly, Larpent et al. have reported the synthesis of nanometer-sized polymer nanoparticles in which they associated a BODIPY derivative and cyclam, a metal chelating receptor.[43] The hydrophobic dye is entrapped within the particle core and the receptor is covalently attached to the polymer backbone. The fluorescence intensity of the BODIPY is quenched upon Cu(II) binding to the cyclam ligand. Cooperation of the ligand subunits bound to the particle surfaces may form binding sites with an increased affinity for the substrate.[53,84,202,203]

2.3.6.2. Quantum dots

In the early 1970s, low dimensional heterostructures known as quantum dots (QDs), were developed.[204] They are luminescent semiconductor nanocrystals of CdS or CdSe with exceptional chemical, electrical, and optical properties. Currently they form the basis of most optoelectronic devices and their importance was recognized by the 2000 Nobel Prize in Physics for Alferov and Kroemer. These luminescent particles, also called artificial atoms, have all three dimensions confined to the 1 to 10 nm length scale. As a result of quantum confinement, they have unique optical and electronic properties such as broad excitation spectra and narrow, symmetric and tunable emission spectra. The main advantage of the nanoparticles for the development of fluorescent sensors is that their luminescent emission depends on the size of the particle. Different size results in different color emissions.[205] Typically, their emission maximum is shifted to longer wavelengths with increasing particle diameter. These particles can be excited efficiently at any wavelength shorter than the emission peak yielding the same narrow and symmetric emission spectrum, characteristic of the quantum dot. Therefore, nanocrystals with many different sizes can be excited with a single wavelength of light resulting in many emission colors that may be detected simultaneously.[206] In comparison with single organic fluorophores the QDs are brighter, more resistant to photobleaching and they have a wide range of emission colors. They can be capped with any organic material (a ligand) to modulate their complexing properties.[207,208] They are very sensitive to surface interactions due to the unique discrete electronic state of each particle. Nevertheless, the mechanisms for the quenching or enhancement of luminescence are not yet clear. The discovery of these luminescent nanoparticles has opened the door to a new exciting approach to fluorescent chemical sensing.

In 1998 Bruchez et al. and Chan et al. reported simultaneously the first two QDs functionalized with biomolecules.[206] The resulting nanoparticles were water-soluble and biocompatible and they were used as biological labels to recognize specific antibodies and antigens for use in ultrasensitive biological detection.[209] Since then, QDs-based approaches to fluorescent sensing have been used extensively for biosensing and labeling of biomolecules.[210-212] The application of QDs to fluorescent chemosensing of abiotic

analytes was not demonstrated until 2002 by Rosenzweig et al.[199] They reported the analysis of Cu(II) and Zn(II) ions by CdS luminescent QDs capped with polyphosphate, L-cysteine, and triglycerol as selective probes in aqueous media. Leblanc et al. have synthesized a peptide-coated CdS QD for the detection of Cu(II) and Ag(I) selectively with sensitivity also in the micromolar range.[37] Liang et al. have reported a new type of water soluble CdSe quantum dots modified with mercaptoacetic acid for the quantitative and selective determination of Ag(I).[213] They obtained detection limits down to 10^{-8} M and high selectivity for Ag(I) in the presence of alkali and alkaline earth ions. Recently, a new method for Cu(II) sensing in water with a new kind of functionalized CdTe nanocrystals has been shown.[214] This system offers some extra advantages such as more stability against photobleaching and narrower emission peaks compared with CdS QDs. The narrow emission spectra allow closer spacing of different sensors without spectral overlap, which might be applied for the development of multianalyte detection schemes.

2.3.7 Nanosensors

The field of fluorescent nanosensors has taken advantage of the recent progress in fluorescence imaging instrumentation which makes it possible to detect single fluorescent molecules and therefore to measure the signal changes of fluorescent nanosensors.[24,139]

In 1998, Kopelman et al. prepared a new type of nanosensor named PEBBLEs[215] (Probes Encapsulated by Biologically Localized Embedding). The PEBBLEs are water-soluble polymer nanoparticles (cross-linked polymers as polyacrylamide, poly-decylmethacrylate, sol-gel silica, etc.) with sizes ranging from 30 nm (the 1 ppm of a normal cell's volume) to 600 nm in which fluorescent analyte-sensitive indicator dyes and analyte-insensitive reference dyes are entrapped in order to perform ratiometric measurements. Their small size and their chemically inert matrices enable intracellular non-invasive analysis with fast response times and high spatial resolution. These nanosensors have been used to fabricate H^+, Ca^{2+}, K^+, Zn^{2+}, Cl^-, NO_2^-, O_2, NO and glucose sensors.[64] They show very high selectivity and reversibility, fast response, and reversible detection. They can be used to obtain information from multiple cells at the

same time. Different systems can be created by combining multiple dyes and ionophores inside the polymeric matrix.[216] For example, Kopelman et al. have reported a ratiometric sensor for intracellular oxygen which was made by the inclusion of a ruthenium complex Ru-DPP, (Ru(Il)tris(4,7-diphenyl-1,10-phenanthroline) chloride) and Oregon green in a polymer nanosphere.[217] The fluorescence emission of the ruthenium complex is quenched strongly in the presence of oxygen while the fluorescence of the Oregon green is not affected, thus allowing ratiometric intensity measurements of the oxygen concentration (Figure 2.19).

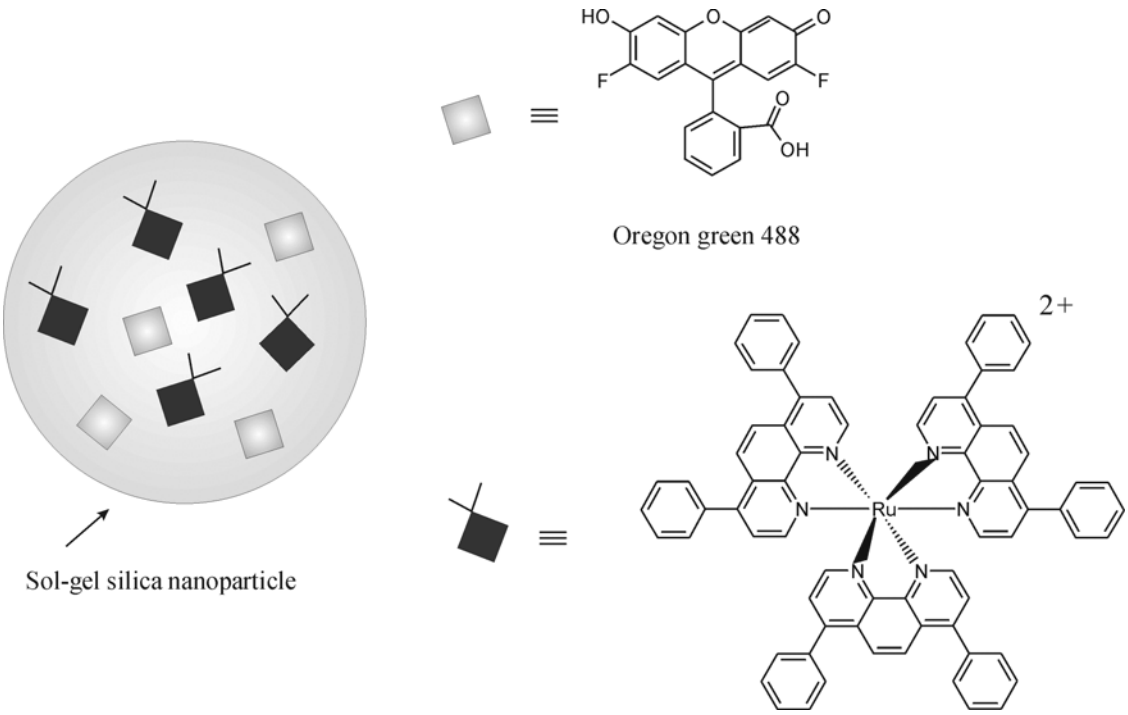

Figure 2.19. *Example of a ratiometric PEBBLE using Ru-DPP sensing dye and Oregon green dye entrapped in a sol-gel silica particle of 20 nm.*

A PEBBLEs nanosensor for intracellular iron (III) sensing has been recently reported.[218] These PEBBLES contain the fluorophore Alexa Fluor 488 as a recognition element and the fluorophore Texas Red as a reference dye in a polyacrylamide matrix. These optical nanosensors have two main benefits: protection of the sensing component

from interfering species within the intracellular environment and protection of the intracellular environment from toxic effects on the sensing component.

Rosenzweig has used liposomes as fluorescent nanosensors[140] for intracellular measurements of pH,[138] Ca^{2+} [219] and O_2.[220] The sensing reagents are encapsulated in the internal aqueous area of the liposomes and they retain their free solution properties. Current research focuses on multi-analyte detection. There is also a large development in the modification of the surfaces of these particles with bioactive molecules for biosensors.[221]

Novel nanostructures such as one-dimensional single-wall carbon nanotubes (SWNTs) appear as highly promising substrates for the development of optical sensors and sensor arrays. They show electrical conductivity comparable to that of conjugated polymers and are sensitive to substances that affect the amount of injected charge.[222] Additionally, they have very good mechanical and thermal properties, and can be tailored with chemically and biologically responsive ligands.[223] Homma reported photoluminescence from individual SWNTs situated in the near-infrared.[224] Quenching of the fluorescence by O_2 absorption was reported by Strano et al.[225] and pH-dependent bleaching has also been observed.[226,227]

2.4. Combinatorial methods for sensing and sensor arrays

The ability of scientists to predict the structural requirements for a perfect fluorescent probe for each analyte is limited and trial and error is still widely used for chemical sensor design.[17] Therefore, combinatorial approaches to both binding and fluorescence building blocks would be powerful if effective library schemes could be invented. The combinatorial concept is based on the relative ease of production of a large number of potential compounds or devices. It is clearly different from the "classical" rational design and individual production of specific targets.[228] It allows the production of a large number of targets, which can be tested to determine successful hits. Linked to a proper screening methodology and data processing, it allows for facile search and

optimization of a target lead structure, e.g. drug discovery, catalysis, bimolecular interaction studies or sensitive probe discovery.[229] Many different types of combinatorial methods have been already employed to obtain new sensitive optical probes.[95,229-237] Solid phase organic synthesis is a well-established tool for the production of combinatorial libraries, but it has been mainly used for drug discovery. Resin bound chemosensors for several analytes have been made by combinatorial methods. Anslyn reported how the split and pool method was used to generate a combinatorial library of more than 4000 different resin bound tripeptides for the discovery of ATP binding receptors. After discovery of the ATP binding receptor, fluorophores were appended to the end of the peptide chains in order to produce a sensing probe.[231] Rivero has reported the use of alkylphosphine sulfide bound resins for Pb^{2+} and Cu^{2+} sensing.[238] Combinatorial chemistry has also been used to improve selectivity in some molecular imprinted polymers.[87] Parallel peptide synthesis was used for a cyclopeptide library attached to a glass surface that works as an amino acid sensor by reflectometric interference spectroscopy.[239] Libraries of fluorescent polymers have been also generated by combinatorial methods by the group of Dordick.[71] They made a sensor array for divalent and trivalent metal ions consisting of fifteen phenolic homopolymers and copolymers generated from five phenolic monomers. The sensing process is based on the change of the intrinsic polyphenol fluorescence upon addition of a metal ion mixture to an aqueous suspension of a polyphenol.

The vast number of targets produced by combinatorial methods creates the need for effective and efficient screening for the hit identification. To this end, surface immobilization and individual addressability of chemical sensing systems are advantageous because they allow for facile analyte sensing to be performed in parallel.[229] For that purpose, platforms have been developed that facilitate high-throughput screening (HTS) technologies, such as microtiter plate or microarray technologies, fiber optic tips, and solid-phase synthesis,[240] originally exploited in the field of biosensors. For instance, Gauglitz et al. have performed a label-free parallel screening of a combinatorial triazine library solid-phase synthesis at the bottom of a microtiterplate.[241] Wolfbeis reported a combinatorial approach for the optimization of hydrogel materials for use in fluorescent

sensing of alkali ions by depositing the sensing layers at the bottom of microtiter plate wells.[242,243]

Combinatorial methods have also been used successfully to generate arrays of nonspecific sensors comprised of partially specific molecular receptors.[228,244] This new approach is inspired by the mammalian olfactory system in which a limited number of not very selective cross-reactive receptors is able to generate a response pattern.[74,245-247] These cross-reactive sensor arrays (artificial noses[248] and tongues[249]) are created such that specificity is distributed across the array's entire reactivity pattern rather than contained in a single recognition element. Such patterns can be then incorporated in an artificial neural network for recognition of mixtures of analytes.[250,251] The first artificial nose was fabricated by Persaud and Dodd and it was based on an array of cross-reactive conjugated polymer sensors.[252] Since then the field of artificial olfaction and gas determination is one of the fastest growing areas in sensing.[253 254]Artificial tongues have been developed for the analysis of liquids.[74,247] The first artificial nose based on organic dyes was reported by Walt et al. in 1996,[255] based on polymer-immobilized dye molecules on optical fiber tips. On exposure to organic vapors different fluorescent response patterns are generated. One year later they reported an improved methodology, which relied on the use of combinatorial methods to generate a library of different polymers.[256] A larger number of elements in a sensor array facilitates the recognition of an analyte or mixture of analytes. The high-density arrays are commonly made by incorporation of micro-sized polymeric beads stained with fluorescent dyes and in the latter case with chemical ionophores in micrometer-sized wells (which can actually go down in size to 250 nm[257]) (Figure 2.20) etched in the fiber core tips. Fiber optic bundles have a miniature feature size (up to 10-micrometer diameter) allowing high-density sensor packing ($2x10^7$ sensors per cm^2). They transmit coherent images enabling combined imaging and sensing, relating the responses monitored by the sensor to observable physical changes.

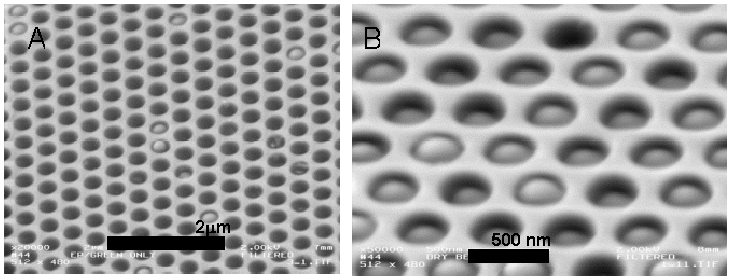

Figure 2.20. *Etched wells in an optical fiber tip filled with nano-spheres, to form a cross reactive sensor array.*

The Walt and Bakker groups have developed high-density microarray optical sensors for explosive-like vapors,[3,71,253] metal ions,[258] and bio-sensors.[259] In a similar approach McDevitt used polystyrene-poly(ethylene glycol) and agarose microspheres arranged in micromachined cavities etched in silicon wafers for analysis of beverages.[249] Indicator molecules are covalently attached to the polymeric microspheres and identification of acids, bases, metal cations, metabolic cofactors, and antibody reagents was done by analysis of the fluorescence or colorimetric changes extracted from digital images obtained with a CCD device.

Crego-Calama et al. have introduced a parallel library generation of fluorescent self-assembled monolayers on glass for ion sensing.[36] Recently Wolfbeis et al. have developed cross reactive sensor arrays in microtiter plate format, in which determination of mixtures of divalent metal ions was performed.[58,260]

2.5 Conclusions and outlook

In this review, a large number of different approaches for the development of fluorescent chemical sensors has been discussed. However, there is still a need of sensors for many different targets. The production of new fluorescent functional materials able to report continuously and reversibly chemical recognition events plays an important role in the development of chemical sensors since the sensor performance depends very much on the properties of the sensory material. Thus, for the successful design of a sensing scheme

the first step is the election of the most suitable material for the target analyte recognition and the device implementation. In this chapter the development of the fluorescent functional materials used for chemical sensing has been reviewed. Many different approaches to the design of these materials are possible due to i) the large variety of substrates e.g. polymers, mesoporous materials, sol-gels, glasses, gold, silica particles, and quantum dots, ii) the variety in the recognition motifs, iii) the probe immobilization methods, iv) the required sensor sizes, and v) the diversity of target analytes. On the other hand, the miniaturization of the sensing probes for the fabrication of non-invasive and non-toxic nanosensors is very important in the field of analytical studies in biosystems.

From the examples published in literature, covalent immobilization of fluorescent probes to several materials has been proven very useful in terms of device implementation because it allows the production of stable and reusable materials. Additionally, combinatorial methods and the fabrication of sensor arrays, either to select the best system or to enhance the performance of non-selective systems by the fabrication of cross-reactive sensor arrays, are paving the way towards efficient sensors. Among the possible substrates, immobilization of the sensing probes on glass surfaces will produce efficient arrays of fluorescent chemosensors because of their simplicity, efficiency and high stability. Similar to protein and DNA microchips, high-density microarray sensors on glass slides for environmental sensing and food control are easily envisioned. Due to the fact that multianalyte sensors and on-line monitoring are requirements for sensor design, microfluidics devices (which so far have been hardly used yet for sensing), appear as a future direction in the development of sensors due to their small size and the possibility of on-line monitoring performance.[192]

Following the original idea of Crego-Calama,[36] a new sensing material for cations and anions based on self-assembled monolayers (SAM) is presented in this thesis. A library of different sensitive substrates is generated by sequential deposition of fluorophores and small ligand molecules onto an amino-terminated SAM coated glass surface. The preorganization provided by the surface avoids the need for complex receptor design, allowing for a combinatorial approach to sensing systems based on individually deposited small molecules. Subsequently, the sensing system has been

miniaturized to the microscale using microcontact printing and integrating the sensory SAMs have been integrated on the walls of microchannels.

2.6 References and Notes

1 B. R. Eggins, *Chemical Sensors and Biosensors (Analytical Techniques in the Sciences)*, Wiley-VCH, ***2002***.

2 H. F. Lodish, *Molecular cell biology*, 5th ed., NY; Freeman, New York ***2004***.

3 Albert, K. J.; Walt, D. R. High-Speed Fluorescence Detection of Explosives-Like Vapors. *Anal. Chem.* ***2000***, 72(9), 1947-1955.

4 Colton, R. J.; Russell, J. N. Making the World a Safer Place. *Science* ***2003***, 299(5611), 1324-1325.

5 Yang, J. S.; Swager, T. M. Fluorescent Porous Polymer Films as TNT Chemosensors: Electronic and Structural Effects. *J. Am. Chem. Soc.* ***1998***, 120(46), 11864-11873.

6 Instrumentation and Sensors for the Food Industry. 2nd Ed. Erika Kress-Rogers and Christopher Brimelow, ***2001***.

7 *Sensors Update*, WILEY-VCH Verlag GmbH & Co. KGaA, Weinheim, ***2003***.

8 Czarnik, A. W. Desperately Seeking Sensors. *Chemistry & Biology* ***1995***, 2 (7), 423-428.

9 Lakowicz, J. R., Topics in Fluorescence Spectroscopy. Kluwer Academic Publishers, New York ***2002***.

10 Lakowicz, J. R., Topics in Fluorescence Spectroscopy, Vol. 4, Probe Desing and Chemical Sensing. Lakowicz, J. R, Kluwer Academic Publishers, New York ***2002***.

11 Lakowicz, J. R., Topics in Fluorescence Spectroscopy. Vol.1, Techniques. Lakowicz, Joseph R. Publication: Kluwer Academic Publishers, New York ***2002***.

12 Irvine, D. J.; Purbhoo, M. A.; Krogsgaard, M.; Davis, M. M. Direct Observation of Ligand Recognition by T Cells. *Nature* ***2002***, 419(6909), 845-849.

13 Pope, A. J.; Haupts, U. M.; Moore, K. J. Homogeneous Fluorescence Readouts for Miniaturized High-Throughput Screening: Theory and Practice. *Drug Discovery Today* ***1999***, 4(8), 350-362.

14 Tsien, R. Y. New Calcium Indicators and Buffers with High Selectivity against Magnesium and Protons: Design, Synthesis, and Porperties of Prototype Structures. *Biochemistry* ***1980***, 19, 2396-2404.

15 Grynkiewicz, G.; Poenie, M.; Tsien, R. Y. A new Generation of Ca^{2+} Indicators with Greatly Improved Fluorescence Properties. *J. Biol. Chem.* ***1985***, 260(6), 3440-3450.

16 Valeur, B.; Leray, I. Design Principles of Fluorescent Molecular Sensors for Cation Recognition. *Coord. Chem. Rev.* ***2000***, 205, 3-40.

17 Bell, J. W.; Hext, N. M. Supramolecular Optical Chemosensors for Organic Analytes. *Chem. Soc. Rev.* ***2004***, 33(9), 589-598.

18 Wolfbeis, O. S. Materials for Fluorescence-based Optical Chemical Sensors. *J. Mater. Chem.* ***2005*** , 15(27-28), 2657-2669.

19 Czarnik, A. W., Fluorescent Chemosensors for Ion and Molecule Recognition, Editor, ACS Books, Washington,***1993***.

20 Steemers, F. J.; Ferguson, J. A.; Walt, D. R. Screening Unlabeled DNA Targets With Randomly Ordered Fiber-Optic Gene Arrays. *Nat. Biotechnol.* ***2000***, 18(1), 91-94.

21 Epstein, J. R.; Biran, I.; Walt, D. R. Fluorescence-Based Nucleic Acid Detection and Microarrays. *Anal. Chim. Acta* ***2002***, 469(1), 3-36.

22 De Lorimier, R. M.; Smith, J. J.; Dwyer, M. A.; Looger, L. L.; Sali, K. M.; Paavola, C. D.; Rizk, S. S.; Sadigov, S.; Conrad, D. W.; Loew, L.; Hellinga, H. W. Construction of a Fluorescent Biosensor Family. *Protein Science* ***2002***, 11(11), 2655-2675.

23 Hellinga, H. W.; Marvin, J. S. Protein Engineering and the Development of Generic Biosensors. *Trends Biotechnol.* ***1998***, 16(4), 183-189.

24 Aylott, J. W. Optical Nanosensors - an Enabling Technology for Intracellular Measurements. *Analyst*

2003, 128(4), 309-312.
25 de Silva, A. P.; Gunaratne, H. Q. N.; Gunnlaugsson, T.; Huxley, A. J. M.; Mccoy, C. P.; Rademacher, J. T.; Rice, T. E. Signaling Recognition Events With Fluorescent Sensors and Switches. *Chem. Rev.* ***1997***, 97(5), 1515-1566.
26 Akkaya, E. U.; Huston, M. E.; Czarnik, A. W. Chelation-Enhanced Fluorescence of Anthrylazamacrocycle Conjugate Probes in Aqueous-Solution. *J. Am. Chem. Soc.* ***1990***, 112(9), 3590-3593.
27 Liu, S. Y.; He, Y. B.; Qing, G. Y.; Xu, K. X.; Qin, H. J. Fluorescent Sensors for Amino Acid Anions Based on Calix[4]Arenes Bearing Two Dansyl Groups. *Tetrahedron: Asymmetry* ***2005***, 16(8), 1527-1534.
28 Meng, L. Z.; Mei, G. X.; He, Y. B.; Zeng, Z. Y. Synthesis and Anion Recognition Properties of Two Novel Tetraamide Calix[4](Aza)Crowns for Optical Anion Sensor. *Acta Chimica Sinica* ***2005***, 63(5), 416-420.
29 Lee, J. Y.; Kim, S. K.; Jung, J. H.; Kim, J. S. Bifunctional Fluorescent Calix[4]Arene Chemosensor for Both a Cation and an Anion. *J. Org. Chem.* ***2005***, 70(4), 1463-1466.
30 Wiskur, S. L.; Ait-Haddou, H.; Lavigne, J. J.; Anslyn, E. V. Teaching Old Indicators New Tricks. *Acc. Chem. Res.* ***2001***, 34(12), 963-972.
31 Tobey, S. L.; Anslyn, E. V. Determination of Inorganic Phosphate in Serum and Saliva Using a Synthetic Receptor. *Org. Lett.* ***2003***, 5(12), 2029-2031.
32 Buryak, A.; Severin, K. An Organometallic Chemosensor for the Sequence-Selective Detection of Histidine- and Methionine-Containing Peptides in Water at Neutral pH. *Angew. Chem., Int. Ed.* ***2004***, 43(36), 4771-4774.
33 Kubo, Y.; Kobayashi, A.; Ishida, T.; Misawa, Y.; James, T. D. Detection of Anions Using a Fluorescent Alizarin-Phenylboronic Acid Ensemble. *Chem. Commun.* ***2005***, (22), 2846-2848.
34 Yoshimura, I.; Miyahara, Y.; Kasagi, N.; Yamane, H.; Ojida, A.; Hamachi, I. Molecular Recognition in a Supramolecular Hydrogel to Afford a Semi-Wet Sensor Chip . *J. Am. Chem. Soc.* ***2004***, 126(39), 12204-12205.
35 Zimmerman, S. C.; Lemcoff, N. G. Synthetic Hosts Via Molecular Imprinting - Are Universal Synthetic Antibodies Realistically Possible? *Chem. Commun.* ***2004***, (1), 5-14.
36 Crego-Calama, M.; Reinhoudt, D. N. New Materials for Metal Ion Sensing by Self-Assembled Monolayers on Glass. *Adv. Mater.* ***2001***, 13(15), 1171-1174.
37 Gattas-Asfura, K. A.; Leblanc, R. M. Peptide-Coated CdS Quantum Dots for the Optical Detection of Copper(II) and Silver(I). *Chem. Commun.* ***2003***, (21), 2684-2685.
38 Zheng, Y.; Orbulescu, J.; Ji, X.; Andreopoulos, F. M.; Pham, S. M.; Leblanc, R. M. Development of Fluorescent Film Sensors for the Detection of Divalent Copper . *J. Am. Chem. Soc.* ***2003***, 125(9), 2680-2686.
39 Aucejo, R.; Alarcon, J.; Soriano, C.; Guillen, M. C.; Garcia-Espańa, E.; Torres, F. New Sensing Devices Part 1: Indole-containing Polyamines Suported in Nanosized Boehmite Particles. *J. Mater. Chem.* ***2005***, 15(27-28), 2920-2927.
40 Wolfbeis, O. S. Fiber-Optic Chemical Sensors and Biosensors. *Anal. Chem.* ***2004***, 76(12), 3269-3283.
41 Potyrailo, R. A.; Hobbs, S. E.; Hieftje, G. M. Optical Waveguide Sensors in Analytical Chemistry: Today's Instrumentation, Applications and Trends for Future Development. *Fresenius. J. Anal. Chem.* ***1998***, 362(4), 349-373.
42 Zourob, M.; Mohr, S.; Fielden, P. R.; Goddard, N. J. An Integrated Disposable Dye Clad Leaky Waveguide Sensor for μ-TAS Applications. *Lab Chip* ***2005***, 5(7), 772-777.
43 Meallet-Renault, R. ; Pansu, R.; Amigoni-Gerbier, S.; Larpent, C. Metal-Chelating Nanoparticles as Selective Fluorescent Sensor for Cu^{2+}. *Chem. Commun.* ***2004***, (20), 2344-2345.
44 Suri, J. T.; Cordes, D. B.; Cappuccio, F. E.; Wessling, R. A.; Singaram, B. Continuous Glucose Sensing With a Fluorescent Thin-Film Hydrogel. *Angew. Chem., Int. Ed.* ***2003***, 42(47), 5857-5859.
45 Lee, S. H.; Kumar, J.; Tripathy, S. K. Thin Film Optical Sensors Employing Polyelectrolyte Assembly. *Langmuir* ***2000***, 16(26), 10482-10489.
46 Adhikari, B.; Majumdar, S. Polymers in Sensor Applications. *Progress in Polymer Science* ***2004***, 29(7), 699-766.
47 Amao, Y. Probes and Polymers for Optical Sensing of Oxygen. *Microchim. Acta* ***2003***, 143(1), 1-12.
48 Albert, K. J.; Gill, S. D.; Pearce, T. C.; Walt, D. R. Automatic Decoding of Sensor Types Within

Randomly Ordered, High-Density Optical Sensor Arrays. *Anal. Bioanal. Chem.* ***2002***, 373(8), 792-802.

49 Dickinson, T. A.; Walt, D. R.; White, J.; Kauer, J. S. Generating Sensor Diversity Through Combinatorial Polymer Synthesis. *Anal. Chem.* ***1997***, 69(17), 3413-3418.

50 Bosch, P.; Catalina, F.; Corrales, T.; Peinado, C. Fluorescent Probes for Sensing Processes in Polymers. *Chem. Eur. J.* ***2005***, 4314-4325.

51 Amao, Y.; Asai, K.; Okura, I.; Shinohara, H.; Nishide, H. Platinum Porphyrin Embedded in Poly(1-Trimethylsilyl-1-Propyne) Film as an Optical Sensor for Trace Analysis of Oxygen. *Analyst* ***2000***, 125(11), 1911-1914.

52 Zhang, Y.; Yang, R. H.; Liu, F.; Li, K. A. Fluorescent Sensor for Imidazole Derivatives Based on Monomer-Dimer Equilibrium of a Zinc Porphyrin Complex in a Polymeric Film. *Anal. Chem.* ***2004***, 76(24), 7336-7345.

53 Doyle, E. L.; Hunter, C. A.; Phillips, H. C.; Webb, S. J.; Williams, N. H. Cooperative Binding at Lipid Bilayer Membrane Surfaces. *J. Am. Chem. Soc.* ***2003***, 125(15), 4593-4599.

54 Qin, W.; Parzuchowski, P.; Zhang, W.; Meyerhoff, M. E. Optical Sensor for Amine Vapors Based on Dimer-Monomer Equilibrium of Indium(III) Octaethylporphyrin in a Polymeric Film. *Anal. Chem.* ***2003***, 75(2), 332-340.

55 Liu, Y.; Mills, R. C.; Boncella, J. M.; Schanze, K. S. Fluorescent Polyacetylene Thin Film Sensor for Nitroaromatics. *Langmuir* ***2001***, 17(24), 7452-7455.

56 Ambrose, T. M.; Meyerhoff, M. E. Optical Ion Sensing With Immobilized Thin Films of Photocrosslinked Decyl Methacrylate. *Anal. Chim. Acta* ***1999***, 378(1-3), 119-126.

57 Shortreed, M. R.; Dourado, S.; Kopelman, R. Development of a Fluorescent Optical Potassium-Selective Ion Sensor With Ratiometric Response for Intracellular Applications. *Sens. Actuators, B* ***1997***, 38(1-3), 8-12.

58 Mayr, T.; Liebsch, G.; Klimant, I.; Wolfbeis, O. S. Multi-Ion Imaging Using Fluorescent Sensors in a Microtiterplate Array Format. *Analyst* ***2002***, 127(2), 201-203.

59 Lin, J. Recent Development and Applications of Optical and Fiber-Optic pH Sensors. *Trac-Trends in Analytical Chemistry* ***2000***, 19(9), 541-552.

60 Weidgans, B. M.; Krause, C.; Klimant, I.; Wolfbeis, O. S. Fluorescent pH Sensors With Negligible Sensitivity to Ionic Strength. *Analyst* ***2004***, 129(7), 645-650.

61 Ceresa, A.; Qin, Y.; Peper, S.; Bakker, E. Mechanistic Insights Into the Development of Optical Chloride Sensors Based on the [9]Mercuracarborand-3 Ionophore. *Anal. Chem.* ***2003***, 75(1), 133-140.

62 Buranda, T.; Huang, J. M.; Perez-Luna, V. H.; Schreyer, B.; Sklar, L. A.; Lopez, G. P. Biomolecular Recognition on Well-Characterized Beads Packed in Microfluidic Channels. *Anal. Chem.* ***2002***, 74(5), 1149-1156.

63 Kermis, H. R.; Kostov, Y.; Harms, P.; Rao, G. Dual Excitation Ratiometric Fluorescent pH Sensor for Noninvasive Bioprocess Monitoring: Development and Application. *Biotechnology Progress* ***2002***, 18(5), 1047-1053.

64 Buck, S. M.; Xu, H.; Brasuel, M.; Philbert, M. A.; Kopelman, R. Nanoscale Probes Encapsulated by Biologically Localized Embedding (PEBBLEs) for Ion Sensing and Imaging in Live Cells. *Talanta* ***2004***, 63(1), 41-59.

65 Brasola, E.; Mancin, F.; Rampazzo, E.; Tecilla, P.; Tonellato, U. A Fluorescence Nanosensor for Cu^{2+} on Silica Particles. *Chem. Commun.* ***2003***, (24), 3026-3027.

66 Wolfbeis, O. S.; Rodriguez, N. V.; Werner, T. Led-Compatible Fluorosensor for Measurement of Near-Neural pH Values. *Mikrochim. Acta* ***1992***, 108(3-6), 133-141.

67 Tanabe, T.; Touma, K.; Hamasaki, K.; Ueno, A. Immobilized Fluorescent Cyclodextrin on a Cellulose Membrane as a Chemosensor for Molecule Detection. *Anal. Chem.* ***2001***, 73(13), 3126-3130.

68 Tanabe, T.; Touma, K.; Hamasaki, K.; Ueno, A. Fluorescent Cyclodextrin Immobilized on a Cellulose Membrane as a Chemosensor System for Detecting Molecules . *Anal. Chem.* ***2001***, 73(8), 1877-1880.

69 Barnard, S. M.; Walt, D. R. A Fiberoptic Chemical Sensor With Discrete Sensing Sites. *Nature* ***1991***, 353(6342), 338-340.

70 Ferguson, J. A.; Healey, B. G.; Bronk, K. S.; Barnard, S. M.; Walt, D. R. Simultaneous Monitoring of pH, CO_2 and O_2 Using an Optical Imaging Fiber. *Anal. Chim. Acta* ***1997***, 340(1-3), 123-131.

71 Epstein, J. R.; Walt, D. R. Fluorescence-Based Fibre Optic Arrays: a Universal Platform for Sensing. *Chem. Soc. Rev.* ***2003***, 32(4), 203-214.

72 Ferguson, J. A.; Steemers, F. J.; Walt, D. R. High-Density Fiber-Optic DNA Random Microsphere Array. *Anal. Chem.* ***2000***, 72(22), 5618-5624.

73 Liu, W. H.; Wang, Y.; Tang, J. H.; Shen, G. L.; Yu, R. Q. Optical Fiber Sensor for Tetracycline Antibiotics Based on Fluorescence Quenching of Covalently Immobilized Anthracene. *Analyst* ***1998***, 123(2), 365-369.

74 Lavigne, J. J.; Savoy, S.; Clevenger, M. B.; Ritchie, J. E.; Mcdoniel, B.; Yoo, S. J.; Anslyn, E. V.; Mcdevitt, J. T.; Shear, J. B.; Neikirk, D. Solution-Based Analysis of Multiple Analytes by a Sensor Array: Toward the Development of an "Electronic Tongue". *J. Am. Chem. Soc.* ***1998***, 120(25), 6429-6430.

75 Kosch, U.; Klimant, I.; Werner, T.; Wolfbeis, O. S. Strategies to Design pH Optodes With Luminescence Decay Times in the Microsecond Time Regime. *Anal. Chem.* ***1998***, 70(18), 3892-3897.

76 Grabchev, I.; Qian, X. H.; Xiao, Y.; Zhang, R. Novel Heterogeneous PET Fluorescent Sensors Selective for Transition Metal Ions or Protons: Polymers Regularly Labelled With Naphthalimide. *New J. Chem.* ***2002***, 26(7), 920-925.

77 Ge, X. D.; Kostov, Y.; Rao, G. High-Stability Non-Invasive Autoclavable Naked Optical CO_2 Sensor. *Biosens. Bioelectron.* ***2003***, 18(7), 857-865.

78 Lopez, E. V.; Luis, G. P.; Suarez-Rodriguez, J. L.; Rivero, I. A.; Diaz-Garcia, M. E. Immobilization of a Boronic Receptor for Fructose Recognition: Influence on the Photoinduced Electron Transfer Process. *Sens. Actuators, B* ***2003***, 90(1-3), 256-263.

79 Balzani, V.; Ceroni, P.; Maestri, M.; Saudan, C.; Vicinelli, V. Luminescent Dendrimers. Recent Advances. *Top. Curr. Chem.*228, 159-191.

80 Balzani, V.; Ceroni, P.; Gestermann, S.; Kauffmann, C.; Gorka, M.; Vogtle, F. Dendrimers as Fluorescent Sensors With Signal Amplification. *Chem. Commun.* ***2000***, (10), 853-854.

81 Pugh, V. J.; Hu, Q. S.; Pu, L. The First Dendrimer-Based Enantioselective Fluorescent Sensor for the Recognition of Chiral Amino Alcohols. *Angew. Chem., Int. Ed.* ***2000***, 39(20), 3638-3641.

82 Pu, L. Synthesis and Study of Binaphthyl-Based Chiral Dendrimers. *J. Photochem. Photobiol., A* ***2003***, 155(1-3), 47-55.

83 Gong, L. Z.; Hu, Q. S.; Pu, L. Optically Active Dendrimers With a Binaphthyl Core and Phenylene Dendrons: Light Harvesting and Enantioselective Fluorescent Sensing. *J. Org. Chem.* ***2001***, 66(7), 2358-2367.

84 Vogtle, F.; Gestermann, S.; Kauffmann, C.; Ceroni, P.; Vicinelli, V.; Balzani, V. Coordination of Co^{2+} Ions in the Interior of Poly(Propylene Amine) Dendrimers Containing Fluorescent Dansyl Units in the Periphery. *J. Am. Chem. Soc.* ***2000***, 122(42), 10398-10404.

85 Grabchev, I.; Chovelon, J. M.; Bojinov, V.; Ivanova, G. Poly(Amidoamine) Dendrimers Peripherally Modified with 4-Ethylamino-1,8-Naphthalimide. Synthesis and Photophysical Properties. *Tetrahedron* ***2003***, 59(48), 9591-9598.

86 Grabchev, I.; Chovelon, J. M.; Qian, X. H. A Polyamidoamine Dendrimer with Peripheral 1,8-Naphthalimide Groups Capable of Acting as a PET Fluorescent Sensor for Metal Cations. *New J. Chem.* ***2003***, 27(2), 337-340.

87 Batra, D.; Shea, K. J. Combinatorial Methods in Molecular Imprinting. *Curr. Opin. Chem. Biol.* ***2003***, 7(3), 434-442.

88 Dickey, F. H. The Preparation of Specific Adsorbents. *Proc. Natl. Acad. Sci. U. S. A.* ***1949***, (35), 227-229.

89 Haupt, K.; Mosbach, K. Molecularly Imprinted Polymers and Their Use in Biomimetic Sensors. *Chem. Rev.* ***2000***, 100(7), 2495-2504.

90 Turkewitsch, P.; Wandelt, B.; Darling, G. D.; Powell, W. S. Fluorescent Functional Recognition Sites Through Molecular Imprinting. A Polymer-Based Fluorescent Chemosensor for Aqueous Camp. *Anal. Chem.* ***1998***, 70(10), 2025-2030.

91 Jenkins, A. L.; Uy, O. M.; Murray, G. M. Polymer-Based Lanthanide Luminescent Sensor for Detection of the Hydrolysis Product of the Nerve Agent Soman in Water. *Anal. Chem.* ***1999***, 71(2), 373-378.

92 Liao, Y.; Wang, W.; Wang, B. H. Building Fluorescent Sensors by Template Polymerization: the Preparation of a Fluorescent Sensor for L-Tryptophan. *Bioorg. Chem.* ***1999***, 27(6), 463-476.

93 Thanh, N. T. K.; Rathbone, D. L.; Billington, D. C.; Hartell, N. A. Selective Recognition of Cyclic GMP Using a Fluorescence-Based Molecularly Imprinted Polymer. *Anal. Lett.* ***2002***, 35(15), 2499-2509.

94 Tong, A. J.; Dong, H.; Li, L. D. Molecular Imprinting-Based Fluorescent Chemosensor for Histamine Using Zinc (II)-Protoporphyrin as a Functional Monomer. *Anal. Chim. Acta* ***2002***, 466(1), 31-37.

95 Wang, W.; Gao, S. H.; Wang, B. H. Building Fluorescent Sensors by Template Polymerization: the Preparation of a Fluorescent Sensor for D-Fructose. *Org. Lett.* ***1999***, 1(8), 1209-1212.

96 Subrahmanyam, S.; Piletsky, S. A.; Piletska, E. V.; Chen, B. N.; Karim, K.; Turner, A. P. F. 'Bite-and-Switch' Approach Using Computationally Designed Molecularly Imprinted Polymers for Sensing of Creatinine. *Biosens. Bioelectron.* ***2001***, 16(9-12), 631-637.

97 Gao, S. H.; Wang, W.; Wang, B. H. Building Fluorescent Sensors for Carbohydrates Using Template-Directed Polymerizations. *Bioorg. Chem.* ***2001***, 29(5), 308-320.

98 Rathbone, D. L.; Su, D. Q.; Wang, Y. F.; Billington, D. C. Molecular Recognition by Fluorescent Imprinted Polymers. *Tetrahedron Lett.* ***2000***, 41(1), 123-126 .

99 Matsui, J.; Higashi, M.; Takeuchi, T. Molecularly Imprinted Polymer as 9-Ethyladenine Receptor Having a Porphyrin-Based Recognition Center. *J. Am. Chem. Soc.* ***2000***, 122(21), 5218-5219.

100 Wandelt, B.; Turkewitsch, P.; Wysocki, S.; Darling, G. D. Fluorescent Molecularly Imprinted Polymer Studied by Time-Resolved Fluorescence Spectroscopy. *Polymer* ***2002***, 43(9), 2777-2785.

101 Zhang, H. Q.; Verboom, W.; Reinhoudt, D. N. 9-(Guanidinomethyl)-10-Vinylanthracene: a Suitable Fluorescent Monomer for Mips. *Tetrahedron Lett.* ***2001***, 42(26), 4413-4416.

102 Kubo, H.; Yoshioka, N.; Takeuchi, T. Fluorescent Imprinted Polymers Prepared With 2-Acrylamidoquinoline as a Signaling Monomer. *Org. Lett.* ***2005***, 7(3), 359-362.

103 Greene, N. T.; Shimizu, K. D. Colorimetric Molecularly Imprinted Polymer Sensor Array Using Dye Displacement. *J. Am. Chem. Soc.* ***2005***, 127(15), 5695-5700.

104 Zhou, Q.; Swager, T. M. Fluorescent Chemosensors Based on Energy Migration in Conjugated Polymers: the Molecular Wire Approach to Increased Sensitivity. *J. Am. Chem. Soc.* ***1995***, 117(50), 12593-12602.

105 Swager, T. M. The Molecular Wire Approach to Sensory Signal Amplification. *Acc. Chem. Res.* ***1998***, 31(5), 201-207.

106 Wang, B.; Wasielewski, M. R. Design and Synthesis of Metal Ion-Recognition-Induced Conjugated Polymers: an Approach to Metal Ion Sensory Materials. *J. Am. Chem. Soc.* ***1997***, 119(1), 12-21.

107 Zhang, Y.; Murphy, C. B.; Jones, W. E. Poly [P-(Phenyleneethynylene)-Alt-(Thienyleneethynylene)] Polymers With Oligopyridine Pendant Groups: Highly Sensitive Chemosensors for Transition Metal Ions. *Macromolecules* ***2002***, 35(3), 630-636.

108 Chen, Z.; Xue, C. H.; Shi, W.; Luo, F. T.; Green, S.; Chen, J.; Liu, H. Y. Selective and Sensitive Fluorescent Sensors for Metal Ions Based on Manipulation of Side-Chain Compositions of Poly(p-Phenyleneethynylene)s. *Anal. Chem.* ***2004***, 76(21), 6513-6518.

109 Crawford, K. B.; Goldfinger, M. B.; Swager, T. M. Na^+ Specific Emission Changes in an Ionaphoric Conjugated Polymer. *J. Am. Chem. Soc.* ***1998***, 120(21), 5187-5192.

110 Tong, H.; Wang, L. X.; Jing, X. B.; Wang, F. S. "Turn-on" Conjugated Polymer Fluorescent Chemosensor for Fluoride Ion. *Macromolecules* ***2003***, 36(8), 2584-2586.

111 Zhou, G.; Cheng, Y. X.; Wang, L. X.; Jing, X. B.; Wang, F. S. Novel Polyphenylenes Containing Phenol-Substituted Oxadiazole Moieties as Fluorescent Chemosensors for Fluoride Ion. *Macromolecules* ***2005***, 38(6), 2148-2153.

112 Saxena, A.; Fujiki, M.; Rai, R.; Kim, S. Y.; Kwak, G. Highly Sensitive and Selective Fluoride Ion Chemosensing, Fluoroalkylated Polysilane. *Macromol. Rapid. Commun.* ***2004***, 25(20), 1771-1775.

113 Kim, T. H.; Swager, T. M. A Fluorescent Self-Amplifying Wavelength-Responsive Sensory Polymer for Fluoride Ions. *Angew. Chem., Int. Ed.* ***2003***, 42(39), 4803-4806.

114 Harrison, B. S.; Ramey, M. B.; Reynolds, J. R.; Schanze, K. S. Amplified Fluorescence Quenching in a Poly(P-Phenylene)-Based Cationic Polyelectrolyte. *J. Am. Chem. Soc.* ***2000***, 122(35), 8561-8562.

115 Naso, F.; Babudri, F.; Colangiuli, D.; Farinola, G. M.; Quaranta, F.; Rella, R.; Tafuro, R.; Valli, L. Thin Film Construction and Characterization and Gas-Sensing Performances of a Tailored Phenylene-Thienylene Copolymer. *J. Am. Chem. Soc.* ***2003***, 125(30), 9055-9061.

116 Sohn, H.; Sailor, M. J.; Magde, D.; Trogler, W. C. Detection of Nitroaromatic Explosives Based on

Photoluminescent Polymers Containing Metalloles. *J. Am. Chem. Soc.* ***2003***, 125(13), 3821-3830.
117 Cumming, C., Fisher, M., Sikes, J., Amplifying Fluorescent Polymer Arrays for Chemical Detection of Explosives. *Electronic Noses and sensors for the Detection of Explosives,* J. W. Gardner and J. Yinon, Eds., Kluwer Academic Publishers, ***2004***, 53 - 70.
118 Cumming, C. J.; Aker, C.; Fisher, M.; Fox, M.; La Grone, M. J.; Reust, D.; Rockley, M. G.; Swager, T. M.; Towers, E.; Williams, V. Using Novel Fluorescent Polymers as Sensory Materials for Above-Ground Sensing of Chemical Signature Compounds Emanating From Buried Landmines. *IEEE Transactions on Geoscience and Remote Sensing* ***2001***, 39(6), 1119-1128.
119 Mcquade, D. T.; Pullen, A. E.; Swager, T. M. Conjugated Polymer-Based Chemical Sensors. *Chem. Rev.* ***2000***, 100(7), 2537-2574.
120 Schulz-Ekloff, G.; Wohrle, D.; Van Duffel, B.; Schoonheydt, R. A. Chromophores in Porous Silicas and Minerals: Preparation and Optical Properties. *Microporous Mesoporous Mater.* ***2002***, 51(2), 91-138.
121 Reisfeld, R. Fluorescent Dyes in Sol-Gel Glasses. *Journal of Fluorescence* ***2002***, 12(3-4), 317-325.
122 Sanchez, C.; Lebeau, B.; Chaput, F.; Boilot, J. P. Optical Properties of Functional Hybrid Organic-Inorganic Nanocomposites. *Adv. Mater.* ***2003***, 15(23), 1969-1994.
123 Loy, D. A.; Shea, K. J. Bridged Polysilsesquioxanes - Highly Porous Hybrid Organic-Inorganic Materials. *Chem. Rev.* ***1995***, 95(5), 1431-1442.
124 Sanchez, C.; Soler-Illia Gjda; Ribot, F.; Lalot, T.; Mayer, C. R.; Cabuil, V. Designed Hybrid Organic-Inorganic Nanocomposites From Functional Nanobuilding Blocks. *Chem. Mater.* ***2001***, 13(10), 3061-3083.
125 Klimant, I.; Ruckruh, F.; Liebsch, G.; Stangelmayer, C.; Wolfbeis, O. S. Fast Response Oxygen Micro-Optodes Based on Novel Soluble Ormosil Glasses. *Mikrochim. Acta* ***1999***, 131(1-2), 35-46.
126 Lebeau, B.; Fowler, C. E.; Mann, S.; Farcet, C.; Charleux, B.; Sanchez, C. Synthesis of Hierarchically Ordered Dye-Functionalised Mesoporous Silica With Macroporous Architecture by Dual Templating. *J. Mater. Chem.* ***2000***, 10(9), 2105-2108.
127 Avnir, D.; Levy, D.; Reisfeld, R. The Natural Silica Glass Cage as Reflected by Spectral Changes and Enhaced Photostability of Trapped Rhodamine 6G. *J. Phys. Chem.*88, 5956-5959.
128 Plaschke, M.; Czolk, R.; Ache, H. J. Fluorometric-Determination of Mercury With a Water-Soluble Porphyrin and Porphyrin-Doped Sol-Gel Films. *Anal. Chim. Acta* ***1995***, 304(1), 107-113.
129 Maccraith, B. D.; Mcdonagh, C. M.; Okeeffe, G.; Mcevoy, A. K.; Butler, T.; Sheridan, F. R. Sol-Gel Coatings for Optical Chemical Sensors and Biosensors. *Sens. Actuators, B* ***1995***, 29(1-3), 51-57.
130 Badini, G. E.; Grattan, K. T. V.; Tseung, A. C. C. Impregnation of a pH-Sensitive Dye Into Sol-Gels for Fiber Optic Chemical Sensors. *Analyst* ***1995***, 120(4), 1025-1028.
131 Zilberstein, J.; Bromberg, A.; Berkovic, G. Fluorescence Study of Pyrene Chemically Bound to Controlled-Pore Glasses. *J. Photochem. Photobiol., A* ***1994***, 77(1), 69-81.
132 Okeeffe, G.; Maccraith, B. D.; Mcevoy, A. K.; Mcdonagh, C. M.; Mcgilp, J. F. Development of a LED-Based Phase Fluorometric Oxygen Sensor Using Evanescent-Wave Excitation of a Sol-Gel Immobilized Dye. *Sens. Actuators, B* ***1995***, 29(1-3), 226-230.
133 Malins, C.; Fanni, S.; Glever, H. G.; Vos, J. G.; Maccraith, B. D. The Preparation of a Sol-Gel Glass Oxygen Sensor Incorporating a Covalently Bound Fluorescent Dye. *Anal. Commun.* ***1999***, 36(1), 3-4.
134 Malins, C.; Glever, H. G.; Keyes, T. E.; Vos, J. G.; Dressick, W. J.; Maccraith, B. D. Sol-Gel Immobilised Ruthenium(II) Polypyridyl Complexes as Chemical Transducers for Optical pH Sensing. *Sens. Actuators, B* ***2000***, 67(1-2), 89-95.
135 Lobnik, A.; Oehme, I.; Murkovic, I.; Wolfbeis, O. S. pH Optical Sensors Based on Sol-Gels: Chemical Doping Versus Covalent Immobilization. *Anal. Chim. Acta* ***1998***, 367(1-3), 159-165.
136 Nguyen, T.; McNamara, K. P.; Rosenzweig, Z. Optochemical Sensing by Immobilizing Fluorophore-Encapsulating Liposomes in Sol-Gel Thin Films. *Anal. Chim. Acta* ***1999***, 400, 45-54.
137 Jaeger, K. E.; Reetz, M. T. Microbial Lipases Form Versatile Tools for Biotechnology. *Trends Biotechnol.* ***1998***, 16(9), 396-403.
138 McNamara, K. P.; Nguyen, T.; Dumitrascu, G.; Ji, J.; Rosenzweig, N.; Rosenzweig, Z. Synthesis, Characterization, and Application of Fluorescence Sensing Lipobeads for Intracellular pH Measurements. *Anal. Chem.* ***2001***, 73(14), 3240-3246.
139 Lu, J. Z.; Rosenzweig, Z. Nanoscale Fluorescent Sensors for Intracellular Analysis. *Fresenius. J. Anal. Chem.* ***2000***, 366(6-7), 569-575.

140 McNamara, K. P.; Rosenzweig, N.; Rosenzweig, Z. Liposome-Based Optochemical Nanosensors. *Mikrochim. Acta* ***1999***, 131(1-2), 57-64.

141 Cho, E. J.; Bright, F. V. Integrated Chemical Sensor Array Platform Based on a Light Emitting Diode, Xerogel-Derived Sensor Elements, and High-Speed Pin Printing. *Anal. Chim. Acta* ***2002***, 470(1), 101-110.

142 Cho, E. J.; Bright, F. V. Pin-Printed Chemical Sensor Arrays for Simultaneous Multianalyte Quantification. *Anal. Chem.* ***2002***, 74(6), 1462-1466.

143 Cho, E. J.; Tao, Z. Y.; Tehan, E. C.; Bright, F. V. Multianalyte Pin-Printed Biosensor Arrays Based on Protein-Doped Xerogels. *Anal. Chem.* ***2002***, 74(24), 6177-6184.

144 Cajlakovic, M.; Lobnik, A.; Werner, T. Stability of New Optical pH Sensing Material Based on Cross-Linked Poly(Vinyl Alcohol) Copolymer. *Anal. Chim. Acta* ***2002***, 455(2), 207-213.

145 Haider, J. M.; Pikramenou, Z. Photoactive Metallocyclodextrins: Sophisticated Supramolecular Arrays for the Construction of Light Activated Miniature Devices. *Chem. Soc. Rev.* ***2005***, 34(2), 120-132.

146 Rudzinski, C. M.; Young, A. M.; Nocera, D. G. A Supramolecular Microfluidic Optical Chemosensor. *J. Am. Chem. Soc.* ***2002***, 124(8), 1723-1727.

147 Wun, A. W.; Snee, P. T.; Chan, YT.; Bawendi, M. G.; Nocera, D. G. Non-linear Transduction Stratergies for Chemo/biosensing on Small Length Scales. *J. Mater. Chem.* ***2005***, 15(27-28), 2697-2706.

148 Lu, Y. K.; Yan, X. P. Preparation and Application of Molecularly Imprinted Sol-Gel Materials. *Chin. J. Anal. Chem.* ***2005***, 33(2), 254-260.

149 Diaz-Garcia, M. E.; Laino, R. B. Molecular Imprinting in Sol-Gel Materials: Recent Developments and Applications. *Microchim. Acta* ***2005***, 149(1-2), 19-36 .

150 Leung, M. K. P.; Chow, C. F.; Lam, M. H. W. A Sol-Gel Derived Molecular Imprinted Luminescent PET Sensing Material for 2,4-Dichlorophenoxyacetic Acid. *J. Mater. Chem.* ***2001***, 11(12), 2985-2991.

151 Graham, A. L.; Carlson, C. A.; Edmiston, P. L. Development and Characterization of Molecularly Imprinted Sol-Gel Materials for the Selective Detection of DDT. *Anal. Chem.* ***2002***, 74(2), 458-467.

152 Kresge, C. T.; Leonowicz, M. E.; Roth, W. J.; Vartuli, J. C.; Beck, J. S. Ordered Mesoporous Molecular-Sieves Synthesized by a Liquid-Crystal Template Mechanism. *Nature* ***1992***, 359(6397), 710-712.

153 Möller, K.; Bein, T. Inclusion Chemistry in Periodic Mesoporous Hosts. *Chem. Mater.* ***1998***, 10(10), 2950-2963.

154 Shi, J. L.; Hua, Z. L.; Zhang, L. X. Nanocomposites from Ordered Mesoporous Materials. *J. Mater. Chem.* ***2004***, 14(5), 795-806.

155 Zhang, Q. M.; Ariga, K.; Okabe, A.; Aida, T. A Condensable Amphiphile With a Cleavable Tail as a "Lizard" Template for the Sol-Gel Synthesis of Functionalized Mesoporous Silica. *J. Am. Chem. Soc.* ***2004***, 126(4), 988-989.

156 Huh, S.; Wiench, J. W.; Trewyn, B. G.; Song, S.; Pruski, M.; Lin, V. S. Y. Tuning of Particle Morphology and Pore Properties in Mesoporous Silicas With Multiple Organic Functional Groups. *Chem. Commun.* ***2003***, (18), 2364-2365.

157 Scott, B. J.; Wirnsberger, G.; Stucky, G. D. Mesoporous and Mesostructured Materials for Optical Applications. *Chem. Mater.* ***2001***, 13(10), 3140-3150.

158 Pellegrino, T.; Kudera, S.; Liedl, T.; Javier, A. M.; Manna, L.; Parak, W. J. On the Development of Colloidal Nanoparticles Towards Multifunctional Structures and Their Possible Use for Biological Applications. *Small* ***2005***, 1(1), 48-63.

159 Wirnsberger, G.; Scott, B. J.; Stucky, G. D. pH Sensing With Mesoporous Thin Films. *Chem. Commun.* ***2001***, (01), 119-120.

160 Fan, H. Y.; Lu, Y. F.; Stump, A.; Reed, S. T.; Baer, T.; Schunk, R.; Perez-Luna, V.; Lopez, G. P.; Brinker, C. J. Rapid Prototyping of Patterned Functional Nanostructures. *Nature* ***2000***, 405(6782), 56-60.

161 Descalzo, A. B.; Jimenez, D.; Marcos, M. D.; Martínez-Máñez, R.; Soto, J.; El Haskouri, J.; Guillem, C.; Beltran, D.; Amoros, P.; Borrachero, M. V. A New Approach to Chemosensors for Anions Using MCM-41 Grafted With Amino Groups. *Adv. Mater.* ***2002***, 14(13-14), 966-969.

162 Descalzo, A. B.; Marcos, M. D.; Martínez-Máñez, R.; Soto, J.; Beltran, D.; Amoros, P. Anthrylmethylamine Functionalised Mesoporous Silica-based Materials as Hybrid Fluorescent

Chemosensors for ATP. *J. Mater. Chem.* ***2005***, 15(27-28), 2965-2973.
163 Lin, V. S. Y.; Lai, C. Y.; Huang, J. G.; Song, S. A.; Xu, S. Molecular Recognition Inside of Multifunctionalized Mesoporous Silicas: Toward Selective Fluorescence Detection of Dopamine and Glucosamine. *J. Am. Chem. Soc.* ***2001***, 123(46), 11510-11511.
164 Radu, D. R.; Lai, C. Y.; Wiench, J. W.; Pruski, M.; Lin, V. S. Y. Gatekeeping Layer Effect: a Poly(Lactic Acid)-Coated Mesoporous Silica Nanosphere-Based Fluorescence Probe for Detection of Amino-Containing Neurotransmitters. *J. Am. Chem. Soc.* ***2004***, 126(6), 1640-1641.
165 Wark, M.; Rohlfing, Y.; Altindag, Y.; Wellmann, H. Optical Gas Sensing by Semiconductor Nanoparticles or Organic Dye Molecules Hosted in the Pores of Mesoporous Siliceous MCM-41. *Phys. Chem. Chem. Phys.* ***2003***, 5(23), 5188-5194.
166 Descalzo, A. B.; Rurack, K.; Weisshoff, H.; Martínez-Máñez, R.; Marcos, M. D.; Amoros, P.; Hoffmann, K.; Soto, J. Rational Design of a Chromo- and Fluorogenic Hybrid Chemosensor Material for the Detection of Long-Chain Carboxylates. *J. Am. Chem. Soc.* ***2005***, 127(1), 184-200.
167 Metivier, R.; Leray, I.; Lebau, B.; Valeur, B. A Mesoporous Silica Functionalized by a Covalently Bound Calixarene-based Fluoroionophore for Selctive Optical Sensing of Mercury(II) in Water. *J. Mater. Chem.* ***2005***, 15(27-28), 2965-2973.
168 Comes, M.; Rodriguez-Lopez, G.; Marcos, M. D.; Martínez-Máñez, R.; Sancenon, F.; Soto, J.; Villaescusa, L. A.; Amoros, P.; Beltran, D. Host Solids Containing Nanoscale Anion-Binding Pockets and Their Use in Selective Sensing Displacement Assays. *Angew. Chem., Int. Ed.* ***2005***, 44(19), 2918-2922.
169 Wolfbeis, O. S.; Schaffar, B. P. H. Optical Sensor: an Ion-selective Optrode for Potassium. *Anal. Chim. Acta* ***1987***, 1-12.
170 Grandini, P.; Mancin, F.; Tecilla, P.; Scrimin, P.; Tonellato, U. Exploiting the Self-Assembly Strategy for the Design of Selective Cu(II) Ion Chemosensors. *Angew. Chem., Int. Ed.* ***1999***, 38(20), 3061-3064.
171 Fernandez, Y. D.; Gramatges, A. P.; Amendola, V.; Foti, F.; Mangano, C.; Pallavicini, P.; Patroni, S. Using Micelles for a New Approach to Fluorescent Sensors for Metal Cations. *Chem. Commun.* ***2004***, (14), 1650-1651.
172 Diaz-Fernandez, Y.; Perez-Gramatges, A.; Rodriguez-Calvo, S.; Mangano, C.; Pallavicini, P. Structure and Dynamics of Micelle-Based Fluorescent Sensor for Transition Metals. *Chem. Phys. Lett.* ***2004***, 398(1-3), 245-249.
173 Kolusheva, S.; Molt, O.; Herm, M.; Schrader, T.; Jelinek, R. Selective Detection of Catecholamines by Synthetic Receptors Embedded in Chromatic Polydiacetylene Vesicles. *J. Am. Chem. Soc.* ***2005***, 127.
174 Crooks, R. M.; Ricco, A. J. New Organic Materials Suitable for Use in Chemical Sensor Arrays. *Acc. Chem. Res.* ***1998***, 31(5), 219-227.
175 Chechik, V.; Crooks, R. M.; Stirling, C. J. M. Reactions and Reactivity in Self-Assembled Monolayers. *Adv. Mater.* ***2000***, 12(16), 1161-1171.
176 Dulkeith, E.; Morteani, A. C.; Niedereichholz, T.; Klar, T. A.; Feldmann, J.; Levi, S. A.; Van Veggel, F. C. J. M.; Reinhoudt, D. N.; Möller, M.; Gittins, D. I. Fluorescence Quenching of Dye Molecules Near Gold Nanoparticles: Radiative and Nonradiative Effects. *Physical Review Letters* ***2002***, 89(20).
177 Imahori, H.; Norieda, H.; Nishimura, Y.; Yamazaki, I.; Higuchi, K.; Kato, N.; Motohiro, T.; Yamada, H.; Tamaki, K.; Arimura, M.; Sakata, Y. Chain Length Effect on the Structure and Photoelectrochemical Properties of Self-Assembled Monolayers of Porphyrins on Gold Electrodes. *J. Phys. Chem. B* ***2000***, 104(6), 1253-1260.
178 Motesharei, K.; Myles, D. C. Molecular Recognition in Membrane Mimics - a Fluorescence Probe. *J. Am. Chem. Soc.* ***1994***, 116(16), 7413-7414.
179 Sun, X. Y.; Liu, B.; Jiang, Y. B. An Extremely Sensitive Monoboronic Acid Based Fluorescent Sensor for Glucose. *Anal. Chim. Acta* ***2004***, 515(2), 285-290 .
180 Sullivan, T. P.; Huck, W. T. S. Reactions on Monolayers: Organic Synthesis in Two Dimensions. *Eur. J. Org. Chem.* ***2003***, (1), 17-29.
181 Panicker, R. C.; Huang, X.; Yao, S. Q. Recent Advances in Peptide-Based Microarray Technologies. *Comb. Chem. High Throughput Screening* ***2004***, 7(6), 547-556.
182 Walsh, D. P.; Chang, Y. T. Recent Advances in Small Molecule Microarrays: Applications and Technology. *Comb. Chem. High Throughput Screening* ***2004***, 7 (6), 557-564.

183 Adronov, A.; Robello, D. R.; Frechet, J. M. J. Light Harvesting and Energy Transfer Within Coumarin-Labeled Polymers. *J. Polym. Sci., Part A: Polym. Chem.* ***2001***, 39(9), 1366-1373.

184 Chrisstoffels, L. A. J.; Adronov, A.; Frechet, J. M. J. Surface-Confined Light Harvesting, Energy Transfer, and Amplification of Fluorescence Emission in Chromophore-Labeled Self-Assembled Monolayers. *Angew. Chem., Int. Ed.* ***2000***, 39(12), 2163-2167.

185 Saari, L. A.; Seitz, W. R. *Anal. Chem.* ***1982***, 54, 821.

186 Harper, B. G. *Anal. Chem.* ***1975***, 47, 348.

187 Urbano, E.; Offenbacher, H.; Wolfbeis, O. S. Optical Sensor for Continuous Determination of Halides. *Anal. Chem. Abstract* ***1984***, 56, 427-429.

188 Xavier, M. P.; Garcia-Fresnadillo, D.; Moreno-Bondi, M. C.; Orellana, G. Oxygen Sensing in Nonaqueous Media Using Porous Glass With Covalently Bound Luminescent Ru(II) Complexes. *Anal. Chem.* ***1998***, 70(24), 5184-5189.

189 Flink, S.; Van Veggel, F. C. J. M.; Reinhoudt, D. N. A Self-Assembled Monolayer of a Fluorescent Guest for the Screening of Host Molecules. *Chem. Commun.* ***1999***, (21), 2229-2230.

190 Van der Veen, N. J.; Flink, S.; Deij, M. A.; Egberink, R. J. M.; Van Veggel, F. C. J. M.; Reinhoudt, D. N. Monolayer of a Na^+-Selective Fluoroionophore on Glass: Connecting the Fields of Monolayers and Optical Detection of Metal Ions. *J. Am. Chem. Soc.* ***2000***, 122(25), 6112-6113.

191 Van der Boom, T.; Evmenenko, G.; Dutta, P.; Wasielewski, M. R. Self-assembly of Photofunctional Siloxane-based Calix[4]arene on Oxide Surfaces. *Chem. Mater.* ***2005***, 15, 4068-4074.

192 Mela, P.; Onclin, S.; Goedbloed, M. H.; Levi, S.; García-Parajó, M. F.; Van Hulst, N. F.; Ravoo, B. J.; Reinhoudt, D. N.; Van den Berg, A. Monolayer-Functionalized Microfluidics Devices for Optical Sensing of Acidity. *Lab Chip* ***2005***, 5(2), 163-170.

193 Cejas, M. A.; Raymo, F. M. Fluorescent Diazapyrenium Films and Their Response to Dopamine. *Langmuir* ***2005***, 21, 5795-5802.

194 Nath, N.; Chilkoti, A. Label Free Colorimetric Biosensing Using Nanoparticles. *Journal of Fluorescence* ***2004***, 14(4), 377-389.

195 Shi, J. J.; Zhu, Y. F.; Zhang, X. R.; Baeyens, W. R. G.; Garcia-Campana, A. M. Recent Developments in Nanomaterial Optical Sensors. *Trac-Trends in Analytical Chemistry* ***2004***, 23(5), 351-360.

196 Drechsler, U.; Erdogan, B.; Rotello, V. M. Nanoparticles: Scaffolds for Molecular Recognition. *Chem. Eur. J.* ***2004***, 10(22), 5570-5579.

197 Montalti, M.; Prodi, L.; Zaccheroni, N. Fluorescence quenching amplification in silica nanosensors for metal ions. *J. Mater. Chem.* ***2005***, 15(27-28), 2810-2814.

198 Montalti, M.; Prodi, L.; Zacheroni, N.; Zattoni, A.; Reschiglian, P.; Falini, G. Energy Transfer in Fluorescent Silica Nanoparticles. *Langmuir* ***2004***, 20(7), 2989-2991.

199 Chen, Y. F.; Rosenzweig, Z. Luminescent CdS Quantum Dots as Selective Ion Probes. *Anal. Chem.* ***2002***, 74(19), 5132-5138.

200 Sasaki, K.; Shi, Z. Y.; Kopelman, R.; Masuhara, H. Three-Dimensional pH Microprobing With an Optically-Manipulated Fluorescent Particle. *Chem. Lett.* ***1996***, (2), 141-142.

201 Ayadim, M.; Jiwan, J. L. H.; de Silva, A. P.; Soumillion, J. P. Photosensing by a Fluorescing Probe Covalently Attached to the Silica. *Tetrahedron Lett.* ***1996***, 37(39), 7039-7042.

202 Rampazzo, E.; Brasola, E.; Marcuz, S.; Mancin, F.; Tecilla, P.; Tonellato, U. Surface modification of silica nanoparticles: a new stratergy for the realization of self-organized fluorescence chemosensors. *J. Mater. Chem.* ***2005***, 15(27-28), 2687-2696.

203 Major, R. C.; Zhu, X. Y. The Surface Chelate Effect. *J. Am. Chem. Soc.* ***2003***, 125(28), 8454-8455.

204 .
Jacak, L., Hawrylak, P.,Wojs, A., *Quantum Dots*, Springer, Germany, ***1998***.

205 Lakowicz, J. R.; Gryczynski, I.; Gryczynski, Z.; Murphy, C. J. Luminescence Spectral Properties of CdS Nanoparticles. *J. Phys. Chem. B* ***1999***, 103(36), 7613-7620.

206 Bruchez, M.; Moronne, M.; Gin, P.; Weiss, S.; Alivisatos, A. P. Semiconductor Nanocrystals as Fluorescent Biological Labels. *Science* ***1998***, 281(5385), 2013-2016.

207 Kalyuzhny, G.; Murray, R. W. Ligand Effects on Optical Properties of CdSe Nanocrystals. *J. Phys. Chem. B* ***2005***, 109(15), 7012-7021.

208 Lin, Z. B.; Su, X. G.; Mu, Y.; Jin, Q. H. Methods for Labeling Quantum Dots to Biomolecules. *J. Nanosci. Nanotechno.* ***2004***, 4(6), 641-645.

209 Chan, W. C. W.; Nie, S. M. Quantum Dot Bioconjugates for Ultrasensitive Nonisotopic Detection.

Science ***1998***, 281(5385), 2016-2018.
210 Wang, L.; Wang, L. Y.; Zhu, C. Q.; Wei, X. W.; Kan, X. W. Preparation and Application of Functionalized Nanoparticles of CdS as a Fluorescence Probe. *Anal. Chim. Acta* ***2002***, 468(1), 35-41.
211 Michalet, X.; Pinaud, F.; Lacoste, T. D.; Dahan, M.; Bruchez, M. P.; Alivisatos, A. P.; Weiss, S. Properties of Fluorescent Semiconductor Nanocrystals and Their Application to Biological Labeling. *Single Molecules* ***2001***, 2(4), 261-276.
212 Wang, L. Y.; Wang, L.; Gao, F.; Yu, Z. Y.; Wu, Z. M. Application of Functionalized CdS Nanoparticles as Fluorescence Probe in the Determination of Nucleic Acids. *Analyst* ***2002***, 127(7), 977-980.
213 Liang, J. G.; Ai, X. P.; He, Z. K.; Pang, D. W. Functionalized CdSe Quantum Dots as Selective Silver Ion Chemodosimeter. *Analyst* ***2004***, 129(7), 619-622.
214 Bo, C.; Ping, Z. A New Determining Method of Copper(II) Ions at $ng \cdot ml^{-1}$ Levels Based on Quenching of the Water-Soluble Nanocrystals Fluorescence. *Anal. Bioanal. Chem.* ***2005***, 381(4), 986-992.
215 Clark, H. A.; Barker, S. L. R.; Brasuel, M.; Miller, M. T.; Monson, E.; Parus, S.; Shi, Z. Y.; Song, A.; Thorsrud, B.; Kopelman, R.; Ade, A.; Meixner, W.; Athey, B.; Hoyer, M.; Hill, D.; Lightle, R.; Philbert, M. A. Subcellular Optochemical Nanobiosensors: Probes Encapsulated by Biologically Localised Embedding (PEBBLEs). *Sens. Actuators, B* ***1998***, 51(1-3), 12-16.
216 Buck, S. M.; Koo, Y. E. L.; Park, E.; Xu, H.; Philbert, M. A.; Brasuel, M. A.; Kopelman, R. Optochemical Nanosensor PEBBLEs: Photonic Explorers for Bioanalysis With Biologically Localized Embedding. *Curr. Opin. Chem. Biol.* ***2004***, 8(5), 540-546.
217 Xu, H.; Aylott, J. W.; Kopelman, R.; Miller, T. J.; Philbert, M. A. A Real-Time Ratiometric Method for the Determination of Molecular Oxygen Inside Living Cells Using Sol-Gel-Based Spherical Optical Nanosensors With Applications to Rat C6 Glioma. *Anal. Chem.* ***2001***, 73(17), 4124-4133.
218 Sumner, J. P.; Kopelman, R. Alexa Fluor 488 as an Iron Sensing Molecule and Its Application in PEBBLE Nanosensors. *Analyst* ***2005***, 130(4), 528-533.
219 Nguyen, T.; Rosenzweig, Z. Calcium Ion Fluorescence Detection Using Liposomes Containing Alexa-Labeled Calmodulin. *Anal. Bioanal. Chem.* ***2002***, 374(1), 69-74.
220 McNamara, K. P.; Rosenzweig, Z. Dye-Encapsulating Liposomes as Fluorescence-Based Oxygen Nanosensors. *Anal. Chem.* ***1998***, 70(22), 4853-4859.
221 Ma, A. H.; Rosenzweig, Z. Synthesis and Analytical Properties of Micrometric Biosensing Lipobeads. *Anal. Bioanal. Chem.* ***2005***, 382(1), 28-36.
222 Baughman, R. H.; Zakhidov, A. A.; De Heer, W. A. Carbon Nanotubes - the Route Toward Applications. *Science* ***2002***, 297(5582), 787-792.
223 Wong, S. S.; Joselevich, E.; Woolley, A. T.; Cheung, C. L.; Lieber, C. M. Covalently Functionalized Nanotubes as Nanometre-Sized Probes in Chemistry and Biology. *Nature* ***1998***, 394(6688), 52-55.
224 Lefebvre, J.; Fraser, J. M.; Finnie, P.; Homma, Y. Photoluminescence From an Individual Single-Walled Carbon Nanotube. *Phys. Rev. B* ***2004***, 69(7).
225 Strano, M. S.; Huffman, C. B.; Moore, V. C.; O'connell, M. J.; Haroz, E. H.; Hubbard, J.; Miller, M.; Rialon, K.; Kittrell, C.; Ramesh, S.; Hauge, R. H.; Smalley, R. E. Reversible, Band-Gap-Selective Protonation of Single-Walled Carbon Nanotubes in Solution. *J. Phys. Chem. B* ***2003***, 107(29), 6979-6985.
226 Dukovic, G.; White, B. E.; Zhou, Z. Y.; Wang, F.; Jockusch, S.; Steigerwald, M. L.; Heinz, T. F.; Friesner, R. A.; Turro, N. J.; Brus, L. E. Reversible Surface Oxidation and Efficient Luminescence Quenching in Semiconductor Single-Wall Carbon Nanotubes. *J. Am. Chem. Soc.* ***2004***, 126(46), 15269-15276.
227 Barone, P. W.; Baik, S.; Heller, D. A.; Strano, M. S. Near-Infrared Optical Sensors Based on Single-Walled Carbon Nanotubes. *Nature Materials* ***2005***, 4(1), 86-116.
228 Lavigne, J. J.; Anslyn, E. V. Sensing a Paradigm Shift in the Field of Molecular Recognition: From Selective to Differential Receptors. *Angew. Chem., Int. Ed.* ***2001***, 40(17), 3119-3130.
229 Gauglitz, G. Optical Detection Methods for Combinatorial Libraries. *Curr. Opin. Chem. Biol.* ***2000***, 4(3), 351-355.
230 Szurdoki, F.; Ren, D. H.; Walt, D. R. A Combinatorial Approach to Discover New Chelators for Optical Metal Ion Sensing. *Anal. Chem.* ***2000***, 72(21), 5250-5257.
231 Schneider, S. E.; O'neil, S. N.; Anslyn, E. V. Coupling Rational Design With Libraries Leads to the

Production of an ATP selective Chemosensor. *J. Am. Chem. Soc.* ***2000***, 122(3), 542-543.
232 Iorio, E. J.; Shao, Y. F.; Chen, C. T.; Wagner, H.; Still, W. C. Sequence-Selective Peptide Detection by Small Synthetic Chemosensors Selected From an Encoded Combinatorial Chemosensor Library. *Bioorg. Med. Chem. Lett.* ***2001***, 11(13), 1635-1638.
233 Chen, C. T.; Wagner, H.; Still, W. C. Fluorescent, Sequence-Selective Peptide Detection by Synthetic Small Molecules. *Science* ***1998***, 279(5352), 851-853.
234 Hioki, H.; Kubo, M.; Yoshida, H.; Bando, M.; Ohnishi, Y.; Kodama, M. Synthesis of Fluorescence-Labeled Peptidocalix[4]arene Library and Its Peptide Sensing Ability. *Tetrahedron Lett.* ***2002***, 43(44), 7949-7952.
235 Davis, C. J.; Lewis, P. T.; Mccarroll, M. E.; Read, M. W.; Cueto, R.; Strongin, R. M. Simple and Rapid Visual Sensing of Saccharides. *Org. Lett.* ***1999***, 1 (2), 331-334.
236 James, T. D.; Sandanayake Kras; Shinkai, S. Saccharide Sensing With Molecular Receptors Based on Boronic Acid. *Angew. Chem., Int. Ed. Engl.* ***1996***, 35(17), 1911-1922.
237 Lu, Y.; Liu, J. W.; Li, J.; Bruesehoff, P. J.; Pavot, C. M. B.; Brown, A. K. New Highly Sensitive and Selective Catalytic DNA Biosensors for Metal Ions. *Biosens. Bioelectron.* ***2003***, 18(5-6), 529-540.
238 Castillo, M.; Rivero, I. A. Combinatorial Synthesis of Fluorescent Trialkylphosphine Sulfides as Sensor Materials for Metal Ions of Environmental Concern. *Arkivoc* ***2003***, 193-202.
239 Leipert, D.; Nopper, D.; Bauser, M.; Gauglitz, G.; Jung, G. Investigation of the Molecular Recognition of Amino Acids by Cyclopeptides With Reflectometric Interference Spectroscopy. *Angew. Chem., Int. Ed.* ***1998***, 37(23), 3308-3311.
240 Havrilla, G. J.; Miller, T. C. High-Throughput Screening With Micro-X-Ray Fluorescence. *Rev. Sci. Instrum.* ***2005***, 76(6).
241 Birkert, O.; Tunnernann, R.; Jung, G.; Gauglitz, G. Label-Free Parallel Screening of Combinatorial Triazine Libraries Using Reflectometric Interference Spectroscopy. *Anal. Chem.* ***2002***, 74(4), 834-840.
242 Chojnacki, P.; Werner, T.; Wolfbeis, O. S. Combinatorial Approach Towards Materials for Optical Ion Sensors. *Microchim. Acta* ***2004***, 147(1-2), 87-92 .
243 Apostolidis, A.; Klimant, I.; Andrzejewski, D.; Wolfbeis, O. S. A Combinatorial Approach for Development of Materials for Optical Sensing of Gases. *J. Comb. Chem* ***2004***, 6(3), 325-331.
244 Schwabacher, A. W.; Johnson, C. W.; Geissinger, P. Linear Combinatorial Synthesis With Fourier Transform Library Analysis. *Macromol. Rapid. Commun.* ***2004***, 25(1), 108-118.
245 Lundstrom, I. Artificial Noses - Picture the Smell. *Nature* ***2000***, 406(6797), 682-683.
246 Stopfer, M.; Jayaraman, V.; Laurent, G. Intensity Versus Identity Coding in an Olfactory System. *Neuron* ***2003***, 39(6), 991-1004.
247 Rakow, N. A.; Suslick, K. S. Novel Materials and Applications of Electronic Noses and Tongues (Vol 406, Pg 710, 2000). *Mrs Bulletin* ***2004***, 29(12), 913.
248 Dickinson, T. A.; White, J.; Kauer, J. S.; Walt, D. R. Current Trends in 'artificial-Nose' Technology. *Trends Biotechnol.* ***1998***, 16(6), 250-258.
249 Goodey, A.; Lavigne, J. J.; Savoy, S. M.; Rodriguez, M. D.; Curey, T.; Tsao, A.; Simmons, G.; Wright, J.; Yoo, S. J.; Sohn, Y.; Anslyn, E. V.; Shear, J. B.; Neikirk, D. P.; Mcdevitt, J. T. Development of Multianalyte Sensor Arrays Composed of Chemically Derivatized Polymeric Microspheres Localized in Micromachined Cavities. *J. Am. Chem. Soc.* ***2001***, 123(11), 2559-2570.
250 Bishop, C. M., *Neural Networks for Pattern Recognition,* Bishop, C. M, Oxford University Press: Oxford, U.K. ***1995***.
251 Lyons, W. B.; Lewis, E. Neural Networks and Pattern Recognition Techniques Applied to Optical Fibre Sensors. *Trans. Inst. Measurm. Control* ***2000***, 22(5), 385-404.
252 Persaud, K.; Dodd, G. Analysis of Discrimination Mechanisms in the Mammalian Olfactory System Using a Model Nose. *Nature* ***1982***, 299, 352-355.
253 Albert, K. J.; Lewis, N. S.; Schauer, C. L.; Sotzing, G. A.; Stitzel, S. E.; Vaid, T. P.; Walt, D. R. Cross-Reactive Chemical Sensor Arrays. *Chem. Rev.* ***2000***, 100(7), 2595-2626.
254 James, D.; Scott, S. M.; Ali, Z.; O'hare, W. T. Chemical Sensors for Electronic Nose Systems. *Microchim. Acta* ***2005***, 149(1-2), 1-17.
255 Dickinson, T. A.; White, J.; Kauer, J. S.; Walt, D. R. A Chemical-Detecting System Based on a Cross-Reactive Optical Sensor Array. *Nature* ***1996***, 382(6593), 697-700.
256 Dickinson, T. A.; Walt, D. R.; White, J.; Kauer, J. S. Generating Sensor Diversity Through Combinatorial Polymer Synthesis. *Anal. Chem.* ***1997***, 69(17), 3413-3418.

257 Pantano, P.; Walt, D. R. Ordered Nanowell Arrays. *Chem. Mater.* ***1996***, 8(12), 2832-2835.
258 Wygladacz, K.; Bakker, E. Imaging Fiber Microarray Fluorescent Ion Sensors Based on Bulk Optode Microspheres. *Anal. Chim. Acta* ***2005***, 532(1), 61-69.
259 Biran, I.; Rissin, D. M.; Ron, E. Z.; Walt, D. R. Optical Imaging Fiber-Based Live Bacterial Cell Array Biosensor. *Anal. Biochem.* ***2003***, 315(1), 106-113 .
260 Mayr, T.; Igel, C.; Liebsch, G.; Klimant, I.; Wolfbeis, O. S. Cross-Reactive Metal Ion Sensor Array in a Micro Titer Plate Format. *Anal. Chem.* ***2003***, 75(17), 4389-4396.

Chapter 3

Self-Assembled Monolayers on Glass; A Combinatorial Approach to Sensor Discovery *

Self-assembled monolayers (SAMs) on glass are used as a platform to sequentially deposit fluorophores and small molecules for ion sensing. The preorganization provided by the surface avoids the need for complex receptor design, allowing for a combinatorial approach to sensing systems based on small molecules. The resulting libraries are easily screened, and show varied responses to a series both of cations and anions in organic solvents.

* This chapter has been published in: Basabe-Desmonts, L.; Beld, J.; Zimmerman, R. S.; Hernando, J.; Mela, P.; García Parajó, M. F.; Van Hulst N. F.; Van der Berg A.; Reinhoudt, D. N.; Crego-Calama, M.; *J. Am. Chem Soc.* ***2004***, *126*, (23), 7293-7299

3.1. Introduction

The importance of chemical sensing of ions and small organic molecules is obvious for different areas such as medical diagnostics, environmental monitoring, and the food industry. Surface-confinement of chemical systems has facilitated the process of sensor testing. A device which allows for facile, simultaneous, multiple analyte sensing is a microsensor array. Microsensor arrays, comprised of spatially addressable ensembles of different receptors on such varied platforms as polymer supports, agarose beads or glass slides, allow for rapid assessment of targets with a desired catalytic or biological activity.[1] This strategy has been widely used for biological purposes that need rapid screening such as determining enzyme activity,[2] recognizing DNA sequences,[3] and characterizing monosaccharide solutions.[4] Microarray technology has also been introduced for chemical sensing, as evidenced by the rapid development of electronic tongues[5,6] and noses.[7] Unlike biologically based arrays, which rely on the highly specific and selective interactions between substrates and targets, the few examples of chemical arrays are based on what is known as differential sensing. Here the individual sensors are not designed to complex one unique analyte, but rather are intended to be generally responsive through less specific interactions to a range of analytes.[8,9]

The inherent strength of microarrays is enhanced by combining the technology with combinatorial chemistry. The use of combinatorial chemistry to generate microarrays has resulted in a broad range of DNA,[10] protein,[11] antibody,[12] and peptide[13] microarrays on surfaces such as optical fiber tips, microbeads and microwells.[1] The generation of small molecule arrays for the purpose of ion sensing, however, has thus far been limited to polymer-immobilized dye molecules.[14,15]

By combining the use of combinatorial chemistry with the generation of small molecule microarrays, we have developed an effective, simple, and new methodology for the production of fluorescent surface sensing systems. This methodology is comprised of randomly functionalized self-assembled monolayers (SAMs) with different complexing functionalities and fluorophores on a glass substrate. The approach combines the advantages imparted by such factors as: (a) a combinatorial approach to the generation of sensing surfaces, (b) label-free analytes and binding groups, (c) determination of receptor

"hits" without deconvolution, (d) no need for a complicated analytical interface, and (e) the potential for high throughput screening. As a proof of principle, we have fabricated simple sensing systems capable of selective detection of metal cations and inorganic anions in organic solvents.

SAMs have successfully been used to demonstrate that the molecular recognition process is feasible at the monolayer solution interface.[16-18] The advantages of SAMs for surface-confined sensing are fast response times, ease and reproducibility of synthesis,[17] and the introduction of additional chelating effects from the preorganization of the surface platform.[19] Thus SAMs on a glass substrate are used as a 2D scaffold to impart sufficient molecular orientation to make it possible to separately deposit various binding functionalities (rather than the entire receptor molecule)[20] and the fluorophore on the surface to achieve analyte selectivity (Figure 3.1).

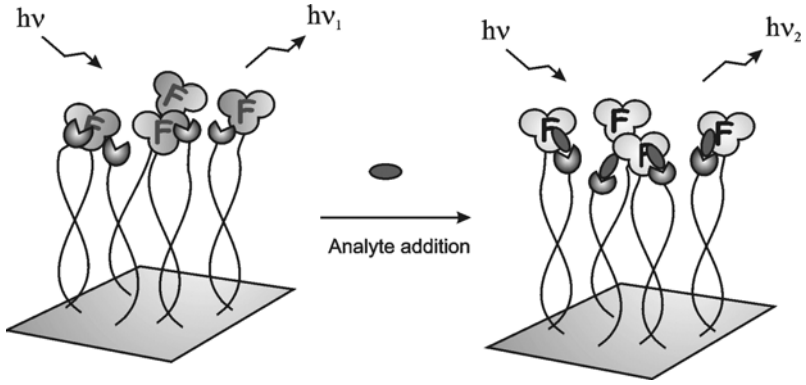

Figure 3.1. *Schematic representation of a fluorescent sensitive monolayer (SAM) on a glass surface. The sensitive fluorescent monolayer comprises a monolayer modified with fluorophores (F) and the binding molecules. In the presence of an analyte the fluorescence emission of the SAM changes due to interaction of the analyte with the layer.*

The phenomenon of proximal but spatially separable receptor-fluorophore communication has been recorded in solution by Tonellato et al.[21] Fluorescence detection is particularly desirable due to its high sensitivity and sub millisecond temporal resolution, but it has hardly ever been used to determine host-guest interactions at the monolayer surface, mainly because most of the systems designed so far have been on

gold, which causes quenching of the fluorescence.[22-24] Glass, however, is an appropriate substrate for the purpose of fluorescent detection of chemical sensing, as demonstrated by Reinhoudt et al.[20]

The directional preorganization inherent in the SAM as well as random lateral distribution brings the binding groups and fluorophores in close enough proximity that the binding group-analyte interaction is communicated to the fluorophore, resulting in a modulation of the fluorescence intensity. The monolayers can be considered as an enormous macromolecule with an infinite number of sensitive binding pockets and reporters. In contrast to the traditional design of molecular receptors as chemical sensors based on geometric and electronic complementarity of the fluorophore-appended host to match that of the guest, our method avoids the design and the laborious synthetic efforts necessary to both label the receptor (and/or the analyte) and to obtain binding selectivity.

3.2. Results and discussion

3.2.1. Synthesis of the fluorescent monolayer libraries

To explore the broad scope of this approach regarding component variability, two small libraries[†] of fluorescent sensitive monolayers were made on SiO_2 surfaces for cation and anion sensing. Monolayers were made on two types of SiO_2 substrates, quartz and silicon wafers for fluorescence sensing and characterization of the layers respectively. Each monolayer of the library constitutes a sensor system, and each sensor system is comprised of an amino terminated SAM tailored with two building blocks, small molecules that supply different functionalities acting as binding groups (ureas, amides, thioureas, sulfonamides, etc..) and fluorescent probes (pH independent long excitation wavelength fluorophores, Lissamine, TAMRA and TRITC[*], Chart 1.1) for

[†] The term library refers to a collection of individual quartz slides, being each one functionalized with a different sensing system.

[*] Lissamine rhodamine B sulfonyl chloride, 5-(and-6)-carboxytetramethylrhodamine, succinimidyl ester (5(6)-TAMRA, SE), tetramethylrhodamine-5-(and-6)- isothiocyanate (5(6)-TRITC)

reporting the recognition event. In this way a large number of different sensing monolayers can be fabricated by making different binary combinations of the building blocks.

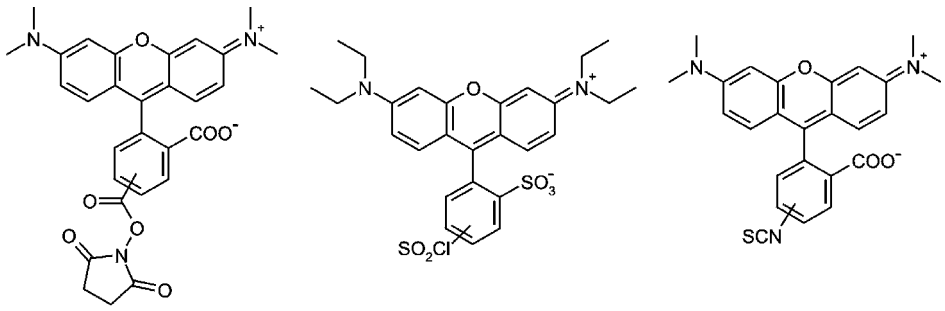

Chart 1.1. *Chemical structures of the fluorophores TAMRA, Lissamine and TRITC.*

The synthesis of the monolayers is depicted in Scheme 3.1. A three-step procedure was followed. First an amino terminated monolayer ***TPEDA*** is formed by silylation of the quartz slides and the silicon wafers with (N-[3-(trimethoxysilyl)propyl]ethylenediamine). Subsequently this layer is converted into a fluorescent-SAM by reaction with an amino reactive fluorescent probe.

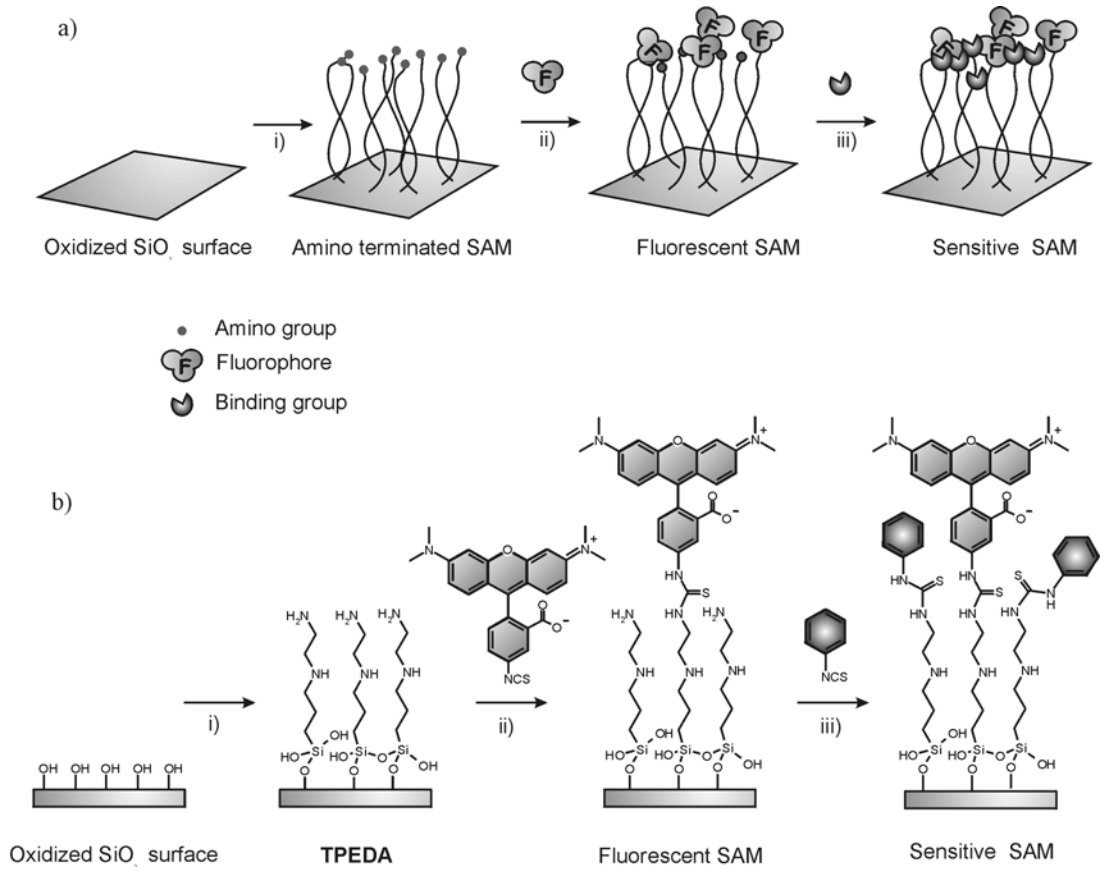

Scheme 3.1. *General schematic cartoon (a), and chemical structures (b) of the fabrication procedure of a fluorescent sensitive monolayer on glass: i) Silanation of the glass slide with N-[3-(trimethoxysilyl)propyl]ethylenediamine to form the amino terminated monolayer* ***TPEDA,*** *ii) reaction with an activated fluorophore and iii) covalent attachment of a binding molecule.*

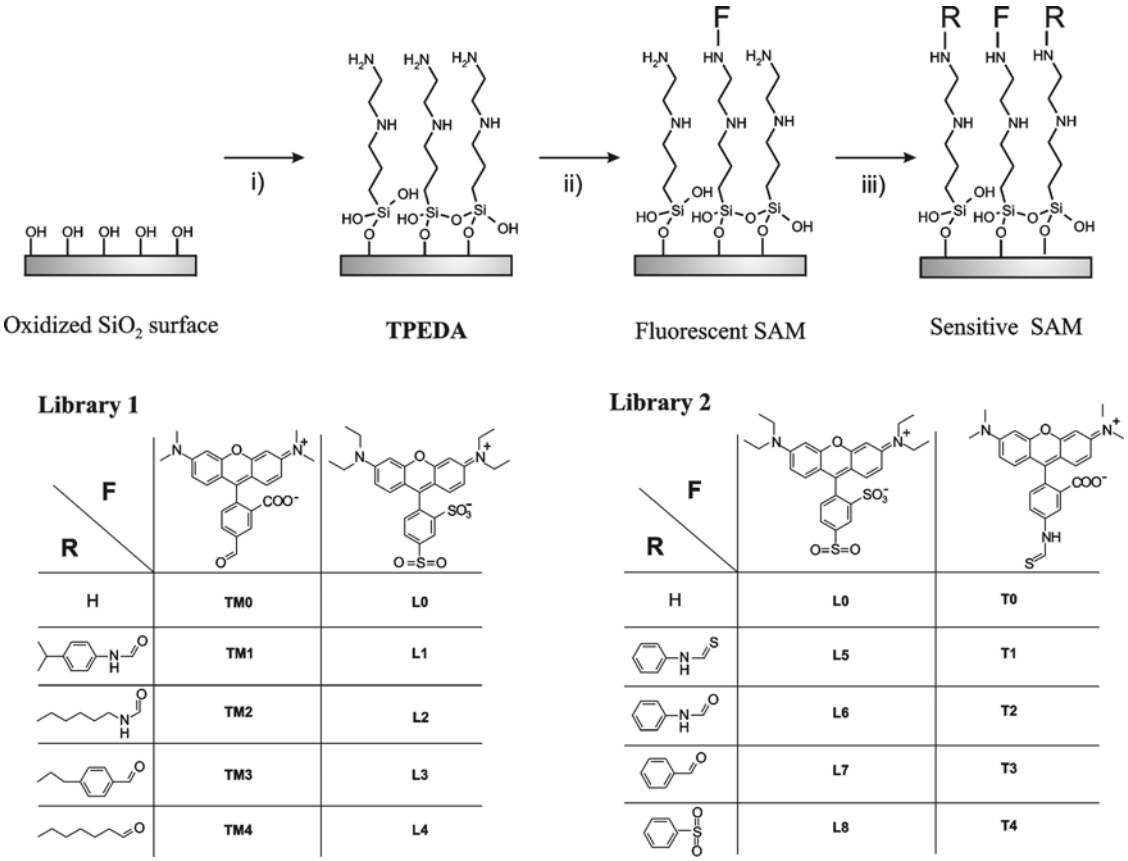

Figure 3.2. *Synthetic scheme for the preparation of* ***Library 1*** *(comprised of layers* ***TM0-TM4*** *and* ***L0-L4****) and* ***Library 2*** *(comprised of layers* ***L0****,* ***L5-L8*** *and* ***T0-T4****) of fluorescent SAMs on glass and silicon surfaces. i) N-[3-(trimethoxysilyl)propyl]ethylenediamine, toluene, rt, 3.5 h, ii) amino reactive fluorophore Lissamine, rhodamine B sulfonyl chloride, 5-(and-6)-carboxytetramethylrhodamine, succinimidyl ester (5(6)-TAMRA, SE) or tetramethylrhodamine-5-(and-6)- isothiocyanate (5(6)-TRITC), acetonitrile, rt, 4 h, iii) isocyanates, thioisocyanates or acid chlorides used as binding molecules, chloroform, rt, 16 h.*

3.2.2 Characterization of the fluorescent monolayers

All monolayers were characterized by contact angle goniometry, ellipsometry, and fluorescence spectroscopy. Additionally, and to assure the introduction of the binding groups, X-ray photoelectron spectroscopy (XPS) measurements were performed with a set of samples. By contact angle measurements[25] the wettability properties of the

surfaces, which depend on the hydrophobicity or hydrophilicity of the monolayer components as well as the layer packing, were analyzed. By ellipsometry,[26] the estimation of thickness of the thin organic film is possible. Fluorescence spectroscopy[27] confirms the presence of the fluorescent molecules by detection of the characteristic spectral emission peaks of the fluorophores. XPS[28] provided elemental analysis data on the composition of the monolayer.

Contact angle and ellipsometry data are summarized in Table 3.1. Amino terminated SAMs formed from N-[3-(trimethoxysilyl)propyl]ethylenediamine (***TPEDA***) have an advancing contact angle (θ_a) of 60^o, and a hysteresis of 25^o, consistent with other literature reports.[18] Values for the other monolayers have not been reported before. Hysteresis (θ_a-θ_r) values range from approximately 25 to 40^o indicating high disorder of the monolayers.[25] Changes in the values of the individual advancing/receding contact angles as well as changes in the hysteresis reflect a variation in the surface hydrophobicity, and therefore variation in the surface functionalization.

Ellipsometry measurements were performed on silicon wafers. The experimental monolayer thicknesses are in good agreement with the thickness modeled with CPK models (software WebLab Viewer v2.01). The calculated values of the layer thickness considering the extended adsorbate lengths are 1.16 nm for ***TPEDA*** SAM, and 2.24 nm for ***L0***, ***TM0*** and ***T0*** SAMs assuming that the molecules of the monolayer are in a perpendicular orientation with respect to the surface. Variations in thicknesses from the calculated values can be due to two factors: i) the molecules are not perpendicular to the surface but tilted and ii) the fluorophore and/or complexing functionalities are lying flat on the amino-surface (***TPEDA***). The introduction of the complexing molecules on the layer does not influence the thickness of the layers because they are smaller molecules than the previously attached fluorophores.

Table 3.1 *Advancing and receding water contact angles ((θ_a) and (θ_r))[a], and ellipsometric thicknesses (nm) of* ***TPEDA***[b] *SAMs of* ***Library 1*** *and* ***Library 2****.*

SAM	θa (°)	θr (°)	Ell. thickness (nm)
TPEDA	60	35	1.35 ± 0.30
TM0	69	32	1.33 ± 0.04
TM1	83	53	1.83 ± 0.20
TM2	55	35	1.13 ± 0.28
TM3	82	58	1.48 ± 0.31
TM4	89	75	1.28 ± 0.30
L0	63	35	1.32 ± 0.15
L1	62	34	1.43 ± 0.09
L2	45	44	1.62 ± 0.19
L3	76	50	1.27 ± 0.11
L4	76	58	2.11 ± 0.23
L5	40	17	*
L6	72	30	*
L7	72	40	1.89 ± 0.14
L8	65	30	2.40 ± 0.43
T0	57	22	1.39 ± 0.1
T1	65	25	1.35 ± 0.16
T2	78	40	1.56 ± 0.15
T3	72	45	1.42 ± 0.18
T4	74	40	1.76 ± 0.19

** Ellipsometry thickness was not measured.*

a) Deviation of the contact angle values are bellow 3^0 in all the cases except ***TM2*** *(θ_a = 55± 6.6 ; θ_r = 35± 7) and* ***L2*** *(θ_r = 44± 13)*
b) N-[3-(trimethoxysilyl)propyl]ethylenediamine

Fluorescent spectroscopy confirmed the introduction of the fluorophores; maximum emission peaks were found at λ of 588 nm for ***L0***, 585 nm for ***TM0*** and 575 nm for ***T0*** in the fluorescence spectra of the functionalized quartz slides (Figure 3.3.A). The maximum emission may be shifted by a few nanometers when the binding molecules are introduced in the fluorescent monolayers. As an example, the fluorescence spectra of layers ***T0-T4*** are depicted in Figure 3.3.B.

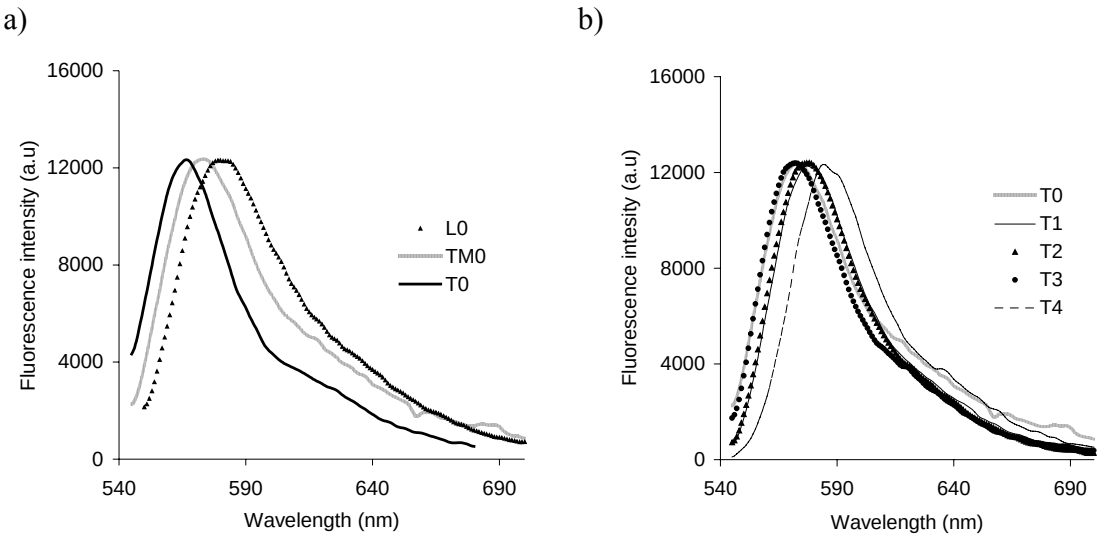

Figure 3.3. *Fluorescence emission spectra of (a) amino-terminated **L0**, **TM0** and **T0** SAMs (λ_{ex} = 545 nm for **L0** and **TM0** and 535 nm for **T0**) and (b) **T1**-**T4,** SAMs functionalized with different binding molecule (amino-terminated SAM **T0** also included) (λ_{ex} = 535 nm). All the measurements are done in acetonitrile.*

The surface elemental composition of the ***TPEDA*** monolayer and the other sensitive monolayers was evaluated by XPS analysis. The XPS analysis of the ***TPEDA*** monolayer (Figure 3.4), indicated a carbon to nitrogen ratio (C1s: N1s) of 69.4% : 30.6% in close agreement with the calculated 71.4% : 28.6%. To study the fluorophore attachment to the ***TPEDA*** SAM, XPS analysis of the monolayer functionalized with lissamine was performed (***L0***, Figure 3.4). In this case, the two sulfur atoms of lissamine can be used as XPS sensitive label. The XPS spectrum of ***L0*** showed a sulfur concentration (S2s) of 3.2 % in the elemental composition, indicating successful monolayer functionalization with the fluorophore. The surface coverage of the samples after their functionalization with the complexing groups was investigated by marking the binding molecule with an XPS sensitive label. A bromine-containing binding molecule was used to form monolayer ***L9*** (Figure 3.4). The XPS spectrum of ***L9*** indicated the appearance of bromine (Br3d) in a concentration 0.8% confirming the successful functionalization of the fluorescent monolayer with the second building block.

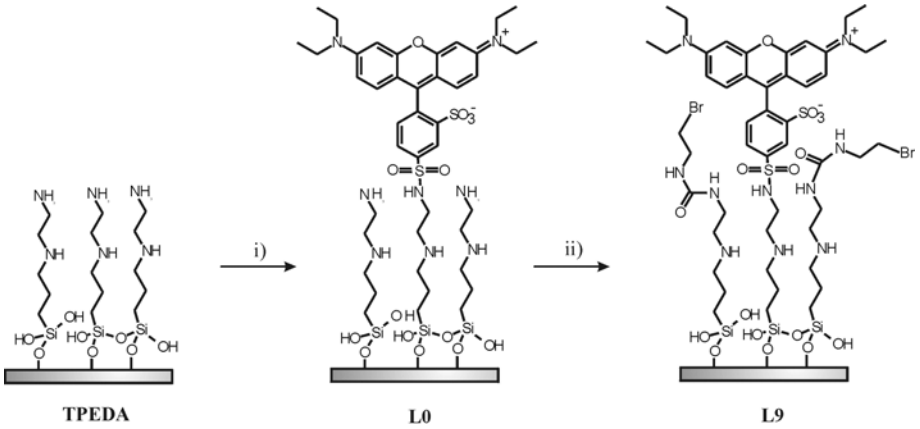

Figure 3.4 *Synthetic scheme for the preparation of* ***L9****, i) Lissamine chloride, toluene, rt, 4h, ii) 2-Bromoethyl isocyanate, chloroform, rt, 16h.*

Once the composition of the SAMs was confirmed, both libraries were subsequently screened for the presence of several metal ions, Cu^{2+}, Co^{2+}, Pb^{2+} and Ca^{2+} and anions like HSO_4^-, NO_3^-, $H_2PO_4^-$, and CH_3COO^- (AcO^-) to determine their sensing properties.

3.2.3. Cation sensing

Library 1 was used for the sensing of Cu^{2+}, Co^{2+}, Ca^{2+} and Pb^{2+} metal ions (Figure 3.5). This library is comprised of ten different monolayers (***TM0-TM4*** and ***L0-L4***) and it is the result of the binary combination (one fluorophore-one binding group) of two fluorophores (Lissamine and TAMRA) and five different functional groups (amino, 4-isopropylphenylurea, hexylurea, 4-propylbenzylamide, and hexylamide).

Fluorescence measurements were performed with 10^{-4} M acetonitrile solutions of Cu^{2+}, Co^{2+}, Pb^{2+} and Ca^{2+} as perchlorate salts. In each case the layer responded to the analytes within seconds. Upon washing with 0.1N HCl the layers were recycled and reproducible results were obtained.[29] The different combinations of binding group and fluorophore resulted in a range of different fluorescent responses (Figure 3.5).

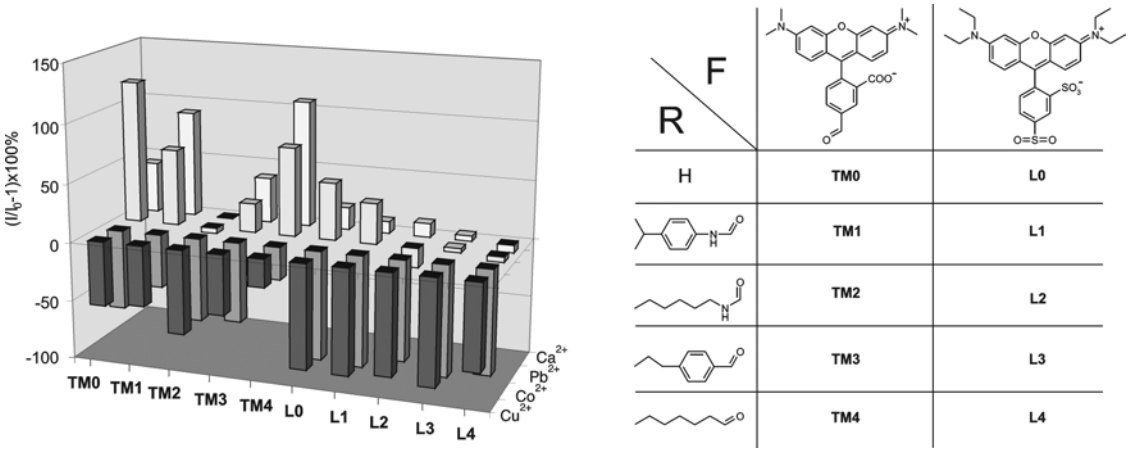

***Figure 3.5**. Relative fluorescence intensity of monolayers **TM0-TM4** and **L0-L4** in the presence of 10^{-4} M solutions of Pb^{2+}, Ca^{2+}, Co^{2+} and Cu^{2+} as perchlorate salts in acetonitrile. The data have been normalized; in the absence of metal cations the maximum fluorescence emission of each layer is set to 0. Positive values correspond to an enhancement in the fluorescence emission intensity of the layer while negative values represent a quenching of the fluorescence emission intensity of the layer.*

Comparing the responses within one fluorophore series, it can be seen that changes in the nature of the binding group significantly affect the binding profiles. For example, both of the fluorophore TAMRA layers, the ureido-substituted ***TM1*** and the amido-substituted ***TM3***, showed an increase in fluorescence upon addition of Ca^{2+} and Pb^{2+}, with a larger increase for the ***TM1*** than for the ***TM3*** layer. More impressive is the comparison of ureido-substituted layers ***TM1*** and ***TM2***. While ***TM1*** shows increased fluorescence for both Pb^{2+} (65%) and Ca^{2+} (90%), ***TM2***, which has a hexyl group instead of a p-isopropylphenyl group shows very little change in fluorescence in the presence of these cations. The differences between binding groups substituted with an aryl versus an alkyl group are remarkable considering that these substituents, in principle, should not directly coordinate either Pb^{2+} or Ca^{2+}, and it is a typical example of the power of the combinatorial method. Due to the ease of generating different sensing system pairs, it requires a minimal effort to synthesize layers with these small variations, which would usually be disregarded in solution state receptor synthesis.

Within the series of lissamine layers (***L0-L4***), amino substituted ***L0*** and ureido substituted ***L1*** showed substantial increases in response to Pb^{2+}, while virtually no response was seen from other amido and ureido layers ***L2-L4***. On the other hand, layers ***L2-L4*** show a very large fluorescence quenching upon addition of and Co^{2+} and Cu^{2+} (~80%), while no response was seen for Ca^{2+} and Pb^{2+}.

When comparing responses between the two fluorophores, there are marked differences between the hexylamido TAMRA system ***TM4***, which shows fluorescence intensity increases for both Ca^{2+} (107%) and Pb^{2+} (75%), and the corresponding hexylamido lissamine system ***L4***, which exhibits virtually no response for these cations. Overall, all systems exhibited a marked fluorescence intensity decrease for Co^{2+} and Cu^{2+}, although more quenching was seen in the lissamine layers than in the corresponding TAMRA layers. Additionally, ***TM0*** is the best for the sensing of Pb^{2+} (121%) versus the other ions due to the large response differences (Ca^{2+} 43%, Co^{2+} -68%, and Cu^{2+} -55%).

Several successful competition studies were performed on hexylureido layer ***L2*** (Figure 3.6) and hexylamido layer ***L4*** (Figure 3.7). Addition of 10^{-4} M Ca^{2+} to layer ***L4*** induced a 10% fluorescence intensity decrease. A further addition of 10^{-4} M Cu^{2+} induced an additional 55% quenching. When reversing the addition, 10^{-4} M of Cu^{2+} caused a 73% decrease in signal, and further addition of 10^{-4} M Ca^{2+} had no effect, indicating that the layer is selective for Cu^{2+} in the presence of Ca^{2+} (Figure 3.6). Similar but more dramatic findings were observed for the ***L2*** system (Figure 3.7). When Ca^{2+} was added the signal increased by 20%, and upon subsequent addition of Cu^{2+} 80% quenching was observed. When the analyte addition was reversed, Cu^{2+} induced a 90% quenching, with no further response upon addition of Ca^{2+}.

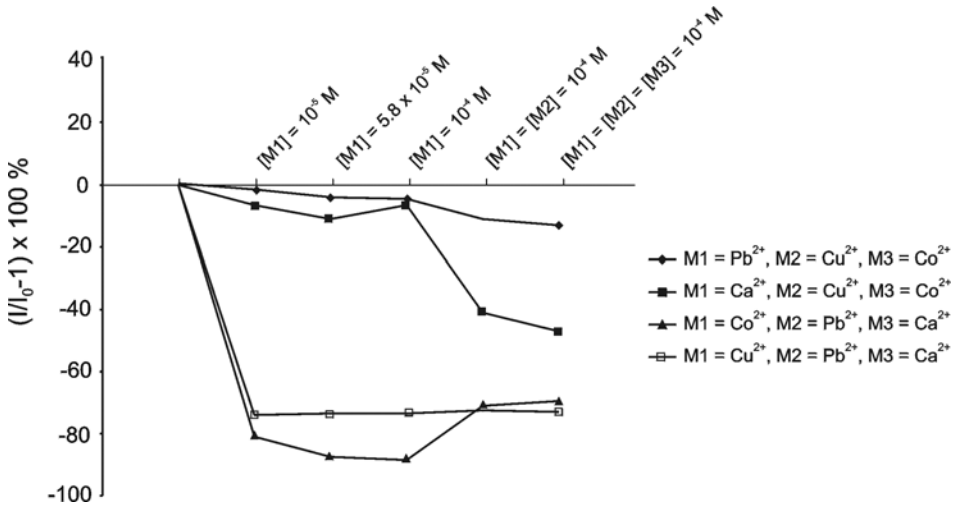

Figure 3.6. *Competition studies with the hexylamido layer* ***L4*** *upon addition of perchlorate salts of Pb^{2+}, Cu^{2+}, Co^{2+} and Ca^{2+} in acetonitrile. The first metal (M1) was added in concentrations ranging from 10^{-5} M to 10^{-4} M, followed by subsequent additions of the second and third metal (M2 and M3) at 10^{-4} M.*

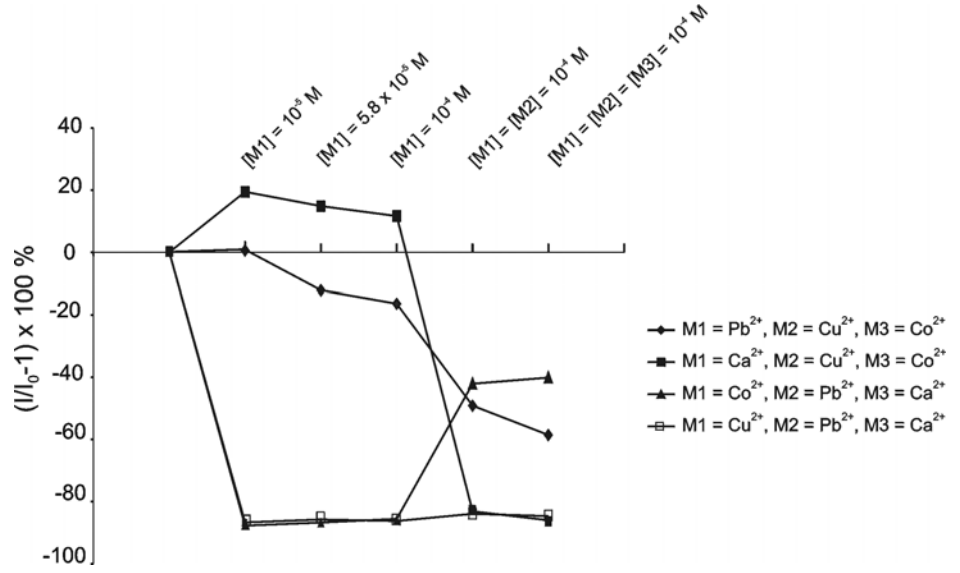

Figure 3.7. *Competition studies with the hexylureido layer* ***L2*** *upon addition of perchlorate salts of Pb^{2+}, Cu^{2+}, Co^{2+} and Ca^{2+} in acetonitrile. The first metal (M1) was added in concentrations ranging from 10^{-5} M to 10^{-4} M, followed by subsequent additions of the second and third metal (M2 and M3) at 10^{-4} M.*

Similar competition experiments for hexylureido and hexylamido layers, ***TM2*** and ***TM4,*** respectively were also performed. Layer ***TM2*** showed high selectivity for Cu^{2+} in presence of Ca^{2+} (Figure 3.8) as observed with layers ***L2*** and ***L4***, while layer ***TM4*** displayed selectivity for Pb^{2+} in the presence of Co^{2+} (Figure 3.9).

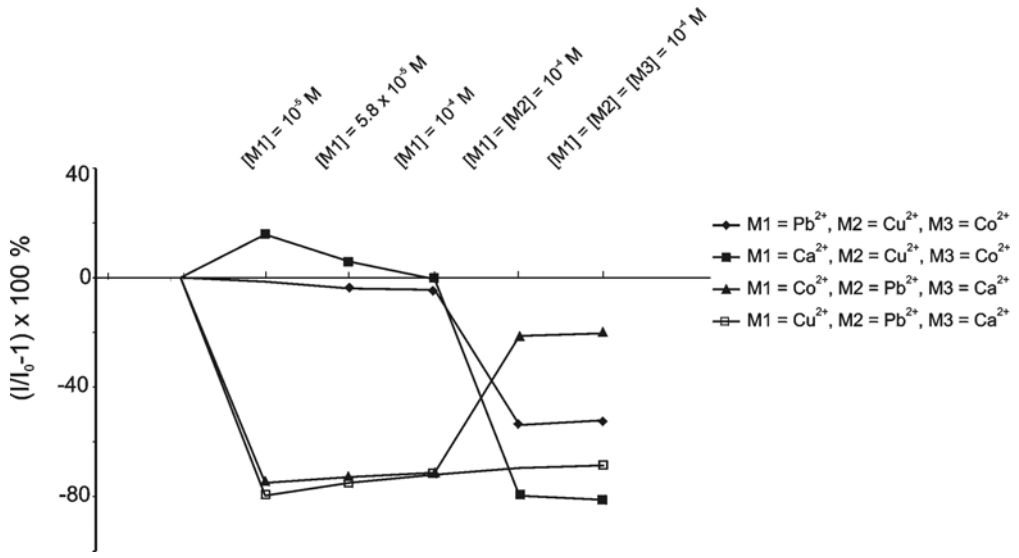

Figure 3.8. *Competition studies with the hexylureido layer* ***TM2*** *upon addition of perchlorate salts of* Pb^{2+}, Cu^{2+}, Co^{2+} *and* Ca^{2+} *in acetonitrile. The first metal (M1) was added in concentrations ranging from* 10^{-5} *M to* 10^{-4} *M, followed by subsequent additions of the second and third metal (M2 and M3) at* 10^{-4} *M.*

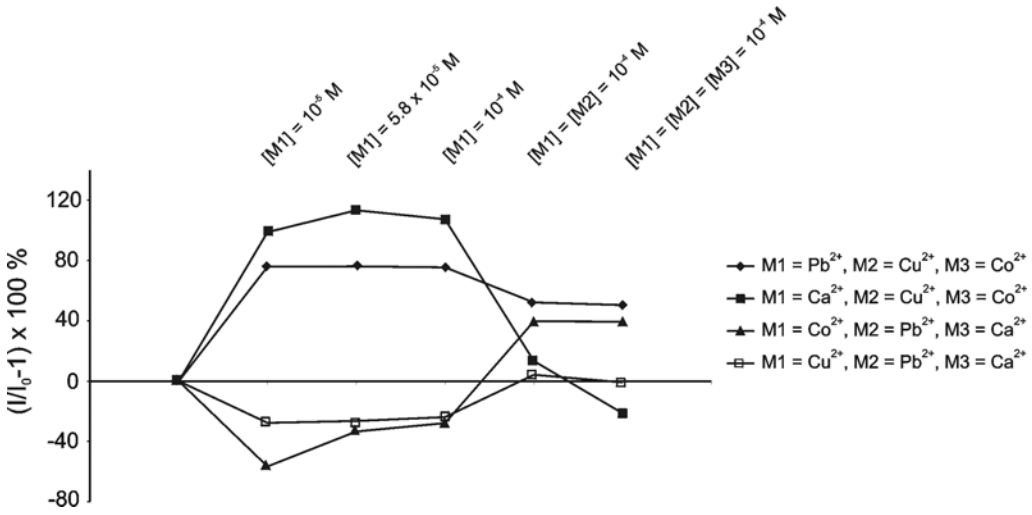

Figure 3.9. *Competition studies with the hexylureido layer* ***TM4*** *upon addition of perchlorate salts of Pb^{2+}, Cu^{2+}, Co^{2+} and Ca^{2+} in acetonitrile. The first metal (M1) was added in concentrations ranging from 10^{-5} M to 10^{-4} M, followed by subsequent additions of the second and third metal (M2 and M3) at 10^{-4} M.*

A detection limit study was performed at concentrations from 10^{-10} M to 10^{-3} M. Responses below 10^{-7} M were negligible. Figure 3.10 shows the fluorescence changes of ***Library 1*** at 10^{-5} M of the analyte concentration.

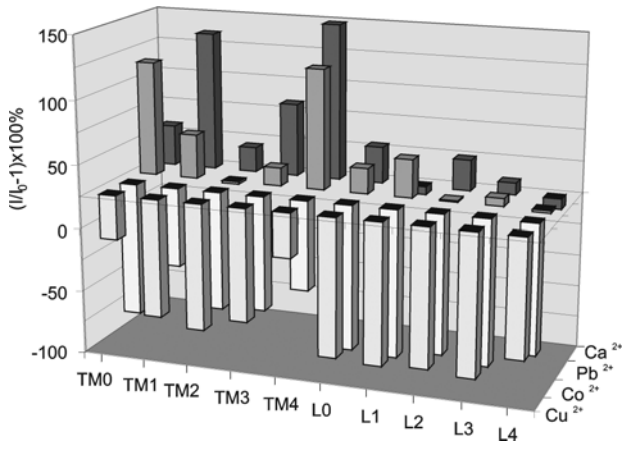

Figure 3.10*. Relative fluorescence intensity of monolayers* ***TM0-TM4*** *and* ***L0-L4*** *in the presence of 10^{-5} M solutions of Pb^{2+}, Ca^{2+}, Co^{2+} and Cu^{2+} as perchlorate salts in acetonitrile. The data*

have been normalized; in the absence of metal cations the maximum fluorescence emission of each layer is set to 0.

Fluorophores, binding groups and their substituents each have a significant impact on the sensitivity and selectivity of the sensing system toward a series of cations. The binding abilities of individual fluorophore-binding group pairs is likely due to a combination of factors such as where the cation binds, whether the binding is shared between various surface functionalities, and whether there are steric constraints or additional intermolecular surface interactions induced by non-coordinating substituents (such as changes in monolayer packing, van der Waals forces, cation-π interactions or π-π interactions between the monolayer substituents). It is likely that some or all of these factors combine to make each pair a truly unique sensing surface. When quenching by the analyte dominates, reduction of the fluorescence is observed. Increased fluorescence, however, is a delicate interplay between quenching by both the analyte and the binding groups. If the binding groups are already quenching the fluorescence, resulting in a lowered initial fluorescence intensity, it is possible that this quenching can be reduced upon addition of the analyte, which will lead to the observed increase in fluorescence. If the binding groups are not quenching, the fluorescence is already at a maximum and no increase can be expected; therefore, in some cases no change in fluorescence is observed.

3.2.4. Anion sensing

Anion sensing development in terms of both sensitivity and selectivity lags behind that of cations for the entire range of sensing systems, from solution state to CHEMFETs and ion selective electrodes.[30] The reasons for this include such factors as their larger size-to-charge ratio, large heat of hydration and geometrical constraints.[31] However, many analytes of interest are anionic and there is a great interest in pushing forward the field of anion sensing.

For this purpose ***Library 2*** was made. Amino terminated SAMs on quartz slides were functionalized sequentially, in the manner previously described for ***Library 1***, with

one fluorophore (TRITC or lissamine) and one anion binding functional group (i.e. amino, amide, sulfonamide, urea, or thiourea, Figure 3.11). The fluorescence response of the layers to 10^{-4} M acetonitrile solutions of tetrabutylammonium salts of HSO_4^-, NO_3^-, $H_2PO_4^-$, and CH_3COO^- (AcO^-) anions was recorded (Figure 3.11). As in the case of cation sensing, each layer revealed a different response pattern for the different anions.

As a general trend, the TRITC functionalized layers ***T0-T4*** exhibited a larger response to all the anions than the corresponding lissamine layers ***L0***, ***L5-L8***. This difference is likely due to the linker functionality. TRITC forms a thiourea bond when reacted with the layer, while lissamine forms a sulfonamide bond. An especially noteworthy response is the large sensitivity of layers ***T1***, ***T2***, and ***T3*** toward $H_2PO_4^-$, with fluorescence quenching from 35% to 50%.

Within the lissamine series, ***L5***, functionalized with a thioureido group, suffers a quenching of 35%, in the presence of AcO^- while the same layer shows a moderate increase of the fluorescence in the presence of HSO_4^- (20%).

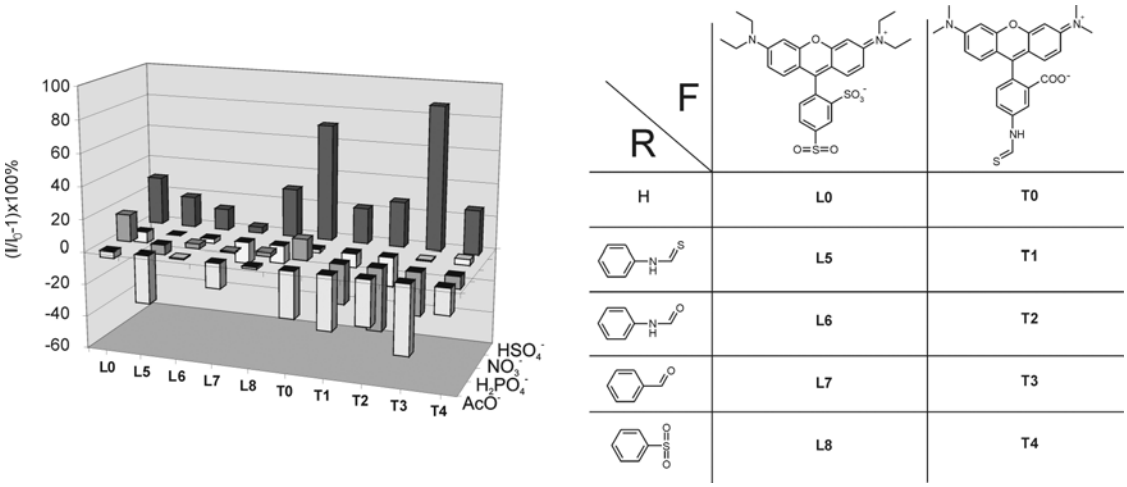

Figure 3.11. *Relative fluorescence intensity of the monolayers **L0**, **L5-L8** and **T0-T4** in the presence of 10^{-4} M solutions of HSO_4^-, NO_3^-, $H_2PO_4^-$ and AcO^- as tetrabutylammonium salts in acetonitrile. The data have been normalized; in the absence of the analytes the maximum fluorescence emission of each layer is set to 0. Positive values correspond to an enhancement in the fluorescence emission intensity of the layer while negative values represent a quenching of the fluorescence emission intensity of the layer.*

Important for sensing purposes is the response of the TRITC functionalized layers ***T1-T3***. The fluorescence response of these layers increased between 24% and 87% in the presence of HSO_4^-, while the same layers showed a decreased fluorescence intensity in the presence of $H_2PO_4^-$ between 35% and 56%. These varied responses (especially the increases in fluorescence) across the library will help to decrease the chance of false positives for the individual analytes. Additionally, the amino-functionalized ***T0*** is an excellent sensor for HSO_4^-; not only is the magnitude of fluorescence increase quite large (72%), but it is the only anion that induces such an increase. The addition of AcO^- induces a quenching of 34%, while NO_3^- and $H_2PO_4^-$ result in virtually no response.

Detection limit studies showed that systems ***T0-T4***, ***L0*** and ***L5*** already exhibit sensitivity towards both AcO^- and HSO_4^- at anion concentrations of 10^{-5} M. Figure 3.12 depicts the fluorescence responses of the library at 10^{-5} M concentration of analytes.

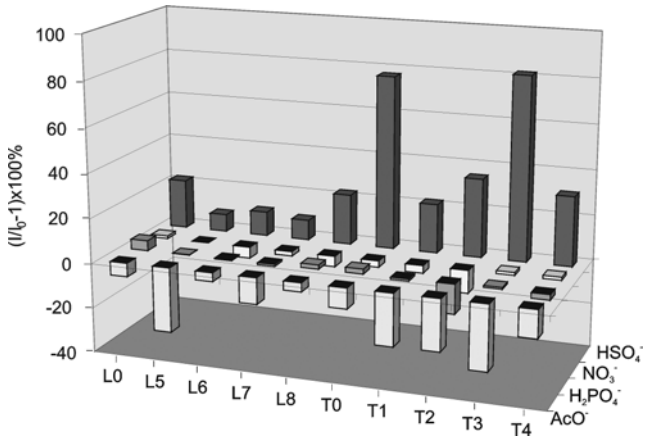

Figure 3.12. *Relative fluorescence intensity of the monolayers **L0**, **L5-L8** and **T0-T4** in the presence of 10^{-4} M solutions of HSO_4^-, NO_3^-, $H_2PO_4^-$ and AcO^- as tetrabutylammonium salts in acetonitrile. The data have been normalized; in the absence of the analytes the maximum fluorescence emission of each layer is set to 0.*

Selectivity studies were performed with layer ***T3,*** which showed selectivity for AcO^- in the presence of NO_3^- and HSO_4^-. Two separate experiments were performed reversing the subsequent addition of solutions of HSO_4^- and AcO^- in presence of NO_3^-. In

both experiments, first 10^{-4} M of NO_3^- was added to a ***T3*** layer, showing no response as expected from the results depicted in Figure 3.11. In the first experiment (Figure 3.13a) four additions of HSO_4^- ranging from 10^{-6} M to 10^{-3} M, produced an enhancement of more than 70 % of the fluorescence intensity of the layer. Subsequently four additions of AcO^- (10^{-6} M-10^{-3} M) quenched the fluorescence of the layer up to 70 % of the initial fluorescence. In a second experiment, (Figure 3.13b) after the addition of 10^{-4} M of NO_3^-, AcO^- was added (10^{-6} M-10^{-3} M), followed by HSO_4^- (10^{-6} M-10^{-3} M). In this case the addition of AcO^- quenched the fluorescence intensity but upon addition of HSO_4^- (10^{-3} M) no enhancement was observed. In both experiments the addition of AcO^- caused 70% fluorescence quenching, but *only* when the HSO_4^- was added *first* the fluorescence intensity increased. Thus, it appears that ***T3*** is able to selectively sense 10^{-5} M AcO^- in the presence of 10^{-4} M NO_3^- and 10^{-3} M HSO_4^- (Figure 3.13).

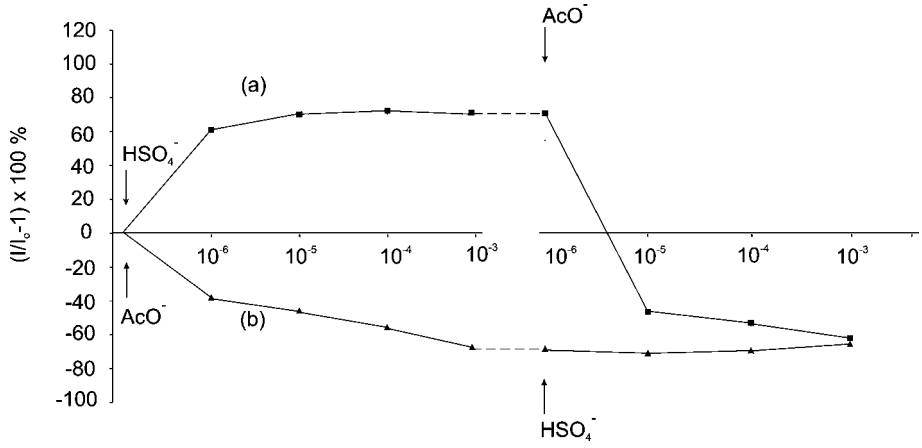

Figure 3.13. *Competition studies with the amido layer* ***T3*** *in acetonitrile. In experiment (a) first an addition of 10^{-4} M NO_3^- was made and no response was observed; subsequently four additions of HSO_4^- (10^{-6} M-10^{-3} M) and then four additions of AcO^- (10^{-6} M-10^{-3} M) were made. In experiment (b) first an addition of 10^{-4} M NO_3^- was made and no response was observed; subsequently AcO^- was added from 10^{-6} M-10^{-3} M, followed by addition of HSO_4^- (10^{-6} M-10^{-3} M).*

These findings could represent an important step forward in the field of anion sensing, which often requires significant synthetic effort in order to achieve binding sensitivity and selectivity. Through a combinatorial approach for the generation of

chemical sensors from commercially available, simple small molecules, and by means of a simple analytical protocol, *in situ* a huge number of sensing surfaces can be obtained without the necessity of target labeling or library deconvolution. It has been shown that a response data set containing a number of general trends represents a unique analyte response, a "fingerprint" of the analyte. The strength of the approach is the overall simplicity of the system, in that it imparts generality to the methodology in terms of both sensing system generation and the exploration of microanalysis technology.

3.3. Conclusions and outlook

Starting with the idea of building an easily generated sensing system by the combinatorial approach, it has been shown that sequential deposition of a fluorophore and a binding group onto monolayer functionalized quartz substrates results in libraries of sensing systems for cations and anions. The simple assembly of many functional groups covalently attached to the surface leads to the formation of a large number of binding groups on the substrate. Because the generated recognition sites are kept together by covalent attachment to the substrate, they operate collectively. Two libraries of sensitive monolayers have been fabricated for cation and anion sensing. The first library discriminates Cu^{2+}, Co^{2+}, Pb^{2+} and Ca^{2+} cations while the anion library discriminates the inorganic anions AcO^-, HSO_4^-, $H_2PO_4^-$ and NO_3^- in acetonitrile. A few systems were tested for selectivity and good results were obtained (substrate ***L2*** exhibited selectivity for Cu^{2+} in presence of Pb^{2+} and Ca^{2+}, and substrate ***T3*** showed high selectivity for AcO^- in presence of NO_3^- and HSO_4^-).

The described monolayer libraries offer many different sensitive substrates, making this approach a surprisingly powerful tool to easily optimize the selectivity and the sensitivity towards a great variety of analytes. The scope of the method is such that many possibilities can be envisioned between combinations of fluorophores and any other complexing groups, reactive molecule, biomolecules, or specific receptors with a compatible functionality for attachment to the surface. The method is particularly amenable for the transition toward miniaturization and subsequent array format, which

would open the possibility for a large number of sensing systems to be quickly synthesized and screened. This would allow both for fingerprints to be made to discern the lead sensing architectures for the detection of analyte mixtures, as well as for hand-picking of particularly selective combinations for a specific analyte.[32]

The extension of the sensing methodology to the microscale by microcontact printing (μCP) and by microchannel technology for future development of microarrays is addressed in Chapters 5, 6 and 7 of this thesis.

3.4. Experimental

Chemicals.

Analytical reagent grade solvents were purchased from Fisher Scientific. Fluorophores TAMRA (5-(and-6)-carboxytetramethylrhodamine (5(6)-TAMRA) *mixed isomers*), Lissamine (Lissamine™ rhodamine B sulfonyl chloride *mixed isomers*), TRITC (tetramethylrhodamine-5-(and-6)-isothiocyanate (5(6)-TRITC) *mixed isomers*) were purchased from Molecular probes (Invitrogen). All other reagents were purchased from Sigma-Aldrich.

Monolayer Preparation

All glassware used to prepare the layers was cleaned by sonicating for 15 minutes in a 2% v/v Hellmanex II solution in distilled water, rinsed four times with high purity (MilliQ, 18.2 MΩcm) water, and dried in an oven at 150º C. The substrates, quartz slides or silicon wafers (four-inch polished, 100 cut, p-doped silicon wafers) were cleaned for 15 minutes in piranha solution (concentrated H_2SO_4 and 33% aqueous H_2O_2 in a 3:1 ratio. ***Warning: Piranha solution should be handled with caution: it has been reported to detonate unexpectedly***). They were then rinsed several times with high purity (MilliQ) water, and dried in a nitrogen stream immediately prior to performing the formation of the monolayer.

*Amino terminated monolayer (**TPEDA**) synthesis*

Formation of the N-[3-(trimethoxysilyl)propyl]ethylenediamine self-assembled monolayer (***TPEDA***) was achieved in a glovebox under an atmosphere of dry nitrogen. The freshly cleaned substrates were immersed in a 5 mM solution of N-[3-(trimethoxysilyl)propyl]ethylenediamine, in dry toluene (freshly distilled over sodium) for 3.5 h. After the substrates were taken from the solution, they were rinsed twice with toluene (under nitrogen atmosphere) to remove excess silane and avoid polymerization. The substrates were then removed from the glovebox and rinsed with ethanol and dichloromethane to remove physisorbed material. The following protocol was repeated twice: stirring of the slide in a beaker filled with EtOH, then rinsing with a stream of EtOH, followed by stirring in CH_2Cl_2, then rinsing with a stream of CH_2Cl_2. The slides were then dried under an air stream.

*Immobilization of the fluorophore on the **TPEDA** monolayer. Synthesis of the layers **TM0**, **L0** and **T0**.*

The attachment of the fluorophores to the amino terminated N-[3-(trimethoxysilyl)propyl]ethylenediamine SAM (***TPEDA***) was achieved by immersing the slides for 4 h. in a 0.23 mM acetonitrile solution of the fluorophore TAMRA (5-(and-6)-carboxytetramethylrhodamine, succinimidyl ester (5(6)-TAMRA, SE)

*mixed isomers)) (TM) to yield layer ***TM0,*** or fluorophore Lissamine (L) (Lissamine rhodamine B sulfonyl chloride) to yield layer ***L0*** for the cation library, a 0.08 mM acetonitrile solution of fluorophore TRITC (T) (tetramethylrhodamine-5-(and-6)-isothiocyanate(5(6)-TRITC) *mixed isomers) to afford layer ***T0*** and fluorophore Lissamine (L) (Lissamine rhodamine B sulfonyl chloride) to afford layer ***L0*** for the anion library. For each library, 100 μL triethylamine was added to the Lissamine solutions. All reactions were carried out in a glovebox under an atmosphere of dry N_2. After the substrates were taken out from the solution they were rinsed with CH_3CN, EtOH, and CH_2Cl_2 to remove physisorbed material. The following protocol was repeated successively for each solvent, twice: stirring of the slide in the solvent followed by rinsing with a stream of the solvent. The slides were then dried under an air stream.

Immobilization of the binding groups on the surface. Synthesis of the layers ***L1-L9, TM1-TM4*** *and* ***T1-T4.***

The slides with the ***L0*** and ***TM0*** SAMs were immersed in 50 mL of 12 mM acetonitrile solution of the appropriate reactive species: *p*-isopropylphenyl isocyanate, hexyl isocyanate, *p*-propylbenzoyl chloride, or hexanoyl chloride to afford the rest of the layers of ***Library 1*** (***TM1-TM4***, ***L1-L4***). A second set of slides with the ***L0*** and ***T0*** SAMs were immersed in 50 mM of 12 mM acetonitrile solution of the appropriate reactive species: of phenyl isothiocyanate, phenyl isocyanate, benzoyl chloride, and benzene sulfonyl chloride to afford the rest of the layers of ***Library 2*** (***T1-T4***, ***L5-L8***). The reaction of layer ***L0*** with 40 mM acetonitrile solution of 2-bromoethyl isocyanate yielded ***L9***. When the reactive specie was an acid chloride, 0.3 mL triethylamine was added to the reaction for the ***Library 1***, and 0.15 mL was added for ***Library 2***. All reactions were carried out under an atmosphere of dry N_2 for 16 h. After the substrates were taken out from the solution they were rinsed sequentially with CH_3CN, EtOH, and CH_2Cl_2 to remove physisorbed material by stirring the slide in each solvent followed by rinsing with a stream of the solvent. The slides were then dried under an air stream.

Characterization of the layers

Ellipsometry measurements of the layers were performed on silicon wafers, and were performed on a Plasmon ellipsometer (λ=632.8 nm) assuming a refractive index of 1.5 for the monolayer over the silicon oxide layer (refractive index 1.46). Raster scans were taken of 25 points per silicon wafer (maximum size $1cm^2$), and their values averaged.

Contact angle measurements of the monolayers were performed on functionalized silicon wafers with MilliQ water. Measurements were performed on a Krüss pendant drop contact angle measurement system G10, a sessile drop system mounted with a CCD camera, using drop shape analysis 1.51 software. Drop fitting was done with DPA32 Tangent 1 and Tangent 2 analysis methods. The MilliQ water inside the syringe was replaced before measuring each silicon wafer.

XPS measurements were performed with a Physical Electronics Quantum2000 equipped with a spherical sector analyzer and a multichannel plate detector (16 detector elements). Analyzer Mode was constant pass energy. For the survey scan the pass energy was 117 eV, the X-ray beam was set to High Powermode 100 Watt/100μm, and the diameter beam scanned over a 1000 μm x 500 μm area; for element scans pass energy was 29.35 eV, the X-ray beam was set to 25 W/100 μm, and the diameter beam scanned over a 1000 μm x 500 μm area. The excitation source was Al K Alpha monochromatic radiation with a source energy = 1486.7 eV. The take-off angle (analyzer angle to sample surface) was set to 30 degrees. Using both low energy electrons and ions controlled the surface potential. The temperature during analysis was 298 K, and the pressure was between 1 and 3 x 10^{-8} Torr (Argon pressure for charge control). For atomic concentration calculation the Shirley background subtraction was employed. The sensitivity factors were provided by Physical Electronics Multipack software version 6.1A. The hydrocarbon C1s signal at 284.8 eV was used as a reference for surface charging.

Spectrofluorometric measurements

Fluorescence experiments were performed on an Edinburgh FS900 spectrofluorimeter with a 450 W Xenon arc lamp as excitation source (λ_{ex} = 545 nm for TAMRA and lissamine, and 535 nm for TRITC). M300 gratings with 1800 l/mm were used on both excitation and emission arms. Signals were detected at an angle

of 90º with regard to the excitation source, by a Peltier element cooled, red sensitive, Hamamatsu R928 photomultiplier system. For the fluorescence spectroscopy measurements a general procedure was followed: the quartz cuvettes (45 mm x 12.5 mm x 12.5 mm, volume 3.5 mL) were cleaned by placement for 15 minutes in a 60º C 2% v/v Hellmanex II solution in demi-water and afterwards rinsed with ultrapure (MilliQ) water and dried in an air stream. 2 mL of dry acetonitrile (dried over molecular sieves) was added, the functionalized quartz slide (H x W x D, 40 mm x 17 mm x 1 mm) was placed at an angle of 45° in the cuvette, and the cuvette placed in a holder on an externally turnable platform. Normally an angle between -10° and -20° was used for the measurements. For all fluorophore systems a 550 nm filter was used. The analytes used for the cation sensing experiments were perchlorate salts of Pb^{2+}, Ca^{2+}, Cu^{2+}, and Co^{2+}, and for the anion sensing experiments, n-tetrabutyl ammonium salts of CH_3COO^- (AcO^-), NO_3^-, HSO_4^-, and $H_2PO_4^-$ were used. After a short stabilization time (5 min) four sequential additions were performed of acetonitrile solutions of the analyte using gastight Hamilton syringes. Some air was then very carefully bubbled through the cuvette with a pipet. Directly after each addition and mixing a spectrum was obtained, followed by an additional spectrum after 5 min. Upon signal stabilization, additional analyte aliquots were added; otherwise, additional spectra were taken until a stable signal was reached. After the additions, the slide was removed and a spectrum of the solvent was obtained. The individual fluorescence values given in the text are the average of two measurements; even though a few measurements had a considerable error, probably due to human error, the average errors of all 104 measurements are below 7% (for error analysis see appendix 3).

3.5. References and notes

1 Lam, K. S.; Renil, M. From Combinatorial Chemistry to Chemical Microarray. *Curr. Opin. Chem. Biol.* ***2002***, 6(3), 353-358.

2 Chen, G. Y. J.; Uttamchandani, M.; Zhu, Q.; Wang, G.; Yao, S. Q. Developing a Strategy for Activity-Based Detection of Enzymes in a Protein Microarray. *Chembiochem* ***2003***, 4(4), 336-339.

3 Steemers, F. J.; Ferguson, J. A.; Walt, D. R. Screening Unlabeled DNA Targets With Randomly Ordered Fiber-Optic Gene Arrays. *Nat. Biotechnol.* ***2000***, 18(1), 91-94.

4 Curey, T. E.; Salazar, M. A.; Oliveira, P.; Javier, J.; Dennis, P. J.; Rao, P.; Shear, J. B. Enzyme-Based Sensor Arrays for Rapid Characterization of Complex Disaccharide Solutions. *Anal. Biochem.* ***2002***, 303(1), 42-48.

5 Lavigne, J. J.; Savoy, S.; Clevenger, M. B.; Ritchie, J. E.; Mcdoniel, B.; Yoo, S. J.; Anslyn, E. V.; Mcdevitt, J. T.; Shear, J. B.; Neikirk, D. Solution-Based Analysis of Multiple Analytes by a Sensor Array: Toward the Development of an "Electronic Tongue". *J. Am. Chem. Soc.* ***1998***, 120(25), 6429-6430.

6 Di Natale, C.; Macagnano, A.; Davide, F.; D'amico, A.; Legin, A.; Vlasov, Y.; Rudnitskaya, A.; Selezenev, B. Multicomponent Analysis on Polluted Waters by Means of an Electronic Tongue. *Sens. Actuators, B* ***1997***, 44(1-3), 423-428.

7 Dickinson, T. A.; White, J.; Kauer, J. S.; Walt, D. R. A Chemical-Detecting System Based on a Cross-Reactive Optical Sensor Array. *Nature* ***1996***, 382(6593), 697-700.

8 Lavigne, J. J.; Anslyn, E. V. Sensing a Paradigm Shift in the Field of Molecular Recognition: From Selective to Differential Receptors. *Angew. Chem., Int. Ed.* ***2001***, 40(17), 3119-3130.

9 Birkert, O.; Tunnernann, R.; Jung, G.; Gauglitz, G. Label-Free Parallel Screening of Combinatorial Triazine Libraries Using Reflectometric Interference Spectroscopy. *Anal. Chem.* ***2002***, 74(4), 834-840.

10 Heller, M. J. Dna Microarray Technology: Devices, Systems, and Applications. *Annual Review of Biomedical Engineering* ***2002***, 4, 129-153.

11 Kawahashi, Y.; Doi, N.; Takashima, H.; Tsuda, C.; Oishi, Y.; Oyama, R.; Yonezawa, M.; Miyamoto-Sato, E.; Yanagawa, H. In Vitro Protein Microarrays for Detecting Protein-Protein Interactions: Application of a New Method for Fluorescence Labeling of Proteins. *Proteomics* ***2003***, 3(7), 1236-1243.

12 Nashat, A. H.; Moronne, M.; Ferrari, M. Detection of Functional Groups and Antibodies on

Microfabricated Surfaces by Confocal Microscopy. *Biotechnol. Bioeng.* ***1998***, 60(2), 137-146.
13 Salisbury, C. M.; Maly, D. J.; Ellman, J. A. Peptide Microarrays for the Determination of Protease Substrate Specificity. *J. Am. Chem. Soc.* ***2002***, 124(50), 14868-14870.
14 Wu, X. Q.; Kim, J.; Dordick, J. S. Enzymatically and Combinatorially Generated Array-Based Polyphenol Metal Ion Sensor. *Biotechnology Progress* ***2000***, 16(3), 513-516.
15 Mayr, T.; Liebsch, G.; Klimant, I.; Wolfbeis, O. S. Multi-Ion Imaging Using Fluorescent Sensors in a Microtiterplate Array Format. *Analyst* ***2002***, 127(2), 201-203.
16 Kaifer, A. E. Functionalized Self-Assembled Monolayers Containing Preformed Binding Sites. *Isr. J. Chem.* ***1996***, 36(4), 389-397.
17 Crooks, R. M.; Ricco, A. J. New Organic Materials Suitable for Use in Chemical Sensor Arrays. *Acc. Chem. Res.* ***1998***, 31(5), 219-227.
18 Crego-Calama, M.; Reinhoudt, D. N. New Materials for Metal Ion Sensing by Self-Assembled Monolayers on Glass. *Adv. Mater.* ***2001***, 13(15), 1171-1174.
19 Major, R. C.; Zhu, X. Y. The Surface Chelate Effect. *J. Am. Chem. Soc.* ***2003***, 125(28), 8454-8455.
20 Van der Veen, N. J. ; Flink, S.; Deij, M. A.; Egberink, R. J. M.; Van Veggel, F. J. C. M.; Reinhoudt, D. N. Monolayer of a Na+-Selective Fluoroionophore on Glass: Connecting the Fields of Monolayers and Optical Detection of Metal Ions. *J. Am. Chem. Soc.* ***2000***, 122(25), 6112-6113.
21 Grandini, P.; Mancin, F.; Tecilla, P.; Scrimin, P.; Tonellato, U. Exploiting the Self-Assembly Strategy for the Design of Selective Cu-Ii Ion Chemosensors. *Angew. Chem., Int. Ed.* ***1999***, 38(20), 3061-3064.
22 Dulkeith, E.; Morteani, A. C.; Niedereichholz, T.; Klar, T. A.; Feldmann, J.; Levi, S. A.; Van Veggel, F. C. J. M.; Reinhoudt, D. N.; Moller, M.; Gittins, D. I. Fluorescence Quenching of Dye Molecules Near Gold Nanoparticles: Radiative and Nonradiative Effects. *Physical Review Letters* ***2002***, 89(20).
23 Motesharei, K.; Myles, D. C. Molecular Recognition on Functionalized Self-Assembled Monolayers of Alkanethiols on Gold. *J. Am. Chem. Soc.* ***1998***, 120(29), 7328-7336.
24 Flink, S.; Van Veggel, F. J. C. M.; Reinhoudt, D. N. Sensor Functionalities in Self-Assembled Monolayers. *Adv. Mater.* ***2000***, 12(18), 1315-1328.
25 Adamson, A. W. *Physical Chemistry of Surfaces, Willey : Chicester* ***1993***.
26 Azzam, R. M. A.; Bashara, N. M. *Ellipsometry and Polarized Light, North-Holland: New York* ***1987***.
27 Mathauer, K.; Frank, C. W. Naphthalene Chromophore Tethered in the Constrained Environment of a Self-Assembled Monolayer. *Langmuir* ***1993***, 9(11), 3002-3008.
28 Wagner, C. D.; Riggs, W. M.; Davis, L. E.; Moulder, J. F. *Handbook of X-Ray Photoelectron Spectroscopy, Muilenberg, G.E.; Ed., Perkin-Elmer Corporation: Eden Prairie, Minesota* ***1979***.
29 After recycling of the surfaces by washing with 0.1 HCl (aq) solution, the response of the layers to the presence of the analytes was smaller, probably due to some degradation of the layers.
30 Antonisse, M. M. G.; Snellink-Ruel, B. H. M.; Lugtenberg, R. J. W.; Engbersen, J. F. J.; Van den Berg, A.; Reinhoudt, D. N. Membrane Characterization of Anion-Selective Chemfets by Impedance Spectroscopy. *Anal. Chem.* ***2000***, 72(2), 343-348.
31 Beer, P. D.; Gale, P. A. Anion Recognition and Sensing: the State of the Art and Future Perspectives. *Angew. Chem., Int. Ed.* ***2001***, 40(3), 487-516 .
32 Phizicky, E.; Bastiaens, P. I. H.; Zhu, H.; Snyder, M.; Fields, S. Protein Analysis on a Proteomic Scale. *Nature* ***2003***, 422(6928), 208-215.

Appendix 3

A3.1. Error analysis

A detailed statistical error analysis of the fluorescence response of the original cation and anion libraries (***Library 1*** and ***Library 2***) at 10^{-4} M concentration of the different analytes is shown bellow depicted by bars. Every data point is the average of between two and six measurements

Cation sensing, ***Library 1***

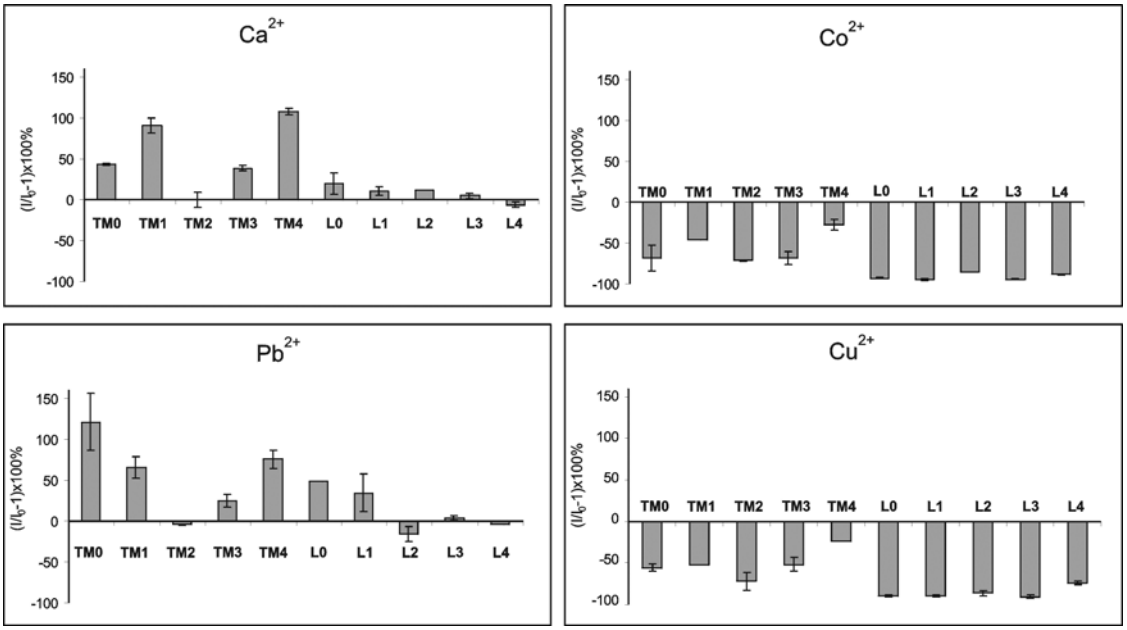

Anion sensing, ***Library 2***

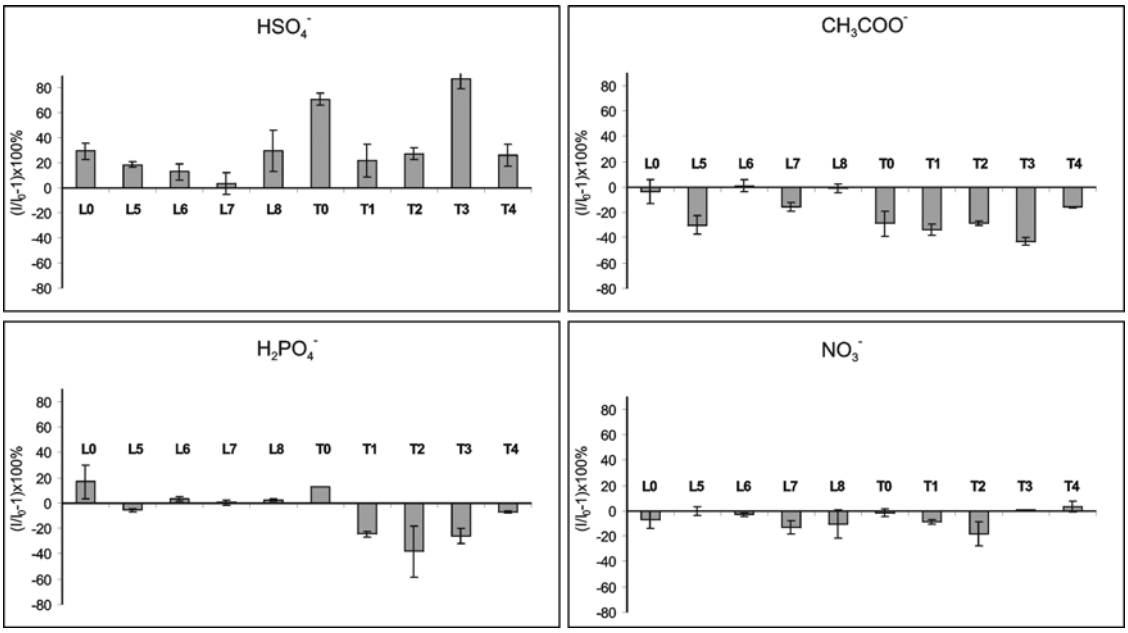

Chapter 4

Self-Assembled Monolayers on Glass for Ion Sensing in Water*

The development of self-assembled monolayers on glass for sensing ions in water via fluorescence spectroscopy is presented. The methodology for detection of inorganic cations and anions in organic solvents,[1,2] described in Chapter 3 of this thesis, is expanded here to sense ions in aqueous solutions. To this end sensitive SAMs that are stable in water have been fabricated. Changes in fluorescence intensity of the layers upon addition of aqueous solutions of different metal ions and inorganic anions confirmed the ability of the monolayer libraries to produce a "fingerprint" response for different analytes with high reproducibility. Additionally, the covalent attachment of the fluorophore moieties to the monolayer allows monitoring of the integrity of the monolayer in contact with aqueous solutions. This is the first example of sensing of ions in water by a self-assembled monolayer covalently attached on glass.

---

* Part of this chapter has been published in: Zimmerman, R. S.; Basabe-Desmonts, L.; Van der Baan F.; Reinhoudt, D. N.; Crego-Calama, M. *Journal of Materials Chemistry*, ***2005***, *15*, (27-28), 2772-2777

4.1. Introduction

Sensing in water is particularly important due to its applicability to real-world analyses including medical diagnostics and detection of environmental contaminants.[3-5] There is a need for the creation of sensing probes for the monitoring of aqueous binding, to facilitate the understanding of biological systems.[6,7] Surface confinement of the sensor systems is very advantageous in terms of reproducibility, remote distance analysis, and in order to avoid leaching problems. As mentioned in Chapter 3 sensing surfaces of self-assembled monolayers (SAMs) offer advantages such as a unidirectional responding surface, minimization of analyte sorption time to receptors, and fast response times,[8] which make them good candidates as sensing surfaces in aqueous media. However, sensing in water using SAMs covalently bound to glass can be hampered by hydrolysis of the Si-O bond, particularly in basic media.[9,10] It is often not possible to monitor in time the layer stability, and most sensing studies on surfaces were reported without consideration of the so important integrity of the monolayer.[11] While an interaction can still be monitored without knowledge of the stability of a monolayer, it becomes problematic to perform reliable quantitative studies.

Thus far, the majority of examples of molecular recognition in water on SAMs has been reported for gold substrates,[12] utilizing mainly electrochemical methods,[13] or surface plasmon resonance,[14,15] to monitor the interaction. Fluorometric techniques offer advantages in terms of sensitivity, selectivity, response times, local observation (e.g by fluorescence microscopy) and minimization of impact on the sample (no use of electrolytes).[16,17] Moreover, remote sensing is possible by using optical fibers with a fluorescent chemosensor immobilized on the tip of the fiber. Therefore, fluorescence spectroscopy is a highly desirable measurement technique for the design of sensors in water. Actually fluorescent imaging has been proven to be the most suitable technique for in vivo monitoring.[18] From the late 1980s, many fluorescent probes have been designed and some have been used successfully for detection of metal ions inside cells.[18] However, fluorescence is not well suited to measuring interactions on top of gold surfaces as it was outlined before in Chapter 3 of this thesis due to quenching of the fluorescence by the

gold.[8,19] Glass is a suitable substrate for fluorescence measurements in contrast to gold surfaces offering the additional advantage of covalent attachment of the sensing monolayer to the surface.[20] In the field of surface-confined biosensing, which often uses glass as a platform for the generation of microarrays, fluorescence has been widely employed to monitor biological interactions such as enzyme activity,[21] recognition of DNA sequences,[22] and protein-protein interactions.[23] Recently, the use of fluorescence has started to emerge to sense molecular recognition processes in water on SAMs on glass,[24-26] silica particles and Langmuir Blodgett monolayers.[27-29]

Here the novel methodology presented previously in Chapter 3 of this thesis, involving a series of glass-confined sensing systems for detecting inorganic cations and anions in organic solvents[1,2] is expanded to sense ions by SAMs on a glass platform in aqueous solutions. At the same time it is shown that this methodology provides a simple method to study the stability of the sensing layers. As explained before, the protocol is a parallel combinatorial approach for the deposition of different complexing functionalities and fluorophores onto an amino-terminated SAM on glass. A number of complexing functionality-fluorophore combinations are generated without the need for designing and synthesizing a complex receptor and target labeling. Due to their binding properties, the analytes interact with the layers and induce different changes in the fluorescence emission intensity of the layers (Figure 4.1).

Our original SAM sensing systems used TPEDA (N-[3-(trimethoxysilyl)propyl]ethylenediamine) to form an amino-terminated monolayer on a glass surface[1,2] to which subsequently the fluorophore and complexing functionality were attached (Chapter 3). However, it is known that direct attachment of amino-terminated silanes onto glass results in monolayers that are not highly ordered,[10] and it is likely that the lack of a well-ordered hydrophobic layer allows water to penetrate the layer and to hydrolyze the Si-O bonds, which will eventually destroy the layer.

Here, we show that by covalent attachment of a fluorophore to a SAM on glass, it is possible to monitor the stability of the layer in aqueous solution. By doing so, a new class of stable monolayers on glass for the fabrication of a parallel library of non-specific sensitive monolayers for ions in aqueous medium was developed.

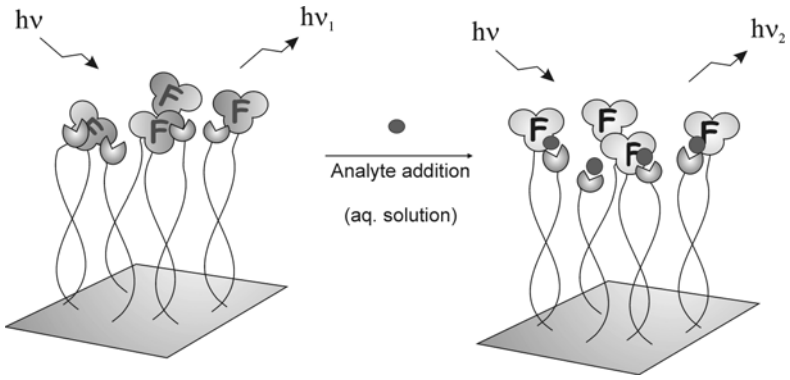

Figure 4.1. *Schematic representation of the working mechanism of a fluorescent sensing monolayer (SAM) on a glass surface in aqueous enviroment. The sensitive fluorescent monolayer is modified with fluorophores (F) and the complexing functionalities. In the presence of an analyte the fluorescence emission of the SAM changes due to interaction of the analyte with the layer.*

4.2. Results and discussion

4.2.1. Water stability of fluorescent self-assembled monolayers on glass

For fluorescent monolayers suitable for measurements in aqueous solution two different amino-terminated monolayers were functionalized with dansyl chloride (Figure 4.2a).[30] Layer ***1*** was fabricated by direct functionalization of the glass substrate with a (N-[3-(trimethoxysilyl)propyl]ethylenediamine) SAM (***TPEDA)*** and subsequent functionalization with the dansyl chloride. Fluorescence stability studies performed with ***1*** at pH 7.0 (see experimental part) showed that the monolayer was unstable over time, with almost total loss of the fluorophore molecules into the solution after 15 min. Because of the instability of these layers, a stepwise chemical synthesis of a long-chain amino-terminated alkylsilane monolayer of 1-amino-11-silylundecane (***3***) was performed (Figure 4.2b). This two steps synthesis of the amino-terminated monolayer yields a well-defined structure of the siloxane network increasing in general the stability of the

monolayer.[25,31] It has been recently used in our group for formation of water stable monolayers used to monitor binding processes.[25,30,32-34]

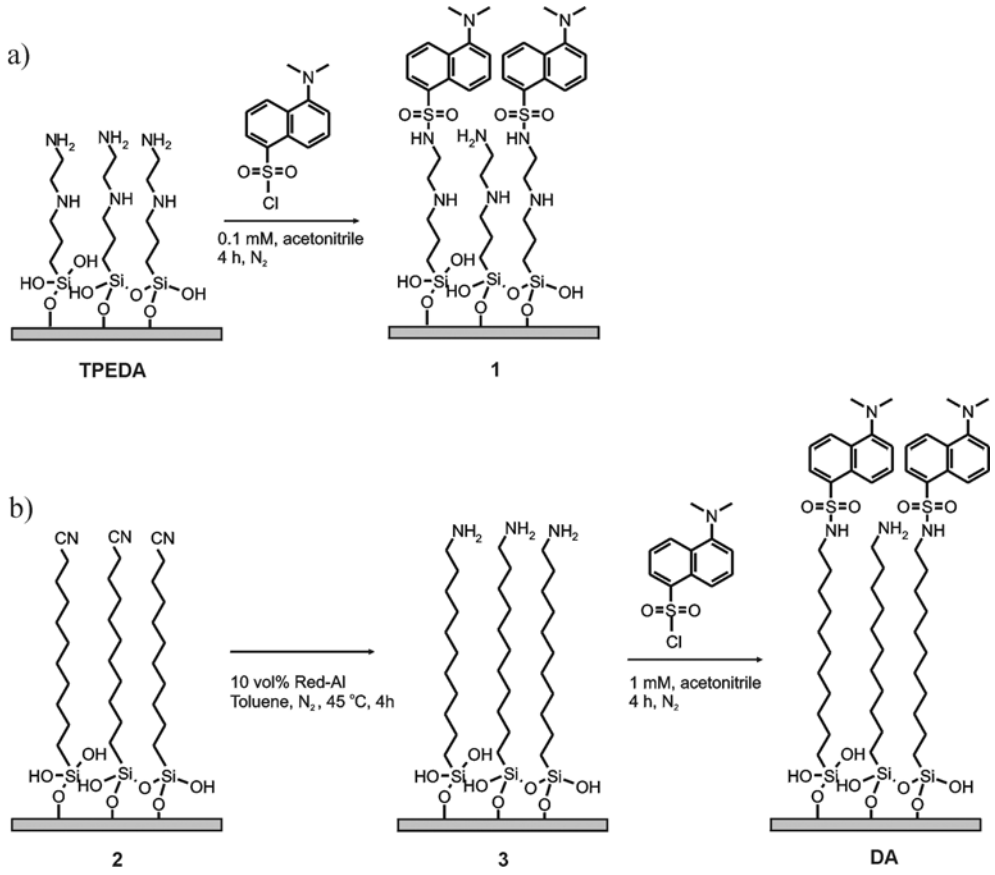

Figure 4.2. *Synthesis scheme for the preparation of the dansyl-substituted N-[3-(trimethoxysilyl) propyl] ethylenediamine SAM (**1**), and dansyl-substituted 1-amino-11-silylundecane SAM (**DA**) on silicon and glass surfaces for water stability testing.*

Dansyl-substituted 1-amino-11-silylundecane SAM ***DA*** (Figure 4.2) was fabricated starting from a SAM formed from 1-cyano-11-trichlorosilylundecane (***2***). Reduction of the cyano groups resulted in the amino-terminated monolayer ***3***. Reaction of ***3*** with dansylchloride afforded ***DA***. The dansyl-substituted SAM ***DA*** showed complete stability and integrity of the fluorescence signal in water at pH 7.0 (solution 0.1 M of HEPES buffer, organic buffer N-2-Hydroxyethylpiperazine-N'-2-ethanesulfonic acid) over at least 1 h (Figure 4.3). Furthermore, no fluorescence signal was detected in the

solution after removal of the functionalized slide from the spectrofluorometer cuvette ruling out the disassembly of the fluorescence material from the glass slide and the presence of physisorbed material. Consequently, monolayer ***3*** was used as starting material for the fabrication of the cation and anion sensing libraries in water.

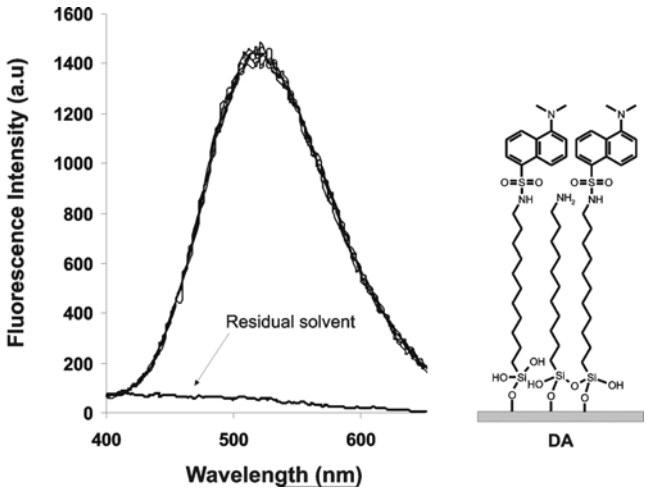

Figure 4.3. *Spectra of the* ***DA*** *SAM after 0, 3, 5, 10, 15, 30 and 60 min immersed in 0.1 M HEPES solution, and the spectrum of the residual solvent after removal of the functionalized glass slide from the spectrofluorometer cuvette.*

4.2.2. Cation sensing in water by self-assembled monolayers on glass

A small library of monolayers based on the functionalization of amino-terminated SAM ***3*** was made to test the response of different monolayers to metal cations in water.

Two binding molecules (benzenesulfonyl chloride and p-isopropylphenyl isocyanate) and three fluorophores (dansyl chloride, 7-dimethylaminocoumarin-4-acetic acid succinimidyl ester, and TAMRA (5-(and-6)-carboxytetramethylrhodamine, succinimidyl ester as mixed isomers) were sequentially reacted with the amino-terminated SAM ***3*** in different combinations, resulting in a library of nine sensing surfaces with different complexing functionality-fluorophore pairs (Figure 4.4). Each sensing layer has one complexing functionality known to bind to cations (i.e., amino (A),

aryl-urea (U), aryl-sulfonamide (S)) and one fluorophore (i.e., short excitation wavelength dansyl (D) or coumarin (C), or long excitation wavelength TAMRA (TM)).

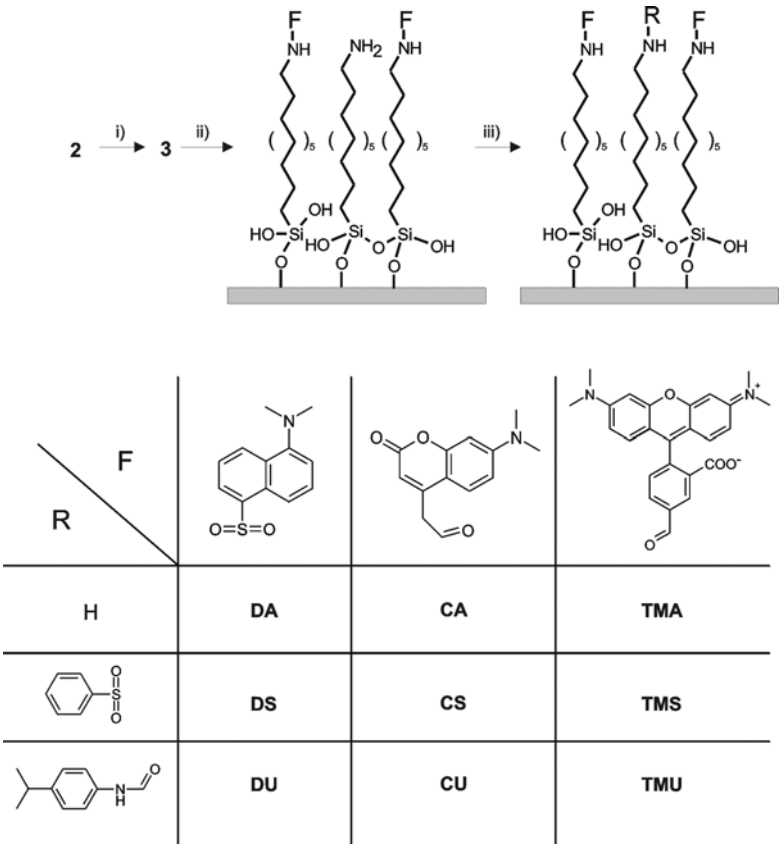

Figure 4.4. *Synthesis scheme for the preparation of the fluorescent SAMs (**DA**, **CA**, **TMA**, **DS**, **CS**, **TMS**, **DU**, **CU** and **TMU**) on glass and silicon surfaces. i) Red Al, toluene, 45°C, ii) dansyl chloride, 7-dimethylaminocoumarin-4-acetic acid succinimidyl ester, or 5-(and-6)-carboxytetramethylrhodamine, succinimidyl ester, acetonitrile, rt. iii) benzenesulfonyl chloride or p-isopropylphenyl isocyanate, acetonitrile, rt.*

The resulting modified layers were characterized by contact angle goniometry and ellipsometry measurements (for description of the contact angle and ellipsometry see Chapter 3) confirming the formation of the monolayers and the covalent linkage of the components. Contact angle and ellipsometry data are summarized in Table 4.1.

Table 4.1. *Advancing (θa) and receding (θr) water contact angles, ellipsometric thicknesses of the monolayers* ***2***, ***3***, ***DA***, ***DS***, ***DU***, ***CA***, ***CS***, ***CU***, ***TMA***, ***TMS***, ***TMU***, ***T0***, ***T1***, ***T2***.

SAM	***Ell. thickness (nm)***	***θa (°)***	***θr (°)***
2	1.44 ± 0.14	65 ± 3	50 ± 3
3	1.44 ± 0.16	60 ± 2	32 ± 6
DA	1.86 ± 0.24	65 ± 3	50 ± 3
DS	2.50 ± 0.37	69 ± 1	30 ± 8
DU	1.95 ± 0.14	67 ± 4	32 ± 6
CA	2.22 ± 0.38	71 ± 5	28 ± 1
CS	2.23 ± 0.34	73 ± 5	32 ± 9
CU	1.89 ± 0.17	70 ± 4	28 ± 1
TMA	1.23 ± 0.11	65 ± 3	35 ± 4
TMS	1.33 ± 0.16	68 ± 2	33 ± 6
TMU	1.57 ± 0.16	66 ± 1	30 ± 4
T0	2.2 ± 0.2	79 ± 6	46 ± 9
T1	*	77 ± 3	53 ± 5
T2	*	79 ± 3	50 ± 7

** Ellipsometry thickness was not measured*

Contact angle values for the cyano and amino-terminated monolayers ***2*** and ***3*** were in good agreement with previous reports in literature.[25] The modest hysteresis value (difference between advancing angle and receding angle values (θ_a-θ_r)) indicates a high order of the formed layer. For the rest of the layers (***DA***, ***DS, DU***, ***CA***, ***CS***, ***CU***, ***TMA***, ***TMS***, ***TMU***) the introduction of the fluorophores and the binding groups resulted in an increase of the disorder of the layers, as reflected in the increased hysteresis. The ellipsometric thickness measured for all the layers ranged from 1.4 and 2.5 nm respectively, in good agreement with the theoretical thickness of the monolayers based on CPK models. Fluorescence spectroscopy of the monolayers showed the characteristic emission peak of each fluorophore, sometimes slightly shifted by the introduction of the binding molecules on the monolayer. Figure 4.5 depicts the fluorescence spectra of the monolayers ***TMA***, ***TMS***, ***TMU***, ***DA***, ***DS***, ***DU***, ***CA***, ***CS*** and ***CU*** in 0.1 M HEPES solution.

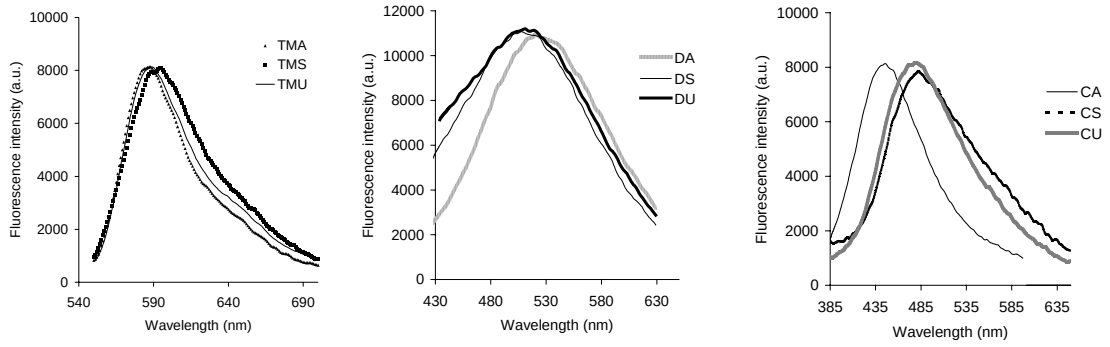

Figure 4.5. *Fluorescence spectra of the monolayers* ***TMA***, ***TMS***, ***TMU*** *(λ_{ex} = 545 nm),* ***DA***, ***DS***, ***DU*** *(λ_{ex} = 320 nm),* ***CA***, ***CS*** *and* ***CU*** *(λ_{ex} = 330 nm) in 0.1 M HEPES solution.*

Each layer was tested for signal stability prior to analyte addition (Figure 4.6). While dansyl layers (***DA***, ***DS*** and ***DU***) were immediately stable, coumarin and TAMRA layers (***CA***, ***CS***, ***CU***, ***TMA***, ***TMS*** and ***TMU***) required sonication in water and in the 0.1 M HEPES buffer to achieve stability. The most effective protocol to achieve stable coumarin and TAMRA layers involved 5 min of sonication in a 0.1 M HEPES solution (pH 7.0) followed by 5 min of sonication in water at 40 ^{o}C.[35] Following this methodology the stability of the siloxane monolayer attached to the glass slide and the absence of physisorbed material is assured.

After formation of the stable monolayers their cation sensing properties were studied. The chloride salts of Hg^{2+}, Ca^{2+}, Co^{2+} and Cu^{2+} were used as analytes. Each of the layers of the sensing library was placed in a spectrofluorometer cuvette filled with 0.1 M aqueous solution of HEPES buffer (pH 7.0) and the fluorescence spectrum was measured. A solution of the corresponding cation was added so that the concentration of the analyte in the cuvette was 10^{-4} M and the fluorescence spectrum was measured again. Two typical examples of the layer fluorescence emission spectra in the presence of analytes are shown in Figure 4.7.

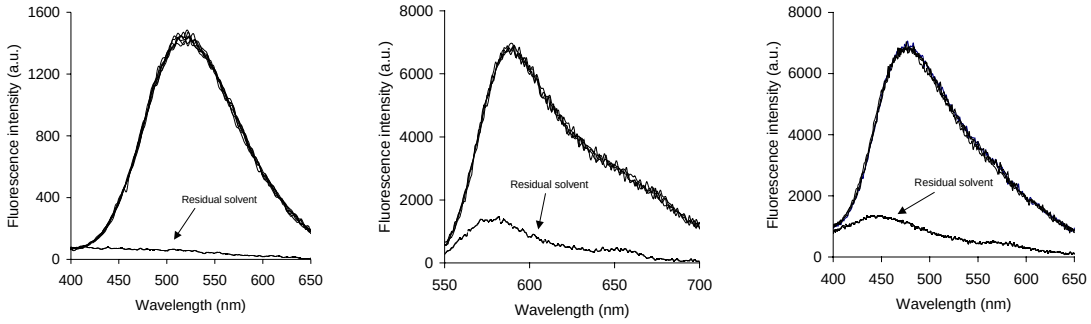

***Figure 4.6**: Fluorescence emission spectra of the **DA**, **TMA** and **CA** SAMs (from left to right) immersed in HEPES 0.1 M after 0, 3, 5, 10, 15, 30 and 60 min for layer **DA** and after 0, 3, 5, 10, 15 min for layers **TMA** and **CA**.*

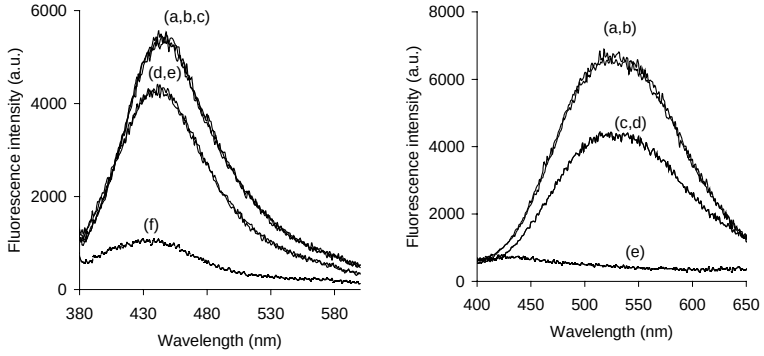

***Figure 4.7**. Left : Spectra of **CA** layer in 0.1 M HEPES solution (a), after 3 min. (b), after 5 min. (c), in 10^{-4} M aqueous solution of $HgCl_2$ (d), 3 min. later (e), and spectrum of the residual solvent after removal of the layer from the fluorescence cuvette (f). Right : Spectra of **DA** layer in 0.1 M HEPES solution (a), after 5 min. (b), in 10^{-4} M aqueous solution of $CuCl_2$ (c), 3 min. later (d), and spectrum of the residual solvent after removal of the layer from the fluorescence cuvette (e). Units of the y axis are counts per second (cps).*

Figure 4.8 shows the fluorescence response of all the layers to 10^{-4} M solutions of Hg^{2+}, Cu^{2+}, Co^{2+} and Ca^{2+} as chloride salts in water (pH 7.0, 0.1 M HEPES).

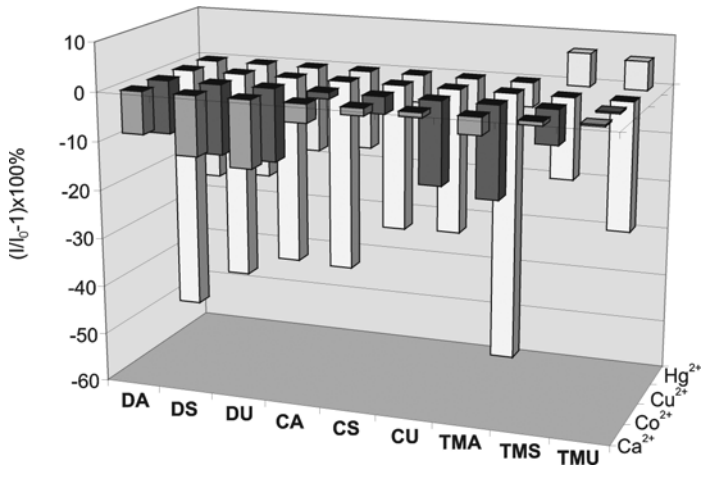

Figure 4.8. *Relative fluorescence intensity of* ***DA***, ***DS***, ***DU***, ***CA***, ***CS***, ***CU***, ***TMA*** *and* ***TMU*** *SAMs in the presence of 10^{-4} M solutions of Hg^{2+}, Cu^{2+}, Co^{2+} and Ca^{2+} as chloride salts in water (pH 7.0, 0.1 M HEPES). The data have been normalized, in the absence of metal cations the maximum fluorescence emission of each layer is set to 0. Positive values correspond to enhancement in the fluorescence emission intensity of the layer while negative values represent quenching of the fluorescence emission intensity of the layer.*

Looking at the library response as a whole, a few overall trends emerge. Among the four analytes the largest fluorescence response of all layers was to Cu^{2+} followed by Hg^{2+} and Ca^{2+}. When the influence of the different fluorophores (dansyl, coumarin and TAMRA) on the monolayer response is compared, the dansyl monolayers exhibit more fluorescence quenching than the monolayers with the other fluorophores. The quenching of the dansyl layers ***DA***, ***DS***, and ***DU*** in response to Ca^{2+} and Hg^{2+} were 9%, 12% and 14% for Ca^{2+}, and 25%, 24% and 18% for Hg^{2+}, respectively. For TAMRA and coumarin bearing layers the response for Ca^{2+} was in all cases lower than 4% fluorescence quenching. In the case of Hg^{2+} only layer ***CA*** showed a fluorescence quenching (16%), comparable with the response of dansyl monolayers to this metal ion. Within each fluorophore series, the effect of the individual complexing groups on the fluorescence response was evaluated. In the dansyl series, all three ligands gave similar responses to each particular analyte, which indicates that the dansyl group has a predominant influence on the analyte response and not the complexing functionality. Notice that when the sulfonyl chloride of the dansyl reacts with the amino-terminated surface a

sulfonamide bond is formed. This sulfonamide functionality is a good binding group for metal ions and may well be responsible of the higher affinity of the metal ions for the dansyl layers. In the coumarin and TAMRA series, the more varied responses illustrate cases where the presence of ligands influences the sensing (Figure 4.8).

There are a few overall trends when we compare the amino, sulfonamide, and urea functionalities and monitor the effect of the fluorophores on the response. For example, the amino layers consistently give a high response for Cu^{2+} for all three fluorophores, whereas not all of the sulfonamide and urea layers respond as strongly. Analysis of both the sulfonamide (***DS***, ***CS***, ***TMS***) and urea (***DU***, ***CU***, ***TMU***) series reveals that some analytes exhibit different responses for different fluorophores. For example the fluorescence of the layers ***DS*** is quenched 24 % in presence of Hg^{2+} while the layer ***CS*** shows a quenching of only 6 % for the same cation. In the same way the layer ***CU*** displayed a 17% quenching for Co^{2+} while layer ***TMU*** does not respond to the presence of Co^{2+}.

The analysis within the current library layers containing the TAMRA fluorophore TMA (amino functionality) and TMU (urea functionality) in the sensing of Ca^{2+}, Co^{2+} and Cu^{2+} offer some degree of comparison with the responses of their counterparts in acetonitrile from the previous library described in Chapter 3. Although direct correlations cannot be made due to differences in the length of the amino SAM upon which the sensing components are placed, as well as differences in counterion (chloride versus perchlorate), it can be noted that the overall responses were not as large as in the acetonitrile system, which is understandable due to the more polar environment as well as the presence of a high concentration of other charged species (the HEPES and NaOH)

Confirming the results shown in Chapter 3, the nature of the functionalities of the fluorophore and the other ligating functionalities seems to influence the sensing ability of the layer resulting in a range of responses to different analytes. Yet whether one component will be predominant in determining the fluorescence response or whether they will work together to form a unique sensing system is unpredictable. The unpredictability of what components will constitute a successful sensing layer underlines the power of utilizing a 2D combinatorial parallel approach to the discovery of successful sensing

systems in aqueous media. The library response towards metal cations can be used to search for either a unique response (individual "hit") or a whole "fingerprint" of responses. Here, the "fingerprint" is the collection of the individual responses of each sensing layer to one cation. Rapid inspection of the library "fingerprint" (Figure 4.9) provides a unique response for each cation.

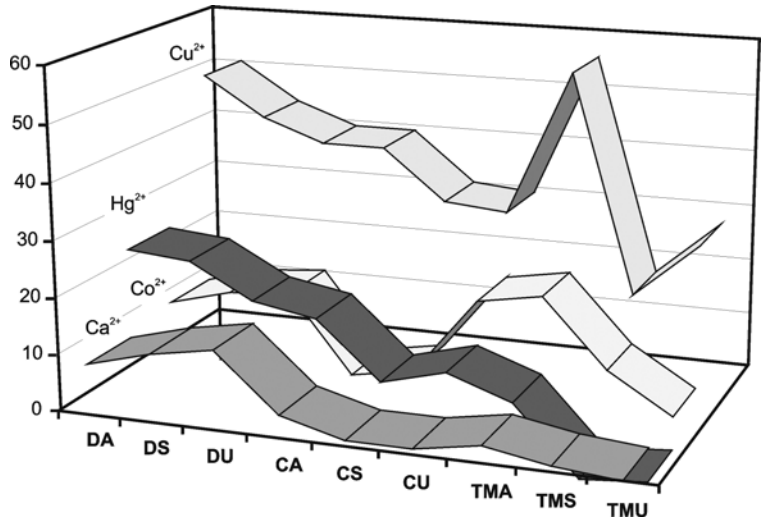

Figure 4.9. *Changes in fluorescence emission intensity of the layers* ***DA***, ***DS***, ***DU***, ***CA***, ***CS***, ***CU***, ***TMA***, ***TMS*** *and* ***TMU*** *in presence of 10^{-4} M Ca^{2+}, Hg^{2+}, Co^{2+} and Cu^{2+} chloride salts in 0.1 M HEPES (pH 7.0). Every line on the graph constitutes a unique "fingerprint" of each analyte. The y axis represents percentage of quenching of the initial fluorescence of the layer upon addition of the analyte. The data have been normalized, the maximum emission of the initial fluorescence of the layers before analyte addition has been set to 0 (see specific data in Figure 4.8).*

The detection limit and reusability of the layers functionalized with dansyl (***DA***, ***DS*** and ***DU***) and TAMRA (***TMA***, ***TMS***, ***TMU***) fluorophores were also studied. The layers exhibited responses to Cu^{2+} down to 10^{-6} M.[36] Furthermore, the sensitive surfaces are fully regenerated by rinsing the analyte away with 0.1M HCl aq. The layers were reused for at least four times without losing their characteristic response.

4.2.3. Anion sensing in water by self-assembled monolayers on glass

To broaden the scope of this methodology for the fabrication of new sensitive materials and to show its applicability for sensing of anions in water, three water stable sensitive monolayers were fabricated, ***T0***, ***T1*** and ***T2***. As in the sensing libraries shown before, the three monolayers are the result of sequential functionalization of the water stable amino-terminated monolayer ***3*** (see Figure 4.2) with a fluorophore and three different molecules with different complexing groups. The choice of the monolayer composition, i.e. fluorophore and anion binding groups is based on the library of anion sensing in acetonitrile presented in Chapter 3. The building blocks (fluorophore and binding molecule) of the layers which displayed the highest response to analytes were chosen. TRITC was chosen as fluorophore and as binding molecules phenyl isocyanate and benzoyl chloride were used, which after attachment to the amino SAMs will result in urea and amido functionalities, respectively. Layers ***T0***, ***T1*** and ***T2*** were prepared and their structures are depicted in Figure 4.10.

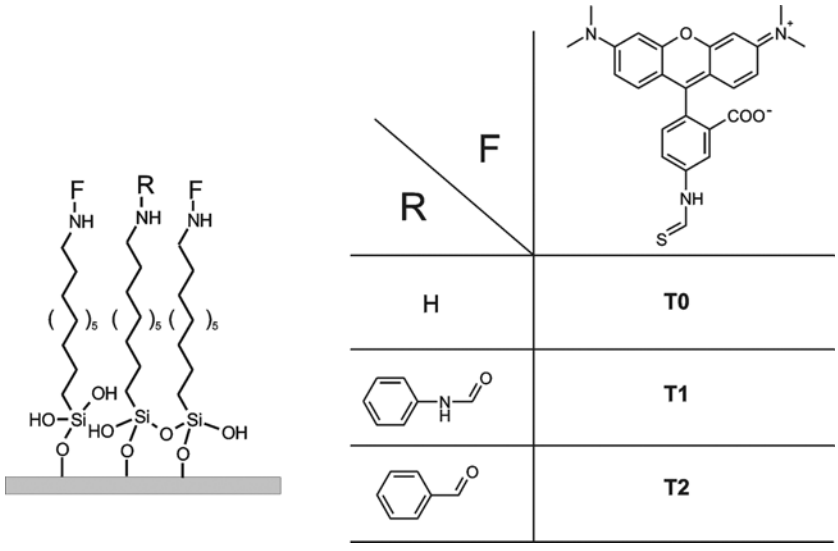

Figure 4.10. *Chemical structure of* ***T0, T1****,* ***T2*** *SAMs used for anion sensing in water.*

After formation of the monolayers the change of fluorescence intensity signal of each monolayer was measured in the presence of the sodium salts of NO_3^-, CH_3COO^- (AcO^-), SO_4^{2-} and HPO_4^{2-}.

Sensing anions in aqueous solutions is complicated by the fact that many anions are strong bases and have influence on the pH of the solution. To keep the solution at neutral pH, the organic buffer HEPES was used (pH = 7.0-8.0). Therefore, each of the layers of the sensing library was placed in a spectrofluorometer cuvette filled with 0.01 M aqueous solution of HEPES buffer (pH 7.2) and the fluorescence spectrum was measured. A solution of the corresponding anion was added so that the concentration of the analyte in the cuvette was 10^{-4} M and the fluorescence spectrum was measured again. The responses of the layers to the presence of the different analytes are graphically represented in Figure 4.11. Control experiments were performed to verify the reproducibility of the library and the changes of fluorescence intensity shown in the graph. The deviation of the measurements were found to be in a range of 0-4% of the absolute fluorescence intensity change value for all the layers.

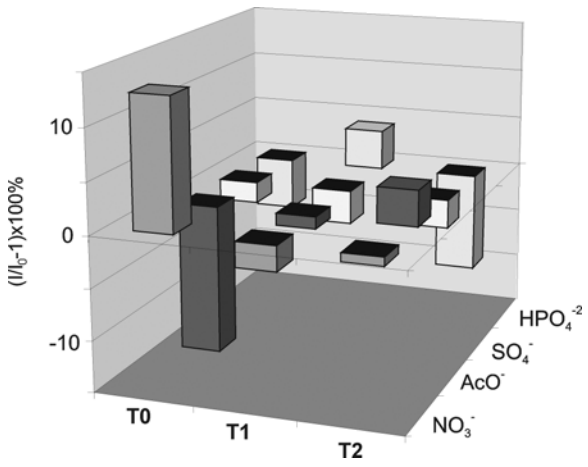

Figure 4.11. *Relative fluorescence intensity of surfaces modified with monolayer* ***T0****,* ***T1*** *and* ***T2*** *in the presence of 10^{-4} M solutions of NO_3^-, AcO^-, SO_4^{2-} and HPO_4^{2-} as sodium salts in water (pH 7.2, 0.01 M HEPES). The data have been normalized; in the absence of metal cations the maximum fluorescence emission of each layer is set to 0.*

The fluorescence responses of the layers to the anions were quite small. Changes ranging from 13 % enhancement to 15 % quenching were obtained. The overall largest response corresponds to ***T0*** in the presence of acetate, with a fluorescence quenching of 15 %, in contrast with the response of ***T1*** (1% quenching), and ***T2*** (3% fluorescence enhancement). ***T0*** showed the highest response to nitrate anions (13% fluorescent enhacement).

A drawback of the use of the buffer solution is that the solution contains additional charged species, which could complicate the sensing.[37-39] Sodium hydroxide is commonly used to adjust the pH of the buffer. The sodium cations could interact with the monolayers interfering in the anion sensing. To evaluate the effect of the sodium cations additional measurements were performed. The layers were tested in the presence of NO_3^-, AcO^-, SO_4^{2-} and HPO_4^{2-} tetrabutylammonium salts[40] in HEPES buffer. To adjust the buffer pH tetrabutylammonium hydroxide was used, avoiding sodium cations. Nevertheless no difference in the response of the layers was found compared with the case where sodium cations are present. Whether or not this specific buffer, HEPES, has an influence on the sensing process has not been determined.

The reason for the low responses is most probably that anions form a solvated complex in aqueous solutions, which is stable due to the formation of a hydrogen bond network, in contrast to the solvation shell of cations where only ion-dipole interactions play a role.[41] In organic solvents the solvating energy of anions is relatively small and electrostatic interaction to the monolayer is more effective, but in aqueous solvents there is strong competition between the solvation shell of the anion with water and the complexation of the anion with the monolayer.

Normally, anion sensing in water is hampered by the low selectivity and sensitivity of the developed probes. The approach presented here for anion sensing in water based on fluorescent sensitive monolayers is not necessarily limited by the unspecificity and low sensitivity of the systems. A large collection of sensitive SAMs may display a unique pattern of responses for each analyte or analyte mixture. Larger

numbers of sensitive systems that have a sensing monolayer library will increase the capacity to identify single analytes or mixtures of analytes.

4.3. Conclusions and outlook

We have demonstrated that commercially available fluorophores and simple, small, off-the-shelf molecules can be used to fabricate a cation and anion responsive library of SAMs on glass in aqueous solution. This is the first example of ion sensing in water by fluorescence of a SAM on a glass surface and shows that our original concept (see Chapter 3) is fully transferable to aqueous medium. Despite the modest response of the systems to anions, this type of sensing library based on monolayers appears as a highly useful probe for cation and anion sensing in water, since it is possible to get different fingerprint responses for different analytes. The monolayers show higher responses to cations than to anions, probably due to the lack of highly specific receptor sites which are necessary to overcome anion salvation in order to efficiently complex the anionic species.

Additionally we have shown that the stability of the monolayer in aqueous solution can be easily monitored by the covalent attachment of a fluorophore to a SAM on glass. This methodology could also be applied to assess the stability, in principle, of other SAMs used in biological and chemical sensing systems where knowledge of the stability of the monolayer or quantification of the molecular recognition event is required.

4.4. Experimental

Chemicals

Analytical reagent grade solvents were purchased from Fisher Scientific. Fluorophores TAMRA (5-(and-6)-carboxytetramethylrhodamine (5(6)-TAMRA) *mixed isomers*), Lissamine (Lissamine™ rhodamine B sulfonyl chloride *mixed isomers*), TRITC (tetramethylrhodamine-5-(and-6)-isothiocyanate (5(6)-TRITC) *mixed isomers*) were purchased from Molecular probes (Invitrogen). 1-cyano-11-trichlorosilylundecane was purchased from Gelest Inc. All other reagents were purchased from Sigma-Aldrich.

Monolayer preparation

All glassware used to prepare the monolayers was cleaned by sonicating for 15 minutes in a 2% v/v Hellmanex II solution in distilled water, rinsed four times with high purity (MilliQ, 18.2 MΩcm) water, and dried in an oven at 150º C. The substrates, quartz slides and silicon wafers (four-inch polished, 100 cut, p-doped silicon wafers), were cleaned for 15 minutes in piranha solution (concentrated H_2SO_4 and 33% aqueous H_2O_2 in a 3:1 ratio. Warning: Piranha solution should be handled with caution: it has been reported to detonate unexpectedly). They were then rinsed several times with high purity (MilliQ) water, and dried in a nitrogen stream immediately prior to performing the formation of the monolayer.

Amino-terminated monolayers (TPEDA and 3 SAMs)

For synthesis of ***TPEDA*** SAM see Chapter 3.

Formation of SAM ***3*** was achieved following a slightly modified protocol described previously by our group.[25] Substrates were submerged in a 0.1 vol.% solution of 1-cyano-11trichlorosilylundecane in freshly distilled toluene previously cooled in an ice bath to afford SAM ***2***. After 35 minutes at 0 ˚C they were removed and rinsed copiously with toluene, then dried in an air stream. Reduction of the cyano group was achieved by submerging the substrates in a 10 vol% solution of Red-Al in freshly distilled toluene under N_2 at 45 ˚C for 4h. The slides were removed and sonicated in a 1 M HCl solution for 5 min, then sonicated with 0.5 M NaOH for 1 min, followed by copious rinsing with millipore water and drying in an air stream.

Inmobilization of the fluorophore on the amino-terminated SAM ***3***. Synthesis of DA, CA, and TMA SAMs

Silicon and glass substrates functionalized with the amino-terminated monolayer 3 were submerged in 50 mL of a 1mM acetonitrile solution of fluorophore (dansyl chloride, 7-dimethylaminocoumarin-4-acetic acid succinimidyl ester, TAMRA (5-(and-6)-carboxytetramethylrhodamine, succinimidyl ester (5(6)-TAMRA, SE) *mixed isomers)) or TRITC (tetramethylrhodamine-5-(and-6)-isothiocyanate(5(6)-TRITC) *mixed isomers) with 100μL Et_3N for 4h under N_2. After the substrates were removed from the fluorophore solution then they were rinsed sequentially with acetonitrile, ethanol and dichloromethane to remove physisorbed material and dried in an air stream.

Immobilization of the binding groups on the surface

Synthesis of DS, DU, CS, CU, TMS and TMU SAMs

Silicon and glass substrates with previously immobilized fluorescent SAM, DA, CA or TMA were submerged in 50 mL of a 50 mM acetonitrile solution of benzenesulfonyl chloride or p-isopropylphenyl isocyanate to yield DS, CS or TMS and DU, CU, and TMU, respectively. In the case of benzenesulfonyl chloride, 100μL Et_3N was added. The reaction took place under N_2 for 16h, at which time the substrates were then sequentially rinsed in acetonitrile, ethanol and dichloromethane to remove physisorbed material, and dried in an air stream.

Synthesis of the layers T1 and T2

Silicon and glass substrates with previously immobilized fluorescent SAM T0, were submerged in 50mL of a 50 mM chloroform solution of phenyl isocianate to yield layer T1, or benzoylchloride to yield the layer T2. 100μL Et_3N was added to the solution in order to prevent protonation of the amines. The reaction took place under N_2 for 16h, at which time the substrates were then sequentially rinsed in chloroform, ethanol and dichloromethane to remove physisorbed material, and dried in an air stream.

Characterization of the layers

For a detailed description of the ellipsometry, contact angle goniometry and spectrofluorometer set up see Chapter 3.

Spectrofluorometric measurements

For a detailed description of the spectrofluorometer set up and cleaning procedure for the spectrofluorometer cuvettes see Chapter 3.

For the measurement of the fluorescence spectra of the fluorescence monolayer and the changes produced upon addition of the analytes the following protocol was followed. Ultrapure (MilliQ) water at pH 7.0 (for cation sensing) or pH 7.2 (for anion sensing) (HEPES) was added to the freshly cleaned spectrofluorometric cuvettes, the functionalized quartz slide (H x W x D, 40 mm x 17 mm x 1 mm) was placed at an angle of 45° in the cuvette, and the cuvette placed in a holder on an externally turnable platform. Normally an angle between -10° and -20° was used for the measurements. For dansyl and coumarin a 375 nm filter was used, for TAMRA and TRITC a 550 nm filter was used. Excitation wavelengths were 340 nm for dansyl, 330 nm for coumarin, 535 nm for TAMRA and 537 nm or 549 nm (for T0 system and T1 or T2 respectively) for TRITC. The analytes used were chloride salts of Hg^{2+}, Ca^{2+}, Cu^{2+}, and Co^{2+}, sodium salts of NO_3^-, AcO^-, SO_4^{2-} and HPO_4^{2-} and tetrabutylamonium salts of NO_3^- and AcO^-. For each analyte, two measurements were first taken in the absence of analyte to ensure layer stability. A solution of the cation was added so that the concentration of the analyte in the cuvette was 10^{-4} M, and a spectrum taken after one minute. An additional spectrum was taken two minutes later to detect any additional changes. The slide was then removed and a spectrum of the solvent was measured. The individual fluorescence values given in the text are the average of between two and six measurements (for error analysis see Appendix 4).

4.5. References and notes

1 Crego-Calama, M.; Reinhoudt, D. N. New Materials for Metal Ion Sensing by Self-Assembled Monolayers on Glass. *Adv. Mater.* ***2001***, 13(15), 1171-1174.

2 Basabe-Desmonts, L.; Beld, J.; Zimmerman, R. S.; Hernando, J.; Mela, P.; García-Parajó, M. F. G.; Van Hulst, N. F.; Van den Berg, A.; Reinhoudt, D. N.; Crego-Calama, M. A Simple Approach to Sensor Discovery and Fabrication on Self-Assembled Monolayers on Glass. *J. Am. Chem. Soc.* ***2004***, 126(23), 7293-7299.

3 Cooper, M. A. Label-Free Screening of Bio-Molecular Interactions. *Anal. Bioanal. Chem.* ***2003***, 377(5), 834-842.

4 Zeng, H. H.; Thompson, R. B.; Maliwal, B. P.; Fones, G. R.; Moffett, J. W.; Fierke, C. A. Real-Time Determination of Picomolar Free Cu(II) in Seawater Using a Fluorescence Based Fiber Optic Biosensor. *Anal. Chem.* ***2003***, 75(24), 6807-6812.

5 O'Connell P.J.; Guilbault G.G. Sensors and Food Quality. *Sens. Update* ***2001***, 9(1), 255.

6 Jiang, P. J.; Guo, Z. J. Fluorescent Detection of Zinc in Biological Systems: Recent Development on the Design of Chemosensors and Biosensors. *Coord. Chem. Rev.* ***2004***, 248(1-2), 205-229.

7 Czarnik, A. W. Desperately Seeking Sensors. *Chemistry & Biology* ***1995***, 2 (7), 423-428.

8 Kaifer, A. E. Functionalized Self-Assembled Monolayers Containing Preformed Binding Sites. *Isr. J. Chem.* ***1996***, 36(4), 389-397.

9 Wasserman, S. R.; Tao, Y. T.; Whitesides, G. M. Structure and Reactivity of Alkylsiloxane Monolayers Formed by Reaction of Alkyltrichlorosilanes on Silicon Substrates. *Langmuir* ***1989***, 5(4), 1074-1087.

10 Bierbaum, K.; Kinzler, M.; Woll, C.; Grunze, M.; Hahner, G.; Heid, S.; Effenberger, F. A Near-Edge X-Ray-Absorption Fine Structure Spectroscopy and X-Ray Photoelectron-Spectroscopy Study of the Film Properties of Self-Assembled Monolayers of Organosilanes on Oxidized Si(100). *Langmuir* ***1995***, 11(2), 512-518.

11 Wang, Z. H.; Jin, G. Silicon Surface Modification with a Mixed Silanes Layer to Immobilize Proteins for Biosensor with Imaging Ellipsometry. *Colloids Surf., B* ***2004***, 34(3), 173-177.

12 Flink, S.; Van Veggel, F. C. J. M.; Reinhoudt, D. N. Sensor Functionalities in Self-Assembled Monolayers. *Adv. Mater.* ***2000***, 12(18), 1315-1328.

13 Gooding, J. J.; Mearns, F.; Yang, W. R.; Liu, J. Q. Self-Assembled Monolayers Into the 21(St) Century: Recent Advances and Applications. *Electroanalysis* ***2003***, 15(2), 81-96.

14 Haes, A. J.; Van Duyne, R. P. A Nanoscale Optical Blosensor: Sensitivity and Selectivity of an Approach Based on the Localized Surface Plasmon Resonance Spectroscopy of Triangular Silver Nanoparticles. *J. Am. Chem. Soc.* ***2002***, 124(35), 10596-10604.

15 Brockman, J. M.; Nelson, B. P.; Corn, R. M. Surface Plasmon Resonance Imaging Measurements of Ultrathin Organic Films. *Annu. Rev. Phys. Chem.* ***2000***, 51, 41-63.

16 Bernhardt, P. V.; Moore, E. G. Functionalized Macrocyclic Compounds: Potential Sensors of Small Molecules and Ions. *Aust. J. Chem.* ***2003***, 56(4), 239-258 .

17 de Silva, A. P.; Gunaratne, H. Q. N.; Gunnlaugsson, T.; Huxley, A. J. M.; McCoy, C. P.; Rademacher, J. T.; Rice, T. E. Signaling Recognition Events with Fluorescent Sensors and Switches. *Chem. Rev.* ***1997***, 97(5), 1515-1566.

18 Ambler, S. K.; Poenie, M.; Tsien, R. Y.; Taylor, P. Agonist-Stimulated Oscillations and Cycling of Intracellular Free Calcium in Individual Cultured Muscle-Cells. *J. Biol. Chem.* ***1988***, 263(4), 1952-1959.

19 Dulkeith, E.; Morteani, A. C.; Niedereichholz, T.; Klar, T. A.; Feldmann, J.; Levi, S. A.; Van Veggel, F. C. J. M.; Reinhoudt, D. N.; Moller, M.; Gittins, D. I. Fluorescence Quenching of Dye Molecules Near Gold Nanoparticles: Radiative and Nonradiative Effects. *Physical Review Letters* ***2002***, 89(20).

20 Netzer, L.; Sagiv, J. A New Approach to Construction of Artificial Monolayer Assemblies. *J. Am. Chem. Soc.* ***1980***, 105(3), 674-676.

21 Chen, G. Y. J.; Uttamchandani, M.; Zhu, Q.; Wang, G.; Yao, S. Q. Developing a Strategy for Activity-Based Detection of Enzymes in a Protein Microarray. *Chembiochem* ***2003***, 4(4), 336-339.

22 Ferguson, J. A.; Steemers, F. J.; Walt, D. R. High-Density Fiber-Optic DNA Random Microsphere Array. *Anal. Chem.* ***2000***, 72(22), 5618-5624.

23 Lynch, M.; Mosher, C.; Huff, J.; Nettikadan, S.; Johnson, J.; Henderson, E. Functional Protein Nanoarrays for Biomarker Profiling. *Proteomics* ***2004***, 4 (6), 1695-1702.

24 Flink, S.; Van Veggel, F. C. J. M.; Reinhoudt, D. N. A Self-Assembled Monolayer of a Fluorescent Guest for the Screening of Host Molecules. *Chem. Commun.* ***1999***, (21), 2229-2230.

25 Onclin, S.; Mulder, A.; Huskens, J.; Ravoo, B. J.; Reinhoudt, D. N. Molecular Printboards: Monolayers of Beta-Cyclodextrins on Silicon Oxide Surfaces. *Langmuir* ***2004***, 20(13), 5460-5466.

26 Van der Veen, N. J. ; Onclin, S.; Deij, M. A.; Flink, S.; Van Veggel, F. C. J. M.; Reinhoudt, D. N. Monolayers on Glass for Optical Sensing of Metal Ions. *Abstracts of Papers of the American Chemical Society* ***2000***, 220, U262.

27 Zheng, Y.; Orbulescu, J.; Ji, X.; Andreopoulos, F. M.; Pham, S. M.; Leblanc, R. M. Development of Fluorescent Film Sensors for the Detection of Divalent Copper . *J. Am. Chem. Soc.* ***2003***, 125(9), 2680-2686.

28 Montalti, M.; Prodi, L.; Zacheroni, N.; Zattoni, A.; Reschiglian, P.; Falini, G. Energy Transfer in Fluorescent Silica Nanoparticles. *Langmuir* ***2004***, 20(7), 2989-2991.

29 Brasola, E.; Mancin, F.; Rampazzo, E.; Tecilla, P.; Tonellato, U. A Fluorescence Nanosensor for Cu^{2+} on Silica Particles. *Chem. Commun.* ***2003***, (24), 3026-3027.

30 Balachander, N.; Sukenik, C. N. Monolayer Transformation by Nucleophilic-Substitution - Applications to the Creation of New Monolayer Assemblies. *Langmuir* ***1990***, 6(11), 1621-1627.

31 Vallant, T.; Kattner, J.; Brunner, H.; Mayer, U.; Hoffmann, H. Investigation of the Formation and Structure of Self-Assembled Alkylsiloxane Monolayers on Silicon Using in Situ Attenuated Total Reflection Infrared Spectroscopy. *Langmuir* ***1999***, 15(16), 5339-5346.

32 Liebmannvinson, A.; Lander, L. M.; Foster, M. D.; Brittain, W. J.; Vogler, E. A.; Majkrzak, C. F.; Satija, S. A Neutron Reflectometry Study of Human Serum Albumin Adsorption in Situ. *Langmuir* ***1996***, 12(9), 2256-2262.

33 Heise, A.; Menzel, H.; Yim, H.; Foster, M. D.; Wieringa, R. H.; Schouten, A. J.; Erb, V.; Stamm, M. Grafting of Polypeptides on Solid Substrates by Initiation of N-Carboxyanhydride Polymerization by Amino-Terminated Self-Assembled Monolayers. *Langmuir* ***1997***, 13(4), 723-728.

34 Fryxell, G. E.; Rieke, P. C.; Wood, L. L.; Engelhard, M. H.; Williford, R. E.; Graff, G. L.; Campbell, A. A.; Wiacek, R. J.; Lee, L.; Halverson, A. Nucleophilic Displacements in Mixed Self-Assembled Monolayers. *Langmuir* ***1996***, 12(21), 5064-5075.

35 The sonication protocol may change depending on the layer composition. After sonication the fluorescence signal of the glass slides and the residual signal in the solvent are measured to check the absence of physisorbed material. The layers were cleaned until stabilization occurred and only minimal signal was seen in the residual solvent.

36 Due to the relatively low magnitude of fluorescence response across the library for Co^{2+}, Hg^{2+} and Ca^{2+} at 10^{-4} M, measurements with these cations were not taken at lower concentrations.

37 Han, M. S.; Kim, D. H. Naked-Eye Detection of Phosphate Ions in Water at Physiological Ph: a Remarkably Selective and Easy-to-Assemble Colorimetric Phosphate-Sensing Probe. *Angew. Chem., Int. Ed.* ***2002***, 41(20), 3809-3811.

38 Palomares, E.; Vilar, R.; Green, A.; Durrant, J. R. Alizarin Complexone on Nanocrystalline Tio2: a Heterogeneous Approach to Anion Sensing. *Adv. Funct. Mater.* ***2004***, 14(2), 111-115.

39 Mizukami, S.; Nagano, T.; Urano, Y.; Odani, A.; Kikuchi, K. A Fluorescent Anion Sensor That Works in Neutral Aqueous Solution for Bioanalytical Application. *J. Am. Chem. Soc.* ***2002***, 124(15), 3920-3925.

40 Tetrabutylammonium salts were used because the layers ***TM0***, ***L0***, and ***T0*** (described in chapter 3) do not respond to the presence of tetrabutylamonium prechlorate salt in acetonitrile, the bulky nature of the tetrabutyl amonium salt prevents from interaction with the layer.

41 Shriver, D. F.; Atkins, P. W.; Langford, C. H. *Inorganic Chemistry 2nd Edition, Oxford University Press, Oxford* ***1994***.

Appendix 4

A4.1. Error analysis

A detailed statistical error analysis of the fluorescence responses of the layers ***DA***, ***DS***, ***DU***, ***CA***, ***CS***, ***CU***, ***TMA***, ***TMS***, ***TMU*** in the presence of the metal cations at 10^{-4} M concentration is shown below. Every data point represents the average of between two and six measurements.

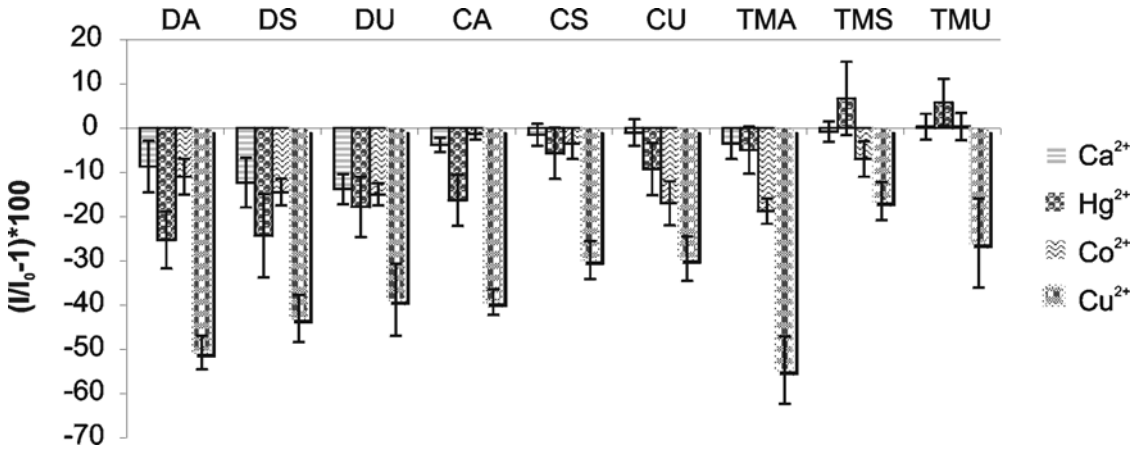

Chapter 5

Cross-Reactive Metal Ion Sensor Array Based on SAMs in a Microtiter-Plate Format*

The novel approach for the fabrication of fluorescent probes for ion sensing based on sensing self-assembled monolayers (SAMs) described in Chapters 3 and 4 has been used to fabricate a cross-reactive array in a microtiter-plate format. A collection of sensing monolayers generated by combinatorial methods has been immobilized on the glass surfaces of a custom-made 140 well microtiter-plate. This SAMs library constitutes a series of unspecific sensing probes. The unselective responses of the library to the presence of different cations generate a characteristic pattern for each analyte, a "finger print" response, which was imaged by confocal microscopy and fluorescence laser scanning. The power and utility of this new fluorescent array fabrication and detection methodology is demonstrated in this chapter for the analysis of Cu^{2+}, Co^{2+}, Pb^{2+}, Ca^{2+} and Zn^{2+}.

*Basabe-Desmonts, L.; Zimmerman, R. S.; Van der Baan F.; Reinhoudt, D. N.; Crego-Calama, M. Manuscript in preparation

5.1. Introduction

Despite several decades of research in optical sensor technology, there is still a substantial need for new sensing materials that can be applied for environmental contaminants, the food industry and in medical analysis.[1] The conventional approach to chemical sensing is to prepare a different sensor for each analyte of interest (one sensor – one analyte approach). It is inspired by the "lock and key" paradigm of molecular recognition.[2] This approach however has many drawbacks. First, the need to create absolute selectivity for analytes is a difficult task and even harder when the analytes are structurally very similar. Significant rational design and computer modeling, as well as trial and error testing has to take place to optimize the ability of the receptor to recognize the guest. Second, the number of sensors grows linearly with the numbers of analytes being measured. An emerging, different approach is the fabrication of cross-reactive sensor arrays.[3,4] These sensors are inspired by the mammalian natural way of sensing, the olfactory system. In the olfactory system, a limited number of cross-reactive receptors that are not highly selective generate a response pattern that is perceived by the brain as a particular odor.[5,6] It is the collection of non-specific receptors that signals the presence of an odor and creates a neuronal response pattern.[7] The large number of response pattern combinations leads to a broadly responsive system able to recognize and detect thousands of distinct odors, including complex mixtures.[8,9] The number of odors that can be detected is limited only by the number of unique receptor patterns that can be generated and recognized. Similar to the sense of smell, the sense of taste occurs as a result of complex chemical analysis that is completed in a parallel fashion at a series of chemical active sites (taste buds).[10]

Inspired by this natural process, chemists have developed artificial cross-reactive sensors known nowadays as artificial noses[6,8] and artificial tongues.[11,12] These sensors are composed of an array of sensing systems which are not highly selective. Identification of the analytes is achieved by recognition of different response patterns using models for data evaluation or neural networks.[13,14]

The evolution from the "lock and key" principle to differential or general sensing has been recently reviewed by Anslyn and coworkers.[15] Different sensing schemes have

been used to approach the fabrication of effective cross-reactive sensors. Since 1982, when Persaud and Dodd reported an approach to chemical sensing based on arrays of cross-reactive conductive polymer sensors,[16] a variety of arrays have been fabricated employing different chemical interaction strategies such as the use of conductive polymers,[17] conductive polymer/carbon-black composites,[18] modified tin oxide sensors,[19,20] polymer coated surface acoustic wave devices,[21,22] quartz crystal microbalances,[23] dye-doped polymer matrixes,[24-27] colorimetric vapor sensors based on vapor-phase interactions with metalloporphyrins immobilized in thin layers of silica-gel,[12,28] and colorimetric and fluorescence changes to receptor and indicator molecules that are covalently attached to polymeric microspheres contained in micro machined cavities.[29] Even an optical imaging fiber-based recombinant bacterial biosensor has been demonstrated.[30] It is composed of an array of thousands of individual bacteria cells expressing a reporter gene that responds to the presence of environmental pollutants. Each microwell at the tip of a fiber was used to accommodate a single living bacterium, allowing simultaneous monitoring of the genetic responses of all the cells in the array.

The potential of organic monolayers (SAMs) as sensing interfaces for array fabrication has been outlined by Crooks in 1997.[21] The application of SAMs for optical sensing of metal cations and inorganic anions in organic and aqueous solvents has been recently reported by our group.[31-33] The synthetic flexibility of the organic monolayers implies that they can be tailored to exhibit a high level of chemical independence and structural order. That is, that each individual type of monolayer responds to an analyte or class of analytes in a manner distinct from other monolayers used in the array. Thanks to the inexpensive procedures to create these materials, families of materials with a range of chemical properties for analyte recognition can be easily generated using simple combinatorial methods. Thicker materials such as polymers provide a much larger quantity of receptors than SAMs, which have a limited number of receptors inherent to the monolayer in which they are confined. Thus, polymers-based optical sensors have an enhanced sensitivity compared to monolayers-based optical sensors,[34] but they have a limiting factor for response rate of the signaling process, which is the chemical and physical permeability of the material; they are commonly inappropriate for time-sensitive

applications.[34] SAMs generally provide very fast responses since all the receptors are exposed to the surface liquid interface.

In this chapter a cross-reactive metal ion sensor array in a microtiter-plate format is described. The microarray sensor is based on the sensing approach described in Chapters 3 and 4. It makes use of SAMs on glass that contain rather unspecific metal ion probes and fluorescent molecules. The fluorescence of the different monolayers is modulated upon analyte addition allowing for generation of sensing SAMs libraries. Generally, these sensitive materials are not highly selective, which makes them good candidates for the fabrication of cross-reactive array-based sensor devices.

An ideal sensor preferentially is based on simple preparation procedures and simple analysis technology to minimize time, effort and cost. To maximize the sensor efficiency, the boundaries of the array were chosen as follows. Fluorophores as reporters with similar excitation and emission wavelength, direct fabrication of the sensitive monolayer array on a custom designed microtiter-plate (MTP), and the use of imaging (either by confocal microscopy or fluorescence laser scanners) which allows for fast discrimination between analytes by simple image comparison. The physical immobilization of the sensing layers in the wells of an MTP enables straightforward preparation of the arrays. Furthermore, the arrays can be conveniently stored, and after rinsing away the analytes the array can be regenerated and reused. Finally standard MTPs enable the rapid screening of large sets of libraries.[26,35]

The power of this novel method for array fabrication and detection is demonstrated in this chapter for the analysis of different metal cations. The overall unselective responses of the array in the presence of cations generates a characteristic fluorescent pattern for each analyte, which is imaged by confocal microscopy and by laser confocal fluorescence scanning in a commercial microarray reader.

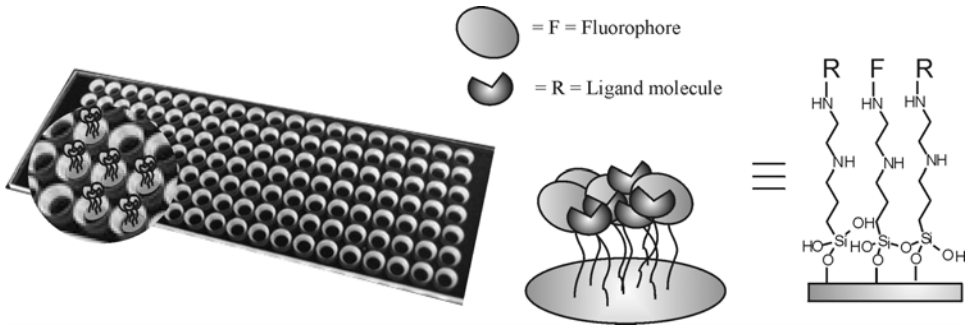

Figure 5.1. *Picture of the 140 well glass microtiter-plate (MTP) and schematic representation of the self-assembled monolayers formed in each well of the MTP.*

5.2. Results and discussion

5.2.1. Synthesis of the fluorescent monolayer array

A collection of 21 sensitive monolayers, generated by parallel combinatorial methods, has been immobilized on glass surfaces of the different wells of a custom-made MTP (Figure 5.1). The MTP was custom designed with dimensions of 75 x 25 mm^2 to allow analysis of the array by commercial fluorescence microarray scanners. It contains 140 wells, of 3 mm diameter which can be filled with a volume up to 7 μL. The glass bottom plate thickness is only 175 μm in order to allow confocal microscopy imaging (Figure 5.2).

Similarly, as described in Chapters 3 and 4, the general procedure for the fabrication of the sensing monolayers on the glass surface of the wells involves the functionalization of the MTP surface with the amino terminated SAM ***TPEDA*** and its sequential modification with a different fluorophore-complexing molecule pair in each well (Figure 5.3). Commercially available amino reactive fluorescent probes (λ_{ex}= 500-550 nm, λ_{em}>550 nm) and complexing functionalities were used, allowing the direct covalent attachment of the array building blocks to the MTP wells (Figure 5.3).

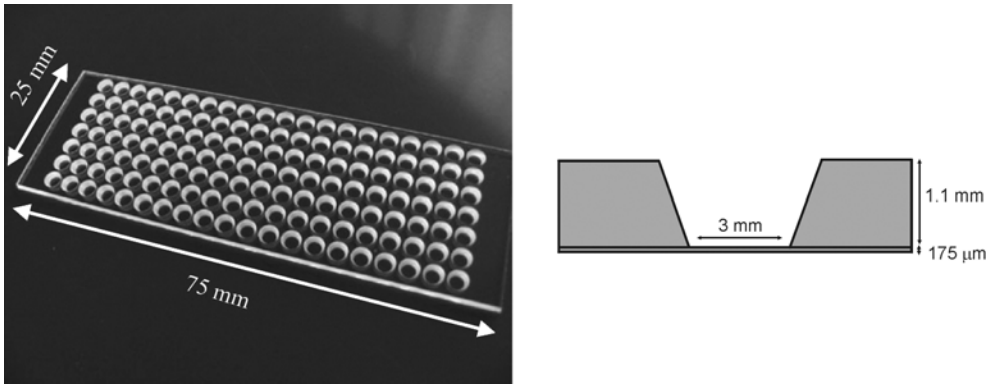

Figure 5.2. *Custom designed 140 well glass microtiter-plate (left) and schematic representation of the wells dimensions (right).*

Scheme 5.1 depicts the three step synthesis and distribution of the parallel combinatorial library of sensing monolayers in the MTP wells. First the amino terminated monolayer A (***TPEDA*** in Figure 5.3) is formed by silylation of the well glass surface by immersion of the MTP in a solution of N-[3-(trimethoxysilyl)propyl]ethylenediamine) in toluene. Sequentially three acetonitrile solutions each containing a different amino reactive fluorophore, TAMRA (TM), TRITC (T), or Lissamine (L) (see chemical structures in Figure 5.4), were pipetted on different columns of the MTP affording fluorescent monolayers ***TM0***, ***T0***, and ***L0***. Six solutions, each containing a different amino reactive binding molecule (1-6), *p*-isopropyl phenyl isocyanate, hexyl isocyanate, phenyl isothiocyanate, hexanoyl chloride, *p*-propyl benzoyl chloride and phenyl isocyanate, were pipetted in different rows. The covalent attachment of the complexing groups onto the fluorescent monolayers results in an array of 21 different sensitive monolayers[36] (***TM0-TM6***, ***T0-T6***, ***L0-L6***). No complexing molecule was added onto the top row, therefore the layers ***TM0***, ***L0***, ***T0***, contain amino groups as coordinating functionalities. The chemical composition of the resulting monolayer library is depicted in Figure 5.4.

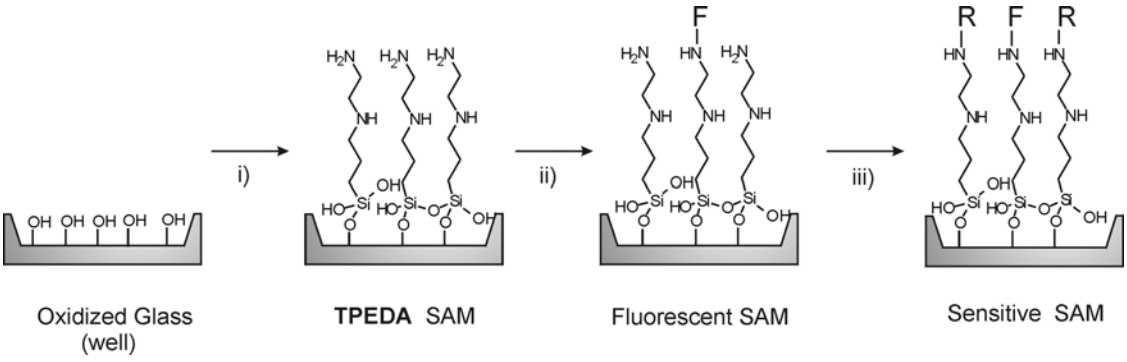

Figure 5.3. *Synthetic scheme of the formation of the sensing SAMs on the MTP wells. i) N-[3-(trimethoxysilyl)propyl]ethylenediamine, toluene, rt, 3.5 h, ii) amino reactive fluorophore (F): Lissamine rhodamine B sulfonyl chloride, 5-(and-6)-carboxytetramethylrhodamine, succinimidyl ester (5(6)-TAMRA, SE) or tetramethylrhodamine-5-(and-6)- isothiocyanate (5(6)-TRITC), acetonitrile, rt, 4 h and iii) isocyanates, thioisocyanates or acid chlorides used as complexing molecules (R), acetonitrile, rt, 16 h.*

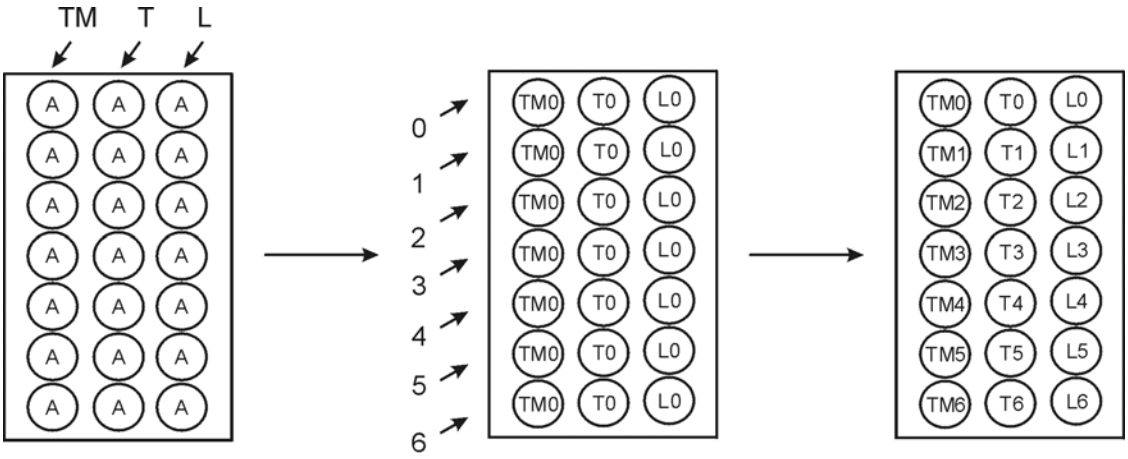

Scheme 5.1. *Schematic representation of the monolayer library synthesis (**TM0**-**TM6**, **T0**-**T6**, **L0**-**L6**) in a microtiter-plate. Three different acetonitrile solutions containing each a different fluorophore, TAMRA (TM), TRITC (T), or Lissamine (L) are pipetted in the wells of three consecutive columns of a MTP coated with **TPEDA** monolayer (A in this figure). Subsequently, six solutions (1-6) containing each a different complexing molecule are pipetted in consecutive rows. No complexing molecule is added onto the top row (wells **TM0**, **L0**, **T0**).*

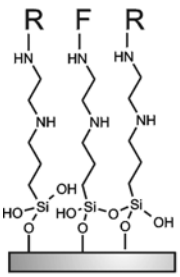

R \ F			
H	TM0	T0	L0
	TM1	T1	L1
	TM2	T2	L2
	TM3	T3	L3
	TM4	T4	L4
	TM5	T5	L5
	TM6	T6	L6

Figure 5.4. *Chemical composition of the library of fluorescent SAMs (**TM0-TM6, L0-L6, T0-T6**) prepared on the MTP glass surface.*

To avoid contamination with unwanted fluorophores and capping molecules from neighboring wells, the MTP was rinsed after each synthetic step with propylamine (0.1 M, acetonitrile) to remove the reactant excess. Figure 5.5 shows the fluorescence microscopy images of two neighboring wells, one functionalized with ***L0*** SAM (Figure 5.5), and the other functionalized only with ***TPEDA*** SAM (Figure 5.5). The images clearly show that the fluorophores have not spread to neighboring wells after this rinsing procedure (see experimental part).

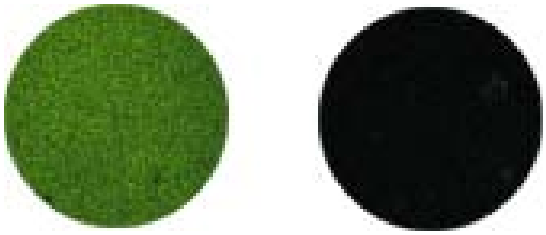

Figure 5.5. *Fluorescence microscope images of two neighboring wells functionalized with* ***L0*** *SAM (left) and* ***TPEDA*** *SAM (right), after rinsing the MTP with propylamine.*

To facilitate the data quantification the MTP was divided in two parts (Figure 5.6). In both parts an identical monolayer library was made. The first part was used as a reference and the second part, the analysis library, was incubated with the corresponding analyte solutions. The fluorescence intensity of both libraries was subsequently measured.

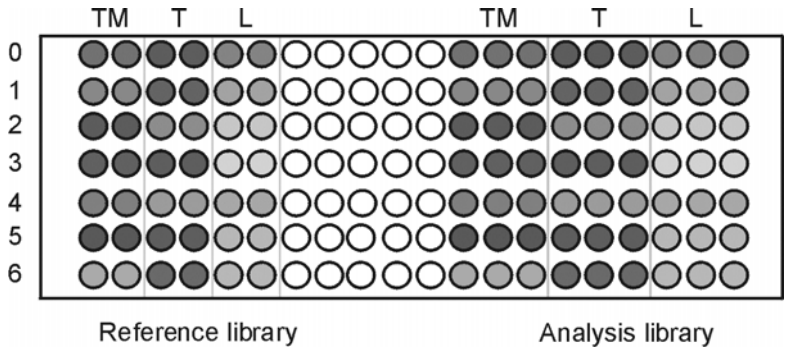

Figure 5.6. *Schematic representation of the functionalized MTP showing two identical monolayer libraries (reference library and analysis library) in the MTP wells. Fluorophores (TM, T, and L) and complexing molecules (1-6) were distributed in the* ***TPEDA*** *functionalized MTP as indicated resulting in 21 different monolayers.*

To control the reproducibility of the measurement and the quality of the data, every monolayer in the analysis library was made in triplicate (in consecutive wells) and in duplicate in the reference library. In total 105 wells were functionalized with 21

different sensing systems. Figure 5.7 shows the plot of the fluorescence intensity of each system (in triplicate). Analysis of the data indicated good inter-well reproducibility.

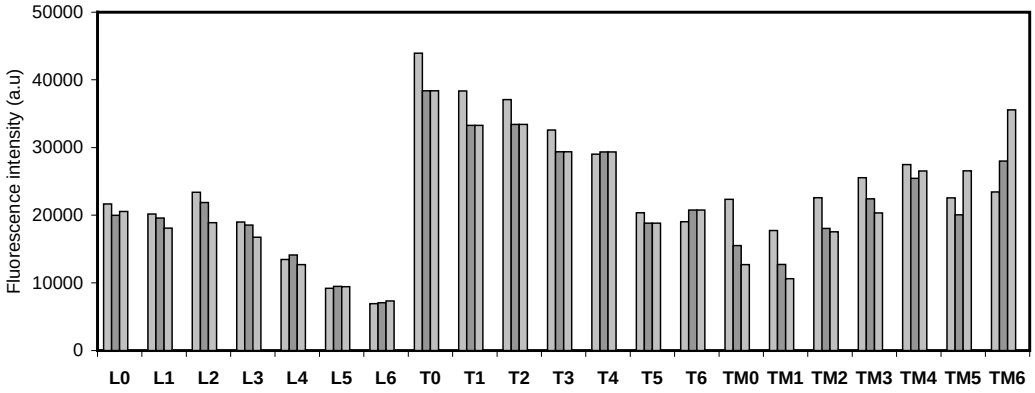

Figure 5.7. *Plot of the original fluorescence intensity of each sensitive monolayer in air (**L0-L6**, **T0-T6**, **TM0-TM6**), made in triplicate in consecutive wells.*

5.2.2. Metal ion sensing with the monolayer array by confocal microscopy

The response of the above described sensor array to Ca^{2+}, Cu^{2+}, Co^{2+}, Pb^{2+}, and Zn^{2+} was studied. First, the MTP was incubated in a 10^{-4} M acetonitrile solution of the perchlorate salts of Ca^{2+}, Cu^{2+}, Co^{2+}, Pb^{2+}, and Zn^{2+}. Afterwards, the fluorescence intensity of each well of the reference and of the analysis libraries was measured using a laser scanning confocal fluorescence microscope (LSCM).[37] Qualitative and quantitive analysis of the microtiter-plate response in the presence of the analytes are both feasible. The fluorescence intensity of each well is measured by LSCM and one colored image is generated for each well, which is easily visualized by eye.[38] The ratio of fluorescence intensities of the reference and the analysis library was calculated providing a quantitative measure of the analyte influence in each well (see experimental part for details).[39]

The interaction of each metal ion with the different sensing wells results in an individual fluorescent signal for each well. The combination of the 21 individual

responses generates a characteristic pattern signature for each analyte. Figure 5.8 shows the fluorescence intensity of each MTP well after incubation with Ca^{2+}, Cu^{2+}, Co^{2+}, Pb^{2+}, or Zn^{2+} solutions (10^{-4} M, acetonitrile). The fluorescence pattern that each analyte induces in the array is unique, allowing analyte identification.[40] Figure 5.9 depicts the changes in fluorescence intensity of each sensing system of the MTP upon analyte complexation.

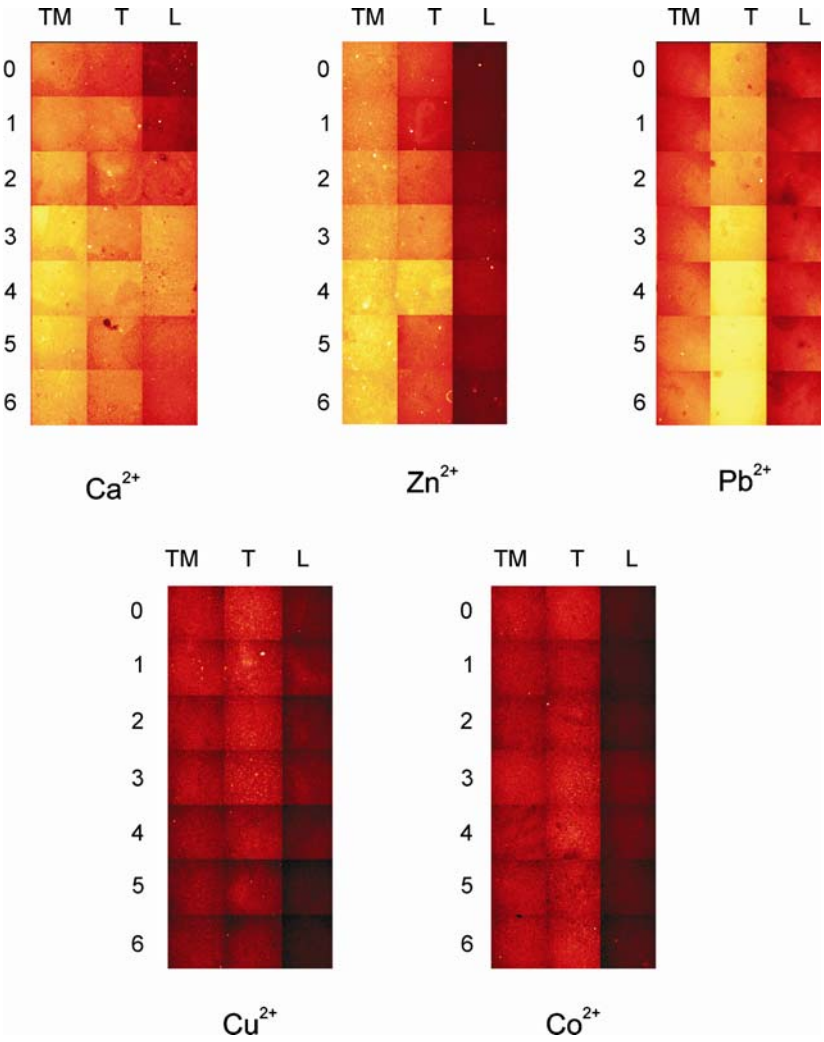

Figure 5.8. *Fluorescence microscopy images of the MTP wells after the MTP was incubated with Ca^{2+}, Zn^{2+}, Pb^{2+}, Cu^{2+} or Co^{2+} (10^{-4} M, acetonitrile). Each square in every image represents an individual signal, and the collection of the individual signals constitutes the response pattern of the array. (For well composition see Figure 5.4).*

Quantification of the data was done by analyzing the fluorescence intensity of each well before and after exposure to the analyte. The maximum fluorescence intensity in absence of the analytes is set to 0. Data were extracted, normalized, and reported as changes in fluorescence emission intensity (see experimental part for details).

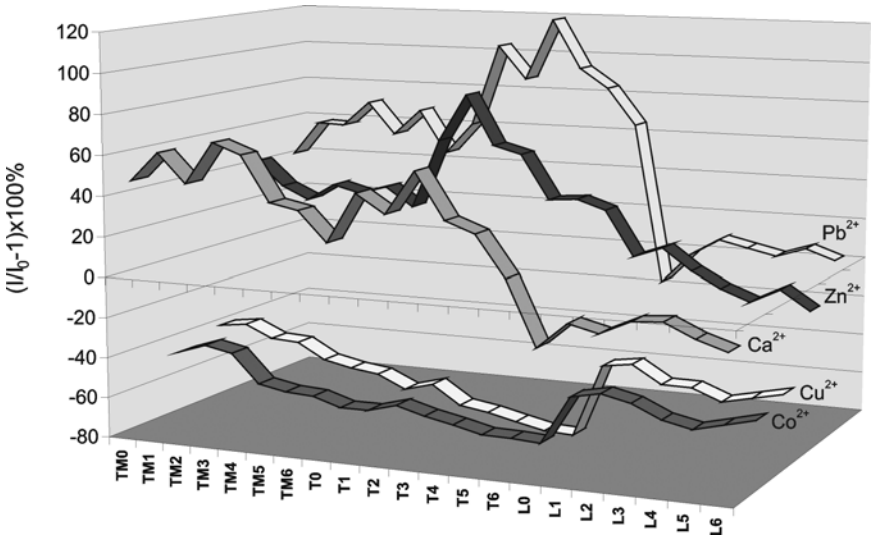

Figure 5.9. *Plot of the fluorescence emission intensity changes of each sensing system in the array upon Pb^{2+}, Zn^{2+}, Ca^{2+}, Co^{2+} and Cu^{2+} complexation. Negative values indicate quenching of fluorescence while positive values indicate enhancement of fluorescence intensity. The data are normalized, the fluorescence intensity of the sensing systems in the reference layer has been set to 0, and compared with the fluorescence intensity of each system after analyte complexation.*[41]

5.2.3 Metal ion sensing with the monolayer array by fluorescence laser scanner

This chapter shows that an array of fluorescent SAMs comprised of rather unspecific metal ions probes constitutes a powerful analysis tool for metal ion sensing. This sensing method allows the use of a standard fluorescent microscope[42] to evaluate the sensing response of the array without additional tagging steps. Nevertheless, quantification of the fluorescence modulation upon analyte addition by fluorescence microscopy allows only imaging of small areas of the MTP, and reduction of the analysis

time for optimization of the method is desirable. Therefore, a commercial confocal fluorescence laser scanner was used to read the micro-sensor array because it allows imaging of the whole array in a shorter time. As mentioned before, the MTP used to form the monolayer array had the dimensions of a standard microscope slide (75 X 25 mm), suitable for measurements in commercial fluorescence scanners. This compact benchtop scanner combines easy-to-use features with advanced optics and solid-state laser technology and provides rapid scan times, image quality, and data reproducibility for accurate and reliable measurements. The simplicity of the analysis technology should enhance the performance of our sensing scheme, allowing fast and accurate measurements.

To prove whether the sensing SAMs array can be measured using a fluorescence array scanner, a few sensing and recycling experiments were performed. Two different MTPs were functionalized with the previously described sensitive SAMs library comprised of 21 different sensing monolayers (for library composition see Figure 5.4). The monolayers were arranged in the MTP according to the pattern given in Figure 5.6 (analysis library). Every monolayer was prepared in triplicate in three consecutive wells to evaluate the reproducibility of the measurements. The MTP was imaged before incubation with the analytes to register the initial fluorescence intensity of each well. Subsequently, the plates ***MTP 1*** and ***MTP 2*** were incubated with Cu^{2+} and Ca^{2+} (10^{-4} M, acetonitrile), respectively, and scanned again.[37] Figure 5.9 shows the pictures of ***MTP 1*** and ***MTP 2*** functionalized with the SAM array before and after Ca^{2+} and Cu^{2+} addition, respectively.

The scanning of the microtiter-plate takes less than 40 s.[43] The fluorescence intensity patterns of the functionalized MTP after exposure to the analytes provide a response signature characteristic for each analyte (Figure 5.9). In this way was proved that the fluorescence laser scanner allows imaging a sensing SAM array in a short time. This constitutes an extra advantage in the screening methodologies for sensor arrays discussed in this thesis.

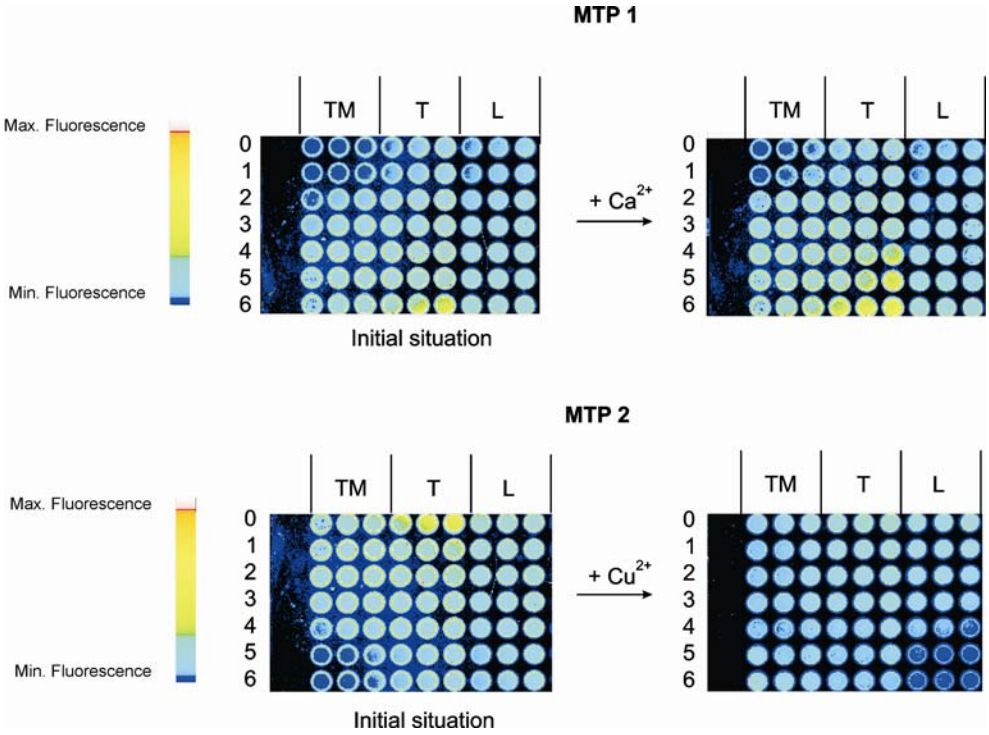

Figure 5.9. *Fluorescence scanner images of* ***MTP 1*** *and* ***MTP 2****, functionalized with a library of 21 SAMs configured into an array (for library composition see Figure 5.4), before and after exposure to a* 10^{-4} *M acetonitrile solution of* $Ca(ClO_4)_2$ *and* $Cu(ClO_4)_2$*, respectively.*

Recycling of the MTP confined sensing array was also studied. A functionalized MTP containing the SAM library described in Figure 5.4, was incubated with Co^{2+} (10^{-4} M, acetonitrile) and produced the fluorescence pattern shown in Figure 5.10 a,b. Subsequently, the MTP was rinsed with a metal scavenger, EDTA solution (ethylenediaminetetraacetic acid, 0.01 M, in H_2O solution). Because the EDTA is a very good chelating agent it removes the Co^{2+} from the layer. Upon rinsing with the EDTA solution the fluorescence intensity of each monolayer increased, indicating that almost all metal ions had been removed from the array (Figure 5.10c). Subsequent exposure of the rinsed MTP to Co^{2+} resulted in almost the same fluorescent pattern found after the initial addition of Co^{2+} (Figure 5.10d). Thus, the complexation is reversible and the surface can be easily recycled for further analysis.

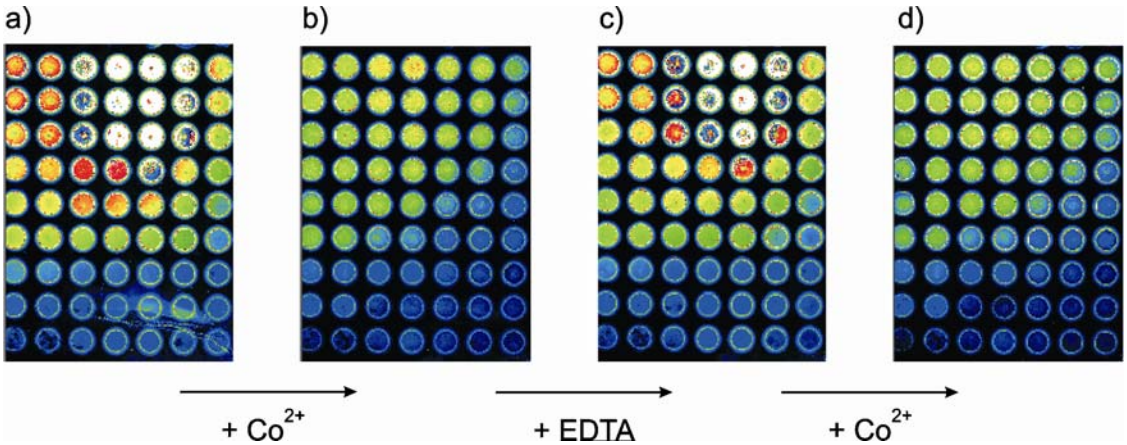

Figure 5.10. *Fluorescence scanner images of a MTP functionalized with the sensing array, a) initial situation, b) after exposure to* Co^{2+} *(*10^{-4} *M, acetonitrile), c) after subsequent rinsing with EDTA (0.01 M, aqueous solution), and d) after re-exposure to* Co^{2+} *(*10^{-4} *M, acetonitrile).*

5.3. Conclusions and outlook

The results herein demonstrate the successful application of parallel combinatorial methods to generate different sensing self-assembled monolayers covalently immobilized in the wells of a glass microtiter-plate. The fluorescence pattern after exposure of the array to different metal ion solutions allows identification of Cu^{2+}, Co^{2+}, Ca^{2+}, Zn^{2+} and Pb^{2+} at 10^{-4} M concentration by laser confocal microscopy and fluorescence laser scanner. The collection of the unselective response of the monolayers in the presence of the cations generates a characteristic fluorescent pattern, a "fingerprint" of each analyte in the array. The array responded extremely fast to the presence of the analytes. It can be reused after removal of the analytes by washing with EDTA.

The work presented here will contribute to the sensor field because it introduces a simple scheme for the fabrication of cross-reactive sensor arrays for analysis of metal ions. The generation of universal arrays containing a vast number of sensitive probes that can be used for identification of any analyte or mixtures of analytes can be easily envisioned due to the versatility and flexibility of this new sensing scheme. Future

applications of this type of sensing array require also the use of elaborate pattern-recognition, chemometrics, and neural networks protocols[14] in order to process the data.

5.4. Experimental

Monolayer microarray fabrication

All glassware used to prepare the layers was cleaned by sonicating for 15 minutes in a 2% v/v Hellmanex II solution in distilled water, rinsed four times with high purity (MilliQ, 18.2 MΩcm) water, and dried in an oven at 150º C. The substrates, costum made 140 well glass micro titer plates were cleaned for 15 minutes in piranha solution (concentrated H_2SO_4 and 33% aqueous H_2O_2 in a 3:1 ratio. ***Warning: Piranha solution should be handled with caution: it has been reported to detonate unexpectedly).*** They were then rinsed several times with high purity (MilliQ) water, and dried in a nitrogen stream immediately prior to performing the formation of the monolayers.

*Synthesis of **TPEDA** monolayers in the MTP wells*

For the synthesis of the N-[3-(trimethoxysilyl)propyl]ethylenediamine SAM ***TPEDA*** in the MTP wells, the whole MTP was treated like one glass slide and the synthetic procedure from Chapter 3 of this thesis for the synthesis of the ***TPEDA*** monolayer onto a glass slide was followed (see experimental part in Chapter 3). The result is the complete coating of the MTP surface with the ***TPEDA*** monolayer.

*Inmobilization of the fluorophores: Synthesis of the layers **TM0**, **L0,** and **T0***

The attachment of the fluorophores onto the ***TPEDA*** SAM in the MTP wells was achieved by pipetting in the corresponding wells a solution (5 μL, 0.1 mM, acetonitrile) of the fluorophore TAMRA (5-(and-6)-carboxytetramethylrhodamine, succinimidyl ester (5(6)-TAMRA, SE) *mixed isomers)) (TM), fluorophore Lissamine (L) (Lissamine rhodamine B, sulfonyl chloride) and fluorophore TRITC (T) (tetramethylrhodamine-5-(and-6)-isothiocyanate(5(6)-TRITC), *mixed isomers) to yield layers ***TM0***, ***L0*** and ***T0***, respectively. 500 μL of triethylamine was added in all the solutions to avoid protonation of the amine groups on the ***TPEDA*** layers. The MTP was kept for 3h in an acetonitrile saturated atmosphere to avoid evaporation. After reaction the MTP was immersed in propylamine (0.1 M, acetonitrile) to quench the reaction and to remove the excess fluorophore. Subsequently, the MTP was gently rinsed with CH_2Cl_2 and dried under an air stream.

*Inmobilization of the coordinating groups: Synthesis of the layers **L1**-**L6**, **T1**-**T6,** and **TM1**-**TM6***

The corresponding MTP wells functionalized with the fluorescent monolayers ***T0***, ***TM0,*** and ***L0*** were filled with 5 μL of a solution of 0.1 mL of *p*-isopropyl phenyl isocyanate, hexyl isocyanate, phenyl isothiocyanate, hexanoyl chloride, *p*-propyl benzoyl chloride and phenyl isocyanate in 20 mL of acetonitrile with 100 μL of triethyelamine, to afford layers ***T1***-***T6***, ***TM1***-***TM6***, and ***L1***-***L6***, respectively. The MTP was kept for 3h in a saturated acetonitrile atmosphere to avoid evaporation. The reactants were taken out of the wells to avoid spreading of the reactive species to other wells. Subsequently the MTP was sonicated for 2 min in a 0.1 M acetonitrile solution of propylamine, for 2 min in CH_3CN, for 2 min in EtOH, and for 2 min in CH_2Cl_2. Finally, the MTP was dried under an air stream.

Metal ion sensing with the microtiter-plate

Ca^{2+}, Co^{2+}, Cu^{2+}, Zn^{2+} and Pb^{2+} sensing with the confined monolayer array was measured using the following protocol: immersion of the analysis part of the MTP in a beaker filled with a 10^{-4} M acetonitrile solution of the corresponding analyte for 5 min followed by gentle rinsing of the MTP first in a beaker filled with CH_2Cl_2 and subsequently with a stream of fresh CH_2Cl_2, and final drying of the MTP under an air stream. Subsequently fluorescent images of the MTP were recorded with laser confocal microscopy (LSCM) and fluorescence scanner (see details below).

Imaging set-up

Laser scanning confocal microscopy

Confocal microscopy images of the functionalized wells of the glass MTP were taken on a Carl Zeiss LSM 510 microscope. Images were acquired using a confocal laser scanning microscope equipped with an argon laser module (Carl Zeiss Inc., Thornwood, NY) using a 10×0.25-na objective. The light was focused through the glass plate on the top side of each well. The image is collected using the focus that gives the maximum initial fluorescence intensity. All the fluorophores were excited at 543 nm with a HeNe laser. The following parameters were kept constant for all types of monolayers: pinhole (17.7 μm), image size (1024 x 1024 pixels), scanning speed (5) and data depth (12 bit). Depending on the initial intensity of the fluorescent monolayers and the expected response in the presence of the analytes (enhancement or quenching of the fluorescence intensity) the following settings were used: for sensing of Ca^{2+}, Pb^{2+} and Zn^{2+}, the detector gain was set to 774, 750 and 772 for TAMRA, TRITC, and Lissamine containing layers, respectively; the amplifier offset was set to -0.115, -0.136 and -0.057 for TAMRA, TRITC, and Lissamine containing layers, respectively; and the amplifier gain was set to 1, 1 and 1.17 for TAMRA, TRITC, and Lissamine containing layers, respectively. For sensing of Cu^{2+} and Co^{2+} the detector gain was set to 901, 849 and 822 for TAMRA, TRITC, and Lissamine containing layers, respectively; the amplifier offset was set to -0.071, -0.136 and -0.057 for TAMRA, TRITC, and Lissamine containing layers, respectively; and the amplifier gain was set to 1, 1 and 1.17 for TAMRA, TRITC, and Lissamine containing layers, respectively. The fluorescence was collected on a PMT R6357. All the images were collected in air.
For data evaluation, two sets of the same monolayer library were made in a MTP (reference library and analysis library). Only the analysis library was exposed to the analyte. After exposure, an image of each functionalized well of both sets was made and the mean fluorescence intensity of each image was extracted. The average value of the duplicate (in the reference library) and the triplicate (in the analysis library) wells in both libraries was calculated. For data evaluation, the fluorescence intensity of each system in the reference library was set to 0 and compared with the intensity of the corresponding well in the analysis library. The values given in the text are the average of two measurements from two different MTP.

Laser confocal fluorescence scanner

Fluorescence laser scanner images of the monolayer array were obtained with an Affymetrix 428 scanner (Affymetrix, High Wycombe, UK), and the Jaguar Software package (Affymetrix). Excitation light was in all the cases 532 nm. For data evaluation, the MTP was scanned before and after analyte addition. The resulting images were analyzed with Imagene 5.0 software (BioDiscovery Inc., El Segundo, CA). Data were further processed. The MTP was placed on the scanner upside down to focus on the bottom part of the wells.

5.5. References and notes

1 Czarnik, A. W. Desperately Seeking Sensors. *Chemistry & Biology* ***1995***, 2 (7), 423-428.

2 J.P. Behr, The Lock and Key Principle, Volume 1, The State of the Art - 100 Years On, Wiley, New York, ***1994***.

3 Jurs, P. C.; Bakken, G. A.; Mcclelland, H. E. Computational Methods for the Analysis of Chemical Sensor Array Data From Volatile Analytes. *Chem. Rev.* ***2000***, 100(7), 2649-2678.

4 Albert, K. J.; Lewis, N. S.; Schauer, C. L.; Sotzing, G. A.; Stitzel, S. E.; Vaid, T. P.; Walt, D. R. Cross-Reactive Chemical Sensor Arrays. *Chem. Rev.* ***2000***, 100(7), 2595-2626.

5 Stopfer, M.; Jayaraman, V.; Laurent, G. Intensity Versus Identity Coding in an Olfactory System. *Neuron* ***2003***, 39(6), 991-1004.

6 Lundstrom, I. Artificial Noses - Picture the Smell. *Nature* ***2000***, 406(6797), 682-683.

7 Shepherd, G. M. Discrimination of Molecular Signals by the Olfactory Receptor Neuron. *Neuron* ***1994***, 13(4), 771-790.

8 Lundstrom, I.; Erlandsson, R.; Frykman, U.; Hedborg, E.; Spetz, A.; Sundgren, H.; Welin, S.; Winquist, F. Artificial Olfactory Images From a Chemical Sensor Using a Light-Pulse Technique. *Nature* ***1991***, 352(6330), 47-50.

9 Lancet, D. Olfaction - the Strong Scent of Success. *Nature* ***1991***, 351(6324), 275-276.

10 Doty, R.L., Handbook of olfaction and gustation, Neurological Disease and Therapy. Vol. 57. Second edition. Marcel Dekker, New York, ***2003***.

11 Rakow, N. A.; Suslick, K. S. Novel Materials and Applications of Electronic Noses and Tongues (Vol 406, Pg 710, 2000). *MRS Bulletin* ***2004***, 29(12), 913.

12 Suslick, K. S.; Rakow, N. A.; Sen, A. Colorimetric Sensor Arrays for Molecular Recognition. *Tetrahedron* ***2004***, 60(49), 11133-11138.

13 Bishop, C. M., Neural networks for pattern recognition, Bishop, C. M, Oxford University Press: Oxford, U.K., ***1995***.

14 Lyons, W. B.; Lewis, E. Neural Networks and Pattern Recognition Techniques Applied to Optical Fibre Sensors. *Trans. Inst. Measurm. Control* ***2000***, 22(5), 385-404.

15 Lavigne, J. J.; Anslyn, E. V. Sensing a Paradigm Shift in the Field of Molecular Recognition: From Selective to Differential Receptors. *Angew. Chem., Int. Ed.* ***2001***, 40(17), 3119-3130.

16 Persaud, K.; Dodd, G. Analysis of Discrimination Mechanisms in the Mammalian Olfactory System Using a Model Nose. *Nature* ***1982***, 299, 352-355.

17 Freund, M. S.; Lewis, N. S. A Chemically Diverse Conducting Polymer-Based Electronic Nose. *Proc. Natl. Acad. Sci. U. S. A.* ***1995***, 92(7), 2652-2656.

18 Lonergan, M. C.; Severin, E. J.; Doleman, B. J.; Beaber, S. A.; Grubb, R. H.; Lewis, N. S. Array-Based Vapor Sensing Using Chemically Sensitive, Carbon Black-Polymer Resistors. *Chem. Mater.* ***1996***, 8(9), 2298-2312.

19 Heilig, A.; Barsan, N.; Weimar, U.; Schweizer-Berberich, M.; Gardner, J. W.; Gopel, W. Gas Identification by Modulating Temperatures of SnO_2-Based Thick Film Sensors. *Sens. Actuators, B* ***1997***, 43(1-3), 45-51.

20 Gardner, J. W.; Shurmer, H. V.; Tan, T. T. Application of an Electronic Nose to the Discrimination of Coffees. *Sens. Actuators, B* ***1992***, 6(1-3), 71-75 .

21 Crooks, R. M.; Ricco, A. J. New Organic Materials Suitable for Use in Chemical Sensor Arrays. *Acc. Chem. Res.* ***1998***, 31(5), 219-227.

22 Grate, J. W.; Abraham, M. H. Solubility Interactions and the Design of Chemically Selective Sorbent Coatings for Chemical Sensors and Arrays. *Sens. Actuators, B* ***1991***, 3(2), 85-111.

23 Brunink, J. A. J.; Dinatale, C.; Bungaro, F.; Davide, F. A. M.; Damico, A.; Paolesse, R.; Boschi, T.; Faccio, M.; Ferri, G. The Application of Metalloporphyrins as Coating Material for Quartz Microbalance-Based Chemical Sensors. *Anal. Chim. Acta* ***1996***, 325(1-2), 53-64.

24 Walt, D. R. Fiber Optic Imaging Sensors. *Acc. Chem. Res.* ***1998***, 31(5), 267-278.

25 Dickinson, T. A.; White, J.; Kauer, J. S.; Walt, D. R. A Chemical-Detecting System Based on a Cross-Reactive Optical Sensor Array. *Nature* ***1996***, 382(6593), 697-700.

26 Chojnacki, P.; Werner, T.; Wolfbeis, O. S. Combinatorial Approach Towards Materials for Optical Ion Sensors. *Microchim. Acta* ***2004***, 147(1-2), 87-92.

27 Mayr, T.; Igel, C.; Liebsch, G.; Klimant, I.; Wolfbeis, O. S. Cross-Reactive Metal Ion Sensor Array in a Micro Titer Plate Format. *Anal. Chem.* ***2003***, 75(17), 4389-4396.

28 Rakow, N. A.; Suslick, K. S. A Colorimetric Sensor Array for Odour Visualization. *Nature* ***2000***, 406(6797), 710-713.

29 Goodey, A.; Lavigne, J. J.; Savoy, S. M.; Rodriguez, M. D.; Curey, T.; Tsao, A.; Simmons, G.;

Wright, J.; Yoo, S. J.; Sohn, Y.; Anslyn, E. V.; Shear, J. B.; Neikirk, D. P.; Mcdevitt, J. T. Development of Multianalyte Sensor Arrays Composed of Chemically Derivatized Polymeric Microspheres Localized in Micromachined Cavities. *J. Am. Chem. Soc.* ***2001***, 123(11), 2559-2570.

30 Biran, I.; Rissin, D. M.; Ron, E. Z.; Walt, D. R. Optical Imaging Fiber-Based Live Bacterial Cell Array Biosensor. *Anal. Biochem.* ***2003***, 315(1), 106-113 .

31 Crego-Calama, M.; Reinhoudt, D. N. New Materials for Metal Ion Sensing by Self-Assembled Monolayers on Glass. *Adv. Mater.* ***2001***, 13(15), 1171-1174.

32 Basabe-Desmonts, L.; Beld, J.; Zimmerman, R. S.; Hernando, J.; Mela, P.; García-Parajó, M. F. G.; Van Hulst, N. F.; Van den Berg, A.; Reinhoudt, D. N.; Crego-Calama, M. A Simple Approach to Sensor Discovery and Fabrication on Self-Assembled Monolayers on Glass. *J. Am. Chem. Soc.* ***2004***, 126(23), 7293-7299.

33 Zimmerman, R. S.; Basabe-Desmonts, L.; Van der Baan, F.; Reinhoudt, D. N.; Crego-Calama, M. A Combinatorial Approach to Surface-Confined Cation Sensors in Water. *J. Mater. Chem.* ***2005***, 15(27-28), 2772-2277.

34 Greene, N. T.; Morgan, S. L.; Shimizu, K. D. Molecularly Imprinted Polymer Sensor Arrays. *Chem. Commun.* ***2004***, (10), 1172-1173.

35 Birkert, O.; Tunnernann, R.; Jung, G.; Gauglitz, G. Label-Free Parallel Screening of Combinatorial Triazine Libraries Using Reflectometric Interference Spectroscopy. *Anal. Chem.* ***2002***, 74(4), 834-840.

36 Due to steric hindrance, some amino groups remain unreacted after addition of the fluorophore molecules. Thus, these groups can be reacted with a small molecule to form the complexing functionalities yielding the final sensitive fluorescent self-assembled monolayer (SAMs).

37 All the fluorescence images shown are made in air. After incubation of the plate with the analyte, it is rinsed with dichloromethene, dried and then imaged.

38 Different color within a gray scale is assigned to different fluorescence intensity values, and with a particular graphical software the gray scale pictures are transformed into colored photos with a red to yellow scale.

39 The imaging of the array in absence and in contact with the analytes was done keeping constant all the parameters of the imaging set-up. The threshold for the fluorescence intensity of the reference library was set differently for layers ***TM0***-***TM6***, ***T0***-***T6*** and ***L0***-***L6*** (see experimental).

40 Every monolayer was made in triple in consecutive wells in the analysis library of the MTP. One image of each well is obtained after the incubation with the analytes. But only one image (out of three) for each of the 21 systems in the array is selected for the final picture.

41 Each point is the average of at least 6 measurements. The average deviation of these values is lower than 5 %.

42 In spite of the fact that during this work a laser scanning confocal microscope has been used, the fluorescence of the monolayer array is visible as well by standard fluorescence microscopes with less powerful light sources.

43 A deviation on the scanner laser focus calibration did not permit the scanning of the whole microtiter plate with high precision. Due to this reason only the half of the plate was imaged each time in order to get the maximum precision along the scanned area.

Chapter 6

Fluorescent Sensor Array in a Microfluidic Chip*

Miniaturization and automation are highly important issues for the development of high-throughput processes. Therefore, the area of micro total analysis systems (μTAS) is growing rapidly and the design of new schemes which are suitable for miniaturized analytical devices is of great importance. In this chapter the immobilization of self-assembled monolayers (SAMs) with metal ion sensing properties, on the walls of glass microchannels is reported. The parallel combinatorial synthesis of sensing SAMs in individually addressable microchannels towards the generation of optical sensor arrays and sensing chips has been developed.

* Part of this chapter has been published in: Basabe-Desmonts, L.; Beld, J.; Zimmerman, R. S.; Hernando, J.; Mela, P.; García Parajó, M. F.; Van Hulst, N. F.; Van den Berg, A.; Reinhoudt, D. N.; Crego-Calama, M.; *J. Am. Chem Soc.* ***2004***, *126*, (23), 7293-7299
Manuscript in preparation: Basabe-Desmonts L.; Gardeniers H.; Van den Berg A.; Reinhoudt D. N.; Crego-Calama M.

6.1 Introduction

Microfluidics-based have been devices are emerging as a powerful tool for analytical applications during the last fifteen years.[1] Microchannels are particularly attractive for analytical purposes because they provide a convenient small platform for rapid analysis and detection. Only small sample volumes are required and flowing of the analyte through the channels enables real-time measurements and consequently fast analysis protocols. These advantages have been demonstrated for the analysis of biological samples[2] and more recently, for chemical analytes.[3-8] Microchannels are small and individually accessible and addressable platforms. The production of high density probe arrays can be achieved within a single device by microfabrication techniques. The concept of cross sensor arrays of non-specific sensing probes, used for example in artificial noses[9,10] and tongues[11] for the analysis of multianalyte mixtures, could be implemented in microchannels. A series of individually addressable microchannels each containing a different sensing probe, would provide a micro total analysis system (μ–TAS).

The glass surface of a microchannel behaves similarly to macro scale glass surfaces, and thus can be chemically activated and modified with SAMs.[12] The integration of (functional) SAMs into microchannels combines the advantages of monolayer chemistry with those of the microfluidics devices *viz* unidirectional responding surfaces, minimization of analyte sorption times to receptors, fast response times, easy synthesis, and reproducibility,[13,14] and high surface-to-volume ratio, faster process, automation resulting in higher reproducibility and precision of the measurements, consumption of tiny amounts of reagents and less waste. SAMs immobilized in microchannels will allow on-line monitoring of the monolayer formation using continuous feeding of fresh reagents. The response of the monolayer upon exposure to different flows and supramolecular interactions on the surface can be monitored in real time. Until now, SAMs on microchannel walls have been studied for surface properties in microreactors,[15] to control surface wetting,[16,17] to create zones for specific immobilization of proteins and biomolecules,[18] and to conduct catalytic reactions.[19] Only recently a pH sensing monolayer confined to a glass microchannel has been reported by our group.[3]

In this chapter, the covalent attachment of fluorescent monolayers on the walls of glass microchannels for cation sensing is reported. The methodology presented in Chapter 3 of this thesis for the fabrication of new fluorescent materials for cation sensing is here applied to microchannel walls. The methodology relies on the sequential deposition of different fluorophores and small ligand molecules on an amino-terminated SAM on the channel glass walls. The tiny dimensions presented by the microchannels enable the parallel generation of differently functionalized channels, and therefore different SAMs, on a single chip resulting in an array of non-specific sensing probes. Thus the monolayer array (confined in a multichannel chip) is prepared by parallel synthesis of monolayers functionalized with different fluorophore-ligand pairs, resulting results in a sensing chip which is able to generate a fingerprint of the network with a single fluorescence "snapshot" for different analytes.

This method combines the advantages of microfluidic real-time analysis with the cost-effectiveness of microanalytical devices. In contrast with the monolayer array confined to a microtiter-plate, it prevents problems such as solvent evaporation during the monolayer formation. Furthermore, it reduces dramatically the occupied space and the amount of reagents, enhances the automation of the fabrication process and allows for continuous monitoring of analyte solutions. Regeneration of the channel activity for the sequential testing of multiple analytes is also possible.

6.2 Results and discussion

6.2.1 Synthesis and characterization of fluorescent SAMs on microchannel walls

The optimized conditions for the coating of glass slides with fluorescent self-assembled monolayers explained in Chapter 3 of this thesis were applied to synthesize a fluorescent SAM on the walls of glass microchannels (Figure 6.1a). For this experiment, a three-inlet borosilicate glass chip with a 20 μm wide, 12 mm long and 2 μm deep microchannel was used (Figure 6.1b). The microchannel was hydroxylated with piranha solution, thoroughly rinsed with MilliQ water and dried with a stream of N_2. Functionalization of the activated glass walls was achieved by sequential pumping of the

reagents in the channel by using syringes (Figure 6.1b). First, a toluene solution of N-[3-(trimethoxysilyl)propyl]ethylenediamine was flushed through the channel *via* the inlets and allowed to react inside for 3.5 h at room temperature to ensure that the **TPEDA** SAM was covalently attached to the channel surface. Subsequently, the channel was filled with an acetonitrile solution of the fluorophore (TAMRA), which was kept inside for 2 h to form the **TM0** SAM. Then a solution of *p*-isopropylphenyl isocyanate was introduced in the channel and kept inside for 16 h to form the final **TM1** SAM on the channel walls. Between each synthetic step the channel was rinsed extensively using pressure driven flows of solvents and dried with a nitrogen stream (see experimental part for further details).

Laser confocal microscopy was used to ascertain the formation of the fluorescent monolayers. Inspection of the bottom wall of the microchannel with a laser scanning fluorescence microscope revealed the monolayer formation on the glass surface. Figure 6.1c shows the fluorescence microscopy image of the **TM1** monolayer functionalized microchannel. The fluorescence intensity profile of the image showed a homogeneous coverage of the monolayer with the fluorophore. Higher intensity of the fluorescence on both edges of the channel was observed due to the adjacent walls that are also fluorescent.[20]

The microchannel surface modification was also characterized by contact angle goniometry. Even though the behavior of fluids inside channels is not comparable to that on flat surfaces[17,21] the variation in the water contact angle inside the channel allows the measurement of the surface hydrophobicity.[22] As an example the contact angles of a glass microchannel washed with piranha solution, subsequently coated with the amino-terminated **TPEDA** SAM and finally functionalized with the fluorophore Lissamine to form the **L0** SAM were measured after each step. Figure 6.2 shows the microscopy images of the channel in each situation.

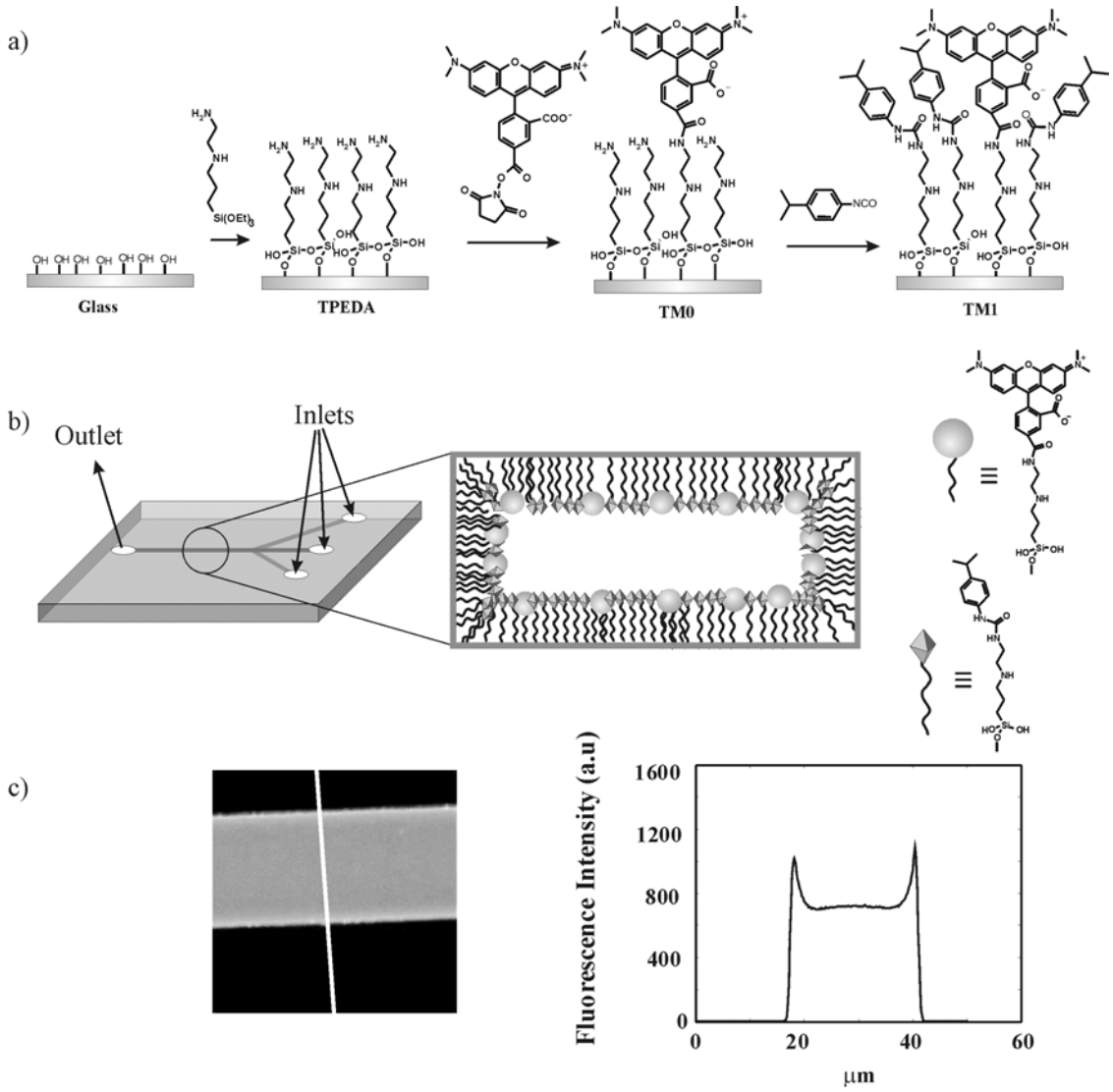

Figure 6.1. *Synthetic scheme for the formation of* ***TM1*** *SAM on the channel walls (a). Schematic representation of a one-channel chip (b). Laser scanning confocal microscopy image (and the fluorescence intensity profile of the cross section defined by the white line) of the channel coated with the fluorescent SAM* ***TM1*** *(c).*

Contact angles of 4°, 24°, and 82° were found for the cleaned, the ***TPEDA*** coated, and the ***L0*** coated channel, respectively. The bare cleaned surface is a highly hydrophilic surface containing mainly hydroxyl groups. As expected, the hydrophobicity of the

channel walls increases gradually upon formation of the amino-terminated monolayer ***TPEDA*** and subsequent functionalization with the fluorophore (***L0*** SAM).

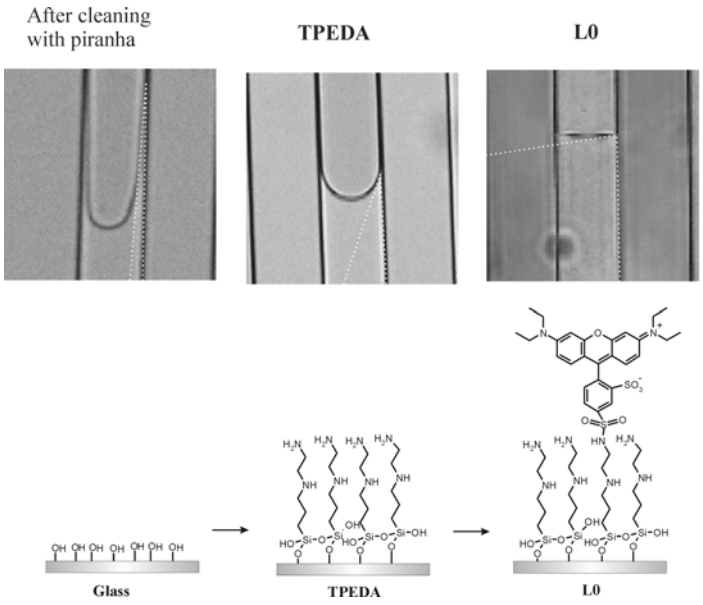

Figure 6.2. *Optical microscopy images of the water meniscus inside the channel after each synthetic step (also shown) of the chip functionalization.*

The response of a **TM1** SAM coated microchannel (Figure 6.1a) to the presence of Pb^{2+} was evaluated. The microchannel was first filled with acetonitrile and imaged using confocal microscopy.[23] Subsequently, Pb^{2+} (perchlorate salt, 10^{-4} M, acetonitrile) was flowed through and the fluorescence microscopy image was registered again. The addition of Pb^{2+} ions resulted in a 50% increase in the monolayer fluorescence intensity (Figure 6.3). These results agree with previous results described in this thesis for the response of this monolayer to the presence of Pb^{2+} ions. The channel was recycled by sequentially rinsing with HCl (0.1 N), $NaHCO_3$ (5%), MilliQ H_2O, EtOH, and CH_2Cl_2, and drying with an air stream. Reproducible changes in the fluorescence intensities were then obtained from a subsequent addition of the Pb^{2+} solution.[24]

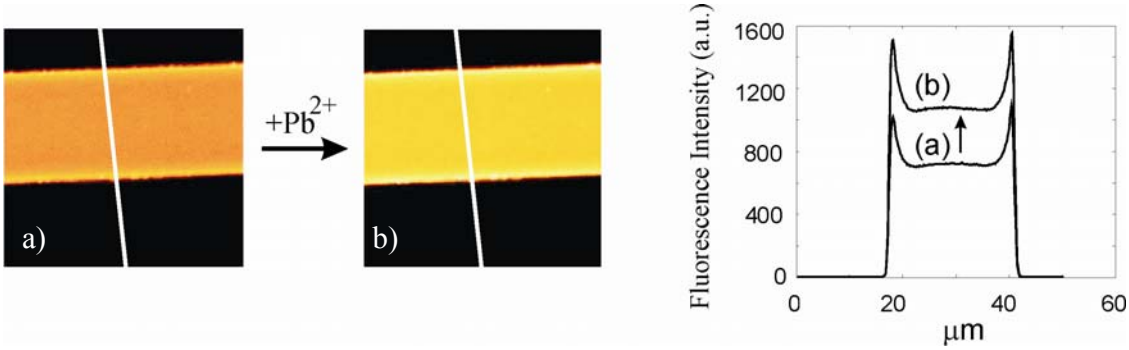

Figure 6.3. *Left: 70 x 70 μm confocal microscopy images of the channel (and the fluorescence intensity profile of the cross section defined by the white line) filled with acetonitrile and (a) with a solution of Pb^{2+} (perchlorate salt, 10^{-4} M, acetonitrile) (b). Right: Fluorescence intensity profiles of the images: (a) channel filled with acetonitrile; (b) channel filled with a solution of Pb^{2+} (perchlorate salt, 10^{-4} M, acetonitrile).*

The combination of these characterization methods and the sensitivity displayed by the surface to the presence of Pb^{2+} ions are consistent with the successful formation of the sensing monolayer on the glass walls of the microchannels.

6.2.2 Sensing microchannel array by parallel synthesis of fluorescent monolayers

6.2.2.1 Chip design

To automate the process of SAM synthesis in the microchannels for the generation of sensing arrays, a multichannel chip suitable for continuous flow of reagents was designed. A microchannel chip (4 x 2.2 cm^2) with five parallel channels confined in an area of 200 μm was fabricated. Each channel can be individually addressed and functionalized with chemically different fluorescent sensing monolayers to produce a sensing array chip (Figure 6.4). The five channels integrated in the chip are 35 mm long, 20 μm wide and 2 μm deep.[25] They share a common outlet and each of them has an independent inlet.

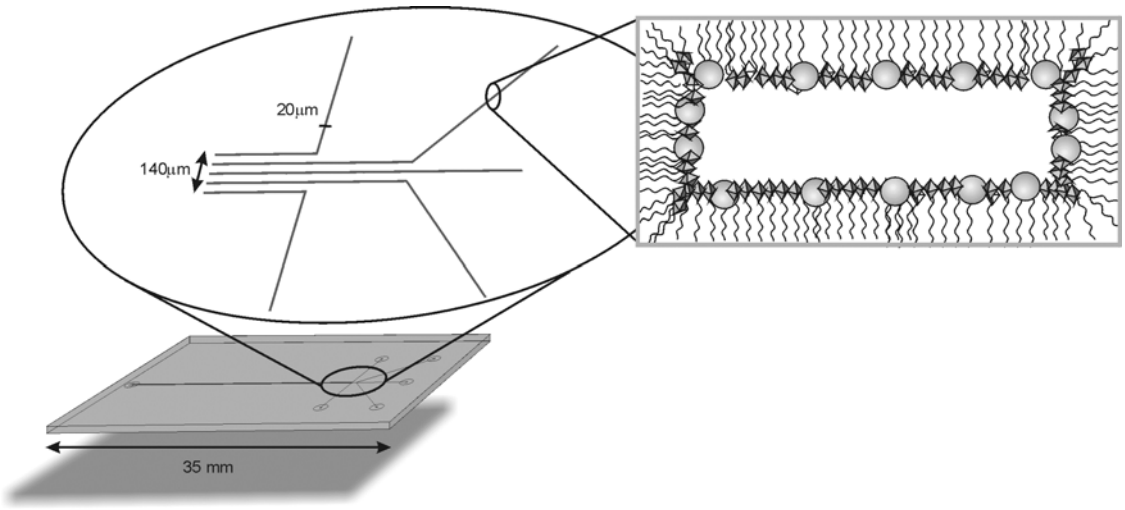

Figure 6.4. *Schematic representation of the five-channel chip.*

Figure 6.5 depicts the protocol for the parallel synthesis of five sensing SAMs in the multichannel chip. After the activation with piranha and the formation of the amino-terminated ***TPEDA*** SAM, the unique functionalization of each monolayer can be achieved by introducing consecutively different fluorophores (Fx, x = 1-5) and ligands (Ly, y = 1-5) in each channel. Common steps such as cleaning, ***TPEDA*** SAM formation or rinsing can be conducted from the outlet, while functionalization of each channel with a different fluorophore and ligand molecule can be carried out by addressing each channel through their independent inlet. As result an array of five fluorescent SAMs (Fx,Ly) confined to a single chip can be achieved.

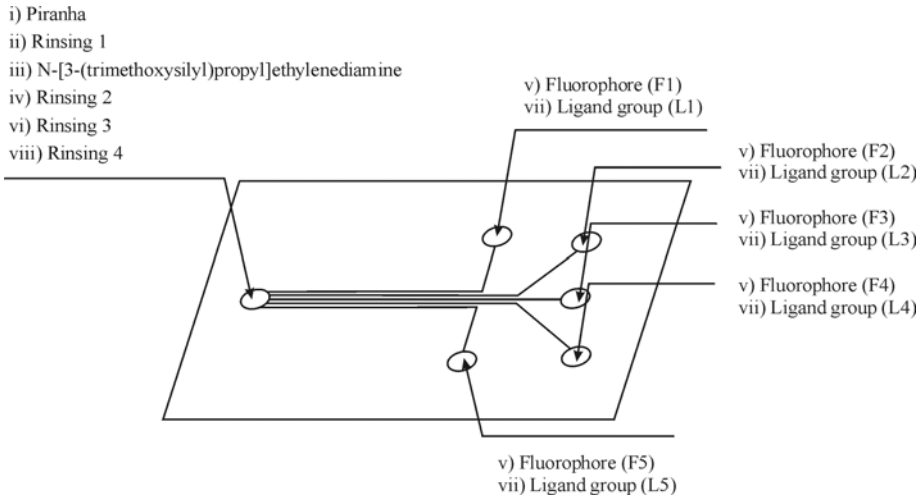

Figure 6.5. *Schematic representation of the parallel synthesis of a sensor array based on a library of fluorescent SAMs (Fx,Ly) (x,y = 1-5) integrated into the walls of the multichannel chip.*

To flush the reagents and the solvents through the channels, the chip is mounted in a holder and connected to the fluid feeders by means of fused silica fibers. The holder is designed for fitting fused silica fibers into the inlet and outlet chip reservoirs using commercially available Nanoport^{TM} assemblies. This system allows flow control in each channel, avoiding cross contamination between different channels. Additionally, the holder is designed to fit on an inverted fluorescence microscope to image the channels. Pictures of the chip and the chip holder are depicted in Figure 6.6. Pictures of the microscope set up are depicted in Figure 6.7 and pictures of the set up for the parallel synthesis of SAMs on the five-channel chip are depicted in Figure 6.8.

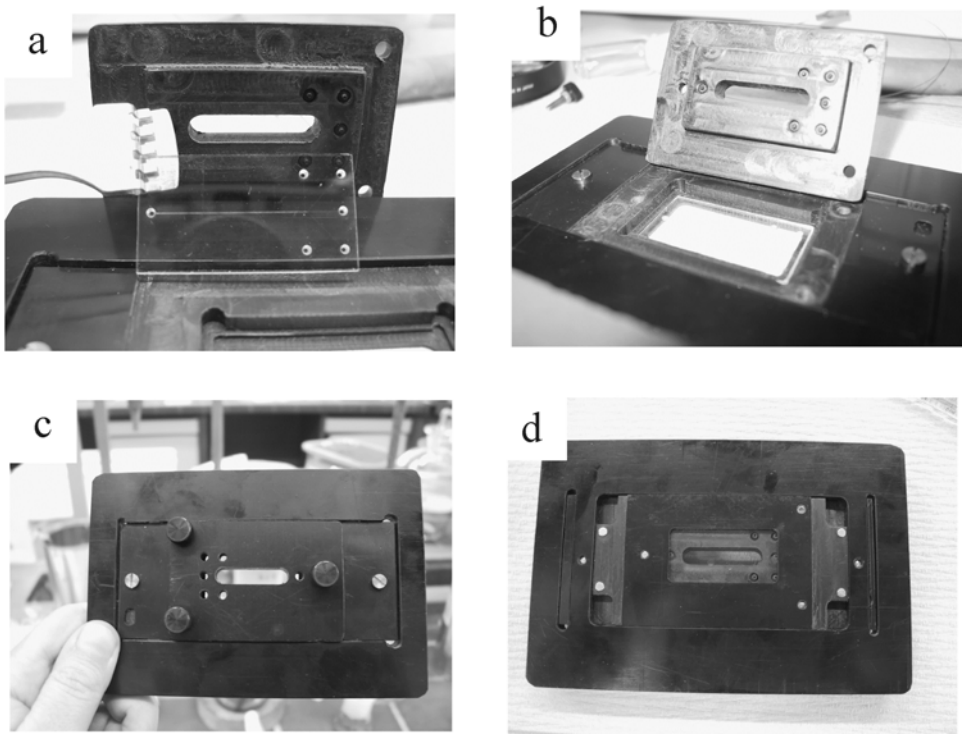

Figure 6.6. *Pictures of the five-channel chip (a) and the chip holder open (b), and closed: front view (c) and back view (d).*

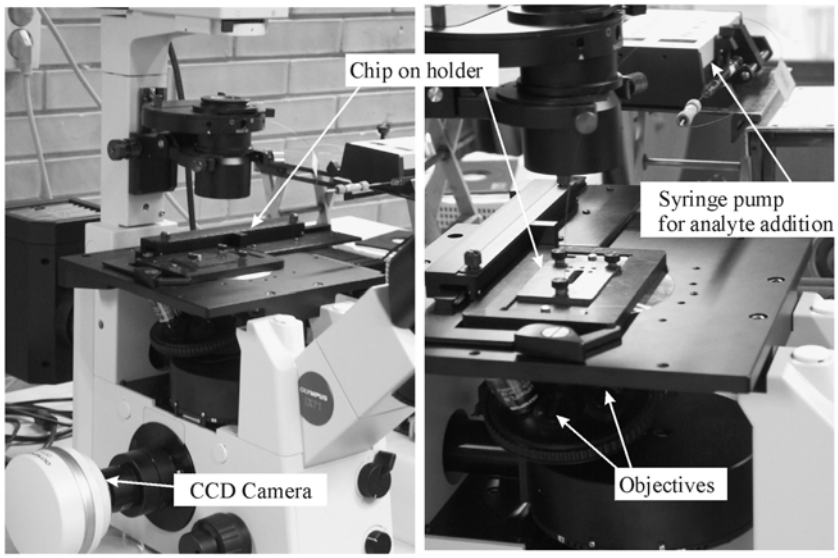

Figure 6.7. *Microscope set-up for the real time fluorescence measurements.*

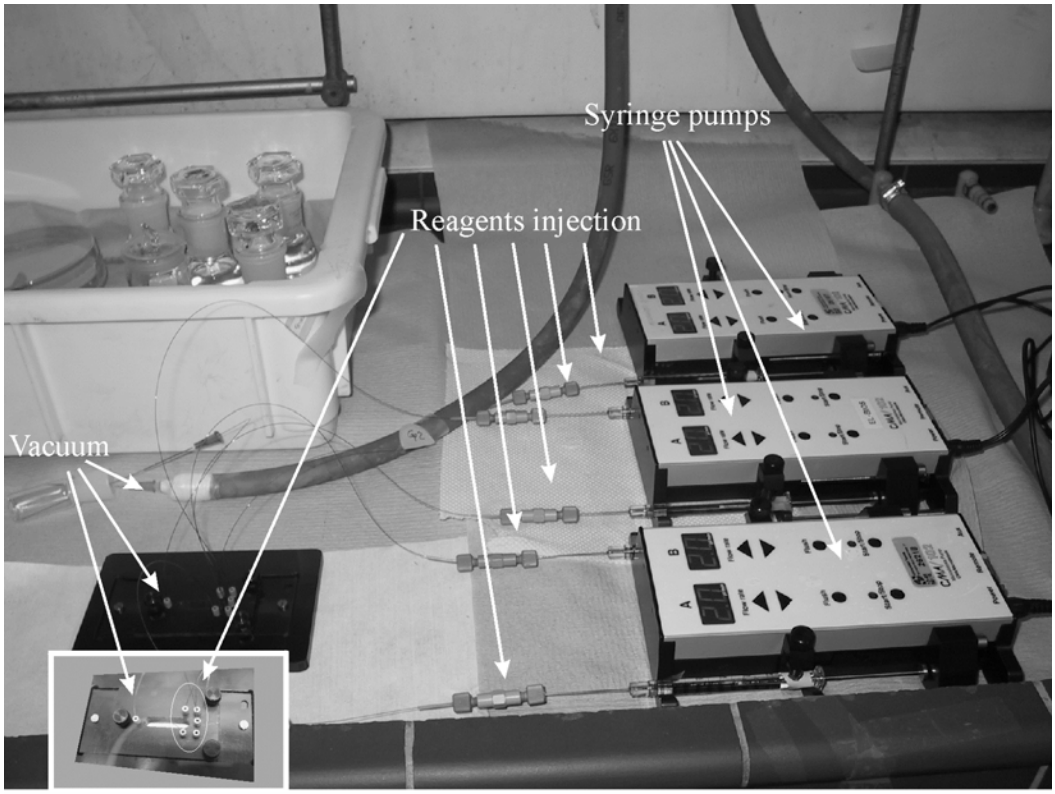

Figure 6.8. *Set-up for the parallel synthesis of SAMs in the channels of the five-channel chip. The inset shows the Nanoport™ connections on the holder for reagents feeding.*

6.2.2.2 Sensor array confined in a multichannel chip

Initially, a five channel-chip (Figure 6.5) was used to verify that the protocol followed for the monolayer formation inside of one microchannel, could be applied to the parallel functionalization of different channels simultaneously, avoiding cross contamination.

The channels C1-C5 (Figure 6.9) of the chip were coated with the amino-terminated SAM ***TPEDA*** after piranha activation (see experimental part). Subsequently, a continuous flow of three different fluorophores (0.01 mM, acetonitrile) was simultaneously injected in the five channels. Lissamine was introduced in channels C1 and C2 to form the ***L0*** SAM (Figure 6.9) while TAMRA was introduced in channels C4

and C5 to form ***TM0*** SAM. A solution of Bengal Rose was injected in channel C3. Bengal rose is a non amino-reactive fluorophore and therefore, its covalent attachment to the ***TPEDA***-coated walls was not expected.

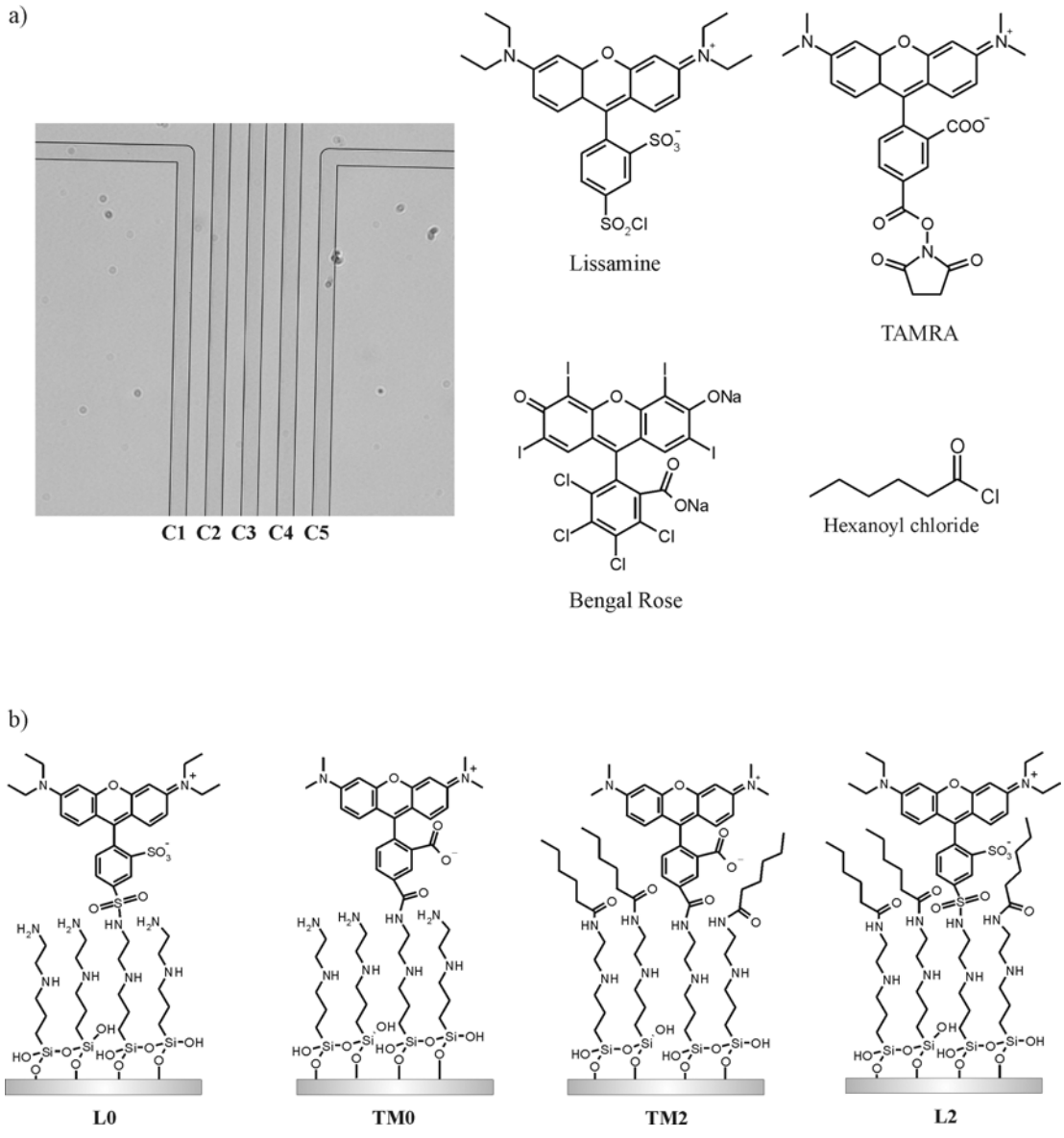

Figure 6.9. *Microscopy image of a section of a five channel chip and chemical structure of the adsorbates (a). Chemical structure of the monolayers* ***L0***, ***TM0***, ***TM2***, ***L2***, *formed inside the microchannel chip (b).*

The solutions of fluorophores were flushed through the channels during 16 h at a flow rate of 0.04 $\mu Lmin^{-1}$ while vacuum was applied to the common outlet to facilitate the fluid flow.[26] Subsequently, the channels were rinsed with EtOH and dried with N_2.

For acquisition of the fluorescence images an inverted fluorescence microscope equipped with a CCD camera was used. Lissamine, TAMRA and Bengal Rose fluorophores have a broad spectral profiles with a maximum absorption at 568 nm, 541 nm and 556 nm, respectively, and therefore, they are suitable for excitation with green light. For imaging of the channels green excitation light ($510 \leq \lambda \leq 550$ nm) was used and red emission light ($\lambda > 590$ nm) was detected (see experimental section for further details). The fluorescence microscopy image of the chip depicted in Figure 6.10a confirmed the successful covalent attachment of Lissamine in channels C1 and C2 and of TAMRA in channels C4 and C5. The fact that channels modified with the same SAM showed similar fluorescence intensities (Figure 6.10a) indicated the reproducibility of the monolayer formation. In agreement with the absorption spectra, higher emission intensity was detected in the TAMRA-modified channels than in the Lissamine-modified channels. The lower fluorescence emission observed in channel C3 indicated poor immobilization of the Bengal Rose, which was not covalently attached to the glass walls and therefore, mostly washed away during the rinsing process.[27] Additionally, the combination of these observations rules out the cross contamination on the channels.

Subsequently, channels C1 and C5 of the same chip were functionalized with a ligating group. A flow of a hexanoyl chloride solution (12 mM, chloroform) was continuously injected in these channels during 16 h at a flow rate of 0.04 $\mu Lmin^{-1}$ at the same time that acetonitrile was flushed through channels C2, C3 and C4 at the same flow rate, and vacuum was applied on the common outlet. After the standard rinsing procedure the fluorescence microscopy images were recorded. They showed a clear change in the fluorescence emission of channel C5 indicating successful functionalization of the fluorescent monolayer with the ligand (Figure 6.10b). This fluorescence enhancement is in agreement with the data shown in Chapter 5 of this thesis, where a higher emission intensity was observed for the ***TM2*** than for ***TM0*** layers. In channel C1 no enhancement was observed, also in agreement with the emission intensity of the hexanoyl functionalized ***L2*** SAMs compared with the ***L0*** SAM**.**

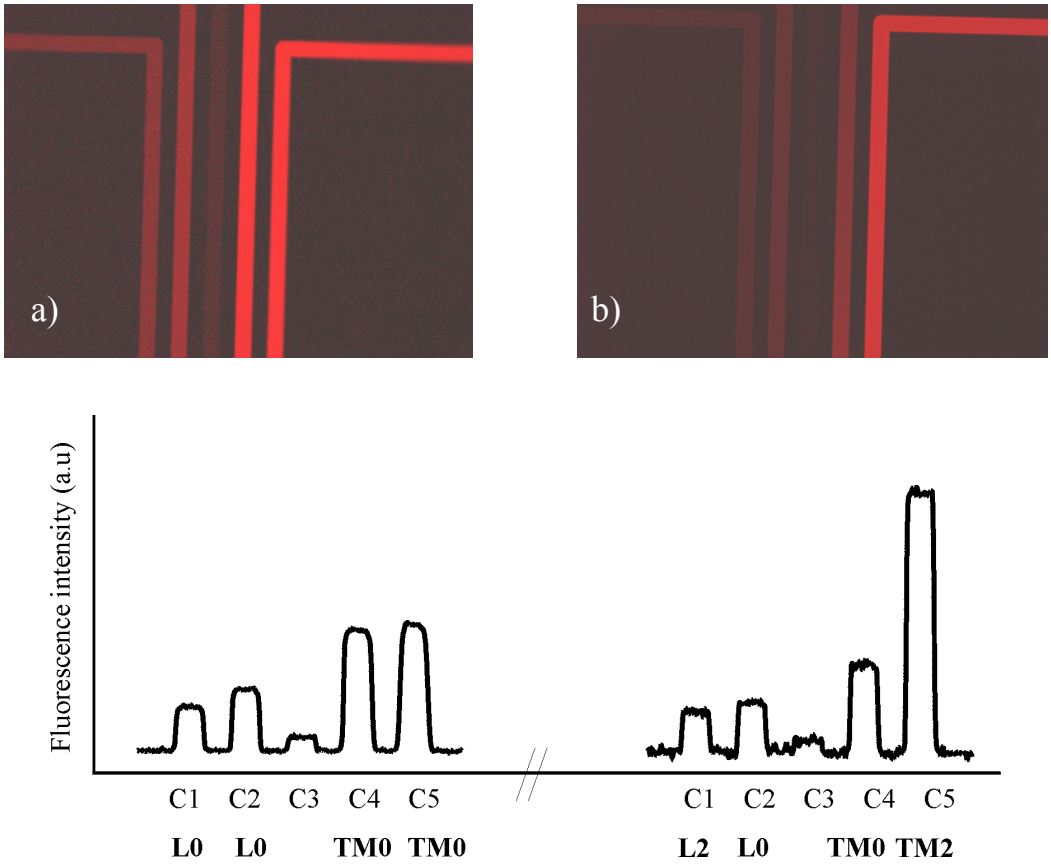

Figure 6.10. *Top: Fluorescence microscopy images ($510 \leq \lambda_{ex} \leq 550$ nm; $\lambda_{em} > 590$ nm) of the multichannel chip, after flow of Lissamine (C1 and C2), Bengal Rose (C3) and TAMRA (C4 and C5) (a) and after flow of hexanoyl chloride to form* ***L2*** *(C1) and* ***TM2*** *(C5) SAMs (b) (see Figure 6.9 for SAMs structures) Bottom: Fluorescence intensity profiles of the images above.*

The result of this experiment proved the control over the modification of the microchannel array with the desired sensing fluorescent monolayer.

Once the protocol for the parallel generation of the sensing channels was optimized, the simultaneous synthesis of five different fluorescent monolayers was performed on a five-microchannel chip. The channels of the chip were coated with the amino-terminated SAM ***TPEDA*** following the procedure explained above (see also experimental part). Subsequently, each channel was exposed to a continuous flow of a different amino-reactive fluorophore solution (0.1 mM, acetonitrile) during 16 h at a flow

rate of 0.04 μLmin^{-1} while vacuum was applied to the outlet. Fluorophores Lissamine, FITC, TRITC, Oregon Green (OG) and TAMRA were injected in channels C1, C2, C3, C4 and C5, respectively (Figure 6.11).

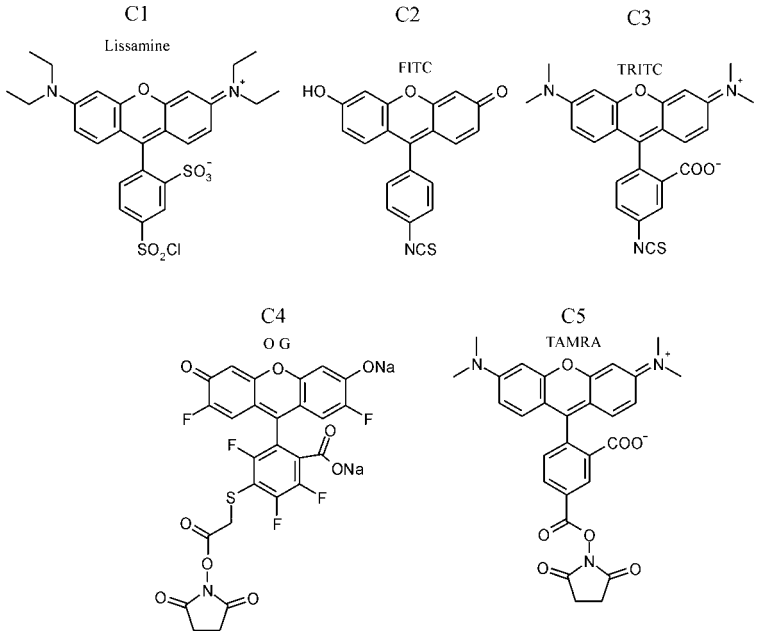

Figure 6.11. *Chemical structures and channel location of the five amino-reactive fluorophores.*

After the reaction, the channels were rinsed with ethanol using the standard procedure (see experimental part) and the fluorescence microscopy images of the chip were acquired. Lissamine, TAMRA and TRITC fluorophores are suitable for excitation with green light while the FITC and OG, with maximum absorption at 494 nm 511 nm, respectively, are suitable for blue light excitation. For visualization of the channels two fluorescent images were recorded; first green excitation light ($510 \leq \lambda \leq 550$ nm) was used and red emission light ($\lambda > 590$ nm) was detected, followed by a second imaging using blue excitation light ($450 \leq \lambda \leq 480$ nm) and green emission ($\lambda > 515$ nm). After acquisition an overlay image was generated with digital imaging software (Figure 6.12) (see experimental section for further details).

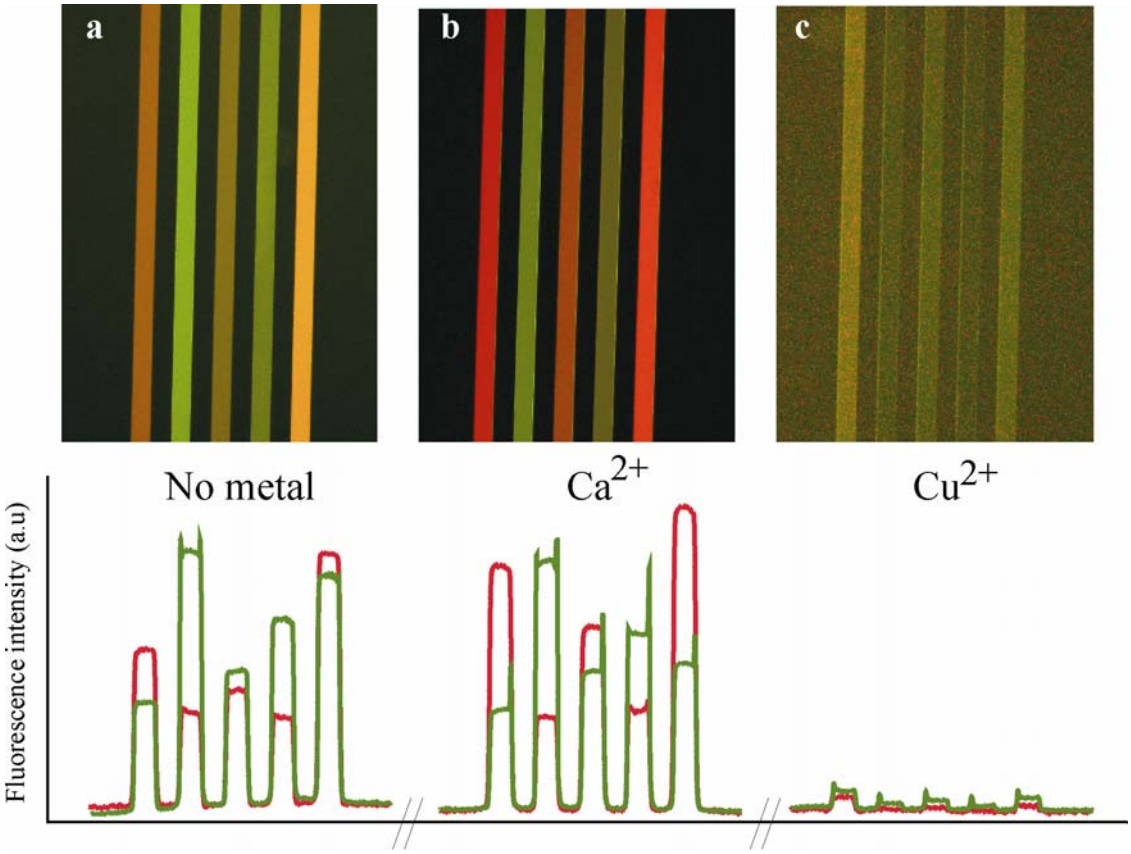

Figure 6.12. *Top: Overlay image of the multichannel chip functionalized with an array of five different fluorescent monolayers filled with acetonitrile (a), Ca^{2+} (perchlorate salt, 10^{-4} M, acetonitrile) (b) and Cu^{2+} (perchlorate salt, 10^{-4} M, acetonitrile) (c). Bottom: Fluorescence intensity profiles of the fluorescent images above. Red lines correspond to the red collecting channel and green lines correspond to the green collecting channel.*

The fluorescence profiles (Figure 6.12) show the emission intensity measured in the red and the green collecting channels. Subsequently, the sensing properties of the monolayer array for Ca^{2+} and Cu^{2+} were evaluated (Figure 6.12).[28] The channels were filled with acetonitrile (Figure 6.12a) and Ca^{2+} (perchlorate salt, 10^{-4} M, acetonitrile) (Figure 6.12b). The fluorescence intensity of each SAM-coated channel varied, which created a fluorescent pattern in the presence of Ca^{2+}. Afterwards a flow of Cu^{2+} (perchlorate salt, 10^{-4} M acetonitrile) was injected during 5 minutes at a flow rate of 0.04 $\mu L min^{-1}$ and different levels of fluorescent quenching in the channels were observed (Figure 6.12,c). These results are in agreement with those previously showed in Chapter 3 and Chapter 5.

The collective response of the sensing chip results in a different finger print for each metal ion.

6.3 Conclusions and outlook

Sensing based on the use of a multichannel chip with parallel synthesis of sensing SAMs has been demonstrated. Fluorescent sensing monolayers have been synthesized on the walls of glass microchannels. These functionalized channels constitute non-specific fluorescent sensing probes which allow for on-line monitoring of analyte solutions in real time. The simple design of the multichannel chip and the straightforward formation of fluorescent self-assembled monolayers inside the channels allowed the fabrication of miniaturized sensor arrays for continuous monitoring of solutions. The parallel synthesis of five different monolayers has been performed in a single multichannel chip containing five parallel 2 μm deep channels for differential sensing of Ca^{2+} and Cu^{2+} ions. Results obtained on the formation and the sensing properties of fluorescent SAMs inside the channels, are in good agrement with those reported in Chapter 3 and Chapter 5 of this thesis for sensing SAMs prepared in glass slides; suggesting that large sensing libraries could be transfer to microfluidic chips. The combination of the approach described here with mathematic tools for pattern recognition will provide enhanced design flexibility to expand the toolbox for fabrication of microfluidics systems for sensing applications.

6.4 Experimental

Materials

Microchips

Monochannel chip: Borosilicate glass microchips were fabricated with conventional wet-etch technology at $MESA^+$ Institute for Nanotechnology (Enschede, The Netherlands) using cleanroom facilities.
Five-channel chip: Borosilicate glass multichannel microchips were designed in collaboration with the BIOS group (University of Twente, The Netherlands) and manufactured for Micronit Microfluidics bv. (Enschede, The Netherlands)

Microchip holder

Microchip holders were fabricated by the BIOS group (University of Twente, The Netherlands) from black Delrin blocks.

Sample injection into microchannels

Monochannel chip: The chip was placed in a Delrin (Dupont) custom made holder onto which syringes could be connected to create pressure driven flows. Magnets were placed in the base of the holder to fix the holder on a steel platform mounted on the scanning stage of the confocal microscope in order to guarantee a fixed relative position between the chip and the objective.

Multichannel chip: The chip was placed in a Delrin (Dupont) custom made holder. Solutions were introduced inside the channels either through the outlet or the independent inlet of the channels by means of dual CMA/102 Microdialysis Pump (flow rate 0.1-20 μLmin $^{-1}$ using 1 mL syringes) on which 100 μL Hamilton syringes were mounted. Syringes were connected to fused silica capillaries of 20 μm inner diameter (i.d.) and 376 μm outer diameter (o.d.) by means of NanoTigh^{TM} Unions and Fittings (Upchurch Scientific).

Chemicals

Analytical reagent grade solvents were purchased from Fisher Scientific. Fluorophores TAMRA (5-(and-6)-carboxytetramethylrhodamine (5(6)-TAMRA) *mixed isomers*), Lissamine (Lissamine™ rhodamine B sulfonyl chloride *mixed isomers*), TRITC (tetramethylrhodamine-5-(and-6)-isothiocyanate (5(6)-TRITC) *mixed isomers*), FITC (fluorescein-5-isothiocyanate), and OG (Oregon Green® 514 carboxylic acid, succinimidyl ester) were purchased from Molecular probes (Invitrogen). Bengal Rose (4,5,6,7-tetrachloro-2′,4′,5′,7′-tetraiodofluorescein sodium salt Acid Red 94) fluorophore and all other reagents were purchased from Sigma-Aldrich.

Visualization

Monochannel chip: The chip was placed in a Delrin (Dupont) custom made holder onto which syringes could be connected to create pressure driven flows. Confocal microscopy images were carried out using an inverted confocal scanning fluorescence microscope (CFM, Zeiss Axiovert) with an oil immersion objective lens (Olympus NA 1.3, 100x). Circularly polarized light coming from an Ar^+/Kr^+ ion laser (Spectra Physics, BeamLok 2060) was used to excite the dye molecules (λ_{ex}=514 nm). The fluorescence light emitted by the fluorophore was collected through the same objective lens, separated from the excitation light by use of a dichroic mirror (Omega 540DRLP) and a rejection band filter (514.5 Raman), and directed to the small detection area (180 μm diameter) of an avalanche photodetector (SPCM-AQ-14, EG&G Electro Optics). Fluorescence images were acquired by raster-scanning the samples over areas of 20 x 20 – 30 x 30 μm^2 at a pixel frequency of 1 kHz and an excitation power within the range 0.1-0.5 kW/cm^2.

Multichannel chip: The chip was placed in a custom made holder designed to connect Nanoport^{TM} assemblies and fused silica capillaries to the chip to create pressure driven flows. Fluorescent and transmission images were made using an Olympus inverted research microscope IX71 equipped with a mercury burner U-RFL-T as light source and a digital camera Olympus DP70 (12.5 million-pixel cooled digital color camera) for image acquisition. Blue excitation light (450 nm ≤ λ ≤480 nm) and green emission light (λ > 515 nm) was filtered using a U-MWB Olympus filter cube. Green excitation light (510 nm ≤ λ ≤ 550 nm) and red emission light (λ > 590 nm) was filtered using a U-MWG Olympus filter cube.

Synthesis of monolayers inside the channels

Monochannel chip: For the synthesis of ***TM1*** on the walls of the microchannel, piranha was flowed into a microchannel and kept for 10 min, followed by rinsing with ultrapure (MiliQ) water and dried with air stream. Immediately afterwards, the channel was placed in a glovebox under a dry N_2 atmosphere, and a 5 mM solution of N-[3-(trimethoxysilyl)propyl]ethylenediamine in dry toluene (freshly distilled over sodium) was flowed into the channel and kept for 3 h. The resulting amino-terminated SAM was rinsed sequentially with toluene, EtOH, and CH_2Cl_2. Still in the glovebox, a 0.2 mM solution of TAMRA fluorophore in acetonitrile was flowed into the channel and kept for 2 h, then rinsed sequentially with CH_3CN, EtOH and CH_2Cl_2. Subsequently a 0.1 mM $CHCl_3$ solution of *p*-isopropylphenyl isocyanate was flowed into the channel, keeping it for 16 h and then rinsing with $CHCl_3$, EtOH and CH_2Cl_2.

*Multichannel chip: Synthesis of **TPEDA** SAM on the microchannels walls*

The chip was introduced in a beaker containing piranha in vertical position in order to immerse only the channel outlet in the solution. The piranha solution was observed to ascend along the walls by capillarity, and it was kept inside the channel for 15 minutes. Afterwards the channels were rinsed with EtOH and subsequently dried using a stream of N_2 at a pressure of 1.5 bar. Immediately afterwards, the channel was placed in a glove box under a dry N_2 atmosphere, and introduced vertically positioned in a beaker containing a 5 mM solution of N-[3-(trimethoxysilyl)propyl]ethylenediamine in dry toluene (freshly distilled over sodium) in order to immerse only the channel outlet in the solution. The silane solution was observed to ascend along the walls by capillarity, and it was kept inside for 3h. After reaction the chip was rinsed two times inside the glove box, by subsequent immersion of the whole chip in two beakers filled with toluene. Then the chip was removed from out of the nitrogen glove box and the channels were rinsed with EtOH using the following procedure: the channels were filled with EtOH and sequentially dried with a N_2 flow at a pressure of 1.5 bars several times through the outlet, and afterwards a flow of EtOH was injected into the channels for 30 min at a flow rate of 0.04 $\mu Lmin^{-1}$.

*Functionalization of the **TPEDA** SAM with fluorophores*

Acetonitrile solutions (0.1 mM) of TAMRA, Lissamine, TRITC, Oregon Green, Bengal Rose and Florescein containing 0.01 % of Et_3N were flowed simultaneously through the independent inlets of each channel of a ***TPEDA***-coated chip at a flow rate between 0.04 and 0.08 $\mu Lmin^{-1}$ during at least 16 h. Vacuum was applied in the outlet to favor the solutions' flow. After fluorophore reaction the channels were rinsed with EtOH with the following procedure: the channels were alternatively filled with EtOH and dried with a N_2 flow at a pressure of 1.5 bars several times through the outlet, and afterwards a flow of EtOH was injected into the channels for 30 min at a flow rate of 0.04 $\mu Lmin^{-1}$.

Functionalization of fluorescent monolayers with ligating groups

A 12 mM solution of hexanoyl chloride in chloroform was flowed through the fluorescent SAM-coated channels to be modified, while at the same time CH_3CN was flowed through the channels that should remain unmodified. A flow rate of 0.04 $\mu Lmin^{-1}$ during 16 h was applied. Vacuum was applied in the outlet to favor the solutions' flow. After ligand reaction the channels were rinsed, alternatively filling them with EtOH and drying with a N_2 flow at a pressure of 1.5 bars several times through the outlet. Afterwards a flow of EtOH was injected to the channels for 30 min at a flow rate of 0.04 $\mu Lmin^{-1}$.

6.5. References and Notes

1 Vilkner, T.; Janasek, D.; Manz, A. Micro Total Analysis Systems. Recent Developments. *Anal.*

Chem. ***2004***, 76(12), 3373-3385.
2 Andersson, H.; Van den Berg, A. Microfluidic Devices for Cellomics: a Review. *Sens. Actuators, B* ***2003***, 92(3), 315-325.
3 Mela, P.; Onclin, S.; Goedbloed, M. H.; Levi, S.; García-Parajó, M. F.; Van Hulst, N. F.; Ravoo, B. J.; Reinhoudt, D. N.; Van den Berg, A. Monolayer-Functionalized Microfluidics Devices for Optical Sensing of Acidity. *Lab Chip* ***2005***, 5(2), 163-170.
4 Buranda, T.; Huang, J. M.; Perez-Luna, V. H.; Schreyer, B.; Sklar, L. A.; Lopez, G. P. Biomolecular Recognition on Well-Characterized Beads Packed in Microfluidic Channels. *Anal. Chem.* ***2002***, 74(5), 1149-1156.
5 Fan, H. Y.; Lu, Y. F.; Stump, A.; Reed, S. T.; Baer, T.; Schunk, R.; Perez-Luna, V.; Lopez, G. P.; Brinker, C. J. Rapid Prototyping of Patterned Functional Nanostructures. *Nature* ***2000***, 405(6782), 56-60.
6 Rudzinski, C. M.; Young, A. M.; Nocera, D. G. A Supramolecular Microfluidic Optical Chemosensor. *J. Am. Chem. Soc.* ***2002***, 124(8), 1723-1727.
7 Guijt, R. M.; Baltussen, E.; Van der Steen, G.; Schasfoort, R. B. M.; Schlautmann, S.; Billiet, H. A. H.; Frank, J.; Van Dedem, G. W. K.; Van den Berg, A. New Approaches for Fabrication of Microfluidic Capillary Electrophoresis Devices with On-Chip Conductivity Detection. *Electrophoresis* ***2001***, 22(2), 235-241.
8 Sato, K.; Hibara, A.; Tokeshi, M.; Hisamoto, H.; Kitamori, T. Microchip-Based Chemical and Biochemical Analysis Systems. *Adv. Drug Delivery Rev.* ***2003***, 55(3), 379-391.
9 Epstein, J. R.; Walt, D. R. Fluorescence-Based Fibre Optic Arrays: a Universal Platform for Sensing. *Chem. Soc. Rev.* ***2003***, 32(4), 203-214.
10 James, D.; Scott, S. M.; Ali, Z.; O'hare, W. T. Chemical Sensors for Electronic Nose Systems. *Microchim. Acta* ***2005***, 149(1-2), 1-17.
11 Lavigne, J. J.; Savoy, S.; Clevenger, M. B.; Ritchie, J. E.; Mcdoniel, B.; Yoo, S. J.; Anslyn, E. V.; Mcdevitt, J. T.; Shear, J. B.; Neikirk, D. Solution-Based Analysis of Multiple Analytes by a Sensor Array: Toward the Development of an "Electronic Tongue". *J. Am. Chem. Soc.* ***1998***, 120(25), 6429-6430.
12 Munro, N. J.; Huhmer, A. F. R.; Landers, J. P. Robust Polymeric Microchannel Coatings for Microchip-Based Analysis of Neat PCR Products. *Anal. Chem.* ***2001***, 73(8), 1784-1794.
13 Crooks, R. M.; Ricco, A. J. New Organic Materials Suitable for Use in Chemical Sensor Arrays. *Acc. Chem. Res.* ***1998***, 31(5), 219-227.
14 Kaifer, A. E. Functionalized Self-Assembled Monolayers Containing Preformed Binding Sites. *Isr. J. Chem.* ***1996***, 36(4), 389-397.
15 Brivio, M.; Oosterbroek, R. E.; Verboom, W.; Goedbloed, M. H.; Van den Berg, A.; Reinhoudt, D. N. Surface Effects in the Esterification of 9-Pyrenebutyric Acid Within a Glass Micro Reactor. *Chem. Commun.* ***2003***, (15), 1924-1925.
16 Zhao, B.; Moore, J. S.; Beebe, D. J. Surface-Directed Liquid Flow Inside Microchannels. *Science* ***2001***, 291(5506), 1023-1026.
17 Zhao, B.; Moore, J. S.; Beebe, D. J. Principles of Surface-Directed Liquid Flow in Microfluidic Channels. *Anal. Chem.* ***2002***, 74(16), 4259-4268.
18 Smith, E. A.; Thomas, W. D.; Kiessling, L. L.; Corn, R. M. Surface Plasmon Resonance Imaging Studies of Protein-Carbohydrate Interactions. *J. Am. Chem. Soc.* ***2003***, 125(20), 6140-6148.
19 Kobayashi, J.; Mori, Y.; Okamoto, K.; Akiyama, R.; Ueno, M.; Kitamori, T.; Kobayashi, S. A Microfluidic Device for Conducting Gas-Liquid-Solid Hydrogenation Reactions. *Science* ***2004***, 304(5675), 1305-1308.
20 The confocal microscopy measurements were imaged in the xy plane. The intensity of the laser was focused only on the bottom wall of the microchannels resulting in the higher intensity of the edges.
21 The contact angle of a monolayer containing a ligand group was not measured. From previous results described in Chapters 3 and 4 it is known that the contact angle of the fluorescent monolayer containing a ligand group does not differ significantly from the contact angle of the fluorescent monolayer without the ligand group, relevant data could not be obtained from such measurement and therefore was not performed.
22 Choi, C. H.; Westin, K. J. A.; Breuer, K. S. Apparent Slip Flows in Hydrophilic and Hydrophobic Microchannels. *Physics of Fluids* ***2003***, 15(10), 2897-2902.
23 Higher fluorescence intensity emission was observed arising from a dried monolayer than from a

monolayer in contact with acetonitrile therefore the emission intensity of the surface in contact with neat acetonitrile must be recorded before applying the analyte solution .

24 After recycling of the channels by washing with 0.1N HCl solution, the fluorescence enhancement in the presence of Pb^{2+} was smaller than the fluorescence enhancement in the presence of Pb^{2+} before the cleaning, probably due to some degradation of the layers.

25 The thickness of the glass bottom plate was 175 μm to allow fluorescent microscopy imaging of the bottom surface of the channel even with oil inmersion objectives for aquisition of higher resolution images if needed.

26 If vacuum is not applied, cross contamination is observed between channels. When the fluid reaches the common outlet it may get inside the adjacent channels due to capillary forces .

27 The small fluorescent signal obtained in channel C3 may correspond to physiabsorbed material or to cross contamination during the washing steps from the common outlet or to physiabsorbed fluorophore. Nevertheless, Bengal Rose has a lower quantum yield than TAMRA and Lissamine and therefore its emission intensity should also be lower. Corrections for this have not been done.

28 Two fluorescence images were obtained each time and then combined, one using blue light and the other using green light for excitation of the fluorophores.

Chapter 7

Combinatorial Fabrication of Fluorescent Patterns with Metal Ions on Glass by Soft and Probe Lithography*

The fluorescent monolayers on glass described in Chapters 3 and 4 of this thesis have been used for the generation of sub-millimeter fluorescent metal ion patterns on glass substrates. Two combinatorial approaches based on monolayer chemistry, fluorescence microscopy and microcontact printing or dip-pen nanolithography are presented. In the first approach, a library of fluorescent patterns is obtained by modification of amino-terminated monolayers with different fluorophores by microcontact printing. The fluorescence of these patterns can be modulated upon exposure to a variety of metal ion solutions. In the second approach, full fluorescent monolayers are made in solution and different metal ions are locally deposited onto these fluorescent SAMs by microcontact printing or dip-pen nanolithography. Modulation of the original SAM fluorescence is achieved exclusively only where the metal ion has been deposited.

---

* Part of this chapter has been published in: Basabe-Desmonts, L.; Beld, J.; Zimmerman, R. S.; Hernando, J.; Mela, P.; García Parajó, M. F.; Van Hulst, N. F.; Van den Berg, A.; Reinhoudt, D. N.; Crego-Calama, M.; *J. Am. Chem Soc.* ***2004***, *126*, (23), 7293-7299
Part of this chapter has been submitted to *Adv. Mater*: Basabe-Desmonts, L.; Reinhoudt, D. N.; Crego-Calama, M.
Manuscript in preparation: Basabe-Desmonts L.; Peter, M.; Reinhoudt, D. N.; Crego-Calama, M.

7.1. Introduction

Pattern fabrication is an important issue in many fields ranging from microelectronics to biological microarray production and nanotechnology.[1,2] Soft and probe lithography techniques such as microcontact printing (μCP) and dip-pen nanolithography (DPN) are frequently used to pattern surfaces,[3,4] mainly by immobilizing a self-assembled monolayer (SAM) onto a bare substrate which can serve as an etch resist.[3] Conventional μCP is an efficient and low-cost method for patterning with feature sizes between ca. 0.5 μm and few millimeters. μCP uses conformal contact of a patterned elastomer with a surface to transfer a chemical ink from the elastomer to localized areas of the surface due to the physical properties of the rubber-elastic polymer stamp.[3] The targets printed on a SAM[3] vary from molecules (and/or biomolecules) with different sizes to catalysts,[5] polymers,[6] dendrimers,[7] and only recently metal ion salts.[8,9] Microcontact printing can be used as well to construct functionalized patterns on a surface via covalent attachment of a molecule to a reactive monolayer,[10-14] or via non-covalent synthesis using supramolecular interactions for the immobilization of molecules on functionalized surfaces.[7] Many procedures for the direct fabrication and visualization of functional monolayer patterns often rely on specific binding between molecules. Specific interactions between antibody and antigen have been used for fabrication and visualization of patterned surfaces.[15] Smart methods like affinity microcontact printing have been used to produce reproducible protein arrays by μCP.[16] Ligand-metal interactions and other supramolecular interactions have been used to build up 3D structures[17] and fluorescent patterns[18] on surfaces. [19]Nevertheless, the diversity in the patterned structures is restricted by the elaborate design and by the use of a very limited number of substrate-ligand pairs with highly specific interactions.

Dip-pen nanolithography is a high resolution patterning technique that enables the creation of patterns from the sub 100 nm to many micrometers length scale.[4] This technique uses an ink-coated AFM (atomic force microscopy) tip as a nanopen. The ink molecules are transported from the tip to a substrate, normally by capillary forces when the tip is in contact with the surface of the substrate.[4,20] The driving force for such transport is chemisorption of the ink to the underlying substrate due to a chemical[21] or

electrochemical force.[22] Since its discovery in 1999,[23] DPN has been performed with inks like alkanethiols, proteins and DNA on gold surfaces as well as with or metal salts, metal oxides, silanes, alkanoxysilanes, organic dyes, dendrimers, polymers and trichlorosilanes on silicon oxide surfaces.[4] Metal salts have also been deposited on semiconductor substrates using electrochemistry as the driving force to generate metallic patterns.[9,22,24] However, deposition of metal ions on glass substrates by DPN has never been reported before, and in the literature only a few examples deal with the generation of fluorescent patterns by DPN.[18] In this chapter the pattern generation by DPN using metal salt solutions as ink onto a glass (nonconductive) substrate will be presented.

Even though soft-lithography techniques (μCP) have been applied to combinatorial methods, the scope of these studies has been limited to the immobilization of arrays of proteins[25] or nanocrystals[26] on surfaces, in order to optimize the patterning of molecular organic semiconductors by organic vapor jet printing,[27] and to optimize the properties of polymers anchored to surfaces.[28] DPN can be used to generate a large number of different patterns from the same or different chemical inks, which can be screened under identical conditions. Parallel probe cantilevers[29] and fountain tips[30] are being developed. Combinatorial approaches using DPN have been used to fabricate particle arrays,[31] to generate libraries of patterns for studying ink exchanges between the ink and nanostructures on the substrate[32] and to deposited monolayer-based resists with micrometer to sub 100 nm dimensions on different substrates for the generation of solid-state features.[33] All these cases are restricted to a unique, printable substrate and they are not systematically expanded to the fabrication of different substrates and to the use of different ligand-substrate combinations. In contrast to these specificity-based patterning methods, and using the combinatorial approach described in Chapter 3 for the parallel synthesis of sensing fluorescent monolayers, two unprecedented combinatorial approaches for the generation of libraries of luminescent patterns on glass are presented in this chapter.

In the first approach, fluorescent patterns on glass slides are generated by μCP of fluorophores onto amino-terminated monolayers (Approach 1, Figure 7.1). An elastomeric stamp is inked with a fluorophore (Fx) solution and placed onto a glass slide functionalized with an amino-terminated SAM (***TPEDA***) (Figure 7.1). The fluorophore is

covalently attached to the amino-terminated SAM generating a fluorescent patterned surface P (Fx). Subsequently, the unreacted amino groups are functionalized with ligand molecules (Ly) by immersing the patterned substrate P (Fx) in a Ly solution. Using different fluorophores (Fx)-ligand (Ly) combinations a library of patterned surfaces can be achieved (P (Fx, Ly) (x, y = 1, 2, 3…, n)) (Figure 7.1). In this way the sensing systems presented in Chapters 3 and 4 of this thesis are miniaturized to micrometer feature sizes. Each component of this library is a patterned fluorescent glass substrate with different complexing abilities for metal ions. Modulation of the fluorescence of the pattern, i.e. different degrees of fluorescence enhancement or quenching, is achieved by delivering different metal ions Mz (z = 1, 2, 3,…, n) onto the layers (Figure 7.1).

In the second approach (Approach 2, Figure 7.1) fluorescent metal ion patterns are achieved by deposition of the metal ion salts on discrete areas of glass substrates fully covered with fluorescent SAMs (SAM (Fx,Ly)). First a library of non-patterned fluorescent self-assembled monolayer SAMs (Fx,Ly) (x,y = 1,2,3,…, n; Figure 7.1) is made by sequential deposition of fluorophores Fx and ligand molecules Ly onto an amino-terminated monolayer on glass using solution synthesis (see Chapter 3). Modulation of the fluorescence is achieved by delivering different metal ions Mz (z = 1, 2, 3,…, n) onto the layer by μCP (see section 7.2. 2) or DPN (see section 7.2.3). The fluorescence modulation is produced in the contact areas between the stamp (μCP) and the AFM tip (DPN) and the fluorescent SAM. As in *Approach 1,* a library of fluorescent patterns is obtained where each pattern P(Fx,Ly,Mz) (x,y,z = 1,2,3,…,n), is the result of the combination of three building blocks, i.e. a fluorophore, a ligand molecule and a metal ion.

The basic concept of these approaches is the fast generation and screening of substrates which store fluorescent and/or metal ion patterns. Besides the simplicity in the pattern generation, the approaches presented here offer the advantage of easy high throughput analysis. Visualization of the generated patterns is simply analyzed by fluorescence microscopy.

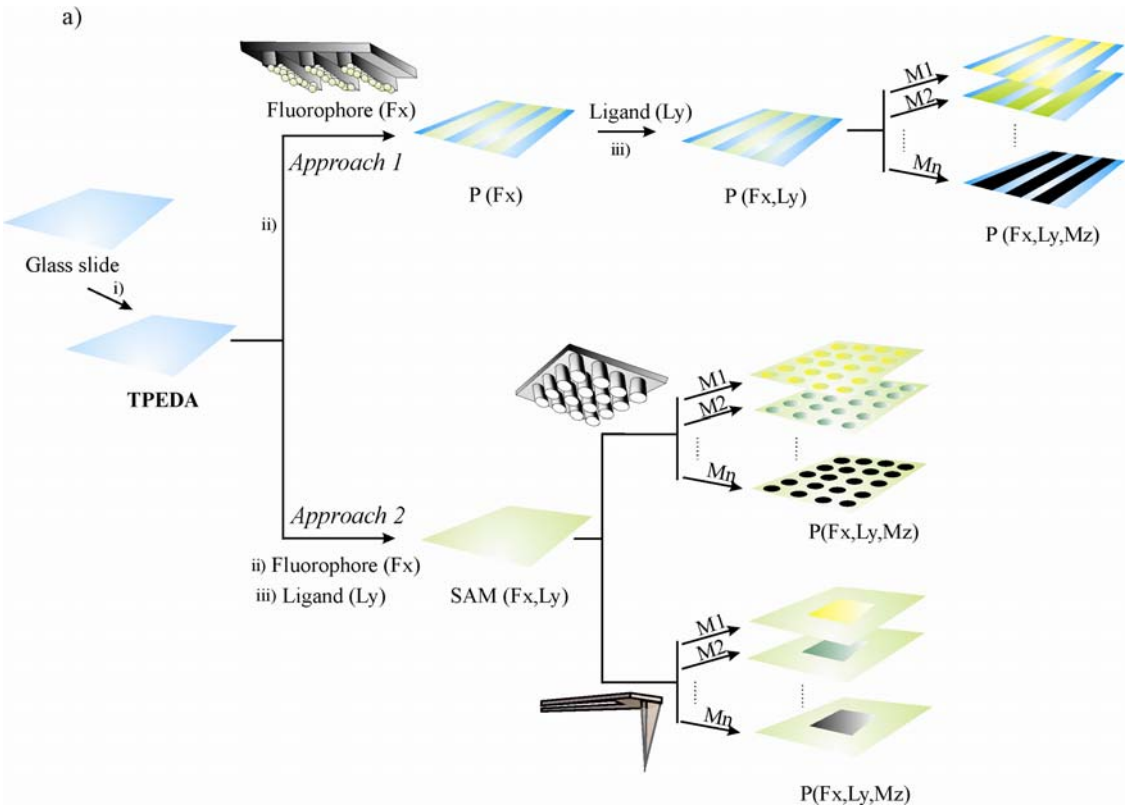

Figure 7.1. *Approach 1: Functionalization of a glass slide with the amino-terminated* ***TPEDA*** *SAM (i); formation of a fluorescent patterned monolayer (P (Fx)) by μCP of a fluorophore (Fx) onto the* ***TPEDA*** *SAM-coated glass slide (ii); Subsequent modification of the P (Fx) by reaction with a ligand molecule (Ly) in solution to form the patterned SAM P (Fx,Ly) (iii). Exposure of P (Fx,Ly) to different metal ion solutions (Mz) enhances or quenches the fluorescence emission of the pattern. Approach 2: Functionalization of a glass slide with the amino-terminated* ***TPEDA*** *SAM (i); functionalization of the* ***TPEDA*** *SAM with a fluorophore (Fx) (ii) and with a ligand molecule (Ly) (iii) in solution to produce a fully covered non-patterned fluorescent SAM (Fx,Ly). Subsequently μCP or DPN are used to transfer metal ions (Mz) from a PDMS stamp or an AFM tip onto the substrates thus creating metal ion patterns. Modulation of the fluorescence of the substrate is observed where the metal ions have been deposited.*

Additional labeling steps are not required and more demanding and sophisticated scanning probe microscopy techniques such as atomic force microscopy (AFM) or scanning electron microscopy (SEM)[34] are avoided. Areas of the patterned surfaces can be obtained with millimeter to nanometer resolution while techniques such as AFM are

limited to an area range smaller than 150 μm. A number of applications for these patterned surfaces are envisioned, such as materials for rewritable data storage, sub-millimeter luminescent and metallic patterns, nanosensors, and multicolor patterns.[35-37]

7.2 Results and discussion

In this chapter two lithographic techniques, microcontact printing (μCP) and dip-pen nanolithography (DPN), have been used for the generation of fluorescent patterns. The use of μCP for pattern fabrication using *Approach 1* and *Approach* 2 (see above) will be discussed in section 7.2.1 and 7.2.2 respectively. The use of DPN for the generation of patterns using the *Approach* 2 concludes this chapter (section 7.2.3).

7.2.1 Fabrication of fluorescent patterns by microcontact printing (Approach 1)

An amino-terminated N-[3-(trimethoxysilyl) propyl] ethylenediamine SAM ***TPEDA*** was synthesized on a glass surface as described previously (see Chapter 3). Subsequently, a PDMS (poly(dimethoxysiloxane)) stamp was first inked with an acetonitrile solution of the fluorophores TAMRA and Lissamine* and brought into contact with the ***TPEDA (***during 1 and 2.5 min. respectively), resulting in the covalent attachment of the fluorophore to the glass substrate. The result is the patterned fluorescent monolayer ***TM0*** and ***L0*** respectively, with 5μm wide parallel lines separated by 3μm.

* (5(6)- TAMRA (5(6)-carboxytetramethylrhodamine, succinimidyl ester) or Lissamine (rhodamine B, sulfonyl chloride))

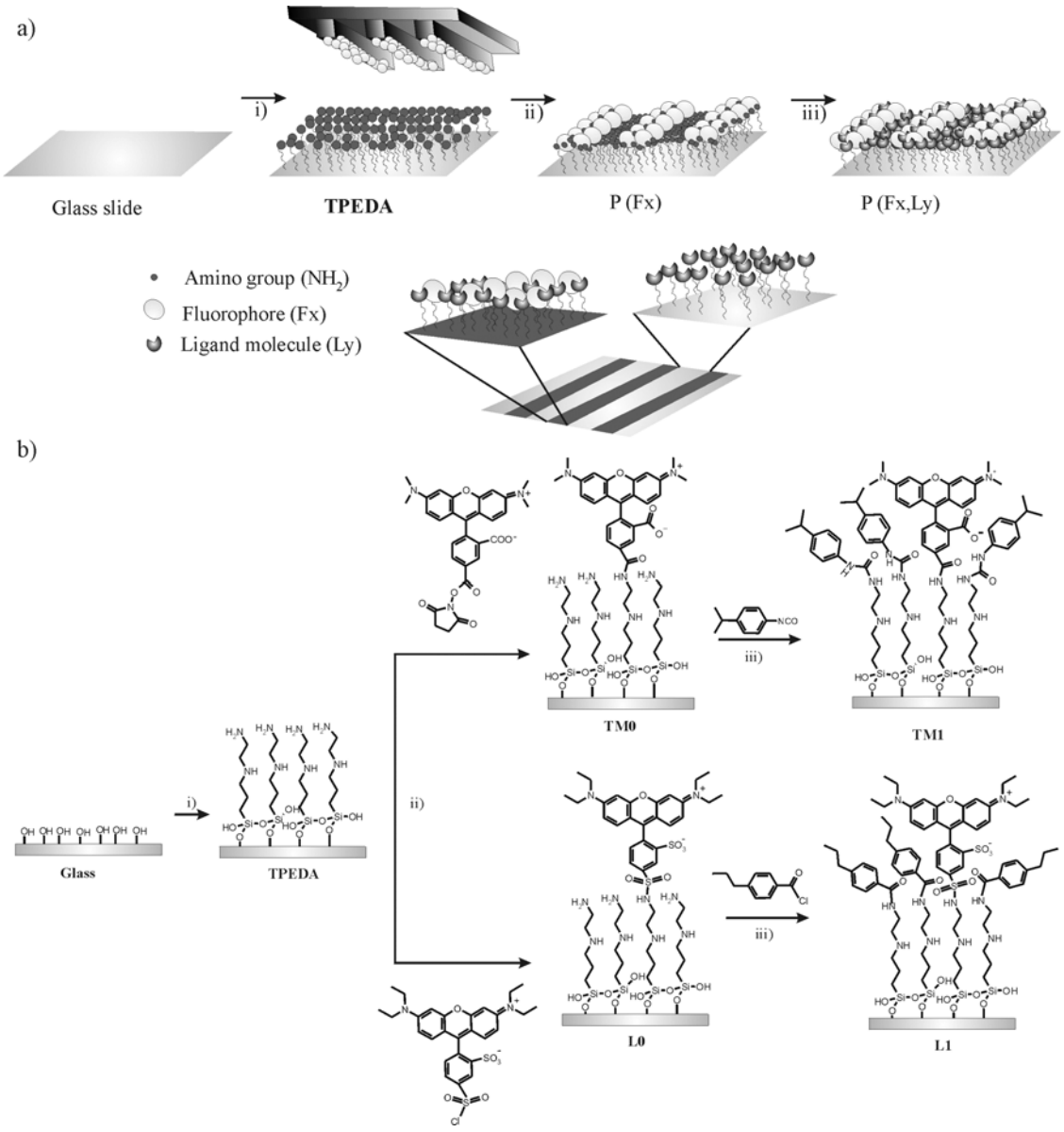

Figure 7.2. *a) Cartoon of the fabrication process of fluorescent patterned glass substrates P (Fx, Ly). b) Synthetic scheme for the formation of* ***TM1*** *and* ***L1****: i) Functionalization of a glass slide with N-[3-(trimethoxysilyl)propyl]ethylenediamine, (toluene, rt, 3.5 h) to form an the amino-terminated SAM* ***TPEDA*** *ii) μCP of the acetonitrile solution of the fluorophore Lissamine or TAMRA during 1 and 2.5 min., respectively, to afford* ***TM0*** *and* ***L0,*** *respectively iii) Reaction of the patterned fluorescent SAM with p-isopropylphenyl isocyanate or p-propylbenzoyl chloride (chloroform, 16h) in solution.*

After vigorous rinsing,[38] the slide was subsequently immersed in an acetonitrile solution of *p*-isopropylphenyl isocyanate or *p*-propylbenzoyl chloride, resulting in the attachment of the ligands on the surface at the sites of the unreacted amino groups (Figure 7.2). The results of this process are fluorescent patterned substrates ***TM1*** and ***L1*** (Figure 7.3).

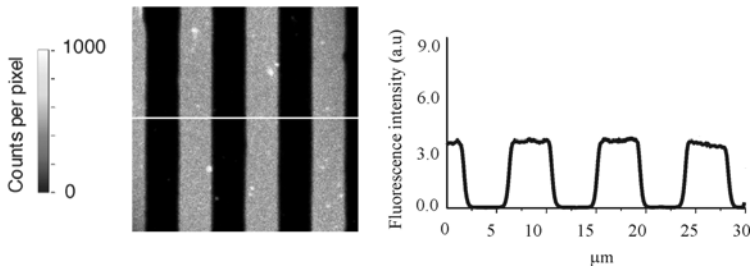

Figure 7.3. *30 x 30 μm^2 confocal fluorescence microscopy image of* ***TM1*** *(left) and plot of the fluorescence intensity profile of the image along the white line (right), showing that only the areas where the fluorophore has been printed are fluorescent.*

The slides were first imaged in acetonitrile by laser confocal microscopy. Then, using a custom built liquid cell, the different slides were put in contact with a 10^{-4} M acetonitrile solutions of perchlorate salts of Co^{2+}, Cu^{2+}, Ca^{2+}, or Pb^{2+} and imaged for fluorescence changes (Figure 7.4). For example, layer ***L1***, microcontact printed with the Lissamine fluorophore and reacted with *p*-propylbenzoyl chloride, resulted in a fluorescence quenching of 70% for Cu^{2+} and 82% and for Co^{2+} while little response towards Pb^{2+} and Ca^{2+} was observed (Figure 7.4). On the other hand, for the ***TM1*** SAM with the TAMRA fluorophore and an ureido ligand responses were completely different. A dramatic 179% increase in the fluorescence was seen for Ca^{2+} (Figure 7.4) and a 98% increase for Pb^{2+}, while there was very little response for both Co^{2+} and Cu^{2+}. Figure 7.4b shows the different fluorescence intensities which arise from the different combinations of fluorophore-ligand molecule and metal ion.

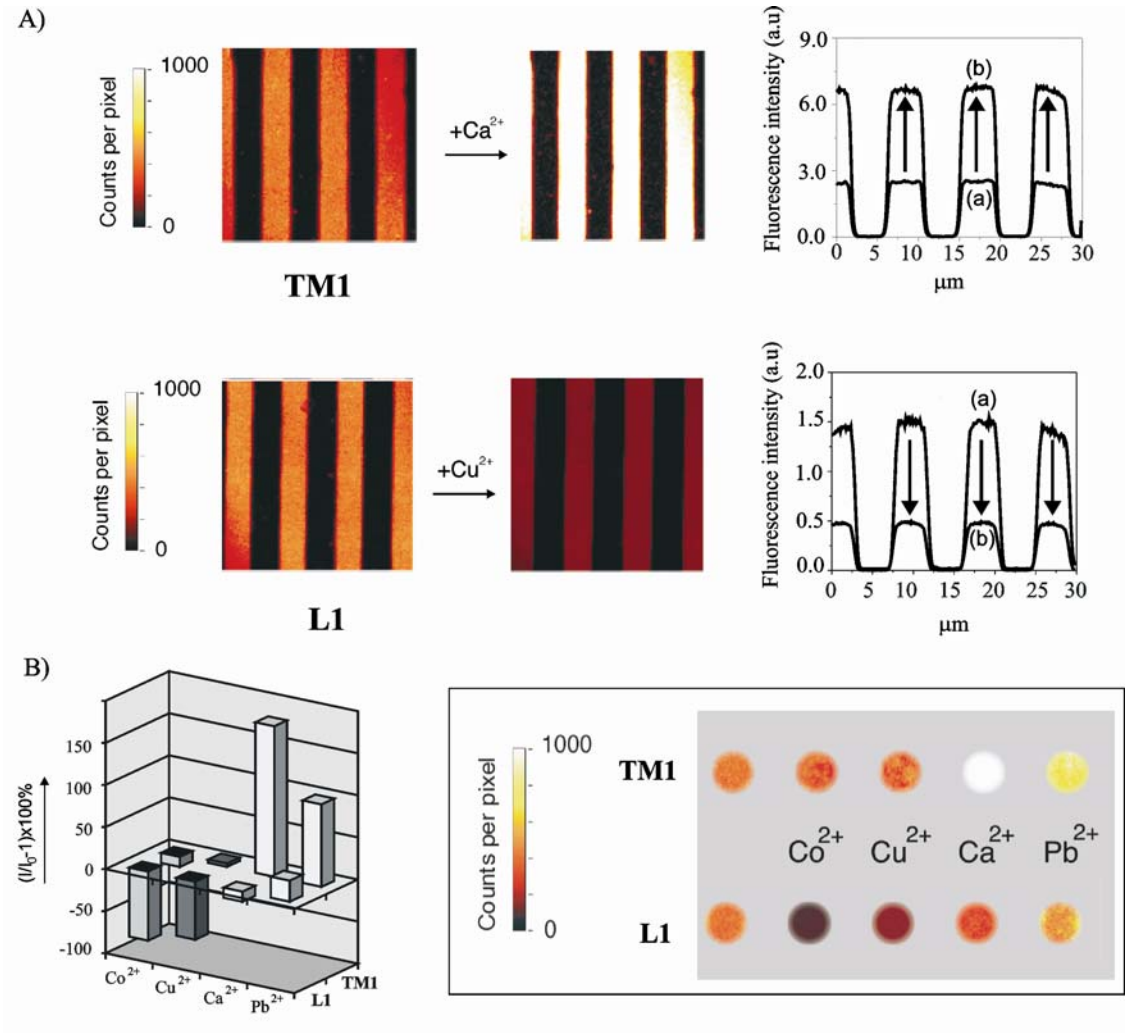

Figure 7.4. *A) (left) Fluorescence confocal microscopy images of the systems* ***TM1*** *and* ***L1*** *in contact with acetonitrile and in contact with* Ca^{2+} *and* Cu^{2+} *(10^{-4} M, acetonitrile) respectively. Profiles of cross sections of the images of* ***TM1*** *and* ***L1*** *before (a) and after (b) addition of* Ca^{2+} *and* Cu^{2+} *(right); B) (Left) Relative fluorescence intensity of systems* ***TM1*** *and* ***L1*** *in the presence of* Pb^{2+}, Cu^{2+}, Co^{2+} *or* Ca^{2+} *(10^{-4} M, acetonitrile). (Right) Array of fluorescence confocal microscopy images of the systems* ***L1*** *and* ***TM1*** *in contact with acetonitrile (first spot) and the metal salt solutions.*[39]

Although quantitative comparison between solution (described in Chapter 3 of this thesis) and µCP is not possible, qualitatively these results correlate well with what was previously seen for the same layers in the macroscale cation library described in

Chapter 3, indicating that it is possible to transfer the methodology concept from the macro to the micro scale. Additionally, the system has a built-in transducer allowing the direct visualization of the pattern and modulation of the fluorescence properties upon addition of analytes.

7.2.2 Patterning of fluorescent SAMs by μCP (Approach 2)

As explained in the introduction of this chapter, a second approach for the generation of fluorescent patterns with metal ion on glass surfaces is based on the fluorescence modulation of discrete areas of a non-patterned fluorescent SAM by μCP (Figure 7.1). Initially, the printing of Cu^{2+}, Co^{2+}, Ca^{2+}, and Pb^{2+} onto the differently functionalized fluorescent SAMs (Fx,Ly), ***TM2***, ***TM3*** and ***L0*** was studied using a PDMS stamp (Figure 7.5). For the fabrication of the fluorescent glass substrates, the amino-terminated N-[3-(trimethoxysilyl) propyl] ethylenediamine SAM ***TPEDA*** (Figure 7.5) was first functionalized with different pairs of fluorophore-ligand molecules. This allows for the parallel generation of a small library of fluorescent monolayers (SAM (Fx,Ly) (x,y = 1,2,3,…,n)) whose individual members have different complexing and sensing properties for a variety of metal ions.[12,40] For example, the reaction of the ***TPEDA*** monolayer with the fluorophores TAMRA and Lissamine yielded the fluorescent SAMs ***TM0*** and ***L0***, respectively (Figure 7.5). The unreacted free amino groups can be subsequently functionalized with smaller ligands. Reaction of the fluorescent layer ***TM0*** with hexanoyl chloride and hexyl isocyanate resulted in the formation of the layers ***TM2*** and ***TM3***, respectively. After the fabrication of the fluorescent monolayers, a PDMS stamp was used to deliver metal ions by μCP to the specific areas where the PDMS stamp was brought into contact with the functionalized substrate.

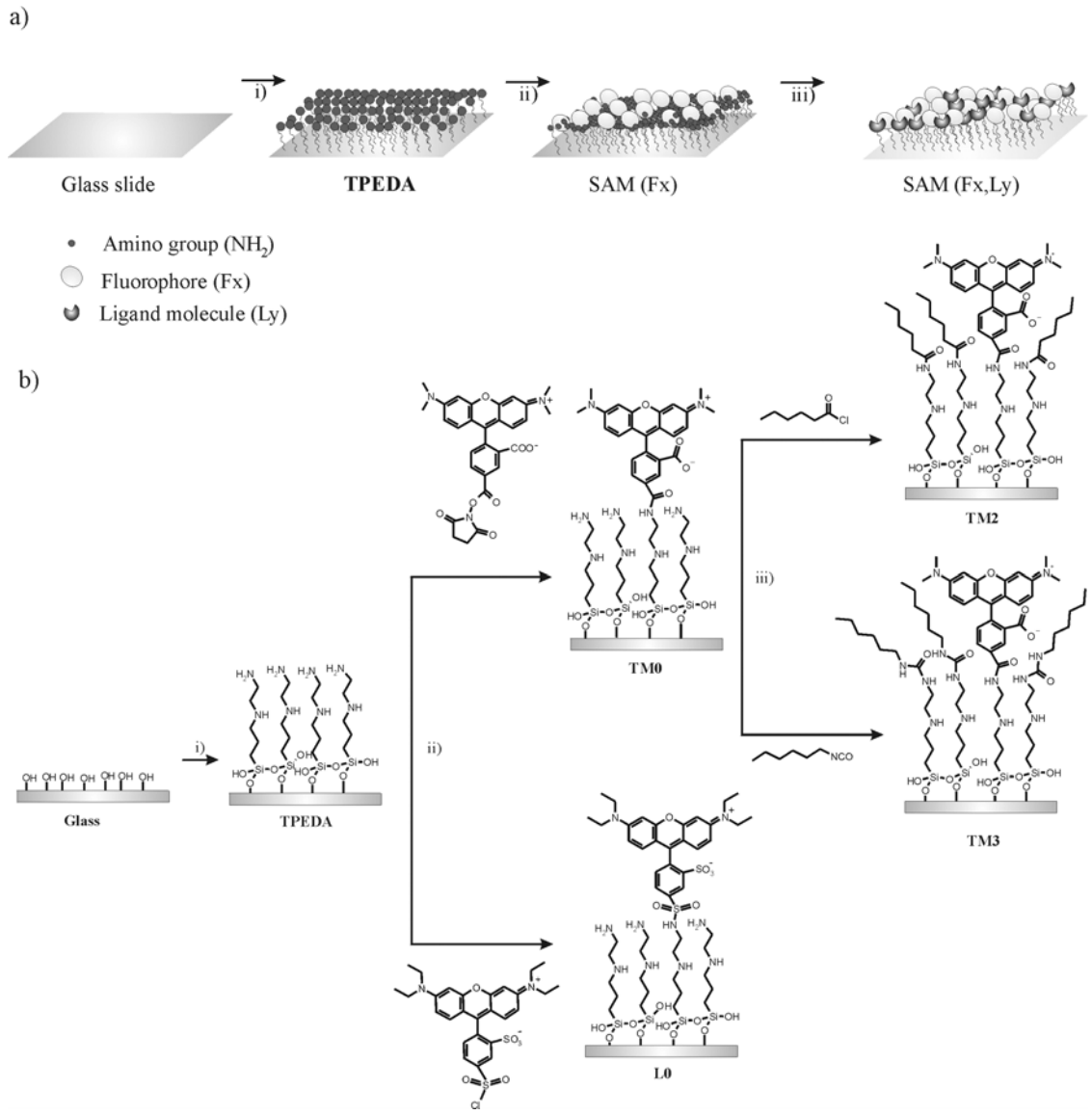

Figure 7.5. *Cartoon (a) and synthetic scheme (b) of the fabrication of four different non-patterned fluorescent self-assembled monolayers* ***TM0***, ***TM2***, ***TM3*** *and* ***L0****. i) N-[3-(trimethoxysilyl)propyl]ethylenediamine, toluene, rt, 3.5 h, ii) amino reactive fluorophore TAMRA and Lissamine to yield* ***TM0*** *and* ***L0*** *SAMs, respectively, acetonitrile, rt, 4 h, and iii) hexanoyl chloride and hexyl isocyanate to afford the layers* ***TM2*** *and* ***TM3*** *respectively, chloroform, rt, 16 h.*

Metal ions Cu^{2+}, Co^{2+}, Ca^{2+}, and Pb^{2+} were transferred by μCP to the ***TM2*** SAM. The printing experiments were performed with freshly prepared PDMS stamps with 10

μm dot features separated by a period of 5 μm, inked with 10^{-3} M acetonitrile solutions of different metal ions.[41,42] After the μCP process, the layers were imaged with a fluorescence microscope. The images showed that the fluorescence emission intensity of the glass substrate in the areas where the metal ion was printed had changed. Figure 7.6 shows two fluorescence microscopy images of two sections of a glass slide coated with ***TM2*** SAM where both dot arrays were generated by printing with Cu^{2+} or Ca^{2+}. This image clearly shows that the fluorescence of the glass slide was quenched and enhanced where the Cu^{2+} and the Ca^{2+} ions, respectively, were printed, i.e. the dotted pattern. It is important to notice that the image shows an area of 650 x 650 μm^2. Such a large patterned area can only be recorded easily by fluorescence microscopy because all the other surface analytical techniques, such as AFM, are limited to a much smaller image range.[43]

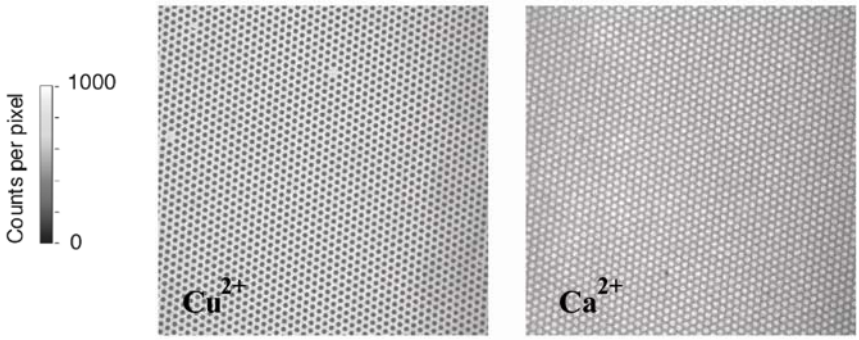

Figure 7.6. *650 x 650 μm^2 fluorescence microscopy image of the **TM2** fluorescent monolayer on glass in which Cu^{2+} and Ca^{2+} ($Cu(ClO_4)_2$ and $Ca(ClO_4)_2$, 10^{-3} M, acetonitrile) were printed with PDMS stamps with an array of 10 μm dots.*

When comparing the patterns produced by the printing of different metal ions, it can be seen that Pb^{2+} and Ca^{2+} induced a fluorescence intensity enhancement of the native monolayer, creating a pattern with brighter dots while Co^{2+} and Cu^{2+} quenched the initial fluorescence intensity, resulting in a pattern with darker dots (Figure 7.7). Ca^{2+} produced higher fluorescence intensity enhancement than Pb^{2+}. The quenching effect produced by Cu^{2+} deposition was slightly higher than the quenching by the Co^{2+} ions.

The luminescent patterns were easily erased and the initial fluorescence recovered by washing away the printed metal ions with HCl (0.1 M, aqueous solution).

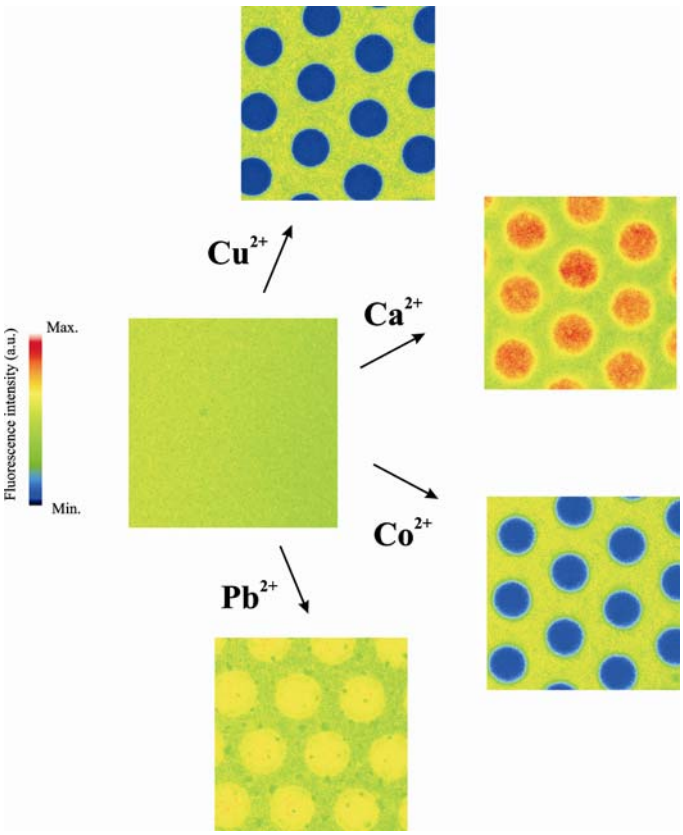

Figure 7.7. *Fluorescence microscopy images of the* ***TM2*** *fluorescent monolayer on glass in which 10^{-3} M acetonitrile solutions of different metal ions were printed with a PDMS stamp with 10 μm diameter dot features separated by a period of 5 μm in an array of dots. The image without dots corresponds to the initial fluorescence image of the* ***TM2*** *SAM before printing the metal ions. The color bar on the left side represents the fluorescence emission intensity scale of the images.*

Similar printing experiments were performed with a differently functionalized glass substrate ***TM3***, which contains hexylurea instead of hexylamide as the ligand group. Figure 7.8 shows the fluorescence images of SAMs ***TM2*** and ***TM3*** after μCP of Ca^{2+}, Cu^{2+}, and Pb^{2+} (perchlorate salts, 10^{-3} M or 10^{-2} M, acetonitrile) with a 10 μm dot array featured stamp. Comparing the pattern created on both substrates upon printing the Ca^{2+}

ions (Figure 7.8), the largest fluorescence enhancement is obtained for layer ***TM2***. The quenching produced by the Cu^{2+} ink is far more intense for ***TM2*** (100%) than for ***TM3*** (50%). With Pb^{2+} (10^{-2} M, acetonitrile) both substrates display a pattern with almost the same fluorescent intensity (Figure 7.8).

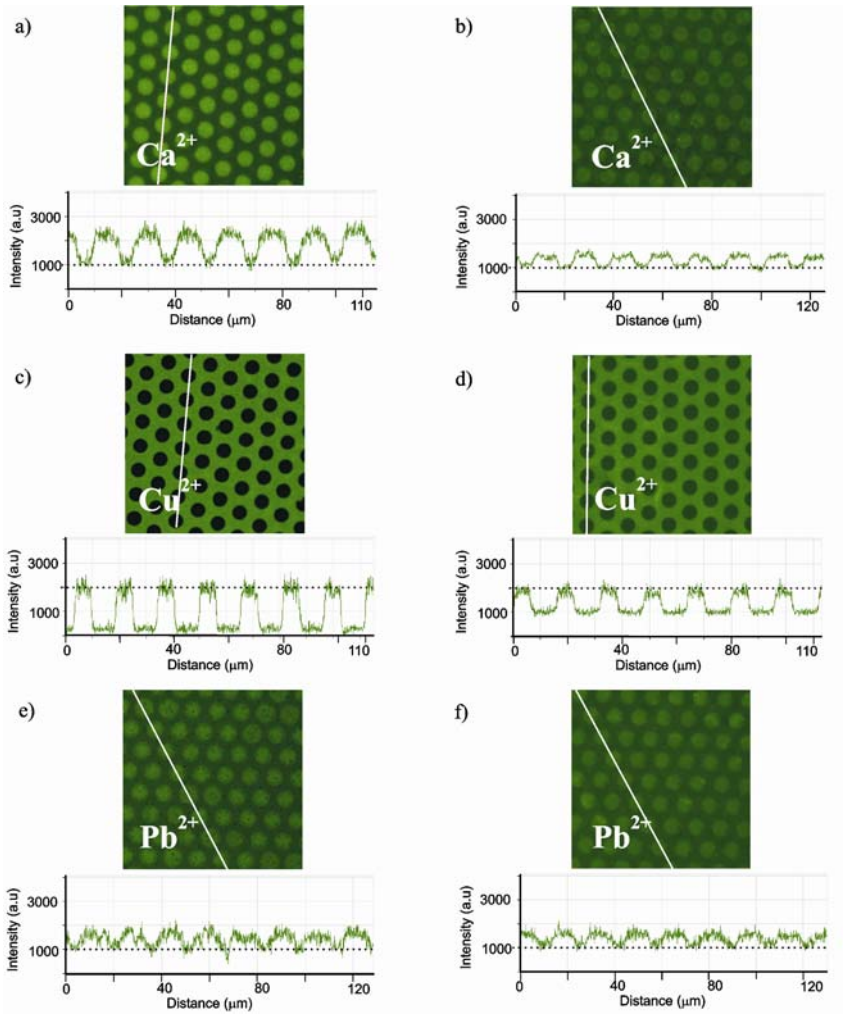

Figure 7.8. *Fluorescence microscopy images (and the fluorescence intensity profile of the cross sections defined by the white line) of* ***TM2*** *(a, c, e) and* ***TM3*** *(b, d, f) SAMs onto which Ca^{2+} (10^{-3} M, acetonitrile) (a, b), Cu^{2+} (10^{-3} M, acetonitrile) (c, d) or Pb^{2+} (10^{-2} M, acetonitrile) (e, f) have been microcontact printed with 10 μm dots array featured PDMS stamp. For comparison the images have been normalized, the dotted horizontal line in the profile plots indicated the initial fluorescence of the layers before the printing of the analyte.*

These differences in fluorescence intensity are remarkable since the composition of ***TM2*** and ***TM3*** substrates differs only in the amido (***TM2***) and ureido (***TM3***) groups. The type of ligating functionalities and fluorophores on the layers determine the properties of the layers and therefore the response toward different analytes.

It was observed that the intensity of the fluorescence patterns is related to the metal ion concentration of the ink solution. When ***L0*** (Figure 7.5) was printed with different concentrations of Cu^{2+} (10^{-6} and 10^{-4} M, perchlorate salt in acetonitrile) using a 10 x 5 μm line patterned PDMS stamp following the protocol described previously[41] the quenching of the fluorescence of the monolayer increased gradually with the concentration of the Cu^{2+} ink solution (Figure 7.9). Printing of a 10^{-6} M acetonitrile solution of Cu^{2+} already produced a quenching of the fluorescence emission of the layer while a negligible effect can be seen in the blank experiment, in which a solution of acetonitrile without metal ion was printed to check the effect of the printing process itself.

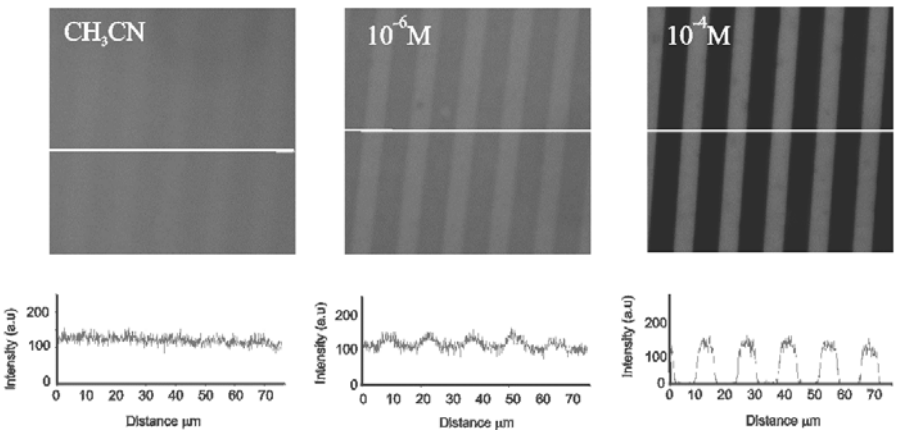

Figure 7.9. *Fluorescence microscopy images (and the fluorescence intensity profile of the cross sections defined by the white line) of the fluorescent monolayer* ***L0*** *after μCP with 0 M, 10^{-6} M and 10^{-4} M solutions of Cu^{2+} (perchlorate salt, acetonitrile).*

Following the same printing procedure and using the Cu^{2+}-***L0*** combination (10^{-3} M $Cu(ClO_4)_2$ in water[44]) a metal ion pattern with electrical circuit features was created on

the glass substrate and visualized by fluorescence microscopy. Figure 7.10 shows sections of the fluorescence image of the glass substrate coated with the ***L0*** SAM after successful transfer of a circuit shape pattern of Cu^{2+} onto the monolayer. The created metal ion pattern with features ranging from 2 - 100 μm is well defined and directly visualized by fluorescence microscopy due to the fluorescence quenching of the layer where Cu^{2+} ions have been deposited.

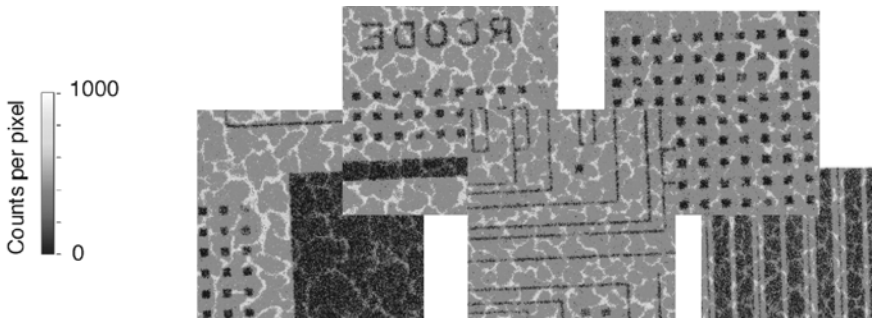

Figure 7.10*. Different sections of a fluorescence confocal microscopy image of a glass slide coated with* ***L0*** *SAM in which* Cu^{2+} *(*10^{-3} *M Cu* $(ClO_4)_2$ *in water) was printed with a PDMS stamp with 2 - 100 μm circuit features. The dark features correspond to the areas where the fluorescence is quenched upon deposition of* Cu^{2+}*.*

7.2.3 Patterning fluorescent SAMs by dip-pen nanolithography (Approach 2)

DPN has some advantages over microcontact printing. Direct creation of arrays by different surface modification with different inks is possible with direct-write DPN while simple μCP process is normally a single ink process.[45] Because of the flexibility and relatively high throughput of DPN, it allows the preparation of a large number of different patterns on one or more different substrates in a combinatorial fashion. Thus, it can be used to quickly identify the best conditions for the generation of a certain pattern. DPN can be carried out as a serial process, and parallel-probe cantilevers have been fabricated by IBM[46] to be used for high-density data storage. Cantilever arrays with 10.000 cantilevers have been fabricated by Liu[29] and "fountain pens" have been

developed as a nanodispensers[30] by integration of microfluidics systems to control the inking of individual cantilevers in a parallel probe array.

These features make DPN a powerful tool for the development of the combinatorial generation of metal ion (and) fluorescent patterns. Selective deposition of metal ions on glass surfaces have been used for protein immobilization on a surface in a controlled way using well known specific metal-proteins interactions.[47]

In this section, the deposition of several metal ions on glass surfaces by DPN is described. DPN is performed over SAM (Fx,Ly)-coated glass slides. Selective modulation of the fluorescence of the substrate in local areas was achieved upon the transfer of metal ions from the tip of an AFM to the functionalized glass surface, and was studied by AFM and laser scanning confocal fluorescence microscopy (LSCM). First, the transfer of Cu^{2+} and Ca^{2+} to a ***TM2*** SAM and Ca^{2+} to a ***T1*** SAM using DPN was studied (Figure 7.11). AFM tips were immersed for 10 min. in a solution of $Cu(ClO_4)_2$ or $Ca(ClO_4)_2$ (10^{-2} M, acetonitrile or ethanol) then dried and used to scan square areas of 20 x 20 μm^2 on a glass substrate functionalized with the fluorescent SAM. The resulting patterns were immediately imaged by AFM and by LSCM (Figure 7.12). For the AFM imaging a larger area of 40 x 40 μm^2 was scanned without withdrawing the tip. Height and friction images were scanned simultaneously. Height AFM images did not show any feature in any case indicating that there is neither mechanical deformation of the SAM nor material removal by scratching (Figure 7.12a,d,g,j). The first experiment was carried out using Cu $(ClO_4)_2$ (10^{-2} M, acetonitrile) as the ink and ***TM2*** as the substrate. The friction AFM image of the pattern written with Cu^{2+} showed a brighter square in the middle of the image corresponding to the area where the metal ion was deposited. LSCM images of the surfaces written with Cu^{2+} showed a 20 x 20 μm^2 pattern where the initial fluorescence of the ***TM2*** was quenched (Figure 7.12c). In a second experiment Ca^{2+} (10^{-2} M, acetonitrile) was used as the ink and ***TM2*** as the fluorescent substrate. A bright fluorescent square feature was observed in the LSCM image of the AFM-written area (Figure 7.12f). A 40 x 40 μm^2 pattern was observed in the fluorescence image which corresponded to the size of the final AFM image (40 x 40 μm^2) and not to the size of the written area (20 x 20 μm^2). The reason could be that the same AFM tip was used to

image and write the pattern, and residual ink on the AFM tip could cause further ink transfer. Also spreading of ink already on the surface would produce a larger feature size.

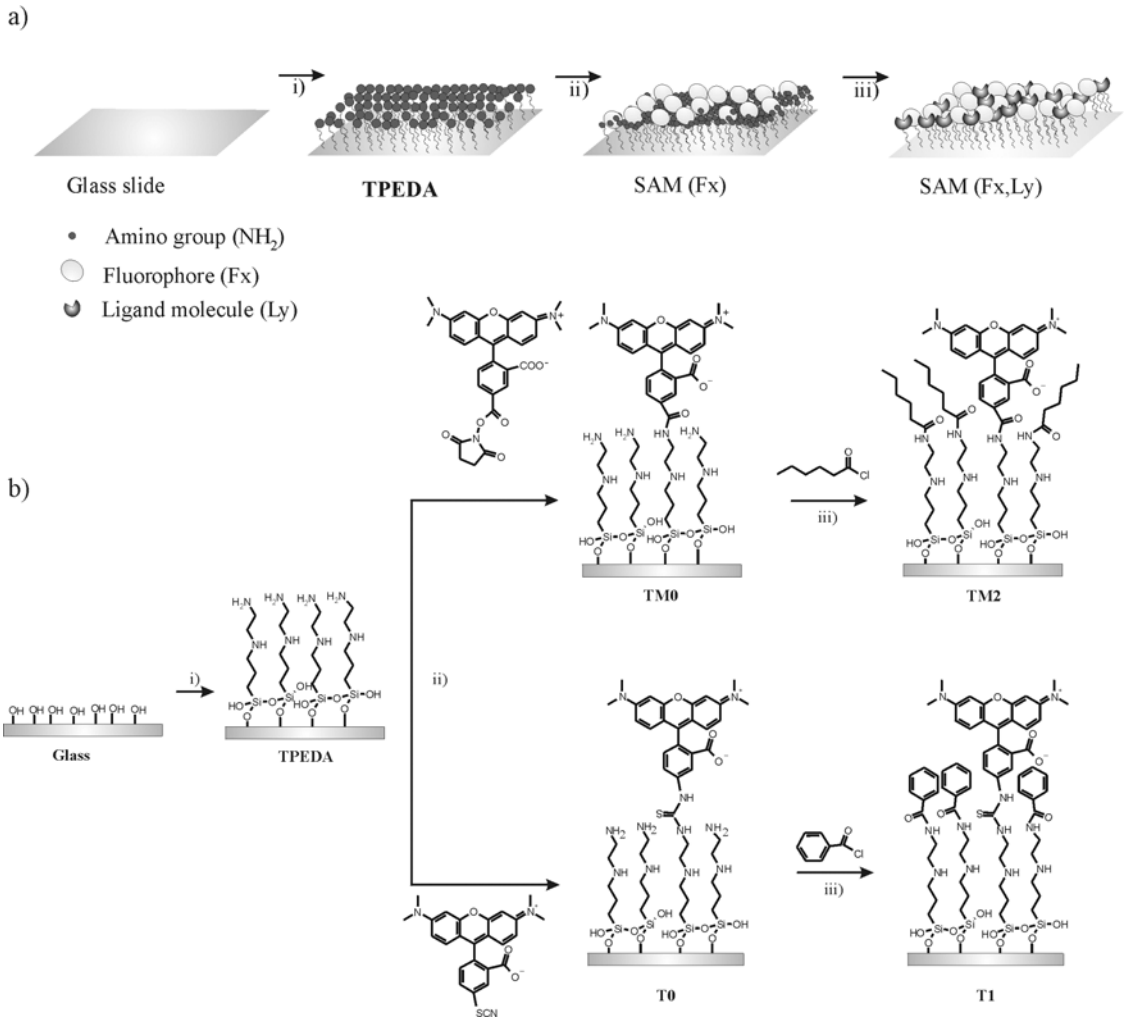

Figure 7.11. *Cartoon (a) and synthetic scheme (b) of the fabrication of the* ***TM2*** *and* ***T1*** *non-patterned SAMs (Fx, Ly) i) N-[3-(trimethoxysilyl) propyl] ethylenediamine, toluene, rt, 3.5 h, ii) amino reactive fluorophore TAMRA and TRITC*[*] *to yield* ***TM0*** *and* ***T0*** *SAMs, respectively, acetonitrile, rt, 4 h, and iii) hexanoyl chloride or bencyl chloride to afford the layers* ***TM2*** *and* ***T1*** *respectively, chloroform, rt, 16 h.*

A similar writing experiment was done on the ***TM2*** with Ca^{2+} in EtOH instead of acetonitrile as the ink. The transfer of Ca^{2+} ions to the substrate produced an

[*] T*etramethylrhodamine-5-(and-6)- isothiocyanate*

enhancement of the fluorescence intensity where the Ca^{2+} was deposited (Figure 7.12i). In another experiment Ca^{2+} ions (Ca $(ClO_4)_2$, 10^{-2} M, acetonitrile) were deposited on ***T1*** (Figure 7.11).

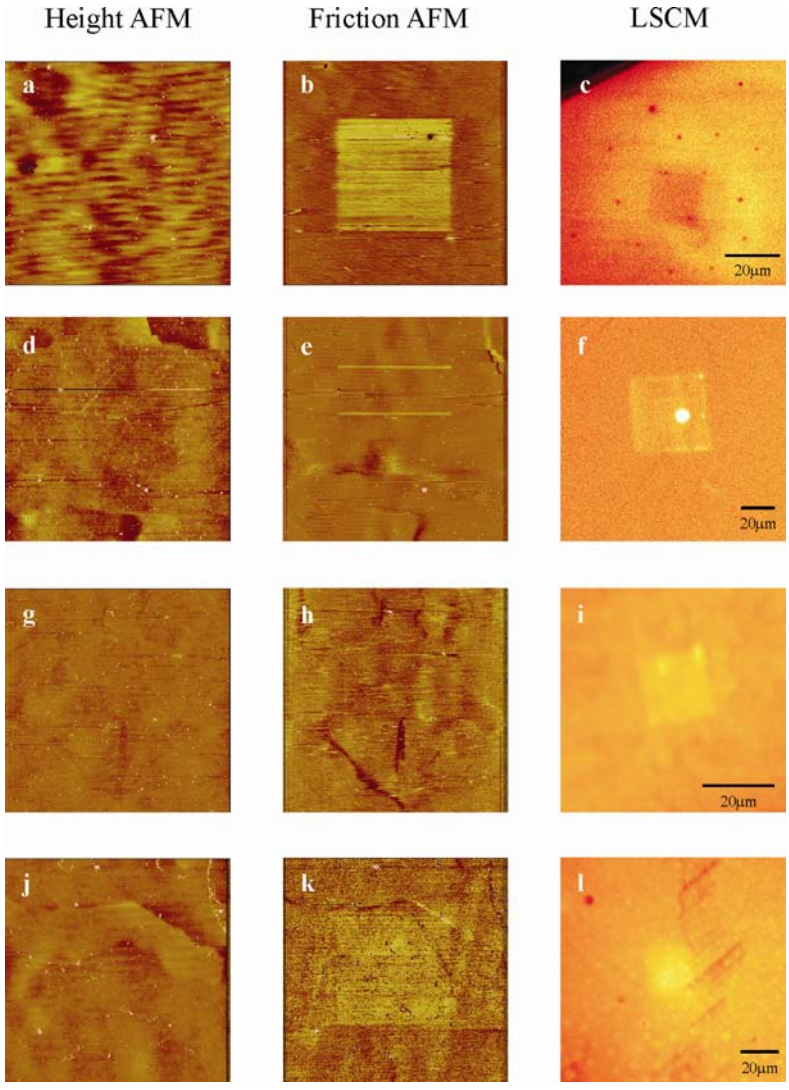

Figure 7.12. *Friction and height AFM 40 x 40 μm images and confocal microscopy (LSCM) images with different sizes of the fluorescent monolayers* ***TM2*** *(images a-i) and* ***T1*** *(images k-l) in which 20 x 20 μm^2 metal ion patterns were written by DPN.* ***TM2*** *SAMs were patterned with Cu^{2+} (Cu $(ClO_4)_2$, 10^{-2} M, acetonitrile) (images a-c), with Ca^{2+} (Ca $(ClO_4)_2$, 10^{-2} M, acetonitrile) (images d-f) or EtOH (images g-i).* ***T1*** *SAM was patterned with Ca^{2+}(Ca $(ClO_4)_2$, 10^{-2} M, acetonitrile) (images j-l).*

The friction AFM image showed contrast in the written area. In the LSCM image an enhanced luminescent fluorescence pattern of 20 x 20 μm^2 was observed (Figure 7.12l). These results demonstrate the transfer of metal ions to non-conductive functionalized glass substrates by DPN. One important point to note is that the extreme cases in which the pattern is only visible by fluorescence microscopy must correspond to a lower metal ion concentration deposited on the surface than in those cases in which the pattern is visible also in the friction AFM image. An important conclusion from these experiments and a strong advantage of the system is that these new fluorescent substrates allow the pattern visualization even in cases where AFM does not reveal any feature.

A pattern with a cross shape was generated on the ***TM2*** substrate (Figure 7.13). Two perpendicular lines of 60 μm long and 1.87 μm wide were written with an AFM tip loaded with a Cu^{2+} ink ($Cu(ClO_4)_2$, 10^{-2} M, acetonitrile). LSCM images revealed the presence of two fluorescence-quenched areas corresponding to the scanned areas in the AFM (Figure 7.13). In the LSCM image, lines widths of ca. 6.62 μm and ca. 1.4 μm for the first and second written lines, respectively, were observed. In the AFM image only one line of 1.95 μm wide was observed corresponding to the first written line.[48] The second line was invisible even though the transfer of Cu^{2+} metal ions to the substrate in that area was already confirmed by fluorescence. The images suggest that a major deposition was done during the scan of the first line, producing a shortage of ink on the tip for the second line. Additionally, fluorescence images revealed that the diffusion of the ink on the substrate was much larger than observed in the AFM images. Depending on the imaging technique a difference of 4.67 μm has been observed for width of the first written line. This difference is more than two times the size of the programmed line width. Due to diffusion processes, a concentration gradient from a high concentration in the center towards the borders of the line exists. Therefore, only the central part with higher concentration of Cu^{2+} is visible by AFM while far from the center the concentration of Cu^{2+} is lower and the line is only visible only by LSCM.[49]

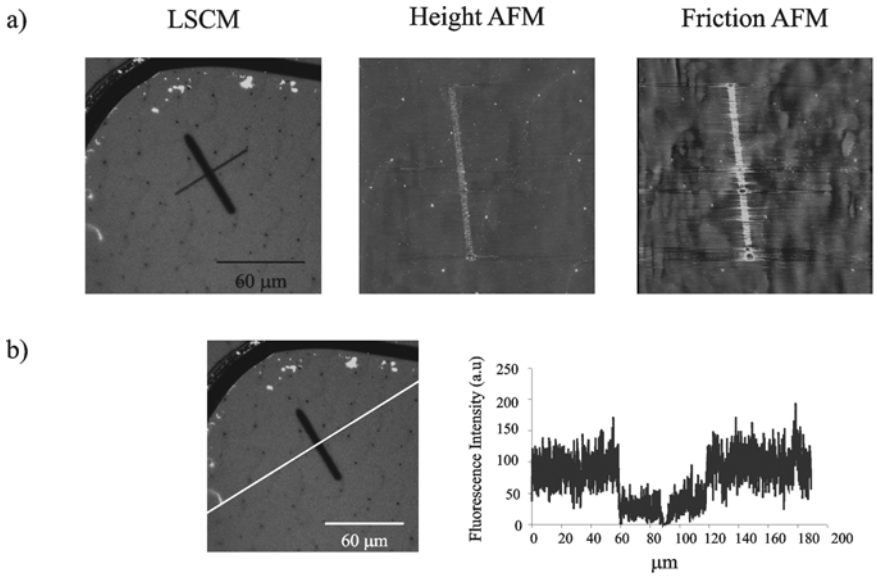

Figure 7.13. *a) LSCM image (left) and friction and height AFM (center and right, respectively) 40 x40 µm images of the fluorescent monolayer* ***TM2*** *in which a cross pattern of two lines (60 x 1.87 µm) has been generated by dip-pen nanolithography using an AFM tip inked with* $Cu^{2+}(Cu(ClO_4)_2,\ 10^{-2}$ *M, acetonitrile). b) Fluorescence intensity profiles of the cross sections defined by the white line.*

Additionally, this approach easily allows observation that successive scanning over the same area results in transport of higher amounts of metal ions to the substrate. Careful inspection of the fluorescence intensity profile (Figure 7.13b) along the second scanned line shows that the fluorescence intensity in the cross intersection (90µm) has a higher quenching of the initial fluorescence intensity, corresponding presumably to a higher concentration of Cu^{2+} ions in that area. Therefore, quantitative data could be extracted using this approach. Quantification of the amount of material transferred from the AFM tip to the substrate can be done by evaluating the magnitude of the produced modulation of fluorescence.

As deduced from the above experiment the results presented here could help to clarify the ink process in DPN, since the substrate properties are modulated proportionally to the ink deposition. The special substrates used for these experiments,

i.e. intrinsically fluorescent self-assembled monolayers, allow direct and more accurate determination of the real diffusion of the ink in the DPN processes. These observations might have important implications in nanotechnology. Diffusion models to study how diffusion dynamics affect patterns generated in DPN are important.[50]

7.2.3.1 Dip-pen nanolithography with a combined AFM-confocal fluorescence microscope (AFFM)

Writing metal ion patterns on fluorescent SAMs (Fx,Ly) on glass by DPN has also been performed using a custom-designed atomic force fluorescence microscope (AFFM).[51] The AFFM setup is emerging as a powerful analysis tool that combines the topographic resolution of AFM and the single molecule sensitivity of fluorescence microscopy. AFFM setups have been used for the study of single biomolecules or cell membranes[51,52] and multichromophoric polymers for the design of molecular photonic devices.[53] However, there is no precedent of DPN using an AFFM. Only recently related work has been published by Zumbusch in which atomic force and far-field fluorescence microscopy are used for the simultaneous atomic force manipulation and optical visualization of individual dye-labeled DNA molecules.[54]

Patterns of Cu^{2+} and Ca^{2+} were written on a ***TM2*** substrate (Figure 7.11). First an AFM tip was immersed for 30 min. in a solution of Cu^{2+} ($Cu(ClO_4)_2$, 10^{-2} M, acetonitrile) then dried and used to scan an area of 10.1 x 10.1 μm^2 on a glass substrate functionalized with the fluorescent ***TM2***. The sample was scanned between the fluorescence microscope objective and the AFM tip. During the scanning period both the fluorescence excitation light and the AFM were switched off in order to avoid photobleaching of the sample. After the writing process the resulting pattern was immediately imaged using the fluorescence objective. Figure 7.14a shows the fluorescence microscopy image of the pattern generated by deposition of Cu^{2+}. A dark square is observed which corresponds to the written area. Quenching of the fluorescence of the ***TM2*** was observed where the Cu^{2+} metal ions were transferred from the tip to the surface. A similar experiment was

performed using Ca^{2+} as a 20 x 20 μm^2 size pattern. Figure 7.14b shows the fluorescence microscopy image of the surface after the writing experiment. Due to a misalignment of the AFM tip and the fluorescence objective only part of the written area is observed. Enhancement of the fluorescence was observed in the written area indicating the transfer of the Ca^{2+} metal ions from the AFM tip to the substrate.

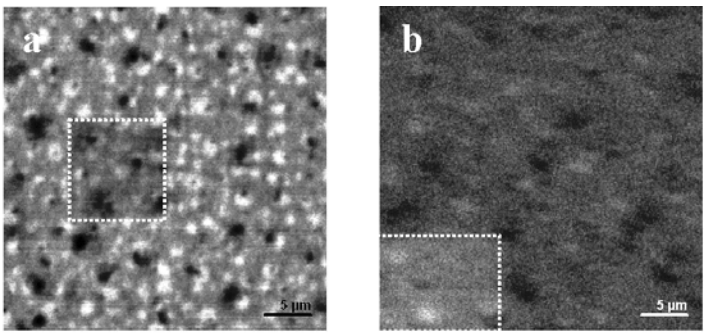

Figure 7.14. *Fluorescence microscopy images of a glass substrate coated with the fluorescent monolayer* ***TM2*** *in which a square pattern has been generated by dip-pen nanolithography using an AFM tip inked with (a) Cu^{2+} or (b) Ca^{2+}. To guide the eye a dotted white line has been drawn bordering the written area.*

Using the AFFM, fluorescent ion patterns can be written on fluorescent SAMs and immediately visualized without any transport of the sample to another instrument. This method could speed up the process of writing and visualizing metal ion patterns tremendously, and it could be conveniently used to generate and visualize also multicolor nanopatterns in a very short time.

7.3 Conclusions and outlook

Two novel combinatorial methods for the generation of fluorescent patterns with metal ions of micrometer dimensions by the combination of fluorescent SAMs, metal ions using μCP and DPN have been presented. The approaches use the sensing abilities of the fluorescent SAMs on glass toward metal cations described in Chapter 3 and 4. In

the first approach μCP printing is used to deposit different fluorophores onto glass surfaces. By introduction of different ligands on these fluorescent monolayers the complexing properties of the patterned SAM are modified. The fluorescence of the pattern can be enhanced or quenched upon exposure to metal ion solutions. In the second approach, μCP and DPN are used to deposit metal ions onto homogeneous fluorescent SAMs. Modulation of the fluorescence of the SAM is produced in discrete areas where the metal ion is deposited. This approach allows the writing of metal ion patterns and their direct visualization by simple fluorescence microscopy. The patterns can be erased upon washing away the analyte with HCl aqueous solution or a chelate solution. The strength of this combinatorial generation of patterns is the use of simple and easily accessible technology i.e. monolayer chemistry to produce fluorescent complexing glass substrates, μCP or DPN as delivery tools to create the patterns and fluorescence microscopy to visualize them. Moreover, the combined fluorescence microscopy and AFM in a single setup, AFFM, speeds up the generation and screening of fluorescent patterns.

These systems are fully compatible with high throughput screening techniques without labeling steps. The fast generation of numerous combinations of fluorophores, ligand molecules and metal ions allows for easy and quick production of different fluorescent patterns and to screen for their binding and fluorescence modulation abilities. These combinatorial approaches offer a "painting-kit" for pattern generation, by the combination of different "papers" (fluorescent SAMs), "inks" (metal ion solutions), and different "drawings" (patterns).

7.3 Experimental

General procedures

All glassware used to prepare the layers was cleaned by sonicating for 15 minutes in a 2% v/v Hellmanex II solution in distilled water, rinsed four times with high purity (MilliQ, 18.2 MΩcm) water, and dried in an oven at 150º C. The substrates, microscope glass slides were cleaned for 15 minutes in piranha solution (concentrated H_2SO_4 and 33% aqueous H_2O_2 in a 3:1 ratio. ***Warning: Piranha solution should be handled with caution: it has been reported to detonate unexpectedly***). They were then rinsed several times with high purity (MilliQ) water, and dried in a nitrogen stream immediately prior to performing the formation of the monolayer.

Fabrication of PDMS stamps

Patterned poly(dimethylsiloxane) (PDMS) stamps were fabricated by pouring a 10:1 (v/v) mixture of Sylgard 184 elastomer and curing agent over a patterned silicon master (stripes of 5x3 μm, or array of dots of 5 μm distanced by 10 μm). The mixture was cured for one hour in the oven at 60º C, then carefully peeled away from the master and left in the oven for another 18 h at 60º C to ensure complete curing. Prior to inking of the stamps, all the stamps were oxidized by exposure to UV/ozone for 60 min. This process favored the hydrophilicity of the stamp and the homogeneous spreading of the ink.[42] After ozone treatment the stamps were directly dipped in the ink solutions. All the stamps were freshly prepared within two days prior to use.

Monolayer preparation

*Preparation of the fluorescent patterned **TM0** and **L0** by microcontact printing*

Glass slides were functionalized with the amino-terminated monolayer N-[3-(trimethoxysilyl)propyl]ethylenediamine SAM (***TPEDA***) following the procedure described in Chapter 3 of this thesis. The covalent attachment of the fluorophore to the amino-terminated SAM ***TPEDA*** was achieved by putting the amino functionalized glass slide in contact with a PDMS stamp inked with a 0.23 M acetonitrile solution of the fluorophore TAMRA (5-(and-6)-carboxytetramethylrhodamine, succinimidyl ester (5(6)-TAMRA, SE) *mixed isomers)) to yield the ***TM0*** SAM or the fluorophore Lissamine (Lissamine rhodamine B sulfonyl chloride) to yield ***L0***. The stamp was dipped in the ink solution immediately after ozone treatment for at least 15 min. then removed from the ink solution, blown dry with an air stream to remove excess fluorophore solution and brought in conformal contact with the ***TPEDA*** functionalized glass substrate and kept for 2.5 min in the case of TAMRA and for 1 min in the case of the more reactive Lissamine before careful removal. After each printing the stamp was introduced for a few seconds in the ink solution, blown dry with air to remove excess fluorophore solution and used again. Each stamp was used to print three samples, then discarded and a new one used. The patterned slides were then extensively rinsed once with a stream of EtOH and once with a stream of CH_2Cl_2, and dried in an air stream.

*Preparation of the fluorescent patterned **TM1** and **L1***

The fluorescent patterned slides ***TM0*** and ***L0*** were immersed in an ehrlenmeyer with 50 mL of a 12.5 mM chloroform solution of the ligand molecule, *p*-isopropylphenyl isocyanate for ***TM0*** and *p*-propylbenzoyl chloride with 0.3 μL of triethylamine for ***L0,*** for 16 h. Then the substrates were taken out from the solution and rinsed with $CHCl_3$, EtOH, and CH_2Cl_2 to remove physisorbed material. The following protocol was repeated successively for each solvent, twice: shaking of the slide in the solvent followed by rinsing with a stream of the solvent. The slides ***TM1*** and ***L1*** were then dried under an air stream.

*Preparation of the fluorescent non-patterned **TM0, TM2, TM3, L0, T0,** and **T1***

Glass slides were functionalized with the amino-terminated monolayer N-[3-(trimethoxysilyl)propyl]ethylenediamine SAM ***TPEDA*** following the procedure described in Chapter 3 of this thesis. For the synthesis of the ***TM0***, ***L0***, and ***T0*** SAMs, the attachment of the fluorophores to the ***TPEDA*** SAM was achieved by immersing the slide for 4 h. in an ehrlenmeyer with 50 mL of a 0.23 mM acetonitrile solution of the fluorophore TAMRA (5-(and-6)-carboxytetramethylrhodamine, succinimidyl ester (5(6)-TAMRA, SE) *mixed isomers)), fluorophore Lissamine (L) (Lissamine rhodamine B sulfonyl chloride) or fluorophore TRITC (T) (tetramethylrhodamine-5-(and-6)-isothiocyanate (5(6)-TRITC) *mixed isomers) to yield ***TM0***, ***L0***, ***T0,*** respectively. Et_3N (100 μL) was added to the Lissamine solutions. All

reactions were carried out in a glove box under an atmosphere of dry N_2. Then the substrates were taken out from the solution and rinsed with CH_3CN, EtOH, and CH_2Cl_2 to remove physisorbed material. The slides were then dried under an air stream. For the synthesis of the ***TM2*** and ***TM3*** SAMs, the ***TM0*** functionalized slides were immersed in CH_3CN solution of hexanoyl chloride (50 mM) and hexyl isocyanate (12 mM) to afford ***TM2*** and ***TM3***, respectively. Et_3N (100 μL) was added to the hexanoyl chloride solution. For the synthesis of ***T1,*** the ***T0*** functionalized slides were immersed in CH_3CN solution of benzoyl chloride, (50 mM). Et_3N (100 μL) was added to the solution. All reactions were carried out under an atmosphere of dry N_2 for 16 h. After the substrates were taken out from the solution they were rinsed sequentially with CH_3CN, EtOH, and CH_2Cl_2 to remove physisorbed material. The slides were then dried under an air stream. All the fluorescent ***TM0***, ***TM2***, ***TM3***, ***L0*** and ***T0-T1*** SAM functionalized glass slides were sonicated for 1 min. in a beaker filled with CH_2Cl_2, then rinsed again with a stream of CH_2Cl_2 and dried under a air stream, to assure a clean fluorescent monolayer.

*Microcontact printing (μCP) of metal ions solution on **TM2, TM3** and **L0***

After UV/ozone treatment the PDMS stamps were immediately dipped on the ink solution (10^{-6} – 10^{-2} M solutions in acetonitrile or water of the perchlorate salts of Cu^{2+}, Co^{2+}, Ca^{2+} or Pb^{2+}) for at least 15 min. Then the stamps were removed from the ink and blown dry in a stream of air to remove the excess ink solution. The stamps were brought into conformal contact with the ***TM2***, ***TM3*** and ***L0*** SAM functionalized slides by hand without the use of external pressure and kept in contact for 1 min before careful removal.

*Dip-pen nanolithography with metal ion solutions on **TM2** and **T1***

The dip-pen Nanolithography (DPN) experiments were performed on a Nanoscope III Atomic Force Microscope (AFM) (Veeco-Digital Intruments) operated at ambient conditions in contact mode. The AFM was equipped with a J scanner. Commercial Si_3N_4 cantilevers were used with a nominal spring constant of 0.58 Nm^{-1}. Prior to writing the tips were immersed in 10^{-2} M solutions of Cu^{2+} or Ca^{2+} ions in acetonitrile or ethanol for 5 minutes and dried in air. For the writing of square shaped patterns, during DPN experiments an area of 20 × 20 μm^2 was scanned for 30 minutes using a scan rate of 1 Hz (40 μm s^{-1}). The load applied by the tip to the sample was kept between 5 and 15 nN. The relative humidity of the air was between 48-55% and the temperature between 25 and 28 °C. For the cross shaped pattern, the AFM was also operated to write in contact mode. The cross was written by scanning over an area of 60 × 60/32 μm^2. The speed used was 1 Hz (120 μm s^{-1}). The scanning of each line was performed for 30 minutes. The relative humidity of the air was 32-34 % and the temperature in the room was 25-26 °C.

Laser scanning confocal microscopy (LSCM)

Confocal microscopy images of ***TM1*** and ***L1*** were carried out using an inverted confocal scanning fluorescence microscope (CFM, Zeiss Axiovert) with an oil immersion objective lens (Olympus NA 1.3, 100x). Circularly polarized light coming from an Ar^+/Kr^+ ion laser (Spectra Physics, BeamLok 2060) was used to excite the dye molecules (λ_{ex}=514 nm). The fluorescence light emitted by the fluorophore was collected through the same objective lens, separated from the excitation light by use of a dichroic mirror (Omega 540DRLP) and a rejection band filter (514.5 Raman), and directed to the small detection area (180 μm diameter) of an avalanche photodetector (SPCM-AQ-14, EG&G Electro Optics). Fluorescence images were acquired by raster-scanning the samples over areas of 20x20 – 30x30 μm^2 at a pixel frequency of 1 kHz and an excitation power within the range 0.1-0.5 kW/cm^2. Addition of the analyte solutions was done using a custom designed liquid cell. Acetonitrile (1 mL) was placed in the liquid cell and aliquots of 10μL from a 10^{-2} M acetonitrile solution of the perchlorate salts of the metal ions were added. Beginning between 5 and 10 min after addition, the fluorescence of the system was then checked approximately every 5 min for a total of three measurements to ensure reproducibility. The values given are the average of at least three measurements with an average error of 10% over 24 measurements.

LSCM images of the ***TM0***, ***TM2***, ***TM3***, ***L0*** and ***T1*** surfaces patterned with metal ions, either by μCP or DPN were taken in air on a Carl Zeiss LSM 510 microscope. The system and the parameter used are described in the experimental part of Chapter 5 of this thesis.

Combined AFM and confocal fluorescence microscopy (AFFM)

The AFFM used for the DPN experiments is extensively described elsewhere.[51] During the DPN writing the fluorescence light and the AFM laser were blocked or shut down to avoid photobleaching of the fluorescent monolayer.

7.4. References and notes

1 Xia, Y. N.; Rogers, J. A.; Paul, K. E.; Whitesides, G. M. Unconventional Methods for Fabricating and Patterning Nanostructures. *Chem. Rev.* ***1999***, 99(7), 1823-1848.

2 Bohr, M. T. Nanotechnology Goals and Challenges for Electronic Applications. *IEEE Trans. Nanotech.* ***2002***, 1(1), 56-62.

3 Geissler, M.; Xia, Y. N. Patterning: Principles and Some New Developments. *Adv. Mater.* ***2004***, 16(15), 1249-1269.

4 Ginger, D. S.; Zhang, H.; Mirkin, C. A. The Evolution of Dip-Pen Nanolithography. *Angew. Chem., Int. Ed.* ***2004***, 43(1), 30-45.

5 Delamarche, E.; Donzel, C.; Kamounah, F. S.; Wolf, H.; Geissler, M.; Stutz, R.; Schmidt-Winkel, P.; Michel, B.; Mathieu, H. J.; Schaumburg, K. Microcontact Printing Using Poly(Dimethylsiloxane) Stamps Hydrophilized by Poly(Ethylene Oxide) Silanes. *Langmuir* ***2003***, 19(21), 8749-8758.

6 Zheng, H. P.; Rubner, M. F.; Hammond, P. T. Particle Assembly on Patterned "Plus/Minus" Polyelectrolyte Surfaces Via Polymer-on-Polymer Stamping. *Langmuir* ***2002***, 18(11), 4505-4510.

7 Auletta, T.; Dordi, B.; Mulder, A.; Sartori, A.; Onclin, S.; Bruinink, C. M.; Peter, M.; Nijhuis, C. A.; Beijleveld, H.; Schonherr, H.; Vancso, G. J.; Casnati, A.; Ungaro, R.; Ravoo, B. J.; Huskens, J.; Reinhoudt, D. N. Writing Patterns of Molecules on Molecular Printboards. *Angew. Chem., Int. Ed.* ***2004***, 43(3), 369-373.

8 Yang, K. L.; Cadwell, K.; Abbott, N. L. Contact Printing of Metal Ions Onto Carboxylate-Terminated Self-Assembled Monolayers. *Adv. Mater.* ***2003***, 15(21), 1819-1823.

9 Porter, L. A.; Choi, H. C.; Schmeltzer, J. M.; Ribbe, A. E.; Elliott, L. C. C.; Buriak, J. M. Electroless Nanoparticle Film Deposition Compatible With Photolithography, Microcontact Printing, and Dip-Pen Nanolithography Patterning Technologies. *Nano Lett.* ***2002***, 2(12), 1369-1372.

10 Lahiri, J.; Ostuni, E.; Whitesides, G. M. Patterning Ligands on Reactive SAMs by Microcontact Printing. *Langmuir* ***1999***, 15(6), 2055-2060.

11 Yan, L.; Zhao, X. M.; Whitesides, G. M. Patterning a Preformed, Reactive SAM Using Microcontact Printing. *J. Am. Chem. Soc.* ***1998***, 120(24), 6179-6180.

12 Basabe-Desmonts, L.; Beld, J.; Zimmerman, R. S.; Hernando, J.; Mela, P.; García-Parajó, M. F. G.; Van Hulst, N. F.; Van Den Berg, A.; Reinhoudt, D. N.; Crego-Calama, M. A Simple Approach to Sensor Discovery and Fabrication on Self-Assembled Monolayers on Glass. *J. Am. Chem. Soc.* ***2004***, 126(23), 7293-7299.

13 Sullivan, T. P.; Van Poll, M. L.; Dankers, P. Y. W.; Huck, W. T. S. Forced Peptide Synthesis in Nanoscale Confinement Under Elastomeric Stamps. *Angew. Chem., Int. Ed.* ***2004***, 43(32), 4190-4193.

14 Rozkiewicz, D. I.; Ravoo, B. J.; Reinhoudt, D. N. Reversible Covalent Patterning of Self-Assembled Monolayers on Gold and Silicon Oxide Surfaces. *Langmuir* ***2005***, 21(14), 6337-6343.

15 Bernard, A.; Renault, J. P.; Michel, B.; Bosshard, H. R.; Delamarche, E. Microcontact Printing of Proteins. *Adv. Mater.* ***2000***, 12(14), 1067-1070.

16 Renault, J. P.; Bernard, A.; Juncker, D.; Michel, B.; Bosshard, H. R.; Delamarche, E. Fabricating

Microarrays of Functional Proteins Using Affinity Contact Printing. *Angew. Chem., Int. Ed.* ***2002***, 41(13), 2320-2323.

17 Mahalingam, V.; Onclin, S.; Peter, M.; Ravoo, B. J.; Huskens, J.; Reinhoudt, D. N. Directed Self-Assembly of Functionalized Silica Nanoparticles on Molecular Printboards Through Multivalent Supramolecular Interactions. *Langmuir* ***2004***, 20(26), 11756-11762.

18 Mulder, A.; Onclin, S.; Peter, M.; Hoogenboom, J. P.; Beijleveld, H.; Ter Maat, J.; García-Parajǩ, M. F.; Ravoo, B. J.; Huskens, J.; Van Hulst, N. F.; Reinhoudt, D. N. Molecular Printboards on Silicon Oxide: Lithographic Patterning of Cyclodextrin Monolayers With Multivalent, Fluorescent Guest Molecules. *Small* ***2005***, 1(2), 242-253.

19 Onclin, S.; Huskens, J.; Ravoo B. J.; Reinhoudt, D. N. Molecular Boxes on a Molecular Printboard: Encapsulation of Anionic Dyes in Immobilized Dendrimers. *Small* ***2005***, 852-857.

20 Tseng, A. A.; Notargiacomo, A.; Chen, T. P. Nanofabrication by Scanning Probe Microscope Lithography: a Review. *J. Vac. Sci. Technol., B* ***2005***, 23(3), 877-894.

21 Lim, J. H.; Mirkin, C. A. Electrostatically Driven Dip-Pen Nanolithography of Conducting Polymers. *Adv. Mater.* ***2002***, 14(20), 1474-1477.

22 Li, Y.; Maynor, B. W.; Liu, J. Electrochemical AFM "Dip-Pen" Nanolithography. *J. Am. Chem. Soc.* ***2001***, 123(9), 2105-2106.

23 Piner, R. D.; Zhu, J.; Xu, F.; Hong, S. H.; Mirkin, C. A. "Dip-Pen" Nanolithography. *Science* ***1999***, 283(5402), 661-663.

24 Maynor, B. W.; Li, Y.; Liu, J. Au "Ink" for AFM "Dip-Pen" Nanolithography. *Langmuir* ***2001***, 17(9), 2575-2578.

25 Stoll, D.; Templin, M. F.; Schrenk, M.; Traub, P. C.; Vohringer, C. F.; Joos, T. O. Protein Microarray Technology. *Frontiers in Bioscience* ***2002***, 7, C13-C32.

26 Vossmeyer, T.; Jia, S.; Delonno, E.; Diehl, M. R.; Kim, S. H.; Peng, X.; Alivisatos, A. P.; Heath, J. R. Combinatorial Approaches Toward Patterning Nanocrystals. *J. Appl. Phys.* ***1998***, 84(7), 3664-3670.

27 Shtein, M.; Peumans, P.; Benziger, J. B.; Forrest, S. R. Direct Mask-Free Patterning of Molecular Organic Semiconductors Using Organic Vapor Jet Printing. *J. Appl. Phys.* ***2004***, 96(8), 4500-4507.

28 Wu, T.; Tomlinson, M.; Efimenko, K.; Genzer, J. A Combinatorial Approach to Surface Anchored Polymers. *J. Mater. Sci.* ***2003***, 38(22), 4471-4477.

29 Zhang, M.; Bullen, D.; Chung, S. W.; Hong, S.; Ryu, K. S.; Fan, Z. F.; Mirkin, C. A.; Liu, C. A Mems Nanoplotter With High-Density Parallel Dip-Pen Manolithography Probe Arrays. *Nanotechnol.* ***2002***, 13(2), 212-217.

30 Deladi, S.; Tas, N. R.; Berenschot, J. W.; Krijnen, G. J. M.; De Boer, M. J.; De Boer, J. H.; Peter, M.; Elwenspoek, M. C. Micromachined Fountain Pen for Atomic Force Microscope-Based Nanopatterning. *Appl. Phys. Lett.* ***2004***, 85(22), 5361-5363.

31 Demers, L. M.; Mirkin, C. A. Combinatorial Templates Generated by Dip-Pen Nanolithography for the Formation of Two-Dimensional Particle Arrays. *Angew. Chem., Int. Ed.* ***2001***, 40(16), 3069-3071.

32 Ivanisevic, A.; Mccumber, K. V.; Mirkin, C. A. Site-Directed Exchange Studies With Combinatorial Libraries of Nanostructures. *J. Am. Chem. Soc.* ***2002***, 124(40), 11997-12001.

33 Weinberger, D. A.; Hong, S. G.; Mirkin, C. A.; Wessels, B. W.; Higgins, T. B. Combinatorial Generation and Analysis of Nanometer- and Micrometer-Scale Silicon Features Via "Dip-Pen" Nanolithography and Wet Chemical Etching. *Adv. Mater.* ***2000***, 12(21), 1600-1603.

34 Greene, M. E.; Kinser, C. R.; Kramer, D. E.; Pingree, L. S. C.; Hersam, M. C. Application of Scanning Probe Microscopy to the Characterization and Fabrication of Hybrid Nanomaterials. *Microscopy Research and Technique* ***2004***, 64(5-6), 415-434.

35 Noy, A.; Miller, A. E.; Klare, J. E.; Weeks, B. L.; Woods, B. W.; Deyoreo, J. J. Fabrication of Luminescent Nanostructures and Polymer Nanowires Using Dip-Pen Nanolithography. *Nano Lett.* ***2002***, 2(2), 109-112.

36 Klajn, R.; Fialkowski, M.; Bensemann, I. T.; Bitner, A.; Campbell, C. J.; Bishop, K.; Smoukov, S.; Grzybowski, B. A. Multicolour Micropatterning of Thin Films of Dry Gels. *Nature Materials* ***2004***, 3(10), 729-735.

37 Peng, Q. J.; Liu, S. J.; Guo, Y. K.; Chen, B.; Du, J. L.; Zeng, Y. S.; Zhou, C. X.; Cui, Z. Real-Time Photolithographic Technique for Fabrication of Arbitrarily Shaped Microstructures. *Optical Engineering* ***2003***, 42(2), 477-481.

38 A control experiment was performed to probe the covalent attachment of the fluorophore to the substrate: a nonreactive monolayer prepared with decyl trichlorosilane (DTS) was fabricated following the same procedure as for TPEDA. After printing the fluorophore, the standard rinsing protocol (see experimental) was performed, resulting in the total loss of fluorescence.

39 The printed surface is not perfectly homogeneous, and the array spots depict only a very small area. They are meant to be a pictorial representation only, whereas the quantitative values for the fluorescence intensity changes are taken as an average over the whole measuring surface.

40 Crego-Calama, M.; Reinhoudt, D. N. New Materials for Metal Ion Sensing by Self-Assembled Monolayers on Glass. *Adv. Mater.* ***2001***, 13(15), 1171-1174.

41 Before inking, the stamps were oxidized by exposing them to UV/ozone for 60 min. This process enhanced the hydrophilicity of the stamp and the homogeneous spreading of the ink .[41] After ozone treatment the stamps were directly introduced in 10^{-3} M acetonitrile solutions of Pb^{2+}, Co^{2+} , Cu^{2+} and Ca^{2+} as perchlorate salts for 15 minutes. Then the stamps where dried with a N_2 stream and brought into contact with the sensitive fluorescent substrate for 1 minute.

42 Olah, A.; Hillborg, H.; Vancso, G. J. Hydrophobic Recovery of Uv/Ozone Treated Poly(Dimethylsiloxane): Adhesion Studies by Contact Mechanics and Mechanism of Surface Modification. *Appl. Surf. Sci.* ***2005***, 239(3-4), 410-423.

43 XPS mapping is the only instrumental method which has been shown to be useful to obtain image areas of such size, but it has a spatial resolution of 10 μm, which limits the technique to visualization of big feature size patterns. Additionally XPS is a much less accessible technique.

44 The printing experiments have been done using metal ion solution in acetonitrile as ink, but additional experiments not shown here have revealed that aqueous inks spread less onto the surface and better definition of the pattern can be obtained.

45 Multiple inking is possible using microfluidic networks over the PDMS stamps.Papra, A.; Bernard, A.; Juncker, D.; Larsen, N. B.; Michel, B.; Delamarche, E. Microfluidic Networks Made of Poly(Dimethylsiloxane), Si, and Au Coated With Polyethylene Glycol for Patterning Proteins Onto Surfaces. *Langmuir* ***2001***, 17(13), 4090-4095.

46 Vettiger, P.; Despont, M.; Drechsler, U.; Durig, U.; Haberle, W.; Lutwyche, M. I.; Rothuizen, H. E.; Stutz, R.; Widmer, R.; Binnig, G. K. The "Millipede" - More Than One Thousand Tips for Future AFM Data Storage. *IBM Journal of Research and Development* ***2000***, 44(3), 323-340.

47 Blankespoor, R.; Limoges, B.; Schollhorn, B.; Syssa-Magale, J. L.; Yazidi, D. Dense Monolayers of Metal-Chelating Ligands Covalently Attached to Carbon Electrodes Electrochemically and Their Useful Application in Affinity Binding of Histidine-Tagged Proteins. *Langmuir* ***2005***, 21(8), 3362-3375.

48 Height of the first line scanned was 6.1 nm indicating that more than a monolayer of Cu^{2+} metal ions was deposited on the substrate. Presumably this height value corresponds to the formation of $Cu(ClO_4)_2$ nanocrystal due to the sequential deposition of $Cu(ClO_4)_2$ onto the substrate.

49 LSCM has a lateral resolution of the half value of the excitation wavelength which was in this case 543 nm, thus a resolution of 270 nm was obtained. Therefore the thickness of the lines observed by LSCM (6.62 μm and 1.4 μm for the first and the second writtne line respectively) can have only 270 nm desviation from the real width.

50 Jang, J. Y.; Hong, S. H.; Schatz, G. C.; Ratner, M. A. Self-Assembly of Ink Molecules in Dip-Pen Nanolithography: a Diffusion Model. *J. Chem. Phys.* ***2001***, 115(6), 2721-2729.

51 Kassies, R.; Van der Werf, K. O.; Lenferink, A.; Hunter, C. N. ; Olsen, J. D.; Subramaniam, V.; Otto, C. Combined AFM and Confocal Fluorescence Microscope for Applications in Bio-Nanotechnology. *Journal of Microscopy-Oxford* ***2005***, 217, 109-116.

52 Burns, A. R. Domain Structure in Model Membrane Bilayers Investigated by Simultaneous Atomic Force Microscopy and Fluorescence Imaging. *Langmuir* ***2003***, 19(20), 8358-8363.

53 Hernando, J.; De Witte, P. A. J.; Van Dijk, E. M. H. P.; Korterik, J.; Nolte, R. J. M.; Rowan, A. E.; García-Parajó, M. F.; Van Hulst, N. F. Investigation of Perylene Photonic Wires by Combined Single-Molecule Fluorescence and Atomic Force Microscopy. *Angew. Chem., Int. Ed.* ***2004***, 43(31), 4045-4049.

54 Hards, A.; Zhou, C. Q.; Seitz, M.; Brauchle, C.; Zumbusch, A. Simultaneous AFM Manipulation and Fluorescence Imaging of Single DNA Strands. *ChemPhysChem* ***2005***, 6(3), 534-540.

Summary

Fluorescent self-assembled monolayers (SAMs) on glass surfaces have been studied as a new material for chemical sensing. The new sensing system presented in this thesis is a label-free sensing approach suitable for metal ion and inorganic anions sensing in both organic solvents and aqueous solution. The sensing SAMs are created by sequential deposition of two building blocks, a fluorophore and a ligand molecule onto an amino terminated SAM on glass slides. This produces a flat glass surface provided with a large number of binding pockets. Perturbation of the fluorophore upon binding of the analyte to the surface creates a measurable signal making the sensing of analytes possible. In this way a large number of different systems are fabricated by combinatorial techniques and parallel synthesis. The sensing SAMs displayed good sensitivity for a number of ions with detection limits of 10^{-6} M. Some of fluorescent SAMs have been found to respond specifically to the presence of Cu^{2+} and CH_3COO^- in the presence of other analytes. These sensing SAMs are also used as cross-reactive sensor arrays in which the analyte is identified by differential sensing using the collective response of a series of different SAMs to the analyte instead of the individual response of a single SAM. Arrays of fluorescent SAMs have been produced both in microtiterplate and in multichannel microfluidic chip formats.

In addition, these glass substrates coated with fluorescent SAMs have been used as substrates for chemical patterning. Different metal ion patterns have been created onto fluorescent SAMs coated glass slides. Due to the sensing properties of the substrates, modulation of fluorescence occurs in the localized areas where the metal ions are deposited. Therefore the chemical pattern is easily revealed by a luminescent pattern which is visualized by simple fluorescent microscopy.

In Chapter 2 an overview of the literature on fluorescent materials for chemical sensing is given. The last trends in the development of chemical sensors such as the use of combinatorial chemistry for discovery and development of new sensing probes, sensor

miniaturization, the use of microfluidics, and the fabrication of sensor arrays are also reviewed.

Chapter 3 describes the synthesis, charactezation and sensing properties of two libraries of fluorescent SAMs on quartz for metal ions and inorganic anions. Twenty different fluorescent SAMs were fabricated by parallel synthesis. Monolayer formation was evaluated by ellipsometry, contact angle measurements, X-ray photoelectron spectroscopy (XPS) and fluorescence spectroscopy. The fluorescent SAMs showed sensitivity for metal ions (Ca^{2+}, Co^{2+}, Pb^{2+}, Cu^{2+}) and inorganic anions (HSO_4^-, NO_3^-, $H_2PO_4^-$, CH_3COO^-) in acetonitrile. The detection limit of the system is 10^{-6} M. Selectivity studies showed SAMs that are highly selective for Cu^{2+} in presence of other metal ions such as Pb^{2+} and Ca^{2+}. Systems highly selective for CH_3COO^- in presence of HSO_4^- were also found.

In Chapter 4, new amino-terminated SAMs stable in water were fabricated and subsequently modified with fluorophores and binding groups to create a library of fluorescent SAMs stable in aqueous environments. By using these fluorescent SAMs, the approach described in Chapter 3 was expanded to the sensing of metal ions (Ca^{2+}, Co^{2+}, Hg^{2+}, Cu^{2+}) and inorganic anions (HSO_4^-, NO_3^-, $H_2PO_4^-$, CH_3COO^-) in water. These sensing studies showed that the library displays a unique fluorescent “fingerprint” for the different analytes in aqueous solvents which is used for identification of the analyte.

To apply high-throughput screening techniques, the fabrication of a fluorescent SAM cross-reactive sensor array in a microtiterplate was carried out in Chapter 5. Custom designed 140 well glass microtiterplates were fabricated. A library of fluorescent SAMs was made by parallel synthesis on the microtiter plates by coating the bottom glass of each well with a different monolayer. Inspection of the properties of the array for the sensing of Pb^{2+}, Zn^{2+}, Co^{2+}, Cu^{2+} and Ca^{2+} was made by laser scanning confocal microscopy (LSCM) and by fluorescence scanning. Different fluorescent patterns were obtained for the microtiterplate after exposure to different metal ions demonstrating the good performance of the sensor array for analyte identification.

In Chapter 6 the use of microchannels for the integration of chemical sensing systems in microfluidics devices was demonstrated. Coating of the walls of glass microchannels with fluorescent sensing SAMs have been used to generate sensing channels that respond to the presence of an analyte in the fluid passing through the channel. Monolayer formation was evaluated by contact angle measurements inside the channel and fluorescence microscopy. Additionally, a sensor array has been fabricated in a custom designed multichannel chip for differential sensing of Ca^{2+} and Cu^{2+}.

In Chapter 7 the complexing properties of the fluorescent SAM-coated substrates are exploited to create and easily visualize metal ion patterns on glass substrates. Patterning of fully covered fluorescent surfaces with metal ions (Ca^{2+}, Co^{2+}, Pb^{2+}, Cu^{2+}) has been carried out by soft and probe lithography techniques. Microcontact printing (μCP) and dip pen nanolithography (DPN) of metal ion salts onto the fluorescent SAMs on glass resulted on the successful transfer of the metal ions to the surface.
Additionally, the generation of fluorescent patterns on amino-terminated SAM coated glass slides by covalent attachment of fluorophores moieties to the surface by μCP has been proven. These patterns also function as sensing molds for metal ions.

In conclusion, new fluorescent materials have been developed for chemical sensing. Their performance has been demostrated for the sensing of metal cations and inorganic anions in organic and aqueous solvents. The simple fabrication scheme allows the generation of sensor arrays on glass surfaces, allowing mass screening of a number of different systems. The possibility of using the array format and combinatorial methods for fabrication of this sensing scheme provides the new approach with a high-throughput character. In addition, these sensing SAMs are generated in any glass substrate simplifying its integration in glass microfluidic devices. The new material constitutes a label-free approach in which binding of analytes can be directly monitored by fluorescence without the need of tagging steps.

The developed materials appear as a powerful tool with affinity for metal ions in which chemical patterns can be easily created and visualized. The possibility of

patterning with an almost unlimited number of analytes and substrates expands the tool box for pattern formation towards the discovery of new strategies for nanofabrication protocols. Catalysis and electroless deposition of metals are some of the envisioned applications of theses patterns.

Samenvatting

Fluorescente zelfassemblerende monolagen (SAMs) op glasoppervlakken zijn onderzocht als nieuwe materialen voor chemische sensoren. Het nieuwe sensorsysteem dat gepresenteerd wordt in dit proefschrift is een labelvrije aanpak geschikt voor herkenning van metaalionen en anionen, in zowel organische oplosmiddelen als in water. De sensor SAMs worden gemaakt door de achtereenvolgende depositie van twee bouwstenen, een fluorofoor en een ligandmolecuul, op een aminogetermineerde SAM op glasplaatjes. Dit geeft een glasoppervlak met een groot aantal bindingsgroepen. Verstoring van de fluorofoor na binding van het ion aan het oppervlak geeft een meetbaar signaal dat het herkennen van de ionen mogelijk maakt. Op deze manier werden een groot aantal verschillende systemen gemaakt met behulp van combinatoriële technieken en parallelle synthese. De sensor-SAMs toonden een goede gevoeligheid voor een aantal ionen met detectielimieten van 10^{-6} M. Enkele van de fluorescente SAMs reageerden specifiek op Cu^{2+} en CH_3COO^- in de aanwezigheid van andere ionen. Deze sensor-SAMs worden ook gebruikt als kruisreactieve sensor array waarin het ion wordt geïdentificeerd door middel van differentiële herkenning, gebruikmakend van de gezamenlijke respons van een serie verschillende SAMs op het ion, in plaats van de individuele respons van een enkele SAM. Arrays van fluorescente SAMs zijn gemaakt in zowel microtiterplaten als meerkanaals microfluidische chips.

Daarnaast zijn deze met fluorescente SAMs bedekte glassubstraten gebruikt als substraat voor chemische patronering. Patronen van verschillende metaalionen werden gemaakt op fluorescente SAMs op glassubstraten. Door de sensoreigenschappen van de oppervlakken vindt er modulatie van de fluorescentie plaats op die plekken waar de metaalionen zijn gedeponeerd. Dit chemische patroon kan eenvoudig zichtbaar worden gemaakt met behulp van fluorescentiemicroscopie.

In Hoofdstuk 2 wordt een overzicht gegeven van fluorescente materialen voor chemische sensoren. De laatste trends in de ontwikkeling van chemische sensoren zoals

het gebruik van combinatoriële chemie voor het ontdekken en de ontwikkeling van nieuwe sensoren, miniaturisering van de sensor, het gebruik van microfluidica, en het fabriceren van sensorarrays worden behandeld.

Hoofdstuk 3 beschrijft de synthese, karakterisatie and sensoreigenschappen van twee bibliotheken van fluorescente SAMs op kwarts, voor metaalionen en anionen. Twintig verschillende fluorescente SAMs werden gemaakt door middel van parallelle synthese. Monolaagvorming werd geanalyseerd met behulp van ellipsometrie, contatcthoekmetingen, Röntgen foto-elektron spectroscopie (XPS) en fluorescentie-spectroscopie. De fluorescente SAMs toonden gevoeligheid voor metaalionen (Ca^{2+}, Co^{2+}, Pb^{2+}, Cu^{2+}) en anionen (HSO_4^-, NO_3^-, $H_2PO_4^-$, CH_3COO^-) in acetonitril. De detectielimiet van het systeem is 10^{-6} M. Selectiviteitsstudies lieten zien dat de SAMs zeer selectief zijn voor Cu^{2+} in de aanwezigheid van andere metaalionen zoals Pb^{2+} en Ca^{2+}. Ook werden er systemen gevonden die zeer selectief waren voor CH_3COO^- in aanwezigheid van HSO_4^-.

In Hoofdstuk 4 worden nieuwe aminogetermineerde SAMS beschreven, die vervolgens werden gemodificeerd met fluoroforen en bindingsgroepen en die stabiel zijn in water, om zo een bibliotheek te creëren van fluorescente SAMs voor metingen in waterig milieu. Met behulp van deze SAMs werd de aanpak, beschreven in Hoofdstuk 3, uitgebreid naar het analyseren van metaalionen (Ca^{2+}, Co^{2+}, Hg^{2+}, Cu^{2+}) en anionen (HSO_4^-, NO_3^-, $H_2PO_4^-$, CH_3COO^-) in water. Deze studies lieten zien dat de bibliotheek een unieke fluorescente vingerafdruk bezit voor de verschillende ionen in waterige oplossingen, wat gebruikt kan worden voor de identificatie.

Om “high througput screening” technieken toe te passen werd in Hoofdstuk 5 een fluorescent SAM kruisreactief sensorsysteem in een microtiterplaat gemaakt. Hiervoor werden speciale glazen 140 well microtiterplaten ontworpen en gemaakt. Een bibliotheek van fluorescente SAMs werd gemaakt door middel van parallelle synthese op de microtiterplaten door de glazen bodem van iedere well met een andere SAM te coaten. Met behulp van laser scanning confocale microscopie (LSCM) en fluorescentiescanning

werden de eigenschappen voor het bepalen van Pb^{2+}, Zn^{2+}, Co^{2+}, Cu^{2+} en Ca^{2+} bekeken. Op de microtiterplaat werden verschillende fluorescentiepatronen verkregen na blootstelling aan verschillende metaalionen. Dit laat de goede werking van dit array zien.

In Hoofdstuk 6 wordt het gebruik van microkanalen voor de integratie van chemische sensoren met microfluidica beschreven. Het coaten van de glaswanden van de microkanalen met fluorescente sensor-SAMs werd gebruikt om kanalen te maken die reageren op de aanwezigheid van een ion in de vloeistof die door de kanalen stroomt. De monolaagvorming werd bekeken met contacthoekmetingen in de kanalen en fluorescentiemicroscopie. Daarnaast werd een sensorarray gemaakt in een speciaal ontworpen meerkanaalschip voor de differentiële herkenning van Ca^{2+} en Cu^{2+}.

In Hoofdstuk 7 worden de complexeringseigenschappen van de fluorescente SAM gecoate substraten gebruikt om patronen van metaalionen op glassubstraten aan te brengen en zichtbaar te maken. Patroneren van volledig bedekte fluorescente oppervlakken met metaalionen (Ca^{2+}, Co^{2+}, Pb^{2+}, Cu^{2+}) werd gedaan met behulp van stempel, en probe-lithografische technieken. Microcontact printen (μCP) en dip-pen nanolithografie (DPN) van metaalzouten op de fluorescente SAM gecoate glasplaatjes resulteerden in de succesvolle overbrenging van de metaalionen naar het oppervlak. Daarnaast werd het maken van fluorescente patronen op aminogetermineerde SAM gecoate glasplaatjes door middel van covalente binding van fluorofoorgroepen aan het oppervlak met μCP bewezen. Deze patronen functioneren ook als sensor-oppervlakken voor metaalionen.

Concluderend, zijn er nieuwe fluorescente materialen gemaakt voor chemische sensoren. De eigenschappen werden gedemonstreerd door het herkennen van metaal-ionen en anionen in organische en waterige oplossingen. De eenvoudige fabricage-methoden maken het mogelijk om sensorarrays op glasoppervlakken te maken, wat massale screening van verschillende systemen mogelijk maakt. Deze mogelijkheid om een array te gebruiken en combinatoriële methodes voor de fabricage van dit sensor-systeem geeft deze methode een “high througput” karakter. Daarnaast kunnen deze

SAMs gemaakt worden op elk soort glassubstraat, wat de integratie in glazen microfluidische devices eenvoudig mogelijk maakt. Het nieuwe materiaal maakt het mogelijk om binding van ionen direct te bekijken met fluorescentie zonder dat een labeling stap nodig is.

De gemaakte materialen lijken een krachtig middel te zijn voor herkenning van metaalionen waarin chemische patronen makkelijk gemaakt en bekeken kunnen worden. De mogelijkheid van het patroneren van een groot aantal verschillende ionen en substraten maakt dat deze aanpak ook gebruikt kan worden voor het ontdekken van nieuwe strategieën voor nanofabricage. Katalyse en “electroless depositie” van metalen zijn enkelen voorbeelden van mogelijke applicaties.

Acknowledgments

Writing the final lines of the thesis is a wonderful moment. Since I arrived to Enschede five years ago, time has passed very fast. Nevertheless there has been time enough to accumulate tones of good memories. I would like to thank everyone from who I have learnt, everyone who has listened to me, the ones who have trusted me and very important the ones that made me smile.

I would like to start thanking my promotor Prof. David N. Reinhoudt. David, belonging to the SMCT has been an amazing multicultural experience of constant exchange of people and fun. Scientifically, during four years, I have enjoyed a complete freedom to develop any scientific idea using an unlimited number of facilities. I could present my work in several conferences to other scientist, what was important to me. I respect very much your way of directing the group, which has made all this possible. Thank you for giving me this great opportunity. And I must not forget to thank you for all the free time that you have spent reading and correcting my concept thesis!

Before coming to Enschede, I got the opportunity of starting my research career working in the Supramolecular Chemistry group of Prof. Javier de Mendoza Sanz and Dr. Pilar Prados Hernando in Spain at the Universidad Autónoma de Madrid. I am deeply grateful to them for that opportunity, which actually opened me the door to the University of Twente, and for all what I learnt from them. I would like to dedicate a kind word to all my lab mates in Madrid: Ruth, Michiel, Vicente, Ana, Margot, Alex, Perla and especially to Juanma, Susana, Curra and Marta for teaching me most of what I know about working in the lab. ¡Cómo he echado de menos los desayunos de las 11!

During four years there has been a person who has guided me throughout this “thesis-trip”. I am deeply grateful to my supervisor Dr. Mercedes Crego Calama, not only for having the good ideas behind the work of my thesis… Her permanent good mood, uncountable good ideas and constant willingness to help, are some of the things that keep

surprising me and that have helped me very much during these years. I remember many occasions in which I entered your room with not so good feelings about the work and you were able to awake my enthusiasm again. Thank you Mercedes for all your guidance, for teaching me how to carry out the research, how to present the results, and for encouraging me continuously to collaborate with other people, what has actually enriched my thesis and me very much. Besides all the time and effort you have dedicated to my work, I knew I could always count on you as a friend, thank you very much. I am pleased to present here the result of our team-work. Mi querida "Supervisora" ¡ha sido un verdadero placer!

I would not have been able to carry out this work without the help and collaboration of many people. Starting from Dr. Jordi Hernando Campos. Thank you Jordi for your kindness, for all the hours that you have spent teaching me lessons of fluorescence, teaching me how to use the confocal microscope in the "dark side", doing measurements or analyzing the data coming out of those colorful lines. I feel very lucky because I could work with you. I could even listen to Pedro Guerra in the darkness! At the TN building, if I met Dr. María García Parajó I would always get extra wishes of good luck. I liked that. Thank you María also for the collaboration, and for coming back to Enschede to be part of my committee.

Part of the results presented in Chapter 5 of this thesis were obtained at the Medical Genetics, Groningen Universitair Medisch Centrum. I want to thank Prof. Buys for making it possible and especially to Dr. Klaas Klok and his team for his kind attention and help during my visits to Groningen. I want to thank Petra Mela for her contribution to Chapter 6 and to Han Gardeniers and Rob Duwel for the nice design and manufacturing of the multichannel-chips and the multichannel chip holder used for the last experiments of Chapter 6. Thanks to Monica Brivio, Meng Lin Chem and Fernando Benito for the good tips on microfluidics. I would like to thank Maria Peter for her contribution to Chapter 7. Maria (de la O!) thank you for all the time you spend at the AFM to draw micro size squares in the right place! And I am grateful to Henk-Jan van Manen, for all the time that he spent teaching me how to use the confocal microscope. I also would like to thank Prof. Vinod Subramanian, Dr. Ine Seger-Nolte and especially Martijn van Raaij

for making possible the experiments with the AFFM set-up described in Chapter 7. Thanks as well to Ruben Sharpe always willing to help. Thank you Ruben for the nice discussions and your help with the microcontact printing experiments. I am grateful to Philips for providing some of the PDMS stamps used in Chapter 7.

Things would have been completely different if during the second year of my PhD Rebecca Zimmerman hadn't come to the SMCT for a postdoc. Work at the lab is completely different and much more fun when you can share and discuss ideas. Becky, I am indebted to you for the enormous contribution you have made to this thesis until the really end, working on the lab, writing, correcting and discussing. Besides the work, I am happy for counting on you as a dear friend. I will not forget the chatting corner at the lab! Two students chose our project as their graduation project. First with Joris Beld, and after with Frederieke van der Baan, the fruitful Sensing Team I and II were formed. Thank you to both of you for the input and enthusiasm you put on the project, and the lessons about "Dutch cultuur"! The nice results that you got are part of the chapters 3, 4 and 5.

Thanks to Becky, Steffen, and Bart Jan, who accepted to read and correct the concept thesis. Thank you for the meticulous work that you made, which help me to improve the manuscript and made me think about many things. Also thank you very much to Emiel who translated the summary into Dutch

Since I was welcomed at the train station in Enschede by Marta Reinoso García and Francesca Corbellini, five years ago, I have not stopped meeting kind and helpful people in the SMCT. At that time I was coming to the group for a short period of four months within the Erasmus program. I want to thank Marta and Francesca for their help, attention and friendship during those months (and after), trying to make me feel part of the group in and outside the lab (even though they brought a poor student to a very expensive hotel in Amsterdam!). That period in the SMCT was the beginning of a nice experience. Thank you to Dr. Willem Verboon and Marta for the kind supervision of my work in the lab at that time.

After my Erasmus period, I left, but I came back to the same place. I would like to thank all my lab mates during these years that made the work in the lab easier and fun. Starting from Steffen Onclin, the one who taught me how to make monolayers just telling me “don’t get nervous”, Roberto Fiammengo, “el maestro de la química”, Francesca Corbellini, the kindest desk mate and stretching woman, Christiaan Bruinink, what a good idea the oxygen plasma!, Tommaso Auletta, Andrea Sartori, “el músico”, Choon Woo Lin, always smiling and ready for any scientific discussion, Soco (Buenos dias!!), Xing Yi (“Buenos días. – Buenos días.- ¿Qué tal? - Bien, gracias, ¿y tú? – Bien, gracias”), Deborah, the best cookies at the coffee^{+}, “Matarilerileron…”, Pascale (Pascalina: me, me , me , me), András, the quite man, and Dorota, my last fluorophore provider.

I want to thank Marcel de Bruine (“Marcelino”), Richard Egberink, Izabel Katalank and Marieke Slotman, for all your help, always smiling, concerning lab equipment, computers, or paperwork, “without you, the SMCT, doesn’t have a clue!”

Thank you to all the present and former members of the SMCT for generating a pleasant and enjoyable working atmosphere. Special thanks to all the people who has made this experience so exceptional sharing their time outside the lab with me (listed in completely random order): Mattijs, always omnipresent, a good friend and the first one who knew I was coming back!; Juanjo, the big brother; Floren (que alegria!); Tomasso, Roberto (Robertiño); Marta; Francesca; Hans, Emiel; Monica; Bas; Barbara; Mónica and Marco; Kazu (Bon); Jessica; Manon, Alessio; Olga; Fernando; Soco, the winner of IDOLS!; Rob; Deborah; Paolo; Andrea; Becky; Michel; Marina; Mirko; Francesca; Meng Lin; Henk and Marloes, you were exceptional, our Dutch reference, always willing to enjoy with us and good friends; Charu, my dear Indian friend and cook!; Francesca and Laura, you were always willing to organize a funny party. What birthday parties!; Aldrik, Ana, y ¡el resto de los Físicos!! Thank you to all of you for the great time together.

My time at Javastraat has also been special. I have had the fortune of sharing the house with several special girls from around the world, France, Italy, Spain, EEUU and Argentina. I would like to thank Maria Cadic for the nice time together and your help for

all the house staff when I arrived here. My dear friend Irene Mazzitelli, thank you for your friendship, the ethernal conversations on the sofa ("sobre filosofia barata o los nerinos del Congo") and all the time we were laughing together when we were traveling to deserted towns on Sundays, cooking or gardening! Also my dear friend Olga Crespo, almost like a mother when she starts giving orders! ☺ We have had so many things together… living at Javastraat, working at the same office, starting the PhD, finishing the PhD, going to our boyfriends' house…what a number of great memories. Extra thanks to Olga and Irene for being my "Paranimfen". I am happy that you will be with me, up there, "that DAY". Rebecca Zimmerman, very silence at home, we could almost not hear you. It was fun watching movies with you, even though you were laughing at the jokes much more than us! And Marina Giannotti was the last one to arrive to Javastraat. What a girl! we could be friends from the really beginning, even though you didn't believe me when I told you that the sun in The Netherlands is something you must take advantage of from the moment that it appears. Since I saw your old big photographic camera I knew we would have fun!

Speaking about photography, the real Photo-team were Mirko, Marina and I. Since we were seeking for an English photocourse, we were making "SELF-portraits" to each other, and we were seeing the ten copies of the same picture in the water pool, I have enjoyed really much. A kind word to our photography teacher Cees Oortwijn and our photo mates Rithyda, Daisy, Muriel and Leoni with whom I had an enjoyable time and fun at the "Doka" and the parties (even though my pullover was on fire!)
Besides all this, Enschede has been special for all the traveling that I did together with friends, all the Thursday afternoons at "De Beiaard", all the Wednesday evenings at the Squash, all the Saturdays at lunch, and all the cinematographic productions! Thank you to all the people who made all this possible.

A special mention to those who knew that the telephone line was working not only from The Netherlands to the outside but also from the outside to The Netherlands!

The last lines are for those who have been friends here in Enschede and have taken care of me. Si algo no podré nunca olvidar de Enschede será la gran familia Basabe

Crespo Giannotti Benito Piermattei Mateos Timoneda. Son demasiadas las anécdotas y las cosas que agradecer. Gracias Olga por que siempre supiste hacer un hueco para mí en tus “apretados esquemas” incluso sin necesidad de que te lo pidiera; son muchas cosas las que hemos pasado juntas y los buenos ratos, me siento afortunada de tenerte como amiga; gracias Alessio por tu carácter y tu buena disposición, cómico y cocinero “genio y figura hasta la sepultura”; Michel (Angelo) siempre cariñoso, sonriendo y dispuesto a ayudar; Marina nuestra última adquisición, siempre lista para reír y escuchar. Y Fernando, un enfermo crónico de alegría. Gracias a todos por haber sido como una verdadera familia, por todos los buenos ratos y vuestro apoyo en todo momento.

Gracias a mis amigos en España, Elena, Miguel, Bea, Arancha y Mª Jesús por demostrarme que la amistad no sabe de distancias y estar cerca de mi durante este tiempo. Itxaro, al fin he terminado, ¡me parece increíble! Y que más te voy a decir Itxarín que no sepas tú ya por que me has acompañado todo este tiempo, muchas gracias. Gracias a Mamen, María, Lucía y Helena por que durante estos años he sabido que pasen los años que pasen sin vernos, seguiremos siendo amigas.

Mi familia es lo más preciado para mí. Su incondicional apoyo, confianza y orgullo es algo fuera del alcance de ningún tipo de agradecimiento, y mi pilar de apoyo. Quiero dar las gracias a mis abuelas, tíos, primos; y especialmente a mis padres y hermano por su constante presencia, la distancia no ha hecho sino acercarnos más. Esta tesis está dedicada a mis padres y hermano, porque sin sus enseñanzas, esfuerzos, constantes cuidados y cariño esto no se habría hecho realidad.

Fernando, he sido muy afortunada de tenerte a mi lado este tiempo y aprender entre tantas otras cosas que la alegría es aquello que no debe perderse nunca, o, “¡qué no hay nada interesante ahí abajo en el suelo!” Gracias por tu alegría, por escucharme con paciencia y especialmente empujarme hacia el final y a hacer las cosas bien cuando me ha hecho falta. Tú has hecho que este tiempo fuera aun más especial. Gracias mi amor por “todas las canciones”.

Lourdes Basabe Desmonts

About the Author

Lourdes Basabe Desmonts was born in Cartagena, Spain, on March 11, 1978. She studied chemistry at the Universidad Autónoma de Madrid from 1996 until 2001. From July 2000 to July 2001, she worked in the synthesis of several organic compounds, derivates of calix[6]arene, and calix[4]arene, in the Supramolecular Chemistry group of the Universidad Autónoma de Madrid directed by Prof. Javier de Mendoza Sanz and Dr. Pilar Prados Hernando. From November 2000 to March 2001, she obtained an Erasmus Fellowship and she worked in the Supramolecular Chemistry and Technology group at the MESA^{+} Research Institute for Nanotechnology directed by Prof. D. N Reinhoudt, in the synthesis of derivates of cavitands, under the supervision of Dr. W. Verboom. From October 2001 until October 2005 she was employed at the same group as a PhD student and she worked under the supervision of Dr. M. Crego Calama. The research carried out in that period is described in this thesis and focuses on the development of fluorescent chemosensing materials based on self-assembled monolayers.